



Universiteit
Leiden
The Netherlands

Developing tissue specific antisense oligonucleotide-delivery to refine treatment for Duchenne muscular dystrophy

Jirka, S.

Citation

Jirka, S. (2017, July 4). *Developing tissue specific antisense oligonucleotide-delivery to refine treatment for Duchenne muscular dystrophy*. Retrieved from <https://hdl.handle.net/1887/51132>

Version: Not Applicable (or Unknown)

License: [Licence agreement concerning inclusion of doctoral thesis in the Institutional Repository of the University of Leiden](#)

Downloaded from: <https://hdl.handle.net/1887/51132>

Note: To cite this publication please use the final published version (if applicable).

Cover Page



Universiteit Leiden



The handle <http://hdl.handle.net/1887/51132> holds various files of this Leiden University dissertation

Author: Jirka, Silvana

Title: Developing tissue specific antisense oligonucleotide-delivery to refine treatment for Duchenne muscular dystrophy

Issue Date: 2017-07-04

**Developing tissue specific antisense
oligonucleotide-delivery to refine treatment
for Duchenne muscular dystrophy**

By Silvana Jirka

Developing tissue specific antisense oligonucleotide-delivery to refine treatment for Duchenne muscular dystrophy

Proefschrift

ter verkrijging van
de graad van Doctor aan de Universiteit Leiden,
op gezag van Rector Magnificus prof.mr. C.J.J.M. Stolker,
volgens besluit van het College voor Promoties
te verdedigen op 4 juli 2017
klokke 15:00 uur

door
Silvana Maria Gerarda Jirka
geboren te Apeldoorn in 1984

Cover design: Vincent Smeenk

Illustrations: Vincent Smeenk

Layout: Remco Peereboom

Printed by: Off Page

ISBN: 978-94-6182-808-8

The studies described in this thesis have been performed at the Leiden University Medical Centre, department of Human Genetics. The work was financially supported by a grant from the Prinses Beatrix Spierfonds, the Netherlands (grant W-OR13-06).

copyright©2017 S.M.G Jirka. All rights reserved. No part of this thesis may be reproduced or transmitted in any form or by any means, without prior permission in writing of the author.

TABLE OF CONTENTS

Chapter 1	General introduction	7
Chapter 2	Update on RNA-targeting therapies for neuromuscular disorders <i>Curr Opin Neurol 2015, 28:515-521</i>	51
Chapter 3	Peptide conjugation of 2'-O-methyl phosphorothioate antisense oligonucleotides enhances cardiac uptake and exon skipping in mdx mice <i>Nucleic Acid Ther. 2014 Feb;24(1):25-36</i>	67
Chapter 4	Phage display screening without repetitious selection rounds <i>Anal Biochem. 2012 Feb 15;421(2):622-31</i>	95
Chapter 5	Cyclic peptides to improve delivery and exon skipping of antisense oligonucleotides for Duchenne muscular dystrophy <i>Submitted</i>	119
Chapter 6	Evaluation of 2'-deoxy-2'-fluoro antisense oligonucleotides for exon skipping in Duchenne muscular dystrophy <i>Mol Ther Nucleic Acids. 2015 Dec 1;4:e265</i>	151
Chapter 7	General discussion	171
Chapter 8	Summary	179
Chapter 9	Samenvatting	183
	Curriculum Vitae	189
	List of Publications	191
	Acknowledgements	194

Promotoren: Prof .Dr. G.J.B. van Ommen
Prof. Dr. A. Aartsma-Rus

Co-Promotor Dr. P.H.A. 't Hoen

Leden promotiecommissie: Prof. Dr. M. Goumans
Prof. Dr. M. Gait¹
Prof. Dr. J. Kuiper²

¹Medical research council, Laboratory of Molecular Biology, Cambridge UK

²Leiden University, Leiden academic centre for drug research, Leiden the Netherlands



CHAPTER 1

General introduction

1. Introduction

1.1.1 Duchenne muscular dystrophy

Duchenne muscular dystrophy (DMD) is a severe and progressive X-linked, muscle-wasting disorder affecting 1 in 5,000 newborn boys (1,2). DMD is caused by mutations in the *DMD* gene, leading to a truncated, non-functional dystrophin protein (figure 1). Dystrophin is an important muscle protein since it provides stability to the muscle fibers upon contraction (3). Without a functional dystrophin protein, muscle fibers are easily damaged during exercise and chronically damaged muscle fibers are eventually replaced by fibrotic and adipose tissues, resulting in a loss of muscle function (4). DMD has an early onset in childhood and patients are in general diagnosed before the age of five. Early symptoms are a delay in time at which children start to stand and walk, hypertrophy of the calf muscles, the need to use their hands to support their legs while rising from the floor (Gower's sign) and difficulties with running and stair climbing. For some patients a delay in cognitive development is seen. Overall the mean IQ is approximately one standard deviation below the mean and about 20-30% of the patients has an IQ of less than 70 (5,6). In general, DMD patients become wheelchair dependent at around the age of 12 years, need assisted ventilation at around 20 years of age, first only at night and later throughout the day as well. Cardiomyopathy manifests around the age of 10 and is prevalent in most patients of 20 years of age (7). The life expectancy of DMD patients is, nowadays, around 30 years in the Western world, where respiratory and cardiac failure is the main cause of death for these patients (8).

1.1.2 Becker muscular dystrophy

In contrast to DMD, which is characterized by the presence of non-functional dystrophin proteins, Becker muscular dystrophy (BMD) is a muscle wasting disorder caused by mutations in the *DMD* gene that result in the production of an internally deleted, but partially functional dystrophin protein (figure 1). Symptoms in patients with BMD are generally milder, however phenotypical variation from mild to moderately severe is seen and within families asymptomatic patients have been identified (5,9). The age of onset of symptoms ranges from ~12 years to late midlife. Patients become wheelchair dependent 20-30 years after diagnosis, however, some patients remain ambulant throughout their life. The life expectancy for the severely affected patients is around 40-50 years of age whereas mildly affected patients have near normal life expectancies.

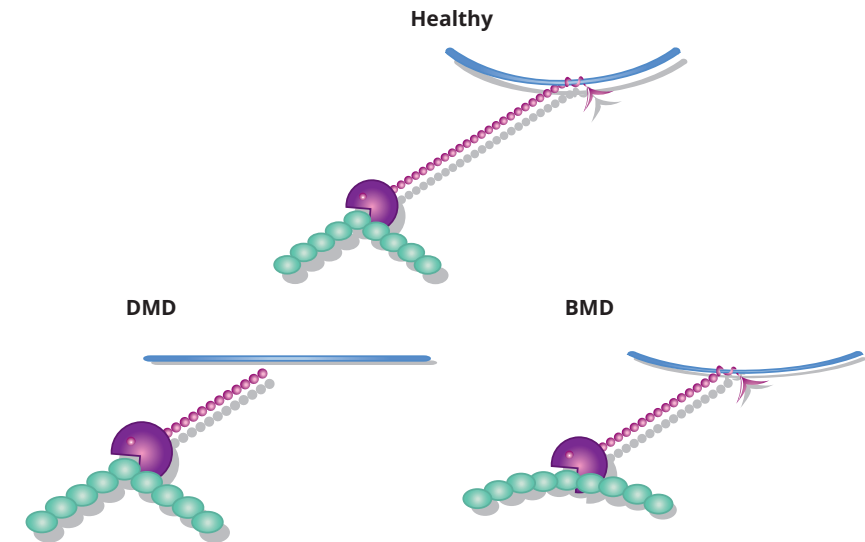


Figure 1. Illustration of dystrophin in healthy individuals versus DMD and BMD patients. Dystrophin is an important muscle protein. It provides stability to the muscle fibers upon contraction by connecting the internal cytoskeleton to the extracellular matrix. In healthy individuals the dystrophin protein is fully functional, however absent in DMD patients and impaired (due to a shorter dystrophin protein) in BMD patients.

1.2 *DMD* gene and protein

The *DMD* gene is the largest known gene of the human genome. It is located on the short arm of the X-chromosome at position 21.2 (Xp21.2) and consists of 2,241,764 base pairs (bp) (www.ensembl.org). The coding region for the full length protein is dispersed over 79 exons, transcribed into a 13,956 bp mRNA and coding for a full-length dystrophin protein of 3,658 amino acids with a molecular weight of 427 kDa (4,10,11). In DMD patients, mutations in the *DMD* gene cause a disruption of the reading frame (if the size of the deletion or insertion in base pairs is not divisible by three) or a premature stop codon. These mutations result in premature truncation of translation and an unstable protein leading to an absence of the dystrophin protein. Mutations can occur throughout the gene, but the region of exon 45-55 is known as a major hotspot for deletions and the region of exon 2-10 as a minor hotspot for duplications (12,13).

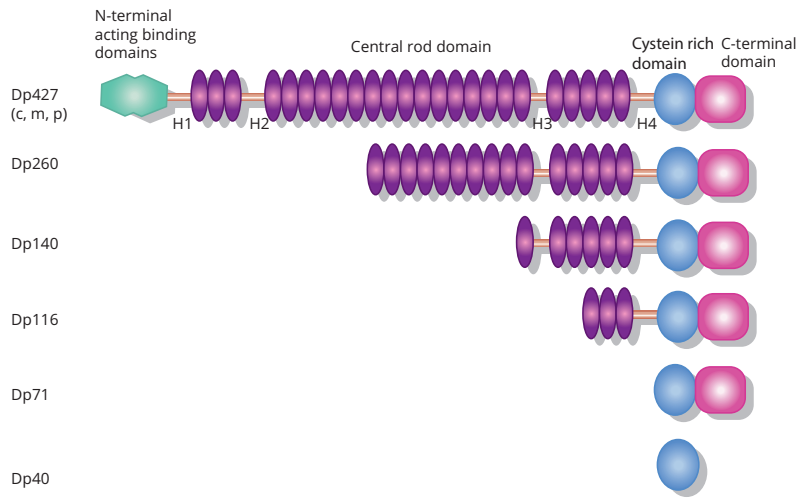


Figure 2. Illustration of dystrophin and its isoforms. Dystrophin contains four domains: N-terminal binding site (green), central rod domain (purple), cysteine rich domain (blue) and the C-terminal binding site (pink). Dystrophin has three full length isoforms regulated by three different promoters and each having unique first exons: Dp427m (skeletal and cardiac muscle), Dp427c (cortical neurons and hippocampus), Dp427p (cerebellar Purkinje cells). There are five shorter dystrophin proteins regulated by internal promoters: Dp260 (retina), Dp140 (central nervous system and kidney), Dp116 (Schwann cells), Dp71 and Dp40 (ubiquitous expressed but not in muscle).

The full length dystrophin protein contains two N-terminal actin-binding domains (encoded by exon 2-8) followed by a central rod domain (encoded by exon 9-63), a cysteine rich domain (encoded by exon 64-70) and the C-terminal domain (encoded by exon 71-79) (figure 2) (11,14,15). Within muscle, dystrophin connects the subsarcolemmal cytoskeleton to the extracellular matrix. With the N-terminal actin-binding domains it connects to the F-Actin in the cytoskeleton. A bridge is formed by binding of the C-terminal cysteine-rich binding domain to the β -dystroglycan protein of the dystrophin glycoprotein complex (DGC complex), which is in turn connected to the extracellular matrix protein laminin (figure 3). Within the muscle the dystrophin connection to the DGC complex provides stability to the muscle fibers upon contraction (3,16,17). Consequently, without a functional dystrophin protein, muscle fibers become vulnerable to exercise-induced damage. Chronically damaged muscle fibers lead to chronic inflammation and eventually these fibers are replaced by non-functional fibrotic and adipose tissues, resulting in muscle loss as seen in DMD patients.

In BMD patients, mutations do not lead to premature truncation of translation, but result in an internally deleted (shorter) but partly functional

dystrophin protein (figure 1). The connection between the subsarcolemmal cytoskeleton and the extracellular matrix is maintained, although with an altered connection and functionality, resulting in muscle fibers that are less vulnerable to exercise-induced damage.

Dystrophin is known to have eight isoforms, expressed from different promoters located throughout the gene (figure 2). Full-length dystrophin is regulated by three different promoters of the first exon. The full length Dp427m isoform is expressed in skeletal muscle and cardiomyocytes. Other two full-length isoforms are Dp427c, expressed in the brain (cortical neurons and hippocampus) and Dp427p expressed in cerebellar Purkinje cells. There are four internal promoters responsible for the expression of shorter proteins. Dp260 which is expressed in the retina. Dp140 which is expressed in the central nervous system and kidney. Dp116 which is expressed in Schwann cells and Dp71 and Dp40 (both expressed from the same promotor) are ubiquitous expressed but not in muscle tissue. DP71 is known to be highly expressed in brain compared to other tissues (3,18).

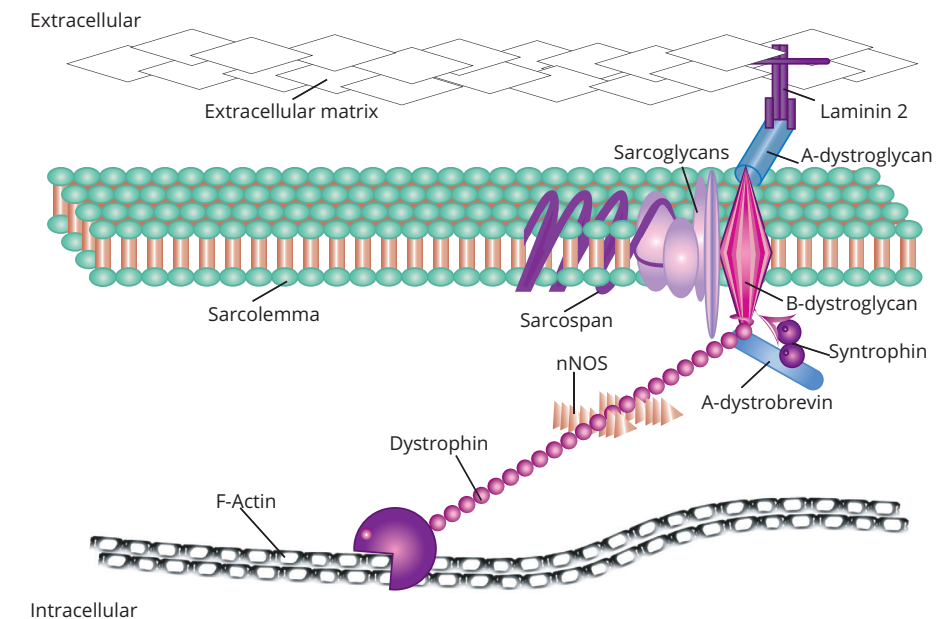


Figure 3. Location of dystrophin in muscle. Dystrophin binds with the N-terminal actin binding domains to F-actin and with the C-terminal cysteine rich binding domain to β -dystroglycan. A bridge is formed connecting the internal cytoskeleton to the extracellular matrix, providing stability upon muscle fiber contraction.

1.3 Therapeutic approaches

1.3.1 Multidisciplinary care

Currently there is no therapy for the majority of DMD patients. As part of the standard of care, patients receive symptomatic treatment (19,20). In general, corticosteroids (prednisone/prednisolone and deflazacort) are used and have shown, in various retrospective studies and clinical trials, to slow down disease progression (7,21-23). However, the use of steroids is associated with side effects like weight gain, loss of vertebral bone mass, growth inhibition and late onset of puberty.

In parallel, improved technology has led to the development of equipment like cough-assists and non-invasive mechanical ventilation devices and improved cardiac care. Furthermore, care standards involve multiple disciplines, e.g. neuromuscular, rehabilitation, orthopedic, pulmonary, cardiac, gastrointestinal and psychosocial management. Together this multidisciplinary approach has greatly improved the quality of life of Duchenne patients and nowadays resulted in a life expectancy into the fourth decade of life (8).

1.3.2 Dystrophin restoring therapeutic approaches

Various therapeutic approaches are currently under development aiming to restore the primary genetic defect i.e. absence of dystrophin protein. Other approaches aim to improve secondary pathology i.e. reduce fibrosis and inflammation, or improve muscle cell growth and strength. Focusing on dystrophin restoration, cell therapy as well as gene therapy based approaches are currently under development.

Cell therapy

Upon muscle damage, muscle stem cells (so called satellite cells or myoblast cells) are activated to repair the damaged muscle (24). By introducing healthy donor muscle stem cells with a functional copy of the *DMD* gene, one can in theory, gradually restore the whole muscle (25,26). This approach has been evaluated in human clinical trials with DMD patients in the early 1990s using myoblast cells. Disappointingly, no dystrophin restoration was observed (27-30). Failure of the trials was mainly caused by rapid cell death of the transplanted cells and their limited migration within the muscle upon intra muscular injections (myoblasts cannot cross blood vessel walls).

Currently, as an alternative to myoblasts, human pericyte-derived mesoangioblasts (MAB) are investigated. MABs are blood vessel-associated progenitor cells, which can be differentiated in various mesoderm cell types including muscle cells. They can cross blood vessel walls, which makes them applicable for systemic administration. Various preclinical animal studies with MABs have shown improvement of muscle pathology (31,32).

MABs from healthy HLA-identical siblings have been evaluated in a non-randomized open-label phase I-II clinical trial (EudraCT no2011-000176-33) (33). In total five DMD patients received four consecutive intra-arterial infusions of donor derived MABs in the limb arteries with a two month interval, under immunosuppressive therapy. Two months after the last infusion no dystrophin was observed in muscle biopsies nor were functional improvements seen by MRI. The authors concluded the study relatively safe. However one patient developed a thalamic stroke, and although the relation to the MAB infusions remained unclear, this is a serious safety concern.

When using donor cells, lifelong treatment with proper immune suppressants is needed to protect the donor cells from the recipients immune system, however these appear to be detrimental for the donor cells (34). To address this, alternatives are under development e.g. the use of CD133⁺ donor derived cells or the use of genetically modified patient derived stem cells using human artificial chromosomes (35-37). The recently developed cluster regularly interspaced short palindromic repeat (CRISPR) associated nuclease nine (cas9) endonuclease system (CRISPR/Cas9) has shown promising results for genetic correction of patient derived stem cells as well. This system uses the cas9 nuclease to cleave the DNA at specific sequences targeted by guide RNAs (gRNA). Subsequently the loose ends are joined together by non-homologous end joining (NHEJ). For DMD, the CRISPR/Cas9 system is used to genetically correct the *DMD* gene by exon deletion. Using 2 gRNAs, designed to bind in the introns, one near the beginning and the other near the end of the exon of interest, Cas9 makes a cut at these sides. The loose-ends are then joined together by NHEJ (deleting the exon of interest), making the deletion larger but restoring the reading frame. In this way an internally deleted but partly functional dystrophin protein is produced as seen in BMD (figure 4) (38-41). While minimal cellular toxicity is seen for CRISPR/Cas9 *in vitro*, off target effects (cutting elsewhere in the genome) do occur and this demands more research (42-45).

Although a lot of progress in developing cell therapy based approaches has been made in general, delivery and control of stem cells and their niche/microenvironment are remaining challenges today. For DMD body wide delivery to muscle is required but still not feasible. Little is known about the influence of fibrotic tissue and inflammation (present in the muscle of DMD patients) on the stem cell niche/microenvironment. In a healthy situation the cells present in this niche provide a specific microenvironment to maintain and promote cell differentiation of stem cells. Future research should focus on these challenges to make the approach successful.

*Gene therapy**DNA based gene therapy*

DNA based gene therapy aims to restore the expression of a gene from a patient by introducing specific DNA as treatment for the disease. An example for DMD is the introduction of the dystrophin gene in muscle cells, using adeno-associated virus derived delivery vectors (AAVs). AAVs are the only virus derived vectors that are capable of efficiently transducing muscle, however the cloning capacity of ~4.5kb limits the use of the full *DMD* gene which has a coding sequence of around 11kb. Therefore mini- or micro-dystrophin genes are generated, mimicking a BMD like dystrophin protein (46-52). A different approach is the earlier described CRISPR/Cas9 system which, upon AAV delivery, can be used directly in muscle to restore the disrupted reading frame. Recently three papers in the journal *Science* were published using this approach; Nelson *et al.*, Tabebordbar *et al.* and Long *et al.* All showed dystrophin restoration in *mdx* mice after intramuscular and or intraperitoneal administration of CRISPR/Cas9 leading to a targeted exon 23 deletion. Dystrophin protein levels varied from 0.5% to 8% in skeletal muscle tissue and ~0.5% in cardiac muscle tissue (53-55).

There are a few major drawbacks of using the CRISPR/Cas9 system directly in patients. The first drawback is the delivery. Effective delivery of AAVs to all skeletal and cardiac muscle cells upon single administration is still challenging for humans and systemic administration requires high dosing of AAV vectors. Second but most important, upon muscle turnover the muscle transgenes are lost, thereby losing the mini- or micro-dystrophin genes. This is not the case when using the exon deletion strategy by CRISPR/cas9 technology, as this affects patients own genes (however in the case of muscle this is only true if satellite cells are targeted as these are responsible for generating new muscle cells). Repeated injections with AAVs are needed, this may lead to an immunological reaction of patients own immune system towards the vector. Third, restoring the dystrophin gene in fibrotic tissue will not lead to dystrophin restoration as there is no active dystrophin production in this tissue. Damaged tissue cannot be restored, making timing critical for this approach. Fourth, not a lot is known about the safety of the CRISPR/Cas9 system regarding specificity, as off target effects appear to be present (see cell therapy). So far only proof of principle has been shown, years of future work is needed assessing all of the issues before this approach can be evaluated for clinical use (56-59).

*RNA targeting gene therapy**Ataluren*

Around 14% of the DMD patients have a nonsense mutation *i.e.* a point mutation causing a premature stop codon, leading to premature truncation of translation and the absence of the dystrophin protein (60). Ataluren, PTC124 (Translarna™), is an orally available non-aminoglycoside drug with premature stop codon read-through activity, which in principle could restore dystrophin expression in this group of patients (61). In preclinical animal models PTC124 showed dystrophin restoration in skeletal and cardiac muscle and was well tolerated in healthy and DMD patients (62). In a phase 2a open-label clinical trial (38 DMD boys, treated for 28 days) 61% showed an increase of 11% in dystrophin levels assessed from muscle biopsies and treatment was well tolerated (63). In a follow up phase 2/3 clinical trial (174 randomized patients) two different doses (40 and 80 mg/kg) were evaluated for a year. Unfortunately, the primary end point (30 meter difference in the 6 minute walk test (6MWT) between treated and placebo groups) was not met ($\Delta 29.7m$). Nevertheless, patients treated with low dose (40 mg/kg/day) showed less (but not a significant) decline in the 6MWT than placebo and showed meaningful differences in secondary endpoints such as climbing and descending 4 stairs and walk or running 10 meters, thereby offering promise as treatment for DMD (64,65). After a post-hoc analyses PTC requested for conditional approval with the EMA, this was granted with the condition to perform a new study. By this means Ataluren, PTC124 (Translarna™), is the first conditionally approved drug by EMA for ambulant DMD patients age 5 years and older with a nonsense mutation causing premature stop codon (66). On October 15th, 2015 PTC announced their results from the phase 3 ACT-DMD clinical trial (40 mg/kg/day vs placebo for the duration of a year) showing a significant benefit of 47 meters in the 6MWT for patients who could walk 300-400 meters at baseline and a non-significant increase of 15 meters in the 6 MWT in the overall study population. In line they saw a benefit over placebo for secondary and tertiary endpoints, *i.e.* climbing and descending 4 stairs, walking or running 10 meters and North Star Ambulatory Assessment test (ir.ptcbio.com). In January 2016 PTC completed the New Drug Application (NDA) submission to FDA, but this was rejected. In parallel they submitted the data from the new phase 3 ACT DMD clinical trial to EMA, this is still pending.

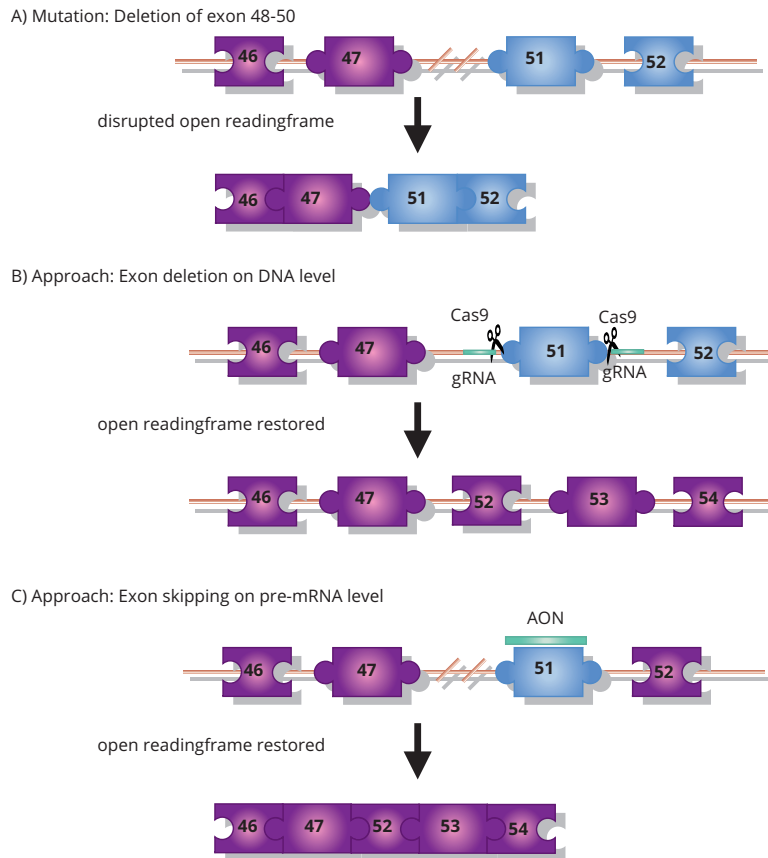


Figure 4. Targeted exon deletion versus exon skipping. Targeted exon deletion by genome editing as well as exon skipping are both applications to restore the disrupted reading frame of the DMD gene. CRISPR/cas9 technology is designed to delete an exon on DNA level. Exon skipping, using AON, is designed to target the pre-mRNA, interfere with pre-mRNA splicing. This results in a skip of the target exon. Both applications result in an internally deleted but partly functional dystrophin protein. A) an example of a disrupted reading frame, deletion of exon 48-50 in the DMD gene. B) restoration of the reading frame using CRISPR/cas9 technology. C) restoration of the reading frame using AON.

Exon skipping

The therapeutic approach that is the focus of this thesis is the restoration of the reading frame on RNA level in DMD patients using antisense oligonucleotides (AON). In theory this approach allows the production of a shorter but partly functional dystrophin protein as seen in patients with BMD (4,67). These AONs bind the target pre-mRNA in the nucleus in a sequence specific way. Here they interfere with splicing factors by binding the exonic splicing enhancer and/or exon inclusion sequences, preventing

exon recognition, and thereby cause the skipping of the target exon (68,69) (figure 4). In 1996 Pramono *et al.*, showed it was feasible to induce exon skipping in an *in vitro* splicing assay (70). Later, Dunckley *et al.*, and Wilton *et al.*, showed the potential of exon skipping in cultured primary myotube cells of *mdx* mice (71,72). The feasibility of exon skipping upon intramuscular and systemic administration of AON, targeted to skip exon 23 in *mdx* mice, was shown by Mann *et al.*, and Lu *et al.*, respectively (73,74). Van Deutekom *et al.*, showed for first time, the skipping of exon 46 in cultured myotube cells of DMD *patients* with a deletion of exon 45, thereby restoring the disrupted reading frame resulting in correctly localized dystrophin protein expression in 75% of the myotubes (75). Later Aartsma-Rus *et al.*, designed AONs for 11 other human DMD exons and showed skipping of these exons in cultured human myotubes (76). In 2007 dystrophin restoration after a local injection of AON, targeting exon 51, in the tibialis anterior of DMD patients was shown by Deutekom *et al.*, (77).

Exon skipping is a mutation specific approach. There is a high variation in mutations between DMD patients. Nonetheless some patients with different mutations can benefit from skipping the same exon, e.g. exon 51 skipping for a deletion of exon 45-50, 47-50, 48-50, 49-50, 50 and 52, making it applicable to the largest group of patients (13-14%) (60,78). Currently AON mediated exon skipping for DMD is evaluated in various clinical trials, further described in paragraph 1.3.4

1.3.3 Exon skipping antisense oligonucleotides

AON are single stranded, short pieces of chemically modified DNA or RNA, which can bind complementary to the target RNA (via Watson and Crick base pairing) and modulate the function of the target RNA. In general AONs can be divided in two main groups based on their mechanism of action. The first group of AON promotes, upon binding, degradation or cleavage of the target RNA by the recruitment of endogenous enzymes. For example, RNase H or RNA-induced silencing complex (79-81). The second group consists of AONs which, upon binding, interfere with the function of the target RNA without degradation, for example by blocking translation, promoting alternative use of exons, exon skipping or exon inclusion (82). The difference between the groups after binding the target RNA depends on the chemistry of AON used, the binding location on the target RNA and the location of the target RNA in the cells.

Throughout the years different chemically modified AON have been developed to enhance nuclease resistance or improve thermodynamic stability, affinity for the target, bio-availability and tissue half-life (83,84). For DMD, the most studied exon skipping AON chemistries are the 2'-O-methyl phosphorothioate (2OMePS) and phosphorodiamidate morpholino oligomers (PMO) (Aartsma-Rus, 2014). 2OMePS AON is a second generation RNA-like AON. It has a 2'-O-methyl modification at the 2'OH position of the

ribose and a phosphorothioate (PS) backbone. It has a net negative charge, is almost completely nuclease resistant and has a high binding affinity for RNA. 2OMePS AONs have a prolonged half-life *in vivo* (plasma half-life ~ 4 weeks in patients) due to fact that PS- modification enables low affinity serum protein binding, thereby preventing acute renal clearance (85,86). It is estimated that 2OMePS AON have a tissue half-life of 10-33 days in skeletal muscle and 46 days in cardiac muscle (87). PMO AON is a third generation, DNA-like AON. The deoxy-ribose sugar ring is replaced by a morpholino ring and the phosphodiester bond by phosphorodiamadate linker. It is charge neutral has a high binding affinity and is completely nuclease resistant. Lacking the PS modification PMOs have a much shorter half-life *in vivo* due to fast renal clearance (plasma half-life ~3-4 hours in patients) (88).

Currently, a new DNA based AON, Tricyclo-DNA (Tc-DNA) is evaluated for exon skipping for DMD in animal models. This AON deviates from DNA by the presence of 3 additional carbon atoms between C5' and C3', is completely nuclease resistant, has a further improved binding affinity, thermodynamic stability, serum stability, and does not elicit RNase H activity (89,90). Serum levels of Tc-DNA rapidly decline in an hour after administration, but are still detectable after 90 minutes in mice (91). Compared to the 2OMePS AON, Tc-DNAs have improved tissue half-life, which is estimated to be 45 days on average and appears to be taken up by cardiac tissue more efficiently (91).

Modifying the 2' position of the sugar moiety of RNA is an attractive approach to improve, for example, affinity, stability and nuclease resistance. The 2OMe modification is an example of such modification. Another possible 2' modification is the substitution of a Fluoro (F) at the 2' position (2'-deoxy-2'-fluoro RNA modification (2F)). In a study from Rigo *et al.*, (Ionis pharmaceuticals) it was shown that 2F modified AONs recruit ILF2/3 proteins upon binding their target RNA. This led to additional steric hindrance, making the target RNA less accessible for splicing factors to bind and resulted in enhanced exon skipping in a model for spinal muscular atrophy (SMA) (92). This is an attractive feature for exon skipping AONs where blocking of the target RNA is essential. In this thesis, 2FPS and isosequential 2OMePS AON counterparts have been compared for DMD. While *in vitro* 2FPS AON resulted in increased exon skipping levels, the modification appeared less effective *in vivo* and was found to be toxic in *mdx* mice (a mouse model for DMD) (this thesis chapter 6).

It is also possible to combine different chemical modifications, making chimeric AONs. Studies from the group of Matsuo have shown increased exon skip levels targeting exon 19, 45 and 46 of the DMD gene, using an chimeric AON consisting of 2OMe RNA and ethylene bridged nucleic acids (ENA) for DMD (2OMe/ENA oligonucleotides)(93,94). In 2015 they showed

improved skipping of exon 45 in primary muscle cells from a patient with a deletion of exon 44 (95). Currently 2OMe/ENA AONs are evaluated in a clinical trial (see next paragraph).

1.3.4 AONs in clinical trials for DMD

AONs are a potential therapeutic approach for DMD and other neuromuscular disorders (e.g. spinal muscular atrophy, myotonic dystrophy). Currently they are evaluated in various pre-clinical and clinical trials. A complete overview of these AONs tested in clinical trials is given in chapter two and recently a nice overview is given by Fletcher *et al* (96). Below you find the most important updates involving clinical trials at this moment.

Recent updates for drisapersen and eteplirsen (DMD)

Drisapersen

Drisapersen (Kyndrisa™), a 2OMePS AON targeting DMD exon 51, has been evaluated in nearly 300 DMD patients via subcutaneous administration and appeared safe. However, mild to moderate side effects have been observed e.g. injection side reaction, proteinuria and thrombocytopenia. In a phase II randomized, double-blind placebo controlled study involving 54 DMD patients (age 6-8), treated patients outperformed placebo treated patients in the 6MWT. Unfortunately in a phase III clinical trial involving 186 DMD patients (age 5-16) no significant difference in the 6MWT has been observed between treated patients and placebo-treated patients. Around the end of this phase III study natural history data came available and showed that it is very difficult to pick up treatment effect in a population with a broad age range. Younger patients respond different to treatment than older patients. By now 8 ambulant patients have been treated for 177 weeks and remained stable in their 6MWT. With new posthoc analyses in age matched groups BioMarin applied for accelerated approval of drisapersen to the Food and Drug Administration (FDA) in April 2015 and with the European Medicines Agency (EMA) in June 2015. On January 14th, 2016, BioMarin announced that the FDA considered the application not to be ready in its current form. On May 31st, 2016, BioMarin announced withdrawal of market authorization application of drisapersen with the EMA, because they anticipated a negative opinion from committee for Medicinal Product for human use. Also they announced to stop all clinical research for drisapersen. Anticipating similar problems for other AONs of the same chemistry, their clinical development was stopped as well. This includes three other first generation AON targeting exon 44, 45 and 53 which were in phase two of clinical development. Nonetheless, BioMarin will continue developing second generation AONs for DMD.

Eteplirsen

Eteplirsen, a PMO targeting DMD exon 51 has been evaluated in clinical trials and appeared safe. However, in some patients proteinuria was found. In the latest clinical trial involving 12 patients, dystrophin restoration has been observed in 30-60% of muscle fibers after 48 weeks of treatment. Moreover 6 patients treated from the onset of the study remained stable in their 6MWT for 120 weeks. Based on this data, Sarepta Therapeutics submitted an application for accelerated approval for eteplirsen, to the FDA on June 26th, 2015. On May 25th, 2016, Sarepta announced that the FDA is not able to complete their evaluation by the prescription drug user fee act goal date of May 26th, 2016, but will continue to complete their work in an as timely manner as possible. On June 6th 2016 Sarepta announced that, on request of the FDA, they will submit dystrophin protein data obtained from muscle biopsies (13 patients) to the ongoing evaluation. September 19th 2016, FDA granted accelerated approval to eteplirsen (EXONDYS 51tm) as treatment for DMD patients who benefit from exon 51 skipping (intravenous administration 30 mg/kg, once a week). However, this is based on the fact that dystrophin protein restoration is observed in a small group of patients (13) with a mean increase of just 0.2 to 0.3% of normal. (<http://jamanetwork.com/journals/jama/fullarticle/2572614>). In the whole study population no clinical benefit has been shown and 38% of the patient treated (compared to placebo) experienced side reactions as vomiting and balance disorders with contusion. Other side reactions were excoriation, arthralgia, rash, catheter site pain and upper respiratory tract infection ($\geq 10\%$ compared to placebo). New, placebo controlled clinical trials need to be conducted to prove if eteplirsen is really working (www.sarepta.com).

Recent updates other AON for DMD

Recently two other clinical trials for DMD have been announced. On February 25th, 2016, Daiichi-Sankyo announced the start of a phase 1-2 clinical trial in Japan (now recruiting) with their DS-5141b drug, an chimeric AON (2OMe/ENA) targeting exon 45 of the DMD gene (<https://clinicaltrials.gov/ct2/show/NCT02667483>). On March 23rd 2016 NS-Pharma announced the start of a phase II, placebo controlled double-blind clinical trial in Japan (not yet recruiting) with NS-065/NCNP-01, a PMO targeting DMD exon 53. (<https://clinicaltrials.gov/ct2/show/NCT02740972>)

*Recent updates for Nusinersen (SMA)**Nusinersen*

On August 1st 2016, Ionis pharmaceuticals and BioGen announced that Nusinersen (Isis-SMN_{rx}, a 2'-O-methoxyethyl phosphorothioate (MOEPS) AON) met the primary endpoint pre-specified for interim analysis of ENDEAR, a broad phase 3 clinical trial for the treatment of infants and

children with spinal muscular atrophy (SMA). On November 7th 2016 they announced that Nusinersen met primary endpoint in a phase 3 clinical trial CHERISH with late-onset patients. Nusinersen is found to have an acceptable safety profile as well and now all participants are able to enrol in the open label extension study (SHINE) where all participants receive Nusinersen. BioGen is currently preparing marketing authorization applications in the USA and Europe.

1.3.5. AON delivery

In general, any drug must reach its target site in order to be effective. Without effective drug delivery the drug has no therapeutic activity and might cause side effects through non intended off target interactions. There are multiple routes of administration to effectively deliver drugs to humans e.g. oral, transdermal, transnasal, subcutaneous, intravenous, intrathecal or local (e.g. intramuscular for muscle diseases). Depending on the drug substance itself and the target tissue, the choice of the optimal route of delivery may vary. For DMD patients the target is skeletal and cardiac muscle tissue. Since the human body consists of 30-40% of muscle it is impossible to treat each muscle individually, a body wide approach is necessary. Oral delivery is most convenient for patients and for many drugs oral bioavailability is sufficient to obtain systemic effect. However the bioavailability of AONs after oral delivery is very poor, and uptake after intestinal administration is limited (97). Based on preclinical animal studies and clinical studies, body wide treatment is feasible using subcutaneous (SC) or intravenous (IV) injections. Today this is the most effective way to deliver AON systemically (98-101).

1.3.5.1 Challenges for AON delivery

Even though systemic administration of AON is feasible, the amount taken up by the target tissue is generally limited. For effective AON delivery, several hurdles need to be overcome (for more details see paragraph 1.3.5.2). In general AONs need to distribute throughout the body without degradation, need to be taken up adequately by the target cells in the target tissue and reach the nucleus where splicing takes place (figure 5). In DMD, patients' muscle fibers have, due to the absence of the dystrophin protein and muscle inflammation, leaky endothelium and therefore more easily take up AON than healthy muscle tissue. Pre-clinical animal studies have shown effective AON delivery. Nevertheless upon body wide treatment a great proportion of AONs end up in liver and or kidney and are lost for uptake by skeletal- and cardiac muscle. Furthermore, less (2OMePS) or minimal (PMO) exon skipping levels in cardiac muscle compared to skeletal muscle are seen (87,102). However, 6 months treatment with high dose of PMO (300 mg/kg and 1.5 g/kg) in *mdx* mice, did result in exon skipping and detectable levels of dystrophin protein in cardiac muscle (103).

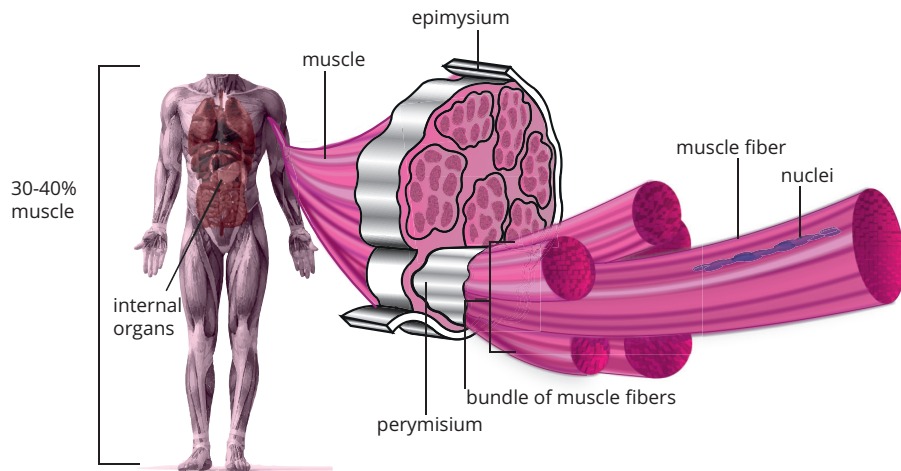


Figure 5. Human body and the location of muscle fiber nuclei. For DMD, the target of AON are muscle fiber nuclei. 30-40% of the human body consist of muscle making systemic treatment necessary. Muscle is built up from muscle fiber bundles surrounded by the epimysium. Each bundle is made from individual muscle fibers and is surrounded by the perimysium, which in turn are made by fusion of individual muscle cells which contain the nuclei.

1.3.5.2 Insight in AON delivery towards muscle

To improve the effective delivery of AON to skeletal and cardiac muscle, insight in the way AON behave *in vivo* is desirable. Upon systemic administration, AON distribute throughout the body via the blood (figure 6). Here, the first biological barrier to overcome is degradation by nucleases. To avoid this, AON are chemically modified making them nuclease resistant (see paragraph 1.3.3). Following SC injections PS modified AON reach peak plasma concentrations within 3-4 hours where after they rapidly decline. The second biological barrier is the endothelium of the blood vessel wall within the tissue. Molecules of 6 nm in diameter or smaller are mainly transported across the endothelium via the paracellular pathway, e.g. via the interendothelial junctions between the cells. Larger molecules, like albumin, are transported via the transcellular pathway, e.g. in vesicles via caveolar-mediated transcytosis. Transport across the endothelium of larger molecules (>100 nm is size) is limited. However, in some tissues like liver, gaps or fenestrations between the cells allow transport of larger molecules (104,105). As AON are small (<6 nm) they readily pass the endothelium of the vessel wall via the paracellular pathway (occurs mostly in kidney and intestinal tract). The uptake of PS modified AON by tissues from blood (but not the central nervous system) takes place within minutes to hours depending on the tissue type. Well perfused organs like liver, kidney and spleen, take up AON more rapidly than less perfused skeletal muscle tissue.

Acute clearance from the body predominantly takes place via the kidneys. However, AON with a PS modification bind serum proteins like albumin and are thereby protected from acute renal clearance (106). When AON have reached the target tissue, they need to overcome a third biological barrier, passing the cell membrane of the target tissue cells. The cell membrane has a dynamic structure, limiting free uptake of large and charged molecules which cannot pass the cell membrane by diffusion. There are various pathways known by which cells can take up larger molecules. In general it is assumed that AON are taken up via some form of endocytosis and are then trapped in cellular compartments like the endosomes. The fourth biological barrier to overcome is the escape from these cellular compartments and reach the nucleus where splicing takes place. It is good to bear in mind that tissues in general are made up of more than one cell type. This means that uptake by a certain tissues not necessarily means uptake by the target cells within that tissue.

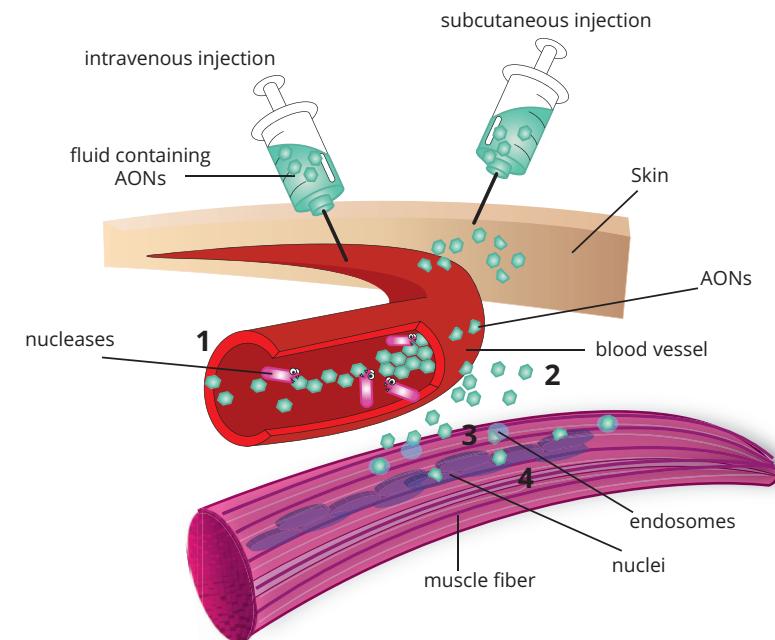


Figure 6. AON delivery, hurdles to overcome. In order to be effective, several hurdles need to be overcome before AONs reach the muscle fiber nuclei. 1) Degradation by nucleases. 2) Escape from endothelium of the blood vessel wall within the tissue. 3) Passing cell membrane of tissue cells. 4) Escape from the endosomes and reach the nucleus.

1.3.5.3 Endocytosis

Endocytosis is the term used for the transport of molecules into cells. Using this pathway cells take up nutrients and communicate with each

other and the environment. There are multiple endocytic pathways known and in general they are classified in two groups: phagocytosis (restricted to specialized cells like macrophages and dendritic cells) and pinocytosis (occurs in all cells)(107). Pinocytosis can be further subdivided in (i) macropinocytosis, (ii) clathrin-dependent endocytosis, (iii) caveolin-dependent endocytosis (iv) clathrin and caveolin independent endocytosis. They differ in coat proteins (when present), vesicle size and intracellular fate (table 1).

Phagocytosis (cell eating), is the process where phagocyte cells take up and clear the body of solids such as parasites, bacteria, death cells, cellular debris etc. It is a commonly known process used by macrophages defending the body against infection, invasion of foreign substances.

Macropinocytosis (cell drinking), shares many features with phagocytosis, but is used by non-phagocytic cells. It is a process of cell membrane ruffling, forming external macropinocytotic vesicles, up to 5 μM in diameter, by which the cell can internalize extracellular fluids containing various molecules (108).

Table 1. Endocytic pathways

Endocytic pathway	Process	Cell type involved
Phagocytosis	Uptake (cell eating) of parasites, bacteria, death cells, cellular debris	Mainly macrophages
Macropinocytosis	Uptake (cell drinking) of extracellular fluids containing molecules	Non-phagocytic cells
Clathrin-dependent endocytosis	Receptor mediated uptake in clathrin coated pits	All cells
Caveolin-dependent endocytosis	Cholesterol dependent uptake in caveolin coated vesicles	Endothelial cells, adipocytes, fibroblast, smooth muscle cells
Clathrin and Caveolin independent	All non-clathrin or caveolin dependent uptake	Various cells

Clathrin-dependent endocytosis, is a process where molecules are taken up by binding a specific receptor in clathrin-coated pits of the cell membrane. After clustering of the ligand-receptor complexes, the clathrin-coated pits invaginate and pinch of the cell membrane forming a clathrin-coated vesicle (100-150 nm in diameter). From these vesicles molecules are further transported through other cellular compartments like early and late endosomes, the golgi apparatus, nucleus and lysosomes. Hereafter

the molecules are released in the cytoplasm or transported back to the cell membrane (107,109,110).

Caveolin-dependent endocytosis is the most commonly reported non clathrin-mediated form of endocytosis. Caveolae are flask-shaped plasma membrane domains formed by the assembly of the caveolin membrane proteins 1, 2 and 3 (60-80 nm in diameter) (111). Caveolae are rich in cholesterol like proteins, and formation of caveolae is cholesterol dependent. Molecules that interact with cholesterol are invaginated and transported from caveolae-coated vesicles directly to other cellular compartment like golgi- or endoplasmic reticulum and often circumvent degradation by lysosomes. Caveolae are especially abundant in endothelial cells, adipocytes, fibroblasts and smooth muscle cells (107,112,113).

Clathrin and Caveolin independent endocytosis is a process that is less understood and basically consists of all uptake that is not clathrin- or caveolin-mediated. Examples are the uptake of molecules depending on DNM2/Dynamin-two, small GTPases or tyrosine kinase for example. What is known is that bacteria and viruses sometimes hijack one of these pathways to enter host cells (114,115).

1.3.6 Strategies taken to improve delivery of AON

Various strategies are being explored to improve the delivery to and uptake by muscle for AON. Examples are, different chemical modifications of the AON, the use of nanoparticles as delivery vehicles or conjugation or co-administration of additive compounds to enhance cell uptake. For delivery of AON to muscle, the ideal delivery system should first of all not interfere with the function of the AON, should have a good safety profile and good biostability. Secondly, the delivery system should be small in size, efficiently taken up by muscle cells and promote endosomal escape. Third, preferably the delivery system is muscle specific thereby limiting or preventing uptake by e.g. liver, kidney and spleen. Finding or developing the perfect delivery system is a major challenge. Throughout the years many approaches have been evaluated. However some are only evaluated after intramuscular administration whereas for DMD systemic administration is the goal.

1.3.6.1 Formulation of AON

To enhance the delivery of 2OMePS AONs, poly(ethylene imine) (PEI) and poly(ethylene glycol) (PEG) copolymers alone, combined with the cell penetrating TAT peptide (GRKKRRQRRPQ), adsorbed colloidal gold (CG) or a combination have been investigated using AONs targeting mouse *Dmd* exon 23 in the *mdx* mouse model. The PEI-PEG copolymer combined with TAT was most potent and resulted, in 6-fold increased dystrophin positive fibers and up to 30% of dystrophin expression compared to wild type levels upon intramuscular administration in tibialis anterior muscle of *mdx* mice (116). However these polyplexes have a cationic charge which

limits their biodistribution due to nonspecific binding to target unrelated components, limiting systemic administration. Later the encapsulation of these polyplexes in biodegradable PLGA nanospheres has been investigated to improve the strategy. Nevertheless, upon intramuscular administration no improvement in dystrophin levels were observed compared to the unencapsulated polyplexes (117). 2OMePS AONs adsorbed onto PMMA/N-isopropyl-acrylamide+ (NIPAM) nanoparticles (ZM2) have been investigated as well. Intraperitoneal administration of these nanoparticles resulted in 20% exon 23 skipping levels and up to 40% dystrophin positive muscle fibers in *mdx* mice (118). Later Bassi *et al.*, showed that this was persistent for over 90 days (119). A next generation of this approach involves ZM4 nanoparticles. Intraperitoneally injected fluorescently labelled ZM4 nanoparticles resulted in detectable fluorescence (analysed with odyssey imaging system) in skeletal muscle and heart. Higher levels of fluorescence were found in liver kidney, spleen and lymph nodes but not in brain (120). Whether ZM4 nanoparticles effectively deliver AON to muscle remains to be evaluated.

1.3.6.2 Co-administration of additive compounds

In addition to formulating AONs, it is also possible to combine AON treatment with compounds that increase exon skipping levels or enhance the uptake of AON. Kendall *et al.*, reported that co-administration of Dantrolene increased exon skipping levels *in vitro* of 2OMePS AONs in cultured cells of *mdx* mice and in reprogrammed myotubes from DMD patients. Systemic administration in *mdx* mice, Dantrolene (intraperitoneal administration) combined with a PMO (intravenous administration), resulted in increased exon 23 skipping levels and dystrophin protein levels in various muscle but not triceps and cardiac muscle (121). However other researchers were not able to reproduce these results in myotube cultures (Aartsma-Rus and van Vliet, personal communication).

Hu *et al.*, showed that PMOs combined with guanine analogues (particularly 6-thioguanine) resulted in improved exon 23 skipping levels (~2-fold) *in vitro* as well as *in vivo* upon intramuscular administration in tibialis anterior muscle of *mdx* mice (122). Verhaart *et al.*, confirmed that 6-thioguanine improved exon skipping levels *in vitro* but, in contradiction, not *in vivo* for 2OMePS and PMO AONs after intramuscular administration in *mdx* mice (123).

Small-sized polyethylenimine (PEI)-conjugated pluronic copolymers (PCMs) have been evaluated to improve the uptake of PMOs. Systemic administration (intravenous) resulted in increased exon 23 skipping levels and on average 15% dystrophin positive muscle fibers (particularly in cardiac muscle tissue) when combining the PMO with PCMs compared to the PMO alone (<5%) in *mdx* mice (124). Nonetheless the overall percentages of exon skipping and dystrophin positive fibers remained low.

1.3.6.3 Conjugation of additive compounds

Cell penetrating peptides (CPPs) are most studied for PMOs. CPPs are short cationic peptides designed to transport drug into cells. They have a long history consisting of a broad range of peptides that have been investigated e.g. Poly-L-lysine, Hiv-1 TAT protein, penetratin and the arginine rich peptides used today (125-128). Moulton *et al.*, was one of the first to describe the use of arginine rich peptides to enhance the delivery and uptake of PMOs in muscle for DMD (so called PPMOs)(128). However these arginine rich peptides resulted in acute toxicity in monkeys (129). Throughout the years various improvements have been made regarding arginine rich CPPs; RXR₄, B-peptide (RXRRBR)₂ and the more recently developed Pip peptides (130-134). The most potent Pip peptides come from the Pip5 and Pip6 series. Conjugates resulted *in vivo*, upon systemic administration, in high levels of exon 23 skipping and dystrophin protein production in skeletal and cardiac muscle. Further evaluation of these conjugates showed improvement of muscle strength and cardiac function in exercised *mdx* mice (131,135). Lehto *et al.*, studied the mechanism by which CPP Pip6a-PMO is taken up. Results showed an energy dependent uptake via caveolin-dependent endocytosis in skeletal muscle with nuclear localization in myotubes but not in myoblast cell cultures (cytoplasm). For cardiac muscle tissue clathrin-dependent endocytosis was found to be the most prominent uptake pathway. However, here Pip6a-PMO was mainly found in the cytoplasm and to a less extent in the nucleus where splicing takes place (133). The newly developed CPPs appear to be well tolerated in *mdx* mice. Nevertheless they contain many arginine residues making it questionable if they are not toxic in higher animals than mice as shown in the early studies of Moulton *et al.*

Despite the fact that the well-studied CPPs have the potential to improve delivery of PMOs, they are not suitable for delivery of 2OMePS. The cationic nature of CPPs have the tendency to strongly form aggregates when combined with the anionic 2OMePS AON backbone. A different approach is needed: e.g. the use of tissue specific homing peptides selected from phage display experiments (see paragraph 1.5).

1.4 Phage display

1.4.1. Phage display

Phage display is a well described, powerful technique to identify peptides, antibodies or other proteins with target specific binding properties from phage libraries. Phage display technology was first introduced by Smith in 1985 (136,137) who later introduced the concept of affinity selection using phage display peptide or antibody libraries. From here the technology has spread rapidly (136,138-140). Nowadays phage display technology has been modified and is used in for example, vaccine development (vaccines consisting of phages that display a disease specific antigen), studying protein-protein interactions (different domains of a protein is displayed on a phage and panned against a specific protein), identification of substrates or inhibitors (analyses of enzyme activity and specificity or identification of enzyme inhibitors) and epitope mapping using antibody libraries (141-143). Phages (or so called bacteriophages), are viruses that consist of DNA or RNA within a protein coat. A phage library is constructed by fusing a foreign peptide or protein with one of the protein coat genes in such a way that these are expressed on the surface of the phage. Phage libraries consist of millions or billions of uniquely constructed phages from which affinity selection takes place, a process called bio-panning. Nowadays the identity of the peptides or proteins of interest can be easily detected using various high throughput sequencing approaches.

1.4.2 Biopanning

Biopanning selections using phage libraries can be undertaken for various targets like specific molecules (e.g. proteins, enzymes, receptors), cultured cells *in vitro* or tissues, or cells within a tissue *in vivo*. The basic principles are the same for all targets. First, the phage library is exposed to the target for binding. Secondly, all non-binders are removed. Third, binding phages are recovered by elution. Fourth, binding phages are amplified and prepared for a next bio-panning round. Fifth, after several rounds of biopanning, binding phages are identified by for example sequencing of candidate phage DNA (figure 7).

1.4.3 Phage display vectors

Different phages have been used for the development of phage display vectors. The M13 filamentous phage is the most used worldwide, the T4, T7 and lambda phages are also often used. Each phage display vector has its own benefits and limitations (table 2).

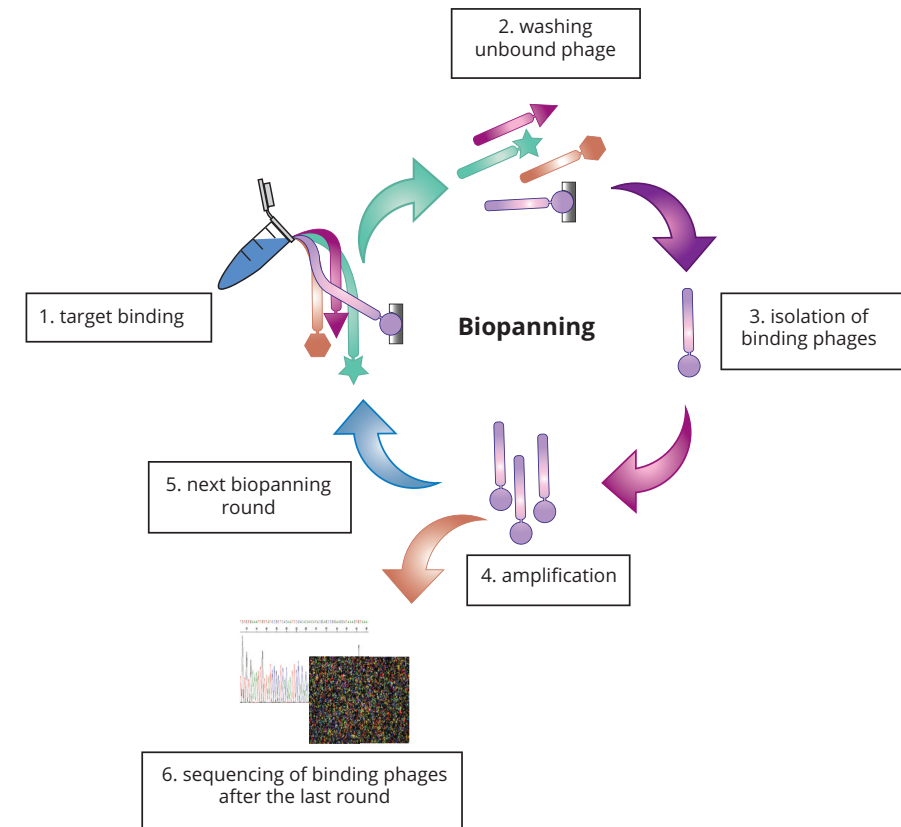


Figure 7. Phage display biopanning. Phage display biopanning is a selection technique to identify high affinity binders for a selected target. Step one, exposing the phage library to the target. Step two, wash away unbound phage. Step 3, isolation of binding phages. Step 4, amplification of isolated phages. Step 5, preparing the amplified isolated phages for another screening round. Step 6, identification of binding phages by sequencing.

M13 filamentous phage display vectors consist of rod shaped linear filamentous phage particles containing single-stranded looped DNA (6.4kb). They can only infect *E-coli* bacteria which express the F-pilus. After infection the F-pilus is depolymerized, preventing multiple phage infections. The advantage of this unique characteristic is that each bacterial clone represents a specific phage with a unique foreign peptide or protein (144). Upon infection, phages are assembled in the periplasmic environment and, after replication, leave the bacterial host via the membrane without killing its host. Another unique characteristic of this phage is the resistance against extreme conditions such as acidic pH, high temperature and enzymatic cleavage, making the phages very convenient to use *in vitro* as well as *in vivo* (144,145). The M13 phage consists of a major PVIII coat protein (2.700

copies) and the minor PIII and PVII coat proteins on one end and PVII, PIX coat proteins on the other end (3-5 copies). In most cases the phages are constructed to express foreign peptides or proteins on the minor PIII (used to infect cells) or major PVIII coat protein, but all 5 coat proteins have been used (136,146). Fusion to the PIII protein can be used for peptides or proteins taking up to 100kb in insertion size. Fusion to the PVIII protein is limited to 6-8 amino acids in length because of the large copy numbers expressed on the phage.

The T4 phage display system has relatively large phages containing double stranded linear DNA (160 kb) packed in a capsid head, which is attached to a contractible tail and tail fibers. Phages infect *E-coli* bacteria upon binding the host with their tail fibers and injecting the phage DNA via their contractible tail directly in the cytoplasm. The phage DNA will be replicated, new phage particles will form and eventually leave the host by cell lysis. The T4 capsid head consist of 3 essential proteins, gp23, gp24 and gp20, and 2 non-essential proteins Hoc (highly antigenic outer capsid protein) and Soc (small outer capsid protein). The Hoc and Soc proteins are used most frequently to express a foreign peptide or protein on the surface. The advantage of using T4 phages over M13 phages is the possibility of fusions with complicated, high molecular weight proteins on the phages surface. T4 phages are most used in vaccine technology by fusion of pathogen antigens to the N- or C-terminus of Hoc and Soc (147,148).

The T7 phage display system is similar to the T4. It consists of a capsid head, a tail, tail fibers and has dsDNA (39kb). T7 differs from the T4 in that the capsid head consists mainly of various combinations of gp10 proteins, and that the tail is not contractible (upon infection the phage builds a protein channel towards the bacterial cytoplasm)(149,150). Foreign proteins can be expressed by fusion with the C-terminus of gp10 protein in high copy numbers for small peptides, or with low or intermediate copy numbers for larger peptides or proteins. The main advantage of T7 phages is their short lytic life cycle, which significantly shortens the screening process. Another advantage is their extreme resistance to various environmental conditions.

Lambda page display vectors contain double stranded linear DNA (48 kb), which is similar to the T4 and T7 phage display systems capsids in a head, and contains tail and tail filaments. The capsids head consists of 2 major coat proteins, pgE and gpD and the major tail protein is gpV. A unique feature of the lambda genome is the 12 nucleotides long GC-rich cos sites (sticky ends) at both 5'ends, which upon infection are used by the host DNA ligase to make the DNA circular (151). Lambda phages can either be lytic or lysogenic (when integrated in the host genome) and are used to express complicated high molecular weight proteins fused to the D head protein (high copy number) or pV tail protein (low copy number).

Table 2. Phage display vectors

Phage vector	Genome size	Size foreign insert	Advantage	Lytic or Lysogenic
M13	6.4kb	Up to 100kb on PIII (3-5 copies) 3-8 amino acids (2.700 copies) on PVIII coat protein	F-Pilus is depolymerized up on infection preventing multiple phage infection	Lysogenic
T4	160kb	High molecular weight proteins to Hoc or Soc coat proteins	Fusion of complicated high molecular weight proteins	Lytic
T7	39kb	Low molecular weight in high copy number. Intermediate to high molecular weight in low copy number to gp10 protein	Short life cycle significantly shortens the screening process	Lytic
lambda	48kb	Complicated high molecular weight to D head protein (high copy number) or pV tail protein (low copy number)	Expression of high molecular weight proteins in high copy number	Lytic and Lysogenic

1.5 Using phage display peptide library screens to improve delivery of AON towards skeletal and cardiac muscle tissue

The advantage of using tissue specific homing peptides over CCPs is that short peptides in general have a better safety profile, do not or minimally provoke an immune reaction and their tissue specificity limits off target effects. The use of tissue specific homing peptides is applicable to 2OMePS and PMO AONs, as well as for other drugs. Various random combinatorial phage display peptide libraries are commercially available ranging from 6 amino acids in length (6-mer) up to 24 amino acids in length (24-mer) in general. Random 7-mer, 9-mer and 12-mer peptide libraries are studied most. These peptides are expressed on the phage coat protein either in linear or circular conformation (e.g. the substitution of cysteines at either end of the random peptide sequence, joint by a disulfide bond, makes the peptide have a circular conformation), and in high or low copy numbers. Using phage display peptide libraries to search for tissue specific homing peptides is not without challenges: Phage display peptide libraries are

known to be prone to parasite sequences i.e. phages with a growth advantage or phages binding plastic or other experimental related but not target related compounds (152). Peptides as therapeutics by themselves have limitations as well. Peptides are known to be aggregation prone, have solubility issues and a pore bioavailability. Nonetheless when peptides are conjugated to an AON most of these issues can be overcome.

In the last couple of years, technology used to analyze phage display outcomes rapidly improved. Various high throughput platforms were integrated in the analyses, resulting in new insights and improved biopanning selections (153,154). This thesis is focused on 7-mer phage display peptide libraries (Ph.D.-7). We integrated for the first time Illumina next generation sequencing (NGS) to analyze phage display biopanning selections (this thesis chapter 4). We showed that high throughput sequencing of the naïve library after one round of bacterial amplification is a powerful tool to identify parasite sequences with a growth advantage. We also showed that by using NGS a single biopanning round is enough to identify candidate peptides. A few months later, a comparable story was published by Matochko *et al.*, (155)

Back in 1999 Samoylova *et al.*, described a phage, expressing a 7-mer peptide ASSLNIA, showing increased uptake (judged on fluorescent intensity) in murine tissues compared to control phages. Later studies showed that the peptide alone was unable to increase delivery or exon skipping levels in *mdx* mice, when conjugated to a PMO (Samoylova and Smith, 1999; Yin *et al.*, 2009). Seow *et al.*, identified after several rounds of *in vivo* biopanning towards heart and quadriceps muscle, peptide T9 (12-mer: SKTFNTHPQSTP). Despite that this peptide appeared to preferentially bind skeletal muscle, they observed limited internalization of muscle cells. In this thesis the first muscle homing peptide for 2OMePS AON is described, peptide P4 (7-mer: LGAQSNF) identified after *in vivo* biopanning towards heart and quadriceps muscle (this thesis chapter 3). P4 conjugated 2OMePS AONs significantly increased exon skipping levels in diaphragm and cardiac muscle tissue, compared to unconjugated AONs, after subcutaneous administration in *mdx* mice.

In search for better muscle specific homing peptides to enhance the delivery of PMOs, Gao *et al.*, identified the M12 peptide RRQPPRSISSHP (Gao *et al.*, 2014), which resulted in improved but variable exon skipping levels in skeletal muscle but not cardiac muscle when conjugated to a PMO. Searching for better muscle specific homing peptides to enhance the delivery 2OMePS AON, a phage display peptide library expressing cyclic 7-mer peptides combined with NGS analyses has been investigated (this thesis chapter 5). The lead peptide CyPep10 (CQLFPLFRC), resulted upon conjugation to 2OMePS AONs, in a significant 2-fold increase in exon skipping levels in all muscle tissues analyzed. All together these results

demonstrate the value of tissue specific homing peptides for the delivery of AON.

Outline of this thesis

The work described in this thesis aimed to optimize delivery of AON towards skeletal and cardiac muscle for DMD. In Chapter 2 an update on RNA-targeting therapies using AON for neuromuscular disorders is given. With emerging new possibilities there is a growing need for improved delivery of AON towards muscle. Conjugation of muscle specific homing peptides is a strategy to accomplish this. In Chapter 3 the first muscle homing peptide for 2OMePS AON is described. This peptide has been identified from a phage display peptide library. Phage display peptide libraries are prone to parasite sequences that dominate the selection. In chapter 4 it is described how NGS improves phage display selections by increased sequencing depth and identification of parasite sequences with a growth advantage. Chapter 5 describes how these improvements have been integrated in new phage display selection experiments towards muscle, which led to the identification of a more potent peptide candidate. In Chapter 6, 2FPS AON have been evaluated as exon skipping AON for DMD. A general discussion where results are put in a broader context is given in chapter 7.

References

1. Moat, S.J., Bradley, D.M., Salmon, R., Clarke, A. and Hartley, L. (2013) Newborn bloodspot screening for Duchenne muscular dystrophy: 21 years experience in Wales (UK). *Eur.J.Hum.Genet.*
2. Mah, J.K., Korngut, L., Dykeman, J., Day, L., Pringsheim, T. and Jette, N. (2014) A systematic review and meta-analysis on the epidemiology of Duchenne and Becker muscular dystrophy. *Neuromuscular disorders : NMD*, **24**, 482-491.
3. Blake, D.J., Weir, A., Newey, S.E. and Davies, K.E. (2002) Function and genetics of dystrophin and dystrophin-related proteins in muscle. *Physiol Rev.*, **82**, 291-329.
4. Muntoni, F., Torelli, S. and Ferlini, A. (2003) Dystrophin and mutations: one gene, several proteins, multiple phenotypes. *The Lancet. Neurology*, **2**, 731-740.
5. Emery, A.E. (2002) The muscular dystrophies. *Lancet*, **359**, 687-695.
6. Pane, M., Scalise, R., Berardinelli, A., D'Angelo, G., Ricotti, V., Alfieri, P., Moroni, I., Hartley, L., Pera, M.C., Baranello, G. *et al.* (2013) Early neurodevelopmental assessment in Duchenne muscular dystrophy. *Neuromuscular disorders : NMD*, **23**, 451-455.
7. Faysoil, A., Nardi, O., Orlikowski, D. and Annane, D. (2010) Cardiomyopathy in Duchenne muscular dystrophy: pathogenesis and therapeutics. *Heart Fail.Rev.*, **15**, 103-107.
8. LoMauro, A., D'Angelo, M.G. and Aliverti, A. (2015) Assessment and management of respiratory function in patients with Duchenne muscular dystrophy: current and emerging options. *Ther.Clin.Risk Manag.*, **11**, 1475-1488.
9. Taglia, A., Petillo, R., D'Ambrosio, P., Picillo, E., Torella, A., Orsini, C., Ergoli, M., Scutifero, M., Passamano, L., Palladino, A. *et al.* (2015) Clinical features of patients with dystrophinopathy sharing the 45-55 exon deletion of DMD gene. *Acta myologica : myopathies and cardiomyopathies : official journal of the Mediterranean Society of Myology*, **34**, 9-13.
10. Roberts, R.G., Coffey, A.J., Bobrow, M. and Bentley, D.R. (1993) Exon structure of the human dystrophin gene. *Genomics*, **16**, 536-538.
11. Koenig, M., Hoffman, E.P., Bertelson, C.J., Monaco, A.P., Feener, C. and Kunkel, L.M. (1987) Complete cloning of the Duchenne muscular dystrophy (DMD) cDNA and preliminary genomic organization of the DMD gene in normal and affected individuals. *Cell*, **50**, 509-517.
12. den Dunnen, J.T., Grootsholten, P.M., Bakker, E., Blonden, L.A., Ginjaar, H.B., Wapenaar, M.C., van Paassen, H.M., van, B.C., Pearson, P.L. and van Ommen, G.J. (1989) Topography of the Duchenne muscular dystrophy (DMD) gene: FIGE and cDNA analysis of 194 cases reveals 115 deletions and 13 duplications. *Am.J.Hum.Genet.*, **45**, 835-847.
13. Aartsma-Rus, A., Ginjaar, I.B. and Bushby, K. (2016) The importance of genetic diagnosis for Duchenne muscular dystrophy. *Journal of medical genetics*, **53**, 145-151.
14. Koenig, M. and Kunkel, L.M. (1990) Detailed analysis of the repeat domain of dystrophin reveals four potential hinge segments that may confer flexibility. *J.Biol.Chem.*, **265**, 4560-4566.
15. Aartsma-Rus, A. (2014) Dystrophin analysis in clinical trials. *JND*, **1**, 41-53.
16. Amann, K.J., Renley, B.A. and Ervasti, J.M. (1998) A cluster of basic repeats in the dystrophin rod domain binds F-actin through an electrostatic interaction. *J.Biol.Chem.*, **273**, 28419-28423.
17. Lai, Y., Thomas, G.D., Yue, Y., Yang, H.T., Li, D., Long, C., Judge, L., Bostick, B., Chamberlain, J.S., Terjung, R.L. *et al.* (2009) Dystrophins carrying spectrin-like repeats 16 and 17 anchor nNOS to the sarcolemma and enhance exercise performance in a mouse model of muscular dystrophy. *J.Clin.Invest*, **119**, 624-635.
18. Monaco, A.P. (1989) Dystrophin, the protein product of the Duchenne/Becker muscular dystrophy gene. *Trends Biochem.Sci.*, **14**, 412-415.
19. Bushby, K., Finkel, R., Birnkrant, D.J., Case, L.E., Clemens, P.R., Cripe, L., Kaul, A., Kinnett, K., McDonald, C., Pandya, S. *et al.* (2010) Diagnosis and management of Duchenne muscular dystrophy, part 1: diagnosis, and pharmacological and psychosocial management. *The Lancet. Neurology*, **9**, 77-93.
20. Bushby, K., Finkel, R., Birnkrant, D.J., Case, L.E., Clemens, P.R., Cripe, L., Kaul, A., Kinnett, K., McDonald, C., Pandya, S. *et al.* (2010) Diagnosis and management of Duchenne muscular dystrophy, part 2: implementation of multidisciplinary care. *The Lancet. Neurology*, **9**, 177-189.
21. Angelini, C. and Peterle, E. (2012) Old and new therapeutic developments in steroid treatment in Duchenne muscular dystrophy.

- Acta Myol.*, **31**, 9-15.
22. Manzur, A.Y. and Muntoni, F. (2009) Diagnosis and new treatments in muscular dystrophies. *Journal of neurology, neurosurgery, and psychiatry*, **80**, 706-714.
 23. Ricotti, V., Ridout, D.A. and Muntoni, F. (2013) Steroids in Duchenne muscular dystrophy. *Neuromuscular disorders : NMD*, **23**, 696-697.
 24. Peault, B., Rudnicki, M., Torrente, Y., Cossu, G., Tremblay, J.P., Partridge, T., Gussoni, E., Kunkel, L.M. and Huard, J. (2007) Stem and progenitor cells in skeletal muscle development, maintenance, and therapy. *Molecular therapy : the journal of the American Society of Gene Therapy*, **15**, 867-877.
 25. Collins, C.A., Olsen, I., Zammit, P.S., Heslop, L., Petrie, A., Partridge, T.A. and Morgan, J.E. (2005) Stem cell function, self-renewal, and behavioral heterogeneity of cells from the adult muscle satellite cell niche. *Cell*, **122**, 289-301.
 26. Collins, C.A. and Partridge, T.A. (2005) Self-renewal of the adult skeletal muscle satellite cell. *Cell cycle (Georgetown, Tex.)*, **4**, 1338-1341.
 27. Huard, J., Roy, R., Bouchard, J.P., Malouin, F., Richards, C.L. and Tremblay, J.P. (1992) Human myoblast transplantation between immunohistocompatible donors and recipients produces immune reactions. *Transplantation proceedings*, **24**, 3049-3051.
 28. Tremblay, J.P., Malouin, F., Roy, R., Huard, J., Bouchard, J.P., Satoh, A. and Richards, C.L. (1993) Results of a triple blind clinical study of myoblast transplantations without immunosuppressive treatment in young boys with Duchenne muscular dystrophy. *Cell transplantation*, **2**, 99-112.
 29. Morandi, L., Bernasconi, P., Gebbia, M., Mora, M., Crosti, F., Mantegazza, R. and Cornelio, F. (1995) Lack of mRNA and dystrophin expression in DMD patients three months after myoblast transfer. *Neuromuscular disorders : NMD*, **5**, 291-295.
 30. Mendell, J.R., Kissel, J.T., Amato, A.A., King, W., Signore, L., Prior, T.W., Sahenk, Z., Benson, S., McAndrew, P.E., Rice, R. *et al.* (1995) Myoblast transfer in the treatment of Duchenne's muscular dystrophy. *The New England journal of medicine*, **333**, 832-838.
 31. Noviello, M., Tedesco, F.S., Bondanza, A., Tonlorenzi, R., Rosaria Carbone, M., Gerli, M.F., Markt, S., Napolitano, S., Cicalese, M.P., Ciceri, F. *et al.* (2014) Inflammation converts human mesoangioblasts into targets of alloreactive immune responses: implications for allogeneic cell therapy of DMD. *Molecular therapy : the journal of the American Society of Gene Therapy*, **22**, 1342-1352.
 32. Bonfanti, C., Rossi, G., Tedesco, F.S., Giannotta, M., Benedetti, S., Tonlorenzi, R., Antonini, S., Marazzi, G., Dejana, E., Sassoon, D. *et al.* (2015) PW1/Peg3 expression regulates key properties that determine mesoangioblast stem cell competence. *Nature communications*, **6**, 6364.
 33. Cossu, G., Previtali, S.C., Napolitano, S., Cicalese, M.P., Tedesco, F.S., Nicastro, F., Noviello, M., Roostalu, U., Natali Sora, M.G., Scarlato, M. *et al.* (2015) Intra-arterial transplantation of HLA-matched donor mesoangioblasts in Duchenne muscular dystrophy. *EMBO molecular medicine*, **7**, 1513-1528.
 34. Hardiman, O., Sklar, R.M. and Brown, R.H., Jr. (1993) Direct effects of cyclosporin A and cyclophosphamide on differentiation of normal human myoblasts in culture. *Neurology*, **43**, 1432-1434.
 35. Hoshiya, H., Kazuki, Y., Abe, S., Takiguchi, M., Kajitani, N., Watanabe, Y., Yoshino, T., Shirayoshi, Y., Higaki, K., Messina, G. *et al.* (2009) A highly stable and nonintegrated human artificial chromosome (HAC) containing the 2.4 Mb entire human dystrophin gene. *Molecular therapy : the journal of the American Society of Gene Therapy*, **17**, 309-317.
 36. Kazuki, Y., Hiratsuka, M., Takiguchi, M., Osaki, M., Kajitani, N., Hoshiya, H., Hiramatsu, K., Yoshino, T., Kazuki, K., Ishihara, C. *et al.* (2010) Complete genetic correction of ips cells from Duchenne muscular dystrophy. *Molecular therapy : the journal of the American Society of Gene Therapy*, **18**, 386-393.
 37. Torrente, Y., Belicchi, M., Marchesi, C., D'Antona, G., Cogiamanian, F., Pisati, F., Gavina, M., Giordano, R., Tonlorenzi, R., Fagiolari, G. *et al.* (2007) Autologous transplantation of muscle-derived CD133+ stem cells in Duchenne muscle patients. *Cell transplantation*, **16**, 563-577.
 38. Ousterout, D.G., Kabadi, A.M., Thakore, P.I., Majoros, W.H., Reddy, T.E. and Gersbach, C.A. (2015) Multiplex CRISPR/Cas9-based genome editing for correction of dystrophin mutations that cause Duchenne muscular dystrophy. *Nature communications*, **6**, 6244.
 39. Li, H.L., Fujimoto, N., Sasakawa, N., Shirai, S., Ohkame, T., Sakuma, T., Tanaka, M., Amano, N., Watanabe, A., Sakurai, H. *et al.* (2015) Precise correction of the dystrophin gene in duchenne muscular dystrophy patient induced pluripotent stem cells by TALEN and CRISPR-Cas9.

- Stem cell reports*, **4**, 143-154.
40. Young, C.S., Hicks, M.R., Ermolova, N.V., Nakano, H., Jan, M., Younesi, S., Karumbayaram, S., Kumagai-Cresse, C., Wang, D., Zack, J.A. *et al.* (2016) A Single CRISPR-Cas9 Deletion Strategy that Targets the Majority of DMD Patients Restores Dystrophin Function in hiPSC-Derived Muscle Cells. *Cell Stem Cell*.
 41. Meng, J., Counsell, J.R., Reza, M., Laval, S.H., Danos, O., Thrasher, A., Lochmuller, H., Muntoni, F. and Morgan, J.E. (2016) Autologous skeletal muscle derived cells expressing a novel functional dystrophin provide a potential therapy for Duchenne Muscular Dystrophy. *Sci. Rep.*, **6**, 19750.
 42. Fu, Y., Foden, J.A., Khayter, C., Maeder, M.L., Reyon, D., Joung, J.K. and Sander, J.D. (2013) High-frequency off-target mutagenesis induced by CRISPR-Cas nucleases in human cells. *Nature biotechnology*, **31**, 822-826.
 43. Hsu, P.D., Scott, D.A., Weinstein, J.A., Ran, F.A., Konermann, S., Agarwala, V., Li, Y., Fine, E.J., Wu, X., Shalem, O. *et al.* (2013) DNA targeting specificity of RNA-guided Cas9 nucleases. *Nature biotechnology*, **31**, 827-832.
 44. Ran, F.A., Hsu, P.D., Lin, C.Y., Gootenberg, J.S., Konermann, S., Trevino, A.E., Scott, D.A., Inoue, A., Matoba, S., Zhang, Y. *et al.* (2013) Double nicking by RNA-guided CRISPR Cas9 for enhanced genome editing specificity. *Cell*, **154**, 1380-1389.
 45. Pattanayak, V., Lin, S., Guilinger, J.P., Ma, E., Doudna, J.A. and Liu, D.R. (2013) High-throughput profiling of off-target DNA cleavage reveals RNA-programmed Cas9 nuclease specificity. *Nature biotechnology*, **31**, 839-843.
 46. Zhang, Y., Yue, Y., Li, L., Hakim, C.H., Zhang, K., Thomas, G.D. and Duan, D. (2013) Dual AAV therapy ameliorates exercise-induced muscle injury and functional ischemia in murine models of Duchenne muscular dystrophy. *Hum.Mol.Genet.*, **22**, 3720-3729.
 47. Lostal, W., Kodippili, K., Yue, Y. and Duan, D. (2014) Full-length dystrophin reconstitution with adeno-associated viral vectors. *Hum. Gene Ther.*, **25**, 552-562.
 48. Seto, J.T., Ramos, J.N., Muir, L., Chamberlain, J.S. and Odom, G.L. (2012) Gene replacement therapies for duchenne muscular dystrophy using adeno-associated viral vectors. *Curr.Gene Ther.*, **12**, 139-151.
 49. Hakim, C.H. and Duan, D. (2013) Truncated dystrophins reduce muscle stiffness in the extensor digitorum longus muscle of mdx mice. *J.Appl.Physiol* (1985.), **114**, 482-489.
 50. Harper, S.Q., Hauser, M.A., DelloRusso, C., Duan, D., Crawford, R.W., Phelps, S.F., Harper, H.A., Robinson, A.S., Engelhardt, J.F., Brooks, S.V. *et al.* (2002) Modular flexibility of dystrophin: implications for gene therapy of Duchenne muscular dystrophy. *Nat.Med.*, **8**, 253-261.
 51. Yue, Y., Pan, X., Hakim, C.H., Kodippili, K., Zhang, K., Shin, J.H., Yang, H.T., McDonald, T. and Duan, D. (2015) Safe and bodywide muscle transduction in young adult Duchenne muscular dystrophy dogs with adeno-associated virus. *Hum.Mol.Genet.*, **24**, 5880-5890.
 52. Gregorevic, P., Blankinship, M.J., Allen, J.M., Crawford, R.W., Meuse, L., Miller, D.G., Russell, D.W. and Chamberlain, J.S. (2004) Systemic delivery of genes to striated muscles using adeno-associated viral vectors. *Nature medicine*, **10**, 828-834.
 53. Nelson, C.E., Hakim, C.H., Ousterout, D.G., Thakore, P.I., Moreb, E.A., Castellanos Rivera, R.M., Madhavan, S., Pan, X., Ran, F.A., Yan, W.X. *et al.* (2016) In vivo genome editing improves muscle function in a mouse model of Duchenne muscular dystrophy. *Science*, **351**, 403-407.
 54. Tabebordbar, M., Zhu, K., Cheng, J.K., Chew, W.L., Widrick, J.J., Yan, W.X., Maesner, C., Wu, E.Y., Xiao, R., Ran, F.A. *et al.* (2016) In vivo gene editing in dystrophic mouse muscle and muscle stem cells. *Science*, **351**, 407-411.
 55. Long, C., Amoasii, L., Mireault, A.A., McAnally, J.R., Li, H., Sanchez-Ortiz, E., Bhattacharyya, S., Shelton, J.M., Bassel-Duby, R. and Olson, E.N. (2016) Postnatal genome editing partially restores dystrophin expression in a mouse model of muscular dystrophy. *Science*, **351**, 400-403.
 56. Chicoine, L.G., Montgomery, C.L., Bremer, W.G., Shontz, K.M., Griffin, D.A., Heller, K.N., Lewis, S., Malik, V., Grose, W.E., Shilling, C.J. *et al.* (2014) Plasmapheresis eliminates the negative impact of AAV antibodies on microdystrophin gene expression following vascular delivery. *Molecular therapy : the journal of the American Society of Gene Therapy*, **22**, 338-347.
 57. Mendell, J.R., Campbell, K., Rodino-Klapac, L., Sahenk, Z., Shilling, C., Lewis, S., Bowles, D., Gray, S., Li, C., Galloway, G. *et al.* (2010) Dystrophin immunity in Duchenne's muscular dystrophy. *The New England journal of medicine*, **363**, 1429-1437.

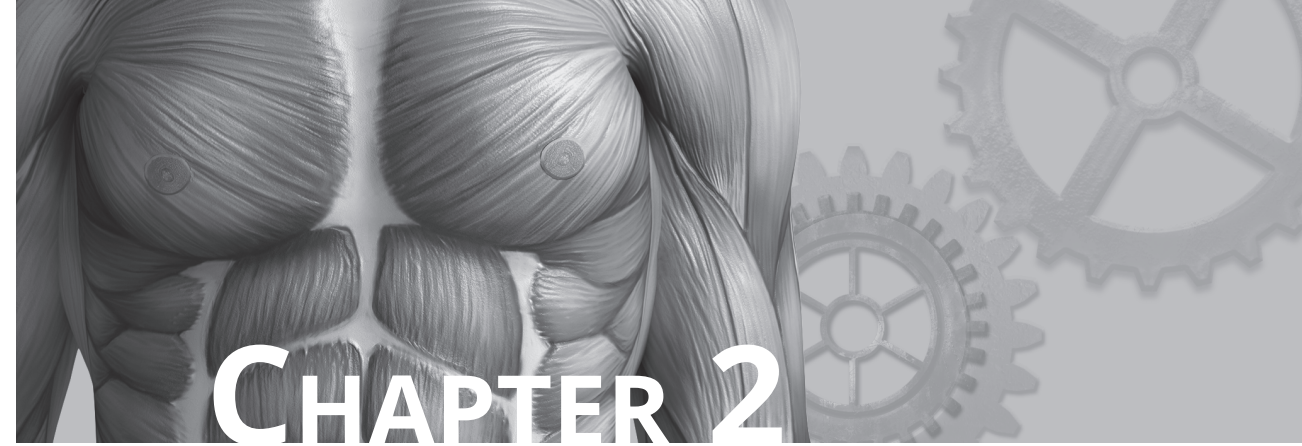
58. Mays, L.E. and Wilson, J.M. (2011) The complex and evolving story of T cell activation to AAV vector-encoded transgene products. *Molecular therapy : the journal of the American Society of Gene Therapy*, **19**, 16-27.
59. Maggio, I., Chen, X. and Goncalves, M.A. (2016) The emerging role of viral vectors as vehicles for DMD gene editing. *Genome medicine*, **8**, 59.
60. Aartsma-Rus, A., Fokkema, I., Verschuuren, J., Ginjaar, I., van Deutekom, J., van Ommen, G.J. and den Dunnen, J.T. (2009) Theoretic applicability of antisense-mediated exon skipping for Duchenne muscular dystrophy mutations. *Human mutation*, **30**, 293-299.
61. Welch, E.M., Barton, E.R., Zhuo, J., Tomizawa, Y., Friesen, W.J., Trifillis, P., Paushkin, S., Patel, M., Trotta, C.R., Hwang, S. *et al.* (2007) PTC124 targets genetic disorders caused by nonsense mutations. *Nature*, **447**, 87-91.
62. Hirawat, S., Welch, E.M., Elfring, G.L., Northcutt, V.J., Paushkin, S., Hwang, S., Leonard, E.M., Almstead, N.G., Ju, W., Peltz, S.W. *et al.* (2007) Safety, tolerability, and pharmacokinetics of PTC124, a nonaminoglycoside nonsense mutation suppressor, following single- and multiple-dose administration to healthy male and female adult volunteers. *Journal of clinical pharmacology*, **47**, 430-444.
63. Finkel, R.S., Flanigan, K.M., Wong, B., Bonnemann, C., Sampson, J., Sweeney, H.L., Reha, A., Northcutt, V.J., Elfring, G., Barth, J. *et al.* (2013) Phase 2a study of ataluren-mediated dystrophin production in patients with nonsense mutation Duchenne muscular dystrophy. *PLoS one*, **8**, e81302.
64. Bushby, K., Finkel, R., Wong, B., Barohn, R., Campbell, C., Comi, G.P., Connolly, A.M., Day, J.W., Flanigan, K.M., Goemans, N. *et al.* (2014) Ataluren treatment of patients with nonsense mutation dystrophinopathy. *Muscle Nerve*, **50**, 477-487.
65. Hoffman, E.P. and Connor, E.M. (2013) Orphan drug development in muscular dystrophy: update on two large clinical trials of dystrophin rescue therapies. *Discovery medicine*, **16**, 233-239.
66. Haas, M., Vlcek, V., Balabanov, P., Salmonson, T., Bakchine, S., Markey, G., Weise, M., Schlosser-Weber, G., Brohmann, H., Yerro, C.P. *et al.* (2015) European Medicines Agency review of ataluren for the treatment of ambulant patients aged 5 years and older with Duchenne muscular dystrophy resulting from a nonsense mutation in the dystrophin gene. *Neuromuscular disorders : NMD*, **25**, 5-13.
67. Monaco, A.P., Bertelson, C.J., Liechti-Gallati, S., Moser, H. and Kunkel, L.M. (1988) An explanation for the phenotypic differences between patients bearing partial deletions of the DMD locus. *Genomics*, **2**, 90-95.
68. Aartsma-Rus, A., de Winter, C.L., Janson, A.A., Kaman, W.E., van Ommen, G.J., den Dunnen, J.T. and van Deutekom, J.C. (2005) Functional analysis of 114 exon-internal AONs for targeted DMD exon skipping: indication for steric hindrance of SR protein binding sites. *Oligonucleotides*, **15**, 284-297.
69. Aartsma-Rus, A., van, V.L., Hirschi, M., Janson, A.A., Heemskerk, H., de Winter, C.L., de, K.S., van Deutekom, J.C., 't Hoen, P.A. and van Ommen, G.J. (2009) Guidelines for antisense oligonucleotide design and insight into splice-modulating mechanisms. *Mol. Ther.*, **17**, 548-553.
70. Pramono, Z.A., Takeshima, Y., Alimsardjono, H., Ishii, A., Takeda, S. and Matsuo, M. (1996) Induction of exon skipping of the dystrophin transcript in lymphoblastoid cells by transfecting an antisense oligodeoxynucleotide complementary to an exon recognition sequence. *Biochemical and biophysical research communications*, **226**, 445-449.
71. Dunckley, M.G., Manoharan, M., Villiet, P., Eperon, I.C. and Dickson, G. (1998) Modification of splicing in the dystrophin gene in cultured Mdx muscle cells by antisense oligoribonucleotides. *Human molecular genetics*, **7**, 1083-1090.
72. Wilton, S.D., Lloyd, F., Carville, K., Fletcher, S., Honeyman, K., Agrawal, S. and Kole, R. (1999) Specific removal of the nonsense mutation from the mdx dystrophin mRNA using antisense oligonucleotides. *Neuromuscul. Disord.*, **9**, 330-338.
73. Mann, C.J., Honeyman, K., Cheng, A.J., Ly, T., Lloyd, F., Fletcher, S., Morgan, J.E., Partridge, T.A. and Wilton, S.D. (2001) Antisense-induced exon skipping and synthesis of dystrophin in the mdx mouse. *Proceedings of the National Academy of Sciences of the United States of America*, **98**, 42-47.
74. Lu, Q.L., Rabinowitz, A., Chen, Y.C., Yokota, T., Yin, H., Alter, J., Jadoon, A., Bou-Gharios, G. and Partridge, T. (2005) Systemic delivery of antisense oligoribonucleotide restores dystrophin expression in body-wide skeletal muscles. *Proceedings of the National Academy of Sciences of the United States of America*, **102**, 198-203.
75. van Deutekom, J.C., Bremmer-Bout, M., Janson, A.A., Ginjaar, I.B.,

- Baas, F., den Dunnen, J.T. and van Ommen, G.J. (2001) Antisense-induced exon skipping restores dystrophin expression in DMD patient derived muscle cells. *Hum.Mol.Genet.*, **10**, 1547-1554.
76. Aartsma-Rus, A., Bremmer-Bout, M., Janson, A.A., den Dunnen, J.T., van Ommen, G.J. and van Deutekom, J.C. (2002) Targeted exon skipping as a potential gene correction therapy for Duchenne muscular dystrophy. *Neuromuscul.Disord.*, **12 Suppl 1**, S71-S77.
77. van Deutekom, J.C., Janson, A.A., Ginjaar, I.B., Frankhuizen, W.S., Aartsma-Rus, A., Bremmer-Bout, M., den Dunnen, J.T., Koop, K., van der Kooij, A.J., Goemans, N.M. *et al.* (2007) Local dystrophin restoration with antisense oligonucleotide PRO051. *The New England journal of medicine*, **357**, 2677-2686.
78. Bladen, C.L., Salgado, D., Monges, S., Foncuberta, M.E., Kekou, K., Kosma, K., Dawkins, H., Lamont, L., Roy, A.J., Chamova, T. *et al.* (2015) The TREAT-NMD DMD Global Database: analysis of more than 7,000 Duchenne muscular dystrophy mutations. *Hum.Mutat.*, **36**, 395-402.
79. Wu, H., Lima, W.F., Zhang, H., Fan, A., Sun, H. and Crooke, S.T. (2004) Determination of the role of the human RNase H1 in the pharmacology of DNA-like antisense drugs. *J.Biol.Chem.*, **279**, 17181-17189.
80. Cerritelli, S.M. and Crouch, R.J. (2009) Ribonuclease H: the enzymes in eukaryotes. *FEBS J.*, **276**, 1494-1505.
81. Vickers, T.A. and Crooke, S.T. (2014) Antisense oligonucleotides capable of promoting specific target mRNA reduction via competing RNase H1-dependent and independent mechanisms. *PLoS.One.*, **9**, e108625.
82. Kole, R., Williams, T. and Cohen, L. (2004) RNA modulation, repair and remodeling by splice switching oligonucleotides. *Acta Biochim.Pol.*, **51**, 373-378.
83. Jarver, P., O'Donovan, L. and Gait, M.J. (2014) A chemical view of oligonucleotides for exon skipping and related drug applications. *Nucleic Acid Ther.*, **24**, 37-47.
84. Bennett, C.F. and Swayze, E.E. (2010) RNA targeting therapeutics: molecular mechanisms of antisense oligonucleotides as a therapeutic platform. *Annu.Rev.Pharmacol.Toxicol.*, **50**, 259-293.
85. Goemans, N.M., Tulinius, M., van den Akker, J.T., Burm, B.E., Ekhardt, P.F., Heuvelmans, N., Holling, T., Janson, A.A., Platenburg, G.J., Sipkens, J.A. *et al.* (2011) Systemic administration of PRO051 in Duchenne's muscular dystrophy. *N.Engl.J.Med.*, **364**, 1513-1522.
86. Watanabe, T.A., Geary, R.S. and Levin, A.A. (2006) Plasma protein binding of an antisense oligonucleotide targeting human ICAM-1 (ISIS 2302). *Oligonucleotides.*, **16**, 169-180.
87. Heemskerk, H., de Winter, C., van Kuik, P., Heuvelmans, N., Sabatelli, P., Rimessi, P., Braghetta, P., van Ommen, G.J., de, K.S., Ferlini, A. *et al.* (2010) Preclinical PK and PD studies on 2'-O-methyl-phosphorothioate RNA antisense oligonucleotides in the mdx mouse model. *Mol.Ther.*, **18**, 1210-1217.
88. Oberbauer, R., Schreiner, G.F. and Meyer, T.W. (1995) Renal uptake of an 18-mer phosphorothioate oligonucleotide. *Kidney Int.*, **48**, 1226-1232.
89. Renneberg, D., Bouliong, E., Reber, U., Schumperli, D. and Leumann, C.J. (2002) Antisense properties of tricyclo-DNA. *Nucleic Acids Res.*, **30**, 2751-2757.
90. Renneberg, D. and Leumann, C.J. (2002) Watson-Crick base-pairing properties of tricyclo-DNA. *J.Am.Chem.Soc.*, **124**, 5993-6002.
91. Goyenvalle, A., Griffith, G., Avril, A., Amthor, H. and Garcia, L. (2015) [Functional correction and cognitive improvement in dystrophic mice using splice-switching tricyclo-DNA oligomers]. *Med.Sci.(Paris)*, **31**, 253-256.
92. Rigo, F., Hua, Y., Chun, S.J., Prakash, T.P., Krainer, A.R. and Bennett, C.F. (2012) Synthetic oligonucleotides recruit ILF2/3 to RNA transcripts to modulate splicing. *Nat.Chem.Biol.*, **8**, 555-561.
93. Yagi, M., Takeshima, Y., Surono, A., Takagi, M., Koizumi, M. and Matsuo, M. (2004) Chimeric RNA and 2'-O, 4'-C-ethylene-bridged nucleic acids have stronger activity than phosphorothioate oligodeoxynucleotides in induction of exon 19 skipping in dystrophin mRNA. *Oligonucleotides.*, **14**, 33-40.
94. Takagi, M., Yagi, M., Ishibashi, K., Takeshima, Y., Surono, A., Matsuo, M. and Koizumi, M. (2004) Design of 2'-O-Me RNA/ENA chimera oligonucleotides to induce exon skipping in dystrophin pre-mRNA. *Nucleic Acids Symp.Ser.(Oxf)*, 297-298.
95. Malueka, R.G., Dwianingsih, E.K., Yagi, M., Lee, T., Nishida, A., Iijima, K., Takeshima, Y. and Matsuo, M. (2015) Phosphorothioate modification of chimeric 2'-O-methyl RNA/ethylene-bridged nucleic acid oligonucleotides increases dystrophin exon 45 skipping capability and reduces cytotoxicity. *Kobe J.Med.Sci.*, **60**, E86-E94.

96. Fletcher, S., Bellgard, M.I., Price, L., Akkari, A.P. and Wilton, S.D. (2016) Translational development of splice-modifying antisense oligomers. *Expert opinion on biological therapy*, 1-16.
97. van Putten, M., Young, C., van den Berg, S., Pronk, A., Hulsker, M., Karnaoukh, T.G., Vermue, R., van Dijk, K.W., de Kimpe, S. and Aartsma-Rus, A. (2014) Preclinical studies on intestinal administration of antisense oligonucleotides as a model for oral delivery for treatment of duchenne muscular dystrophy. *Mol. Ther. Nucleic Acids*, **3**, e211.
98. Flanigan, K.M., Voit, T., Rosales, X.Q., Servais, L., Kraus, J.E., Wardell, C., Morgan, A., Dorricott, S., Nakielny, J., Quarcoo, N. *et al.* (2014) Pharmacokinetics and safety of single doses of drisapersen in non-ambulant subjects with Duchenne muscular dystrophy: results of a double-blind randomized clinical trial. *Neuromuscul. Disord.*, **24**, 16-24.
99. Voit, T., Topaloglu, H., Straub, V., Muntoni, F., Deconinck, N., Campion, G., de Kimpe, S.J., Eagle, M., Guglieri, M., Hood, S. *et al.* (2014) Safety and efficacy of drisapersen for the treatment of Duchenne muscular dystrophy (DEMAND II): an exploratory, randomised, placebo-controlled phase 2 study. *Lancet Neurol.*, **13**, 987-996.
100. Mendell, J.R., Rodino-Klapac, L.R., Sahenk, Z., Roush, K., Bird, L., Lowes, L.P., Alfano, L., Gomez, A.M., Lewis, S., Kota, J. *et al.* (2013) Eteplirsen for the treatment of Duchenne muscular dystrophy. *Ann. Neurol.*, **74**, 637-647.
101. Verhaart, I.E., Tanganyika-de Winter, C.L., Karnaoukh, T.G., Kofschoten, I.G., de Kimpe, S.J., van Deutekom, J.C. and Aartsma-Rus, A. (2013) Dose-dependent pharmacokinetic profiles of 2'-O-methyl phosphorothioate antisense oligonucleotides in mdx mice. *Nucleic Acid Ther.*, **23**, 228-237.
102. Heemskerk, H.A., de Winter, C.L., de Kimpe, S.J., van Kuik-Romeijn, P., Heuvelmans, N., Platenburg, G.J., van Ommen, G.J., van Deutekom, J.C. and Aartsma-Rus, A. (2009) In vivo comparison of 2'-O-methyl phosphorothioate and morpholino antisense oligonucleotides for Duchenne muscular dystrophy exon skipping. *J. Gene Med.*, **11**, 257-266.
103. Wu, B., Xiao, B., Cloer, C., Shaban, M., Sali, A., Lu, P., Li, J., Nagaraju, K., Xiao, X. and Lu, Q.L. (2011) One-year treatment of morpholino antisense oligomer improves skeletal and cardiac muscle functions in dystrophic mdx mice. *Molecular therapy : the journal of the American Society of Gene Therapy*, **19**, 576-583.
104. Komarova, Y. and Malik, A.B. (2010) Regulation of endothelial permeability via paracellular and transcellular transport pathways. *Annual review of physiology*, **72**, 463-493.
105. Tarbell, J.M. (2010) Shear stress and the endothelial transport barrier. *Cardiovascular research*, **87**, 320-330.
106. Geary, R.S. (2009) Antisense oligonucleotide pharmacokinetics and metabolism. *Expert Opin. Drug Metab Toxicol.*, **5**, 381-391.
107. Conner, S.D. and Schmid, S.L. (2003) Regulated portals of entry into the cell. *Nature*, **422**, 37-44.
108. Jones, A.T. (2007) Macropinocytosis: searching for an endocytic identity and role in the uptake of cell penetrating peptides. *Journal of cellular and molecular medicine*, **11**, 670-684.
109. McMahon, H.T. and Boucrot, E. (2011) Molecular mechanism and physiological functions of clathrin-mediated endocytosis. *Nat. Rev. Mol. Cell Biol.*, **12**, 517-533.
110. Takei, K. and Haucke, V. (2001) Clathrin-mediated endocytosis: membrane factors pull the trigger. *Trends in cell biology*, **11**, 385-391.
111. Rothberg, K.G., Heuser, J.E., Donzell, W.C., Ying, Y.S., Glenney, J.R. and Anderson, R.G. (1992) Caveolin, a protein component of caveolae membrane coats. *Cell*, **68**, 673-682.
112. Ferrari, A., Pellegrini, V., Arcangeli, C., Fittipaldi, A., Giacca, M. and Beltram, F. (2003) Caveolae-mediated internalization of extracellular HIV-1 tat fusion proteins visualized in real time. *Molecular therapy : the journal of the American Society of Gene Therapy*, **8**, 284-294.
113. Parton, R.G. and Simons, K. (2007) The multiple faces of caveolae. *Nature reviews. Molecular cell biology*, **8**, 185-194.
114. Mayor, S. and Pagano, R.E. (2007) Pathways of clathrin-independent endocytosis. *Nature reviews. Molecular cell biology*, **8**, 603-612.
115. Doherty, G.J. and McMahon, H.T. (2009) Mechanisms of endocytosis. *Annual review of biochemistry*, **78**, 857-902.
116. Sirsi, S.R., Schray, R.C., Guan, X., Lykens, N.M., Williams, J.H., Erney, M.L. and Lutz, G.J. (2008) Functionalized PEG-PEI copolymers complexed to exon-skipping oligonucleotides improve dystrophin expression in mdx mice. *Human gene therapy*, **19**, 795-806.
117. Sirsi, S.R., Schray, R.C., Wheatley, M.A. and Lutz, G.J. (2009)

- Formulation of polylactide-co-glycolic acid nanospheres for encapsulation and sustained release of poly(ethylene imine)-poly(ethylene glycol) copolymers complexed to oligonucleotides. *Journal of nanobiotechnology*, **7**, 1.
118. Ferlini, A., Sabatelli, P., Fabris, M., Bassi, E., Falzarano, S., Vattemi, G., Perrone, D., Gualandi, F., Maraldi, N.M., Merlini, L. *et al.* (2010) Dystrophin restoration in skeletal, heart and skin arrector pili smooth muscle of mdx mice by ZM2 NP-AON complexes. *Gene Ther.*, **17**, 432-438.
119. Bassi, E., Falzarano, S., Fabris, M., Gualandi, F., Merlini, L., Vattemi, G., Perrone, D., Marchesi, E., Sabatelli, P., Sparnacci, K. *et al.* (2012) Persistent dystrophin protein restoration 90 days after a course of intraperitoneally administered naked 2'OMePS AON and ZM2 NP-AON complexes in mdx mice. *J.Biomed.Biotechnol.*, **2012**, 897076.
120. Falzarano, M.S., Bassi, E., Passarelli, C., Braghetta, P. and Ferlini, A. (2014) Biodistribution studies of polymeric nanoparticles for drug delivery in mice. *Hum.Gene Ther.*, **25**, 927-928.
121. Kendall, G.C., Mokhonova, E.I., Moran, M., Sejbuk, N.E., Wang, D.W., Silva, O., Wang, R.T., Martinez, L., Lu, Q.L., Damoiseaux, R. *et al.* (2012) Dantrolene enhances antisense-mediated exon skipping in human and mouse models of Duchenne muscular dystrophy. *Sci.Transl.Med.*, **4**, 164ra160.
122. Hu, Y., Wu, B., Zillmer, A., Lu, P., Benrashid, E., Wang, M., Doran, T., Shaban, M., Wu, X. and Lu, Q.L. (2010) Guanine analogues enhance antisense oligonucleotide-induced exon skipping in dystrophin gene in vitro and in vivo. *Mol.Ther.*, **18**, 812-818.
123. Verhaart, I.E. and Aartsma-Rus, A. (2012) The effect of 6-thioguanine on alternative splicing and antisense-mediated exon skipping treatment for duchenne muscular dystrophy. *PLoS.Curr.*, **4**.
124. Wang, M., Wu, B., Lu, P., Cloer, C., Tucker, J.D. and Lu, Q. (2013) Polyethylenimine-modified pluronics (PCMs) improve morpholino oligomer delivery in cell culture and dystrophic mdx mice. *Mol.Ther.*, **21**, 210-216.
125. Degols, G., Devaux, C. and Lebleu, B. (1994) Oligonucleotide-poly(L-lysine)-heparin complexes: potent sequence-specific inhibitors of HIV-1 infection. *Bioconjugate chemistry*, **5**, 8-13.
126. Roebuck, K.A., Rabbi, M.F. and Kagnoff, M.F. (1997) HIV-1 Tat protein can transactivate a heterologous TATAA element independent of viral promoter sequences and the trans-activation response element. *AIDS (London, England)*, **11**, 139-146.
127. Derossi, D., Chassaing, G. and Prochiantz, A. (1998) Trojan peptides: the penetratin system for intracellular delivery. *Trends in cell biology*, **8**, 84-87.
128. Moulton, H.M., Nelson, M.H., Hatlevig, S.A., Reddy, M.T. and Iversen, P.L. (2004) Cellular uptake of antisense morpholino oligomers conjugated to arginine-rich peptides. *Bioconjugate chemistry*, **15**, 290-299.
129. Moulton, H.M. and Moulton, J.D. (2010) Morpholinos and their peptide conjugates: therapeutic promise and challenge for Duchenne muscular dystrophy. *Biochim.Biophys.Acta*, **1798**, 2296-2303.
130. Betts, C., Saleh, A.F., Arzumanov, A.A., Hammond, S.M., Godfrey, C., Coursindel, T., Gait, M.J. and Wood, M.J. (2012) Pip6-PMO, A New Generation of Peptide-oligonucleotide Conjugates With Improved Cardiac Exon Skipping Activity for DMD Treatment. *Mol.Ther.Nucleic Acids*, **1**, e38.
131. Yin, H., Saleh, A.F., Betts, C., Camelliti, P., Seow, Y., Ashraf, S., Arzumanov, A., Hammond, S., Merritt, T., Gait, M.J. *et al.* (2011) Pip5 transduction peptides direct high efficiency oligonucleotide-mediated dystrophin exon skipping in heart and phenotypic correction in mdx mice. *Mol.Ther.*, **19**, 1295-1303.
132. Betts, C.A. and Wood, M.J. (2013) Cell penetrating peptide delivery of splice directing oligonucleotides as a treatment for Duchenne muscular dystrophy. *Curr.Pharm.Des*, **19**, 2948-2962.
133. Lehto, T., Castillo, A.A., Gauck, S., Gait, M.J., Coursindel, T., Wood, M.J., Lebleu, B. and Boisguerin, P. (2013) Cellular trafficking determines the exon skipping activity of Pip6a-PMO in mdx skeletal and cardiac muscle cells. *Nucleic Acids Res.*
134. Yin, H., Moulton, H.M., Seow, Y., Boyd, C., Boutilier, J., Iverson, P. and Wood, M.J. (2008) Cell-penetrating peptide-conjugated antisense oligonucleotides restore systemic muscle and cardiac dystrophin expression and function. *Human molecular genetics*, **17**, 3909-3918.
135. Betts, C.A., Saleh, A.F., Carr, C.A., Hammond, S.M., Coenen-Stass, A.M., Godfrey, C., McClorey, G., Varela, M.A., Roberts, T.C., Clarke, K. *et al.* (2015) Prevention of exercised induced cardiomyopathy following Pip-PMO treatment in dystrophic mdx mice. *Sci.Rep.*, **5**, 8986.
136. Smith, G.P. (1985) Filamentous fusion phage: novel expression

- vectors that display cloned antigens on the virion surface. *Science*, **228**, 1315-1317.
137. Parmley, S.F. and Smith, G.P. (1988) Antibody-selectable filamentous fd phage vectors: affinity purification of target genes. *Gene*, **73**, 305-318.
 138. Scott, J.K. and Smith, G.P. (1990) Searching for peptide ligands with an epitope library. *Science*, **249**, 386-390.
 139. McCafferty, J., Griffiths, A.D., Winter, G. and Chiswell, D.J. (1990) Phage antibodies: filamentous phage displaying antibody variable domains. *Nature*, **348**, 552-554.
 140. Devlin, J.J., Panganiban, L.C. and Devlin, P.E. (1990) Random peptide libraries: a source of specific protein binding molecules. *Science*, **249**, 404-406.
 141. Lin, M., McRae, H., Dan, H., Tangorra, E., Laverdiere, A. and Pasick, J. (2010) High-resolution epitope mapping for monoclonal antibodies to the structural protein Erns of classical swine fever virus using peptide array and random peptide phage display approaches. *J.Gen.Virol.*, **91**, 2928-2940.
 142. Guo, A., Cai, X., Jia, W., Liu, B., Zhang, S., Wang, P., Yan, H. and Luo, X. (2010) Mapping of *Taenia solium* TSOL18 antigenic epitopes by phage display library. *Parasitol.Res.*, **106**, 1151-1157.
 143. He, Y., Wang, Y., Struble, E.B., Zhang, P., Chowdhury, S., Reed, J.L., Kennedy, M., Scott, D.E. and Fisher, R.W. (2012) Epitope mapping by random peptide phage display reveals essential residues for vaccinia extracellular enveloped virion spread. *Virology*, **9**, 217.
 144. Schmitz, U., Versmold, A., Kaufmann, P. and Frank, H.G. (2000) Phage display: a molecular tool for the generation of antibodies--a review. *Placenta*, **21 Suppl A**, S106-S112.
 145. Rakonjac, J., Bennett, N.J., Spagnuolo, J., Gagic, D. and Russel, M. (2011) Filamentous bacteriophage: biology, phage display and nanotechnology applications. *Curr.Issues Mol.Biol.*, **13**, 51-76.
 146. Sidhu, S.S. (2001) Engineering M13 for phage display. *Biomol.Eng.*, **18**, 57-63.
 147. Jiang, J., Abu-Shilbayeh, L. and Rao, V.B. (1997) Display of a PorA peptide from *Neisseria meningitidis* on the bacteriophage T4 capsid surface. *Infect.Immun.*, **65**, 4770-4777.
 148. Ren, S., Fengyu, Zuo, S., Zhao, M., Wang, X., Wang, X., Chen, Y., Wu, Z. and Ren, Z. (2011) Inhibition of tumor angiogenesis in lung cancer by T4 phage surface displaying mVEGFR2 vaccine. *Vaccine*, **29**, 5802-5811.
 149. Cerritelli, M.E., Conway, J.F., Cheng, N., Trus, B.L. and Steven, A.C. (2003) Molecular mechanisms in bacteriophage T7 procapsid assembly, maturation, and DNA containment. *Adv.Protein Chem.*, **64**, 301-323.
 150. Chang, C.Y., Kemp, P. and Molineux, I.J. (2010) Gp15 and gp16 cooperate in translocating bacteriophage T7 DNA into the infected cell. *Virology*, **398**, 176-186.
 151. Beghetto, E. and Gargano, N. (2011) Lambda-display: a powerful tool for antigen discovery. *Molecules*, **16**, 3089-3105.
 152. Huang, J., Ru, B., Li, S., Lin, H. and Guo, F.B. (2010) SAROTUP: scanner and reporter of target-unrelated peptides. *J.Biomed.Biotechnol.*, **2010**, 101932.
 153. Dias-Neto, E., Nunes, D.N., Giordano, R.J., Sun, J., Botz, G.H., Yang, K., Setubal, J.C., Pasqualini, R. and Arap, W. (2009) Next-generation phage display: integrating and comparing available molecular tools to enable cost-effective high-throughput analysis. *PLoS.One.*, **4**, e8338.
 154. Derda, R., Tang, S.K., Li, S.C., Ng, S., Matochko, W. and Jafari, M.R. (2011) Diversity of phage-displayed libraries of peptides during panning and amplification. *Molecules (Basel, Switzerland)*, **16**, 1776-1803.
 155. Matochko, W.L., Chu, K., Jin, B., Lee, S.W., Whitesides, G.M. and Derda, R. (2012) Deep sequencing analysis of phage libraries using Illumina platform. *Methods*, **58**, 47-55.



CHAPTER 2

Update on RNA-targeting therapies for neuromuscular disorders

Silvana Jirka and Annemieke Aartsma-Rus

Department of Human Genetics, Leiden University Medical Center, Leiden, the Netherlands

Curr Opin Neurol 2015, 28:515–521

Abstract

Purpose: Antisense-mediated modulation of transcripts is a dynamic therapeutic field, especially for neuromuscular disorders.

Recent findings: For three diseases, this approach has advanced to the clinical trial phase, i.e. Duchenne muscular dystrophy (DMD), spinal muscular atrophy (SMA) and myotonic dystrophy (DM). In parallel, numerous proof of concept studies in cell and animal models have been reported for additional neuromuscular disorders.

Summary: This review discusses the most notable advances in preclinical and clinical studies in the past year. For DMD, SMA and DM trials are ongoing to assess safety and efficacy, while in parallel pre-clinical studies are being conducted to identify ways to improve efficiency and delivery. For other neuromuscular diseases, progress is made as well warranting future clinical trials. However, towards clinical trial readiness, it is important not only to optimize the therapy preclinically, but to also develop the infrastructure that is needed to conduct trials.

1. Introduction

Developing therapies for neuromuscular disorders is challenging because affected tissues are difficult to target due to their abundance (skeletal muscle) or inaccessibility (motor neurons). Antisense oligonucleotides (AONs) are small (20-30 nucleotides) single stranded pieces of chemically modified DNA or RNA that can target gene transcripts. Because they are small they can overcome the delivery challenge. Delivery to the nervous system is especially efficient with intrathecal or intraventricular injection. Following delivery in this manner, AONs are rapidly taken up by neurons in the central and peripheral nervous system[1]. As such AONs offer an attractive therapeutic tool for the treatment of neuromuscular disorders, and in fact AONs have progressed to the clinical trial phase for three neuromuscular disorders: Duchenne muscular dystrophy (DMD), spinal muscular atrophy (SMA) and myotonic dystrophy (DM). In parallel preclinical studies are ongoing to further improve this approach, and reported proof-of-concept studies outline the therapeutic potential of AON therapy for other neuromuscular disorders. This review will focus on the pre-clinical and clinical developments of AON-mediated transcript targeting for neuromuscular disorders of the past 15 months.

2. Clinical trials

2.1 Duchenne muscular dystrophy

AON-mediated transcript targeting has moved into the clinical trial phase

for DMD, SMA and DM. For DMD and SMA AONs modulate the pre-mRNA splicing process. DMD is caused by mutations in the *DMD* gene that disrupt the reading frame, leading to premature truncation of protein translation and non-functional dystrophin proteins. Mutations that maintain the reading frame allow the production of an internally deleted, partially functional dystrophin protein. These are associated with a less severely progressive disease, Becker muscular dystrophy. For DMD AON-mediated transcript targeting is exploited with the aim to reframe dystrophin transcripts to allow the production of internally deleted, partially functional dystrophin proteins, as found in Becker muscular dystrophy. This can be achieved by AONs that target specific exons, hiding them from the splicing machinery and causing them to be 'skipped'. This approach is mutation specific, but because skipping a single exon can be applicable to a variety of different mutations, AONs targeting certain exons can be applied to larger groups of patients, e.g. exon 51 skipping applies to 13-14% of all patients[2;3]. Not surprisingly, AONs targeting exon 51 are most advanced in the clinical development, i.e. Drisapersen (2'-O-methyl phosphorothioate (2OMePS)) and Eteplirsen (phosphorodiamidate morpholino oligomer (PMO) chemistry).

Eteplirsen has been injected intravenously in weekly doses up to 50 mg/kg in 31 DMD patients[4;5]. The drug was well tolerated, occasionally transient proteinuria was reported. In the most recent study 12 patients received 30 or 50 mg/kg Eteplirsen or placebo for 24 weeks, followed by an open label extension phase where all patients received 30 or 50 mg/kg[5]. Dystrophin restoration was reported for 30-60% of muscle fibers in a biopsy taken after 48 weeks of treatment. For 6 of the patients treated from the onset of the study, the distance walked in 6 minutes (6MWD) remained stable for 120 weeks. Currently, patients have been treated for up to 168 weeks. While there is some decline in 6MWD, the 10 ambulant patients performed better than would be expected from natural history, suggesting that Eteplirsen slowed disease progression (Edward Kaye, personal communication).

Drisapersen has been tested in 4 trials using subcutaneous treatment in ~300 DMD patients[6;7]. While the drug was tolerated well, mild to moderate side effects were reported, involving injection site reactions, proteinuria and in some patients thrombocytopenia[7]. These side effects are commonly found for the 2OMePS chemistry, with injection site reactions observed after subcutaneous but not after intravenous delivery. Drisapersen also appears to slow down disease progression. In an open label extension trial following a dose escalation study in 12 patients, 8 ambulant patients had stable 6 MWD for 177 weeks. Furthermore, treated patients (6 mg/kg subcutaneous weekly or intermittently) outperformed placebo treated patients in the 6MWD in a randomized, double-blind placebo controlled trial involving 54 early stage DMD patients (6-8 years of age)[7]. Two other trials have been completed but are not yet published

(Giles Campion and Tony Hall, personal communication). Early stage patients treated with 6 mg/kg subcutaneous Drisapersen for 24 weeks outperformed patients treated with placebo or 3 mg/kg Drisapersen in a dose comparing trial involving 51 patients. The most recently completed trial involved 186 patients of varying ages (5-16 years) and disease stages. After 48 weeks the treated group did not perform significantly better in the 6 minute walk test than the placebo treated group. Recent natural history data for the 6MWD in DMD patients has revealed that it is very difficult to find significant effects in a population as mixed as the one in the phase 3 trial[8-11]. In young patients the decline in 6MWD is slow and therefore it is challenging to pick up a treatment-induced slowing of disease progression in a 48 week trial. By contrast in patients who are in a more advanced disease state, treatment for more than 48 weeks might be required to induce an discernible effect in the 6MWD, as suggested by data of patients who were treated for an additional 48 weeks in the open label study following the phase 3 trial.

Biomarin/Prosensa has submitted a new drug application (NDA) for accelerated approval of Drisapersen with the Food and Drug Administration in April 2015 and filed for conditional approval of Drisapersen with the European Medicine Agency in June 2015. Sarepta plans to file for accelerated approval using a rolling NDA for Eteplirsen while a phase 3 trial is ongoing. In addition trials are ongoing for exons 44, 45 and 53 skipping (coordinated by Biomarin, Sarepta and Nippon-Shinyaku Co)[12;13].

2.2 Spinal muscular atrophy

SMA is caused by mutations in the *SMN1* gene, leading to death or incomplete development of motor neurons. The *SMN2* gene (only present in humans) can produce functional transcripts, if exon 7 could be retained in the transcripts. Exon 7 possesses a silent mutation and intronic splicing silencers located in the regions flanking exon 7. Using AONs targeting intronic silencers, the level of exon 7 inclusion can be increased, enabling patients to produce more functional *SMN2* transcripts and increased amounts of SMN protein. Extensive preclinical screening has resulted in the identification of ISIS-SMN_{rx}, a 2'-O-methoxyethyl phosphorothioate (MOEPS) AON, for which pharmacological properties after central nervous system delivery have been thoroughly investigated in mouse, rats and non-human primates[14]. One exploratory trial with ISIS-SMN_{rx} has been completed by ISIS pharmaceuticals in SMA type 2 and type 3 patients with encouraging preliminary results[15]. Currently, a trial has initiated for severe type 1 patients and additional trials are ongoing in type 2 and 3 patients coordinated by ISIS and Biogen.

2.3 Myotonic dystrophy

For myotonic dystrophy (DM), AONs treatment aims to reduce RNA aggregates formed by the expanded CUG repeat in the *DMPK* gene, which

sequester splicing factors, and as such underlie the missplicing pathology observed in DM patients. An MOE gapmer AON to reduce *DMPK* transcript levels (ISIS-DMPK_{rx}) has been identified, which normalizes splicing patterns in vitro and in an DM animal model[16]. A dose-finding, safety trial has recently been initiated in DM patients by ISIS pharmaceuticals (<https://www.clinicaltrials.gov/ct2/show/NCT02312011>).

3. Preclinical studies for DM, SMA and DMD

3.1 Improving chemistry and delivery

In parallel with the clinical trial, preclinical work is ongoing to further optimize the tools and techniques involved. For DM it was shown that a locked nucleic acid targeting the CUG repeat has potential in vitro and in vivo[17]. The locked nucleic acid chemistry has a very high affinity for RNA transcript and very short AONs (8-10-mers) were able to reduce the amount of DMPK aggregates and restore splicing defects. However, with such short AONs there is an obvious risk that CUG repeats in normal transcripts will be targeted as well.

For SMA, it was reported that intraventricular delivery of ISIS-SMN_{rx} AONs normalizes gene-expression levels in the spinal cords of SMA mouse models[18]. Notably, Keil *et al.*, published that the phenotype of severe SMA models could be ameliorated with an 8-mer AON[19]. While promising, it is obvious that an 8-mer AON will not be specific for only the *SMN2* gene and comprehensive gene expression analysis as done for the ISIS-SMN_{rx} compound would be warranted to study this AON further.

For DMD efforts focus on improving delivery to heart. The tricyclo-DNA modification resulted in increased exon skipping and dystrophin restoration in heart and even resulted in low levels of exon skipping in the brain[20]. Treatment with this chemistry also rescued the phenotype of a severe mouse model lacking dystrophin and its homologue utrophin (*mdx/utrn^{-/-}* mouse). Clinical trials with this chemistry are planned for DMD. However, as yet safety and tolerability in species other than mice has not been assessed. Another concern is that tricyclo-DNA AONs are shorter than PMO and 2OMePS AONs (15-mer vs 20-30-mers). Therefore there is a risk that the AONs will have (off) target sites in addition to the intended dystrophin exon.

Another way to increase uptake is through addition of peptides [21-23]. Conjugation of short arginine rich cationic peptides with a hydrophobic core increased uptake of phosphorodiamidate morpholino oligomers (pip-PMOs) in heart (as well as skeletal muscle), leading to a slower development of cardiomyopathy[21;23]. Since 2OMePS nucleotides are negatively charged, it is not possible to conjugate positively charged peptides to these AON. However, conjugation of a 7-mer peptide identified from a phage display peptide library resulted in increased uptake and exon skipping levels[24].

3.2 Applicability for different mutations

DMD exon skipping is a mutation specific approach. Thus far the focus has been on skipping single exons for deletion mutations, while ~12% of patients have a duplication of 1 or more exons. Exon skipping for duplications is challenging, since the AONs will target both the original and the duplicated exon and generally both exons will be skipped, resulting in an out-of-frame transcript[25]. However, it was recently reported that exon skipping may be possible for the most common single exon duplication, i.e. an exon 2 duplication[26]. Here, if exon skipping is too efficient and both exons 2 are omitted, the resulting transcript (deletion of exon 2) can still give rise to functional dystrophin through the activation of an internal ribosomal entry site in exon 5. Skipping multiple exons (exon 2-7) was reported as an alternative approach to restore an exon 2 duplication[25]. This approach involves a combination of multiple AONs. Multiexon skipping has also been proposed as a 'cocktail' approach to induce skipping of exon 45-55 (i.e. the mutation hotspot)[27;28], which would in theory be therapeutic for a large group of patients (~40-60% depending on which mutation database is queried[2;29]) and produce a highly functional dystrophin. It was recently shown to be feasible to skip exon 45-51 and exon 53-55 and restore dystrophin expression in a mouse model lacking mouse dystrophin exon 52 using a combination of 10 vivo-PMOs (PMOs with an oligodendrimer group for enhanced tissue uptake). While multiexon skipping is feasible in animal models, developing an approach involving 11 individual AONs poses regulatory challenges[30].

3.3 Timing, duration and effects of AON treatment

Preclinical studies have revealed insight on the duration of treatment and the impact of treatment initiation. While 2OMePS AON levels and exon skipping transcripts decline and were barely detectable 12 weeks after treatment was stopped, dystrophin protein levels continued to increase for another 8-12 weeks and were still detectable 24 weeks after treatment termination in *mdx* mice[31]. An elegant study from Wu *et al.*, used peptide conjugated PMOs to restore high levels of dystrophin in the severe *mdx/utrn*^{-/-} model. The level of benefit critically depended on the time of intervention. Animals treated before 4 weeks of age had increased lifespan, normal posture, limited muscle wasting and very limited kyphosis, while no benefit was observed for animals that were treated in ~6-7 week old animal with advanced pathology, despite high levels (>50% of normal) of dystrophin restoration[32].

Multiple studies have focused on the effect of systemic versus CNS treatment in SMA mouse model [21;33-36]. It appears that the combination of CNS and systemic delivery results in a markedly improved increase in survival compared to only CNS or systemic delivery. Since in newborn mice the blood-brain-barrier is not yet mature, systemic treatment with high

doses of AON will result in body-wide delivery, including the central nervous system. In order to investigate the effect of treatment of only peripheral tissues in new born mice, Hua *et al* used a decoy AON (i.e. a sense oligo that can sequester an AON, rendering it ineffective[34]). New-born mice were injected with AONs postnatally and received an injection with the decoy AON through intraventricular injection. As such SMN was restored only in the periphery, which resulted in rescue of ear and tail necrosis in a mild SMA model and increased survival in a severe model. It is not yet clear whether the importance of peripheral SMN restoration is specific for mouse or whether it translates to the human situation. For now, clinical trials for SMA patients involve only intrathecal delivery.

RNA targeting therapies for other neuromuscular disorders

Antisense-mediated transcript targeting has been reported for multiple neuromuscular disorders (Table 1). Here, we will focus only on reports of the past 15 months.

Table 1. Overview of transcript targeting antisense approaches for neuromuscular

Disease	Mechanism	Reference
Amyotrophic lateral sclerosis and frontotemporal degeneration	Reduced levels of mutated transcript (C9ORF72)	[37;38]
Congenital myosthenia	Normalize CHRNA1 splicing	[39]
Duchenne muscular dystrophy	Reading frame restoration	[5;6]
Dysferlinopathies	Bypassing mutation in in-frame exon	[40]
Fukuyama Muscular Dystrophy	Skipping of cryptic retrotransposon exon	[41]
Laminopathies	Bypassing mutation in in-frame exon 5	[42]
Myotonic Dystrophy	Reduced levels of mutated transcript	[16]
Oculopharyngeal muscular dystrophy	Polyadenylation site usage	[43]
Pompe Disease	Reduced levels of glycogen synthase	[44]
Spinal muscular atrophy	Exon inclusion	[45;46]

4.1 Oculopharyngeal muscular dystrophy

Oculopharyngeal muscular dystrophy (OPMD) is caused by an alanine expansion in the polyadenyline binding protein 1 (PABPN1), that makes the PABPN1 protein prone to aggregation. In OPMD lower amounts of soluble PABPN1 protein lead to a genome-wide shift of proximal rather

than distal polyadenylation site usage. This deregulation of gene expression is proposed to underlie the premature aging observed in affected OPMD muscles. ARIH2 E3-ligase is one of the genes misregulated in OPMD. Notably, ARIH2 protein levels positively regulate the amount of total and soluble PABPN1. As such restoring the normal polyadenylation site usage for ARIH2 could also lead to increased levels of PABPN1. Indeed, AONs targeting the proximal polyadenylation signal of ARIH2 resulted in increased levels of ARIH2, higher levels of PABPN1 and improved differentiation of OPMD-derived cell cultures in vitro[43].

4.2 Laminopathies

Mutations in the lamin A/C encoding *LMNA* gene underlie multiple disorders, including neuromuscular disorders such as Emery-Dreifuss muscular dystrophy, limb-girdle muscular dystrophy type 1B and congenital muscular dystrophy. In an effort to identify exons encoding redundant parts of lamin A, a recent study studied expression vectors of lamin A cDNA lacking selected exons. This work revealed that cDNA without the in-frame exon 5 resulted in a lamin protein that was localized normally, could rescue the abnormal nuclear phenotype of laminopathy-patient-derived cells and did not have dominant negative effect in control cells[42]. AONs to induce *LMNA* exon 5 skipping in vitro have been identified[42]. This approach might have therapeutic potential for laminopathy patients with mutations in exon 5, although further studies are required in cell and animal models to fully evaluate the potential.

4.3 Pompe disease

Pompe disease is characterized by progressive accumulation of undegraded glycogen, due to mutations in the *GAA* gene that encodes for acid alpha-glucosidase (GAA), an enzyme involved in breaking down glycogen to glucose. Infusion with recombinant human GAA is an approved treatment for Pompe patients. However, GAA infusion generally is insufficient to completely abolish all aspects of the disease. In an effort to develop an add-on therapy, Clayton *et al.*, tested peptide-conjugated PMOs targeting an out-of-frame exon of the glycogen synthase enzyme as a way to reduce glycogen production. Treatment with these PMOs resulted in lower levels of glycogen synthase and lower amounts of glycogen accumulation in a Pompe animal model[44].

4.4 Congenital myasthenic syndroms

Congenital myasthenic syndroms (CMS) are caused by mutations in genes encoding proteins required for neuromuscular junction formation, maintenance and regulation. The *CHRNA1* encodes the alpha subunit of the nicotinic acetylcholine receptor (nAChR), which is expressed in the post synaptic membrane of the neuromuscular junction. In humans, the *CHRNA1* gene produces two transcripts that either include or exclude exon

P3A. Only the transcript lacking exon P3A encodes a functional protein. Mutations have been identified in CMS patients that result in increased levels of P3A inclusion. Tei *et al.*, have identified AONs that could induce P3A exon skipping in minigenes containing mutated sequences and in wild type cells[39]. Further work is needed to assess the potential of this approach in patient-derived cells and animal models.

5. Forward look

It is clear that antisense-mediated transcript targeting is a dynamic field for the neuromuscular disease space: proof-of-concept studies accumulate and the approach is taken into preclinical and clinical development for some neuromuscular disorders. However, it has become apparent that it is crucial to develop tools and infrastructure to conduct clinical trials in parallel with the development of the potential therapy, rather than at the initiation of the clinical trial phase. In addition to patient registries and trial sites, this involves developing functional and molecular outcome measures to be used in trials as well as natural history data for these measures. When these tools are in place this will allow better trial design and hopefully faster clinical evaluation of potentially therapeutic compounds. In addition, good communication with key regulatory agencies is critical to move these therapies towards clinical practice.

6. Conclusion

RNA targeting is a promising therapeutic approach for multiple neuromuscular disorders. However, in addition to proof-of-concept in cell and animal models, clinical infrastructure is required to further the clinical development of this approach towards clinical application.

RNA targeting is a promising therapeutic approach for neuromuscular disorders

RNA targeting is tested in clinical trials for DMD, SMA and DM

Proof-of-concept has been shown for multiple neuromuscular disorders

Infrastructure for clinical trial needs to be in place for each neuromuscular disorder to facilitate and accelerate clinical development of (RNA targeting) therapies

7. Conflict of Interest

SMGJ declares no conflicts of interest. AAR declares that she is employed by LUMC, which has patents on exon skipping. As co-inventor on some of these patents AAR is entitled to a share of royalties.

8. Acknowledgements

Silvana Jirka's salary is paid by a grant from the Prinses Beatrix Spierfonds and Spieren voor Spieren, the Netherlands to Annemieke Aartsma-Rus (Project number W.OR13-06). The salary of Annemieke Aartsma-Rus is partially paid for by a grant from ZonMw, the Netherlands (Project number 113202001).

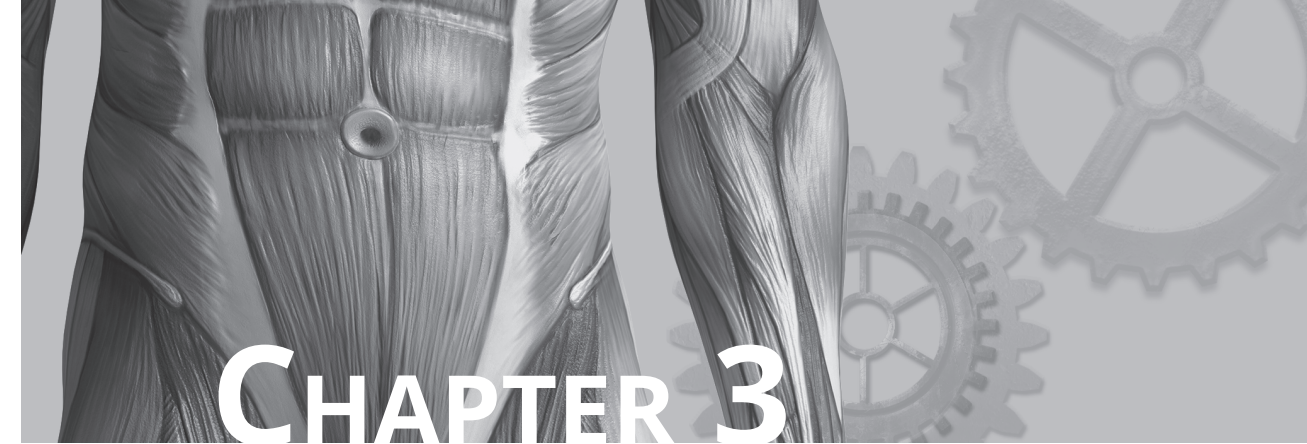
References

1. Rigo F, Chun SJ, Norris DA, Hung G, Lee S, Matson J, Fey RA, Gaus H, Hua Y, Grundy JS, Krainer AR, Henry SP, Bennett CF: Pharmacology of a central nervous system delivered 2'-O-methoxyethyl-modified survival of motor neuron splicing oligonucleotide in mice and nonhuman primates. *J.Pharmacol.Exp.Ther.* 2014, 350:46-55.
*Comprehensive study of the pharmacological effects of AON delivery to the CNS
2. Aartsma-Rus A, Fokkema I, Verschuuren J, Ginjaar I, van DJ, van Ommen GJ, den Dunnen JT: Theoretic applicability of antisense-mediated exon skipping for Duchenne muscular dystrophy mutations. *Hum.Mutat.* 2009, 30:293-299.
3. Bladen CL, Salgado D, Monges S, Foncuberta ME, Kekou K, Kosma K, Dawkins H, Lamont L, Roy AJ, Chamova T, Guergueltcheva V, Chan S, Korngut L, Campbell C, Dai Y, Wang J, Barisic N, Brabec P, Lahdetie J, Walter MC, Schreiber-Katz O, Karcagi V, Garami M, Viswanathan V, Bayat F, Buccella F, Kimura E, Koeks Z, van den Bergen JC, Rodrigues M, Roxburgh R, Lusakowska A, Kostera-Pruszczyk A, Zimowski J, Santos R, Neagu E, Artemieva S, Rasic VM, Vojinovic D, Posada M, Bloetzer C, Jeannet PY, Joncourt F, Diaz-Manera J, Gallardo E, Karaduman AA, Topaloglu H, El SR, Stringer A, Shatillo AV, Martin AS, Peay HL, Bellgard MI, Kirschner J, Flanigan KM, Straub V, Bushby K, Verschuuren J, Aartsma-Rus A, Beroud C, Lochmuller H: The TREAT-NMD DMD Global Database: Analysis of More than 7,000 Duchenne Muscular Dystrophy Mutations. *Hum.Mutat.* 2015.
4. Cirak S, Arechavala-Gomeza V, Guglieri M, Feng L, Torelli S, Anthony K, Abbs S, Garralda ME, Bourke J, Wells DJ, Dickson G, Wood MJ, Wilton SD, Straub V, Kole R, Shrewsbury SB, Sewry C, Morgan JE, Bushby K, Muntoni F: Exon skipping and dystrophin restoration in patients with Duchenne muscular dystrophy after systemic phosphorodiamidate morpholino oligomer treatment: an open-label, phase 2, dose-escalation study. *Lancet* 2011, 378:595-605.
5. Mendell JR, Rodino-Klapac LR, Sahenk Z, Roush K, Bird L, Lowes LP, Alfano L, Gomez AM, Lewis S, Kota J, Malik V, Shontz K, Walker CM, Flanigan KM, Corridore M, Kean JR, Allen HD, Shilling C, Melia KR, Sazani P, Saoud JB, Kaye EM: Eteplirsen for the treatment of Duchenne muscular dystrophy. *Ann.Neurol.* 2013, 74:637-647.
*Paper reporting slower disease progression in Eteplirsen treated DMD patients in an open label study
6. Goemans NM, Tulinius M, van den Akker JT, Burm BE, Ekhardt PF, Heuvelmans N, Holling T, Janson AA, Platenburg GJ, Sipkens JA, Sitsen

- JM, Aartsma-Rus A, van Ommen GJ, Buyse G, Darin N, Verschuuren JJ, Campion GV, de Kimpe SJ, Van Deutekom JC: Systemic administration of PRO051 in Duchenne's muscular dystrophy. *N.Engl.J.Med.* 2011, 364:1513-1522.
7. Voit T, Topaloglu H, Straub V, Muntoni F, Deconinck N, Campion G, de Kimpe SJ, Eagle M, Guglieri M, Hood S, Liefwaard L, Lourbakos A, Morgan A, Nakielny J, Quarcoo N, Ricotti V, Rolfe K, Servais L, Wardell C, Wilson R, Wright P, Kraus JE: Safety and efficacy of drisapersen for the treatment of Duchenne muscular dystrophy (DEMAND II): an exploratory, randomised, placebo-controlled phase 2 study. *Lancet Neurol.* 2014, 13:987-996.
*Paper reporting slower disease progression in Drisapersen treated DMD patients in a placebo-controlled trials
 8. Goemans N, Klingels K, van den Hauwe M, Boons S, Verstraete L, Peeters C, Feys H, Buyse G: Six-minute walk test: reference values and prediction equation in healthy boys aged 5 to 12 years. *PLoS. One.* 2013, 8:e84120.
 9. Lynn S, Aartsma-Rus A, Bushby K, Furlong P, Goemans N, De LA, Mayhew A, McDonald C, Mercuri E, Muntoni F, Pohlschmidt M, Verschuuren J, Voit T, Vroom E, Wells DJ, Straub V: Measuring clinical effectiveness of medicinal products for the treatment of Duchenne muscular dystrophy. *Neuromuscul.Disord.* 2015, 25:96-105.
*Meeting report that lists an overview of and practical considerations for the use of outcome measures for DMD trials
 10. McDonald CM, Henricson EK, Abresch RT, Florence JM, Eagle M, Gappmaier E, Glanzman AM, Spiegel R, Barth J, Elfring G, Reha A, Peltz S: The 6-minute walk test and other endpoints in Duchenne muscular dystrophy: longitudinal natural history observations over 48 weeks from a multicenter study. *Muscle Nerve* 2013, 48:343-356.
 11. Pane M, Mazzone ES, Sivo S, Sormani MP, Messina S, Amico D, Carlesi A, Vita G, Fanelli L, Berardinelli A, Torrente Y, Lanzillotta V, Viggiano E, Ambrosio D, Cavallaro F, Frosini S, Barp A, Bonfiglio S, Scalise R, De SR, Rolle E, Graziano A, Magri F, Palermo C, Rossi F, Donati MA, Sacchini M, Arnoldi MT, Baranello G, Mongini T, Pini A, Battini R, Pegoraro E, Previtali S, Bruno C, Politano L, Comi GP, Bertini E, Mercuri E: Long term natural history data in ambulant boys with Duchenne muscular dystrophy: 36-month changes. *PLoS.One.* 2014, 9:e108205.
 12. Lee JJ, Yokota T: Antisense therapy in neurology. *J.Pers.Med.* 2013, 3:144-176.
 13. Aartsma-Rus A: Dystrophin analysis in clinical trials. *Journal of Neuromuscular Diseases* 2014, 1:41-53.
 14. Hua Y, Vickers TA, Okunola HL, Bennett CF, Krainer AR: Antisense masking of an hnRNP A1/A2 intronic splicing silencer corrects SMN2 splicing in transgenic mice. *Am.J.Hum.Genet.* 2008, 82:834-848.
 15. Zanetta C, Nizzardo M, Simone C, Monguzzi E, Bresolin N, Comi GP, Corti S: Molecular therapeutic strategies for spinal muscular atrophies: current and future clinical trials. *Clin.Ther.* 2014, 36:128-140.
 16. Wheeler TM, Leger AJ, Pandey SK, MacLeod AR, Nakamori M, Cheng SH, Wentworth BM, Bennett CF, Thornton CA: Targeting nuclear RNA for in vivo correction of myotonic dystrophy. *Nature* 2012, 488:111-115.
 17. Wojtkowiak-Szlachcic A, Taylor K, Stepniak-Konieczna E, Sznajder LJ, Mykowska A, Sroka J, Thornton CA, Sobczak K: Short antisense-locked nucleic acids (all-LNAs) correct alternative splicing abnormalities in myotonic dystrophy. *Nucleic Acids Res.* 2015, 43:3318-3331.
*Paper reporting an 8-mer LNA that can reduce the DMPK transcript aggregates in vitro and in vivo
 18. Staropoli JF, Li H, Chun SJ, Allaire N, Cullen P, Thai A, Fleet CM, Hua Y, Bennett CF, Krainer AR, Kerr D, McCampbell A, Rigo F, Carulli JP: Rescue of gene-expression changes in an induced mouse model of spinal muscular atrophy by an antisense oligonucleotide that promotes inclusion of SMN2 exon 7. *Genomics* 2015, 105:220-228.
 19. Keil JM, Seo J, Howell MD, Hsu WH, Singh RN, DiDonato CJ: A short antisense oligonucleotide ameliorates symptoms of severe mouse models of spinal muscular atrophy. *Mol.Ther.Nucleic Acids* 2014, 3:e174.
 20. Goyenvalle A, Griffith G, Babbs A, Andaloussi SE, Ezzat K, Avril A, Dugovic B, Chaussonot R, Ferry A, Voit T, Amthor H, Buhr C, Schurch S, Wood MJ, Davies KE, Vaillend C, Leumann C, Garcia L: Functional correction in mouse models of muscular dystrophy using exon-skipping tricyclo-DNA oligomers. *Nat.Med.* 2015, 21:270-275.
*This report describes the use of tricyclo-DNA AONs which results in efficient exon skipping in skeletal muscle and heart and notably low level exon skipping in brain after systemic treatment.
 21. Betts C, Saleh AF, Arzumanov AA, Hammond SM, Godfrey C, Coursindel T, Gait MJ, Wood MJ: Pip6-PMO, A New Generation of Peptide-oligonucleotide Conjugates With Improved Cardiac Exon

- Skipping Activity for DMD Treatment. *Mol.Ther.Nucleic Acids* 2012, 1:e38.
22. Gao X, Zhao J, Han G, Zhang Y, Dong X, Cao L, Wang Q, Moulton HM, Yin H: Effective dystrophin restoration by a novel muscle-homing peptide-morpholino conjugate in dystrophin-deficient mdx mice. *Mol.Ther.* 2014, 22:1333-1341.
 23. Betts CA, Saleh AF, Carr CA, Hammond SM, Coenen-Stass AM, Godfrey C, McClorey G, Varela MA, Roberts TC, Clarke K, Gait MJ, Wood MJ: Prevention of exercised induced cardiomyopathy following Pip-PMO treatment in dystrophic mdx mice. *Sci.Rep.* 2015, 5:8986.
*Reports prevention of cardiomyopathy in dystrophic mice treated with peptide-conjugated PMOs
 24. Jirka SM, Heemskerk H, Tanganyika-de Winter CL, Muilwijk D, Pang KH, de Visser PC, Janson A, Karnaoukh TG, Vermue R, 't Hoen PA, Van Deutekom JC, Aguilera B, Aartsma-Rus A: Peptide conjugation of 2'-O-methyl phosphorothioate antisense oligonucleotides enhances cardiac uptake and exon skipping in mdx mice. *Nucleic Acid Ther.* 2014, 24:25-36.
*First report of a peptide conjugation to improve delivery and exon skipping for 2OMePS AONs in mdx mice
 25. Greer KL, Lochmuller H, Flanigan K, Fletcher S, Wilton SD: Targeted exon skipping to correct exon duplications in the dystrophin gene. *Mol.Ther.Nucleic Acids* 2014, 3:e155.
 26. Wein N, Vulin A, Falzarano MS, Szigyarto CA, Maiti B, Findlay A, Heller KN, Uhlen M, Bakthavachalu B, Messina S, Vita G, Passarelli C, Gualandi F, Wilton SD, Rodino-Klapac LR, Yang L, Dunn DM, Schoenberg DR, Weiss RB, Howard MT, Ferlini A, Flanigan KM: Translation from a DMD exon 5 IRES results in a functional dystrophin isoform that attenuates dystrophinopathy in humans and mice. *Nat.Med.* 2014, 20:992-1000.
*This report outlines why the exon skipping approach has potential for DMD patients with an exon 2 duplication.
 27. Echigoya Y, Aoki Y, Miskew B, Panesar D, Touznik A, Nagata T, Tanihata J, Nakamura A, Nagaraju K, Yokota T: Long-term efficacy of systemic multiexon skipping targeting dystrophin exons 45-55 with a cocktail of vivo-morpholinos in mdx52 mice. *Mol.Ther.Nucleic Acids* 2015, 4:e225.
 28. Echigoya Y, Yokota T: Skipping multiple exons of dystrophin transcripts using cocktail antisense oligonucleotides. *Nucleic Acid Ther.* 2014, 24:57-68.
 29. Beroud C, Tuffery-Giraud S, Matsuo M, Hamroun D, Humbertclaude V, Monnier N, Moizard MP, Voelckel MA, Calemard LM, Boisseau P, Blayau M, Philippe C, Cossee M, Pages M, Rivier F, Danos O, Garcia L, Clautres M: Multiexon skipping leading to an artificial DMD protein lacking amino acids from exons 45 through 55 could rescue up to 63% of patients with Duchenne muscular dystrophy. *Hum.Mutat.* 2007, 28:196-202.
 30. Aartsma-Rus A, Ferlini A, Goemans N, Pasmooij AM, Wells DJ, Bushby K, Vroom E, Balabanov P: Translational and regulatory challenges for exon skipping therapies. *Hum.Gene Ther.* 2014, 25:885-892.
 31. Verhaart IE, van Vliet-van den Dool, Sipkens JA, de Kimpe SJ, Kolfshoten IG, Van Deutekom JC, Liefwaard L, Ridings JE, Hood SR, Aartsma-Rus A: The Dynamics of Compound, Transcript, and Protein Effects After Treatment With 2OMePS Antisense Oligonucleotides in mdx Mice. *Mol.Ther.Nucleic Acids* 2014, 3:e148.
 32. Wu B, Cloer C, Lu P, Milazi S, Shaban M, Shah SN, Marston-Poe L, Moulton HM, Lu QL: Exon skipping restores dystrophin expression, but fails to prevent disease progression in later stage dystrophic dko mice. *Gene Ther.* 2014, 21:785-793.
*Elegant study that outlines the importance of the time of intervention on therapeutic effects that can be expected
 33. Osman EY, Miller MR, Robbins KL, Lombardi AM, Atkinson AK, Brehm AJ, Lorson CL: Morpholino antisense oligonucleotides targeting intronic repressor Element1 improve phenotype in SMA mouse models. *Hum.Mol.Genet.* 2014, 23:4832-4845.
 34. Hua Y, Liu YH, Sahashi K, Rigo F, Bennett CF, Krainer AR: Motor neuron cell-nonautonomous rescue of spinal muscular atrophy phenotypes in mild and severe transgenic mouse models. *Genes Dev.* 2015, 29:288-297.
*Elegant study that assesses the effect of restoring SMN only in the periphery
 35. Nizzardo M, Simone C, Salani S, Ruepp MD, Rizzo F, Ruggieri M, Zanetta C, Brajkovic S, Moulton HM, Muehlemann O, Bresolin N, Comi GP, Corti S: Effect of combined systemic and local morpholino treatment on the spinal muscular atrophy Delta7 mouse model phenotype. *Clin.Ther.* 2014, 36:340-356.
 36. Hua Y, Sahashi K, Rigo F, Hung G, Horev G, Bennett CF, Krainer AR: Peripheral SMN restoration is essential for long-term rescue of a severe spinal muscular atrophy mouse model. *Nature* 2011, 478:123-126.

37. Donnelly CJ, Zhang PW, Pham JT, Haeusler AR, Mistry NA, Vidensky S, Daley EL, Poth EM, Hoover B, Fines DM, Maragakis N, Tienari PJ, Petrucelli L, Traynor BJ, Wang J, Rigo F, Bennett CF, Blackshaw S, Sattler R, Rothstein JD: RNA toxicity from the ALS/FTD C9ORF72 expansion is mitigated by antisense intervention. *Neuron* 2013, 80:415-428.
38. Lagier-Tourenne C, Baughn M, Rigo F, Sun S, Liu P, Li HR, Jiang J, Watt AT, Chun S, Katz M, Qiu J, Sun Y, Ling SC, Zhu Q, Polymenidou M, Drenner K, Artates JW, McAlonis-Downes M, Markmiller S, Hutt KR, Pizzo DP, Cady J, Harms MB, Baloh RH, Vandenberg SR, Yeo GW, Fu XD, Bennett CF, Cleveland DW, Ravits J: Targeted degradation of sense and antisense C9orf72 RNA foci as therapy for ALS and frontotemporal degeneration. *Proc.Natl.Acad.Sci.U.S.A* 2013, 110:E4530-E4539.
39. Tei S, Ishii HT, Mitsunashi H, Ishiura S: Antisense oligonucleotide-mediated exon skipping of CHRNA1 pre-mRNA as potential therapy for Congenital Myasthenic Syndromes. *Biochem.Biophys.Res. Commun.* 2015.
40. Wein N, Avril A, Bartoli M, Beley C, Chaouch S, Laforet P, Behin A, Butler-Browne G, Mouly V, Krahn M, Garcia L, Levy N: Efficient bypass of mutations in dysferlin deficient patient cells by antisense-induced exon skipping. *Hum.Mutat.* 2010, 31:136-142.
41. Taniguchi-Ikeda M, Kobayashi K, Kanagawa M, Yu CC, Mori K, Oda T, Kuga A, Kurahashi H, Akman HO, DiMauro S, Kaji R, Yokota T, Takeda S, Toda T: Pathogenic exon-trapping by SVA retrotransposon and rescue in Fukuyama muscular dystrophy. *Nature* 2011, 478:127-131.
42. Scharner J, Figeac N, Ellis JA, Zammit PS: Ameliorating pathogenesis by removing an exon containing a missense mutation: a potential exon-skipping therapy for laminopathies. *Gene Ther.* 2015.
*Very comprehensive analysis to assess which exons are potential targets for therapeutic exon skipping for laminopathies
43. Raz V, Buijze H, Raz Y, Verwey N, Anvar SY, Aartsma-Rus A, van der Maarel SM: A novel feed-forward loop between ARIH2 E3-ligase and PABPN1 regulates aging-associated muscle degeneration. *Am.J.Pathol.* 2014, 184:1119-1131.
44. Clayton NP, Nelson CA, Weeden T, Taylor KM, Moreland RJ, Scheule RK, Phillips L, Leger AJ, Cheng SH, Wentworth BM: Antisense Oligonucleotide-mediated Suppression of Muscle Glycogen Synthase 1 Synthesis as an Approach for Substrate Reduction Therapy of Pompe Disease. *Mol.Ther.Nucleic Acids* 2014, 3:e206.
45. Rigo F, Chun SJ, Norris DA, Hung G, Lee S, Matson J, Fey RA, Gaus H, Hua Y, Grundy JS, Krainer AR, Henry SP, Bennett CF: Pharmacology of a central nervous system delivered 2'-O-methoxyethyl-modified survival of motor neuron splicing oligonucleotide in mice and nonhuman primates. *J.Pharmacol.Exp.Ther.* 2014, 350:46-55.
46. Hua Y, Liu YH, Sahashi K, Rigo F, Bennett CF, Krainer AR: Motor neuron cell-nonautonomous rescue of spinal muscular atrophy phenotypes in mild and severe transgenic mouse models. *Genes Dev.* 2015, 29:288-297.



**Peptide conjugation of 2'-O-methyl
phosphorothioate antisense oligonucleotides
enhances cardiac uptake and exon skipping in
mdx mice**

Silvana M.G. Jirka^a, Hans Heemskerk^a, Christa L. Tanganyika-de Winter^a,
Daan Muilwijk^b, Kar Him Pang^b, Peter C. de Visser^b, Anneke Janson^b, Tatyana
G. Karnaoukh^b, Rick Vermue^b, Peter.A.C.'t Hoen^a, Judith C.T. van Deutekom^b,
Begoña Aguilera^b and Annemieke Aartsma-Rus^a

^aDepartment of Human Genetics, Leiden University Medical Center, 2300 RC
Leiden, The Netherlands

^bProsensa Therapeutics B.V., 2333 CH Leiden, The Netherlands

Nucleic Acid Ther. 2014 Feb;24(1):25-36

Abstract

Antisense oligonucleotide (AON)-mediated exon skipping is a promising therapeutic approach for Duchenne muscular dystrophy that is currently being tested in various clinical trials. This approach is based on restoring the open reading frame of dystrophin transcripts resulting in shorter but partially functional dystrophin proteins as found in patients with Becker muscular dystrophy. After systemic administration a large proportion of AONs ends up in the liver and kidneys. Therefore, enhancing AON uptake by skeletal and cardiac muscle would improve the AONs' therapeutic effect. For phosphorodiamidate morpholino oligomer they use nonspecific positively charged cell penetrating peptides to enhance efficacy. However, this is challenging for negatively charged 2'-O-methyl phosphorothioate oligomer. Therefore, we screened a 7-mer phage display peptide library to identify muscle and heart homing peptides *in vivo* in the *mdx* mouse model and found a promising candidate peptide capable of binding muscle cells *in vitro* and *in vivo*. Upon systemic administration in dystrophic *mdx* mice, conjugation of a 2'-O-methyl phosphorothioate AON to this peptide indeed improved uptake in skeletal and cardiac muscle, and resulted in higher exon skipping levels with a significant difference in heart and diaphragm. Based on these results, peptide conjugation represents an interesting strategy to enhance the therapeutic effect of exon skipping with 2'-O-methyl phosphorothioate AONs for Duchenne muscular dystrophy.

1. Introduction

Duchenne muscular dystrophy (DMD) is a severe X-linked muscle-wasting disorder typically caused by out of frame mutations in the *DMD* gene, and affecting 1 in 5,000 newborn boys¹. DMD patients suffer from progressive muscle weakness, are generally wheel-chair dependent before the age of 12, and die around the third decade of their life due to respiratory and cardiac failure². Exon skipping is a promising therapeutic approach for DMD that is currently being tested in clinical trials³. This approach is based on restoration of the dystrophin transcript's open reading frame by manipulating pre-mRNA splicing using antisense oligonucleotides (AONs). This results in shorter but partially functional dystrophin proteins as found in patients with the less severe Becker muscular dystrophy (BMD)⁴⁻⁷. The exon skipping approach depends on adequate uptake by the target tissues of the AONs. Over 30% of the human body consists of muscle; therefore a body-wide effect is required to treat DMD. AONs with 2'-O-methyl phosphorothioate (2OMePS) and phosphorodiamidate morpholino oligomer (PMO) chemistries have been studied in most detail for DMD.

AONs are modified DNA or RNA oligomers, and the modifications render the AONs more resistant to RNases and DNases, improving stability *in vivo*. However, while PMOs are apparently fully resistant to nucleases, 2OMePS

AONs still suffer from some breakdown. Upon systemic treatment there are certain barriers that an AON needs to overcome to reach the nucleus of skeletal muscle fibers. AONs are very small (~8 kDa) and as such will be filtered out by the kidney efficiently. For PMOs the vast majority is cleared through urine within an hour of treatment, leading to very short serum half-lives. By contrast, due to low affinity binding to serum proteins by 2OMePS AONs, renal filtration is largely prevented, leading to longer half-lives. In addition, to be effective, AONs also need to pass the endothelium of their target tissues, enter the tissue and (when taken up by endocytosis) have to escape from the endosomes to reach the nucleus, where splicing takes.

Based on positive results from different preclinical animal experiments and phase 1/2 clinical trials, showing dystrophin restoration after subcutaneous injections with 2OMePS AONs and intravenous injections with PMOs, one can conclude that systemic delivery is feasible⁸⁻¹⁵. However, a large proportion of the AON ends up in liver and kidney (2OMePS) or kidney (PMO), and is lost for targeting muscle¹⁶. Furthermore, while AONs appear to be taken up by dystrophic skeletal muscles, animal models have shown that the effect of AONs in heart is less (2OMePS) or minimal (PMO). Therefore, improving the uptake of AONs by skeletal but especially also by cardiac muscles is anticipated to further enhance the therapeutic effect of AON treatment.

Cell penetrating peptides (CPP) have been explored to improve uptake of PMOs by target tissues. Basic, positively charged, arginine rich peptides (PPMO)¹⁷ indeed enhanced uptake of PMOs by most tissues, including muscle and heart, and significantly increase exon skipping levels and dystrophin restoration after systemic delivery in *mdx* mice¹⁸⁻²⁰. However, in monkeys, 4-9 mg/kg weekly systemic injections during 4 weeks with AVI-5038, a PPMO targeting human dystrophin exon 50, resulted in tubular degeneration in the kidney¹⁸. The fact that apparently higher animals are more sensitive to arginine-rich peptide related toxicity than mice may limit their clinical application^{17,19}.

Tissue-specific homing peptides have also been investigated to improve uptake of AONs. These peptides home to the target of interest and bind or are taken up by the cells of interest, but do not necessarily penetrate the cells like CPPs. Phage display biopanning is a well-described technique to identify homing peptides for specific targets^{21,22}. Several muscle or heart targeting peptides have been reported to date²³⁻²⁵, of which the ASSLNIA muscle targeting peptide²⁴ has been further tested in conjugation to PPMOs, resulting in improved dystrophin restoration. Interestingly, this was only seen when the muscle-specific peptide was located between the arginine-rich peptide and the PMO, while linking the muscle-specific peptide to the 5' end of the PPMO reduced the efficiency²⁶. For 2OMePS AONs, conjugation of highly positively charged peptides (such as arginine rich

peptides) is challenging due to strong electrostatic interactions between the positive peptide and the negatively charged AON backbone, leading to aggregate formation. Therefore in a different approach we screened a 7-mer phage display peptide library for non-charged homing peptides to enhance uptake and exon skipping in muscle and heart *in vivo* in the *mdx* mouse model. We here report the identification of a 7-mer peptide which, after conjugation to a 2OMePS AON, resulted in significantly improved AON uptake and effect by heart and diaphragm upon systemic administration in the *mdx* mouse model.

2. Material and Methods

In Vivo Biopanning

Four to five weeks old *mdx* mice were injected intravenously with 2×10^{11} phages from the naïve or enriched libraries (Ph.D.-7™ Phage Display Peptide Library kit, New England Biolabs, Beverly, Maryland, one animal per round). Mice were perfused with PBS after one hour to remove unbound phages. The gastrocnemius and heart muscles were isolated and washed 3 times with Tris-buffered saline (TBS). Subsequently the organs were homogenized in 2 ml TBS with MagNA Lyser green beads (Roche Diagnostics, the Netherlands) in the MagNA Lyser (Roche Diagnostics, the Netherlands) according to the manufacturer's protocol. The suspension was titrated and amplified according to the protocol provided with the phage library. Up to 4 rounds of biopanning were performed for each fraction. After the third and fourth round, phages were plated and colonies were picked. DNA was isolated and prepared for Sanger sequencing with the ABI PRISM® 3730 Analyzer (Applied Biosystems).

Peptide synthesis

7-mer peptides were synthesized by standard Fmoc solid phase peptide chemistry on a PS3 or Tribute Peptide synthesizer (Protein Technologies, USA), using 5eq. HCTU (Protein Technologies, USA eq.) as activating reagent and DIPEA (10 eq.) as base. A fluorescent label was manually coupled to the resin-bound peptides by treatment with 5(6)-carboxyfluorescein *N*-hydroxysuccinimide ester and triethylamine (all from Acros, Belgium) in *N,N*-dimethylformamide (DMF). After cleavage and deprotection TFA trifluoroacetic acid (TFA)/triisopropylsilane (TIS)/H₂O 95/2.5/2.5 (v/v)

or TFA/ thioanisole/TIS/H₂O 90/2.5/2.5/5 (v/v) for peptide sequences containing Met], filtration, precipitation in cold diethyl ether and centrifugation, crude 5(6)-carboxyfluorescein amide (FAM) - labeled peptides were obtained. Peptides were purified by RP-HPLC and analyzed by electrospray ionization mass spectrometry (ESI-MS) (positive mode). Fluorescently labeled peptide concentrations were determined by spectrophotometric analysis at 490 nm at pH 7.5.

In vitro uptake studies of FAM-labeled peptides

Primary human control myoblasts were grown in NutMix F-10 (HAM) medium supplemented with GlutaMax-I, 20% fetal bovine serum (FBS) and 1% Penicillin/streptomycin (P/S (all from Gibco-BRL, the Netherlands) in flasks coated with purified bovine dermal collagen for cell culture (Nutacon B.V. the Netherlands). Cells were plated on collagen coated glass slides, in 6 wells plates and grown to 90% confluence before switching to differentiation medium (Dulbecco's medium (without phenol red) with 2% FBS, 1% P/S, 2% glutamax and 1% glucose (all from Gibco-BRL, the Netherlands)). Cells were allowed to differentiate for 7-14 days. Peptides were dissolved in water and if necessary acidic acid was used to properly dissolve the peptide. Final concentrations were determined by spectrophotometric analysis at 490 nm at pH 7.5. Upon sufficient differentiation, cells were washed twice with hank's balanced salt solution (HBSS), and 1 ml of medium without serum was added with 0.45 nM or 2.25 nM of fluorescent peptide. After incubation for 3 hours at 37 °C and 5% CO₂, 2 ml of differentiation medium was added. Cells were fixed 2 days later for 5 minutes with methanol (-20 °C) and air dried for 30 minutes. The glass slides were taken out and mounted in mounting medium (Vectashield hard set (Vector laboratories)). After drying for 30 minutes, the glass slides were analyzed with fluorescence microscopy (Leica DM RA2) using a CCD camera (Leica DC 350 FX).

In vivo evaluation of FAM labeled peptides by intramuscular injection in the *mdx* mouse model

Four to six week old *mdx* mice were injected in the gastrocnemius muscle with 2.5 nmol FAM- labeled peptides in 40 µl saline (n=1 for each peptide). After 3 days the mice were sacrificed and the muscles were snap frozen in liquid nitrogen-cooled isopentane. Subsequently, 8 µm sections were cut with a cryotome, perpendicular to the muscle fibers and collected on a positively charged glass slide. The slides were fixed with -20 °C acetone and mounted in mounting medium (Vectashield hard set). The slides were analyzed with fluorescence microscopy (Leica DM RA2) using a charge-coupled device (CCD) camera (Leica DC 350 FX).

Oligonucleotide synthesis

The 20-mer 2'-*O*-methyl phosphorothioate RNA (5'-ggc caa acc ucg gcu uac cu-3') targeting mouse exon 23 (23AON)²⁹ was synthesized on an AKTA prime OligoPilot-100 (GE Healthcare, UK) synthesizer using the protocols recommended by the supplier. The oligonucleotide was cleaved and deprotected in a two-step sequence (diethylamine followed by concentrated ammonia treatment), purified by reversed phase (RP)-HPLC, dissolved in water and an excess of NaCl was added to exchange ions. After evaporation, the oligonucleotide was redissolved in water, desalted by FPLC, and lyophilized. Mass spectrometry confirmed the identity of the AON, and

its purity (determined by UPLC) was 86%.

Peptide oligonucleotide conjugate synthesis

Peptide P4 was assembled on a peptide synthesizer as described above and maleimide propionic acid was subsequently coupled on-line. Deprotection, cleavage from the resin, and subsequent precipitation in cold ether, afforded crude maleimide-peptide, which was used without further purification in the conjugation step. The oligonucleotide for conjugation to the peptide was synthesized with a thiol modifier C6 S-S phosphoramidite (Link Technologies) coupled on-line to the 5' end. Treatment of the crude resin with 40% aqueous ammonia and 0.1 M dithiothreitol led to the concomitant cleavage of the solid support, deprotection of the nucleobases and internucleoside linkages, and reduction of the disulfide bond. Crude thiol-modified oligonucleotide was purified by RP- HPLC, and directly conjugated to the maleimide-peptide (5 eq.) *via* thiol-maleimide coupling in phosphate buffer (pH 7) at ambient temperature for 16 hours. Crude product was purified by HPLC, dissolved in water, and an excess of NaCl was added to exchange ions. After evaporation of the solution, the peptide-conjugated AON (P4-23AON) was redissolved in water, desalted by FPLC and lyophilized. Mass spectrometry confirmed the identity of the compound.

Transfection of (P4-)23AON and sense staining on primary human control myotubes

Differentiated primary human control myoblasts cells were washed twice with HBSS, and 1 ml of medium without serum was added with 2.25 nmol of P4-23AON or 23AON. After incubation for 3 hours at 37 °C and 5% CO₂, 2 ml of fusion medium was added with 2% serum. Two days later the cells were washed three times with PBS and fixed for 30 minutes in fixation buffer. The slides were washed with 1x PBS/5 mM MgCl₂ for 30 minutes and pre-hybridized for 30 minutes in 125 µl pre-hybridization buffer (40% deionized formamide, 2 times SSC buffer (300mM NaCl and 30nM trisodium citrate, pH 7.0)), followed by an overnight incubation in 125µl hybridization mix (32% deionized formamide, 2 times SSC buffer, 0.2mg/ml BSA, 10mg/ml Dextran sulphate, 1 mg/ml fish sperm and the 5'-Cy5 labeled sense oligonucleotide (5'□3', ccg gtt tgg agc cga atg ga) in a water bath at 37 °C in the dark. The slides were washed in wash buffer (40% deionized formamide 2 times SSC buffer) for 2 times 20 minutes in a water bath at 37 °C in the dark followed by a wash step with SSC buffer for 20 minutes at room temperature in the dark and a quick incubation with 1:5,000 4',6-diamidino-2-phenylindole (DAPI) in PBS to stain nuclei. Finally the slides were mounted in mounting medium (vectashield hard set (vector laboratories)) and after 30 minutes drying, the glass slides were analyzed with fluorescent microscopy (Leica DM RA2) using a CCD camera (Leica DC 350 FX).

AON treatment, RNA isolation and RT-PCR analysis of (P4-)23AON in differentiated mouse myogenic cells

C2C12 cells were grown in Dulbecco's medium (without phenol red) supplemented with 10% FBS, 1% P/S, 2% Glutamax and 1% glucose (all from Gibco-BRL, the Netherlands) in collagen coated flasks. Cells were seeded in collagen coated 6 wells plate with proliferation medium and grown until confluence. The cells were washed twice with HBSS and Dulbecco's medium (without phenol red) supplemented with 2% FBS, 1% P/S, 2% Glutamax and 1% glucose (all from Gibco-BRL, the Netherlands) was added to induce differentiation. At day 8 of differentiation the cells were incubated with 500nM P4-23AON or 23AON with or without 3.5 µl PEI (as transfection reagent)/mg AON in differentiation medium (1 ml). After 3 hours the medium was removed and fresh differentiation medium added (3 ml). After 48 hours the cells were washed twice with HBSS and RNA was isolated by adding 500 µl TriPure (Roche diagnostics, the Netherlands) to each well to lyse the cells. This was followed by chloroform extraction in a 1/5 ratio on ice for 5 minutes. The remaining cell debris was pelleted down by centrifugation (4 °C, 15 minutes, 15,4000 rcf) and the upper aqueous phase precipitated for 30 minutes on ice with equal volume of isopropanol. The RNA was pellet down by centrifugation (4 °C, 15 minutes, 15,400 rcf) and the pellet washed with 70% ethanol. The final RNA pellet was dissolved in milli-Q water. For complementary DNA (cDNA) synthesis, 400 ng of RNA was used in a 20 µl reaction with a specific primer (ctt taa ggc ttc ctt tct ggt g) and transcriptase reverse transcriptase (Roche Diagnostics, the Netherlands) for 30 minutes at 55°C and 5 minutes at 85°C to terminate the reaction. For reverse transcriptase PCR (RT-PCR) analysis 3 µl of cDNA was incubated with 0.625 U AmpliTaq polymerase (Roche Diagnostics, the Netherlands), 10 pM of primers (reverse primer ctt taa ggc ttc ctt tct ggt g, forward primer: aga aaa ggg aca ggg gcc a) and 1 times supertaq PCR buffer (Enzyme technologies Ltd) and amplified for 20 cycles each consisting of an incubation for 40 sec at 94 °C, 40 sec at 60 °C and 80 sec at 72 °C. This PCR was followed by a nested PCR. For the nested PCR analysis 1.5 µl of the first PCR was incubated with 1.25 U AmpliTaq polymerase (Roche Diagnostics, the Netherlands), 20 pM of primers (reverse primer: cag cca tcc att tct gta agg, forward primer: atc cag cag tca gaa agc aaa) and 1 times supertaq PCR buffer (Enzyme technologies Ltd) and amplified for 32 cycles each consisting of an incubation for 40 sec at 94 °C, 40 sec at 60 °C and 60 sec at 72 °C. PCR fragments were analyzed using 1% agarose gel electrophoresis. Exon skip levels were semi-quantitatively determined as the percentages of the total (wild type and skipped) product with the Agilent 2100 bioanalyzer.

Systemic study with P4-23AON and 23AON in *mdx* mice

Four to five weeks old *mdx* mice (5 mice per group) were subcutaneous injected 4 times per week, with 50 mg/kg of AON in 100 µl of saline or the molar equivalent of peptide conjugated AON (6.8 µmol) for 6 weeks. Blood samples were obtained from the tail vein for plasma pharmacokinetics analysis (PK) 10 minutes, 30 minutes, 1 hour and 6 hours after the last injection. All mice were sacrificed 1 week after the last injection by perfusion with PBS, after taking blood from the tail vein of all mice to determine plasma parameters. Gastrocnemius, quadriceps, tibialis anterior, triceps and diaphragm muscles, heart, liver and kidney were isolated to determine exon skipping levels and AON concentrations in these tissues.

Plasma parameters

Blood was collected in microvettes (Sarstedt B.V. the Netherlands). Glutamate pyruvate transaminase (GPT), alkaline phosphates (ALP) glutamic oxaloacetic transaminase (GOT) hemoglobin (HB), urea and creatine kinase (CK) were determined using Reflotron strips (Roche Diagnostics, the Netherlands) in the Reflotron Plus machine (Roche Diagnostics, the Netherlands).

Quantification of AON levels in plasma and tissue samples

For measuring the concentration of 23AON in plasma and tissue samples a hybridization-ligation assay based on one previously published was used³⁵. Tissues were homogenized in 100 mM Tris-HCl pH 8.5, 200 mM NaCl, 0.2% SDS, 5 mM EDTA and 2 mg/mL proteinase K using zirconium beads (1.4 mm; OPS Diagnostics, Lebanon, NJ) in a MagNA Lyser (Roche Diagnostics, the Netherlands). Samples were diluted 600 and 6000 times (muscle) or 6000 and 60000 (liver and kidney) in pooled control *mdx* tissue in PBS.

Calibration curves of the analyzed 23AON prepared in 60 times pooled control mouse *mdx* tissue in PBS were included. All analyses were performed in duplicate. For plasma the samples were diluted (t=0 100 times and 200 times, t=10 min, 30 min, 1h 1000 times and 10000 times and t=6h 100 times and 1000 times) in pooled control plasma of *mdx* mice in PBS. Calibration curves of the analyzed 23AON prepared in 100 times pooled control plasma of *mdx* mice in PBS were included.

Determination of exon skipping levels in *mdx* mice

Samples from muscle and heart were homogenized in RNA- Bee (Campro Scientific, Veenendaal, the Netherlands) solution using a MagNA Lyser (Roche Diagnostics, the Netherlands) and MagNA Lyser green beads (Roche Diagnostics, the Netherlands). Total RNA was isolated and purified according manufacturer's instructions. For complementary DNA (cDNA) synthesis, 400 ng of RNA was used in a 20 µl reaction with random

hexamers and transcriptor reverse transcriptase (Roche Diagnostics, the Netherlands) for 45 minutes at 42°C. For PCR analysis 1.5 µl of cDNA was incubated with 1.25 U taq polymerase (Roche Diagnostics, the Netherlands), 20 pM of primers (reverse primer: cag cca tcc att tct gta agg, forward primer: atc cag cag tca gaa agc aaa) and 1 times supertaq PCR buffer (Enzyme technologies Ltd) and amplified for 30 cycles each consisting of an incubation for 30 sec at 94 °C, 30 sec at 60 °C and 30 sec at 72 °C. PCR fragments were analyzed by 1% agarose gel electrophoresis. Exon skipping levels were semi-quantitatively determined as the percentages of the total (wild type and skipped) product with the Agilent 2100 bioanalyzer.

Table 1. Overview of selected peptide sequences

Peptide (P)	Sequence	Detected	Tissue	Comments
1	LYQDYSL	twice	heart 3rd round	
2	LPWKPLG	twice	heart 3rd and 4th round	
3	TPAHPNY	twice	heart 3rd and 4th round	
4	LGAQSNF	once	heart 4th round	low prevalence
5	PGAQSNF	once	heart 3rd round	
6	VNSPETHS	once	heart 3rd round	
7	VNSATHS	once	heart 4th round	
8	YQDSEAKT	once	heart 3rd round	negative control
9	TALPPSY	twice	muscle 3rd and 4th round	
10	AMISAIH	once	muscle 3rd round	low prevalence
11	HVIANAG	once	muscle 3rd round	low prevalence
12	EPLQLKM	twice	heart and muscle 4th round	reported as nuclei targeting
13	GNTPSRA	once	muscle 4th round	negative control

3. Results

To identify peptides homing to muscle and heart, an *in vivo* biopanning was performed in the *mdx* mouse model with a 7-mer phage display peptide library. 2×10^{11} phages from the PhD-7 library were injected intravenously and mice were perfused after 1 hour, after which gastrocnemius and heart muscles were isolated. Tissues were homogenized and recovered phages were amplified for the next screening round. After the third and fourth round of screening, a total of 52 colonies were selected and sequenced. For each peptide sequence we consulted Sarotup²⁷ and Pepbank²⁸ databases to identify false positives. This led to the exclusion of 8 peptides for further experiments, as these peptides had been identified before and were therefore not likely to be target specific binders. A series of peptide sequences occurring more than once or with recurrent stretches of 6 amino acids was identified (Table 1). Because not all amino acids occur in the library with the same frequency, some peptide sequences are less common than others. After calculating the prevalence of each of the found peptide sequences, two peptide sequences (P10 and P11) that were found only once were also included based on the fact that they had a very low prevalence in the library. As negative controls we included three peptide sequences from the selection, which showed up in the Sarotup database (P8, P12 and P13).

To evaluate uptake and intracellular distribution, selected peptides were synthesized with a FAM label and incubated with primary human control myotube cultures for 48 hours (2.25 and 0.8 nM respectively) and analyzed with fluorescence microscopy (figure 1A). Clear fluorescence was observed for 7 of the 12 peptides, also at a lower concentration of 0.8 nM (figure 1B). Based on the highest fluorescence intensity, P1, P2, P4 and P11 were chosen for *in vivo* evaluation. Four to six weeks old *mdx* mice were intramuscularly injected with 2.5 nmol of labeled peptide in the gastrocnemius muscle. Muscles were isolated 3 days after injection, and cross-sections were analyzed with fluorescence microscopy (figure 2). Clear fluorescence was observed for P4 at the membrane. In contrast, P11 was found negative, and P2 showed only some weak staining close to the injection site. P1 resulted in strong fluorescence, but as acetic acid was needed to dissolve this peptide, it is likely that this resulted in damaged muscle fibers leading to the observed uptake of the labelled peptide or to autofluorescence of necrotic cells.

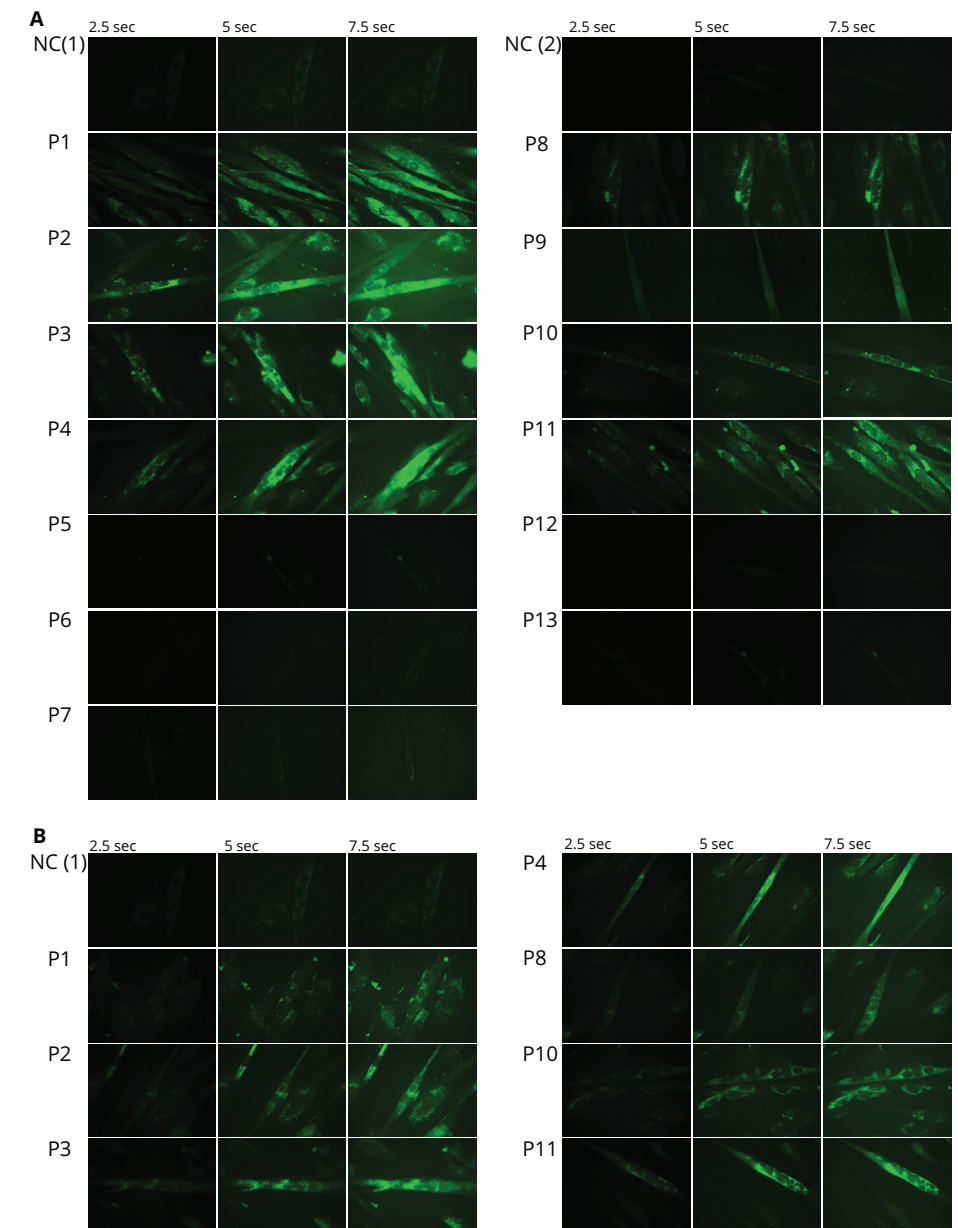


Figure 1. Uptake of FAM-labeled peptides by primary human control myotubes. Primary human control myotubes were incubated with (A) 2.25 or (B) 0.45 nmol of FAM-labeled peptide. After 48 hours the cells were washed and analysed at three different exposure times (2.5, 5 and 7.5 seconds) with fluorescence microscopy. Representative pictures are shown. NC is un-transfected control, P1-13 are the peptides.

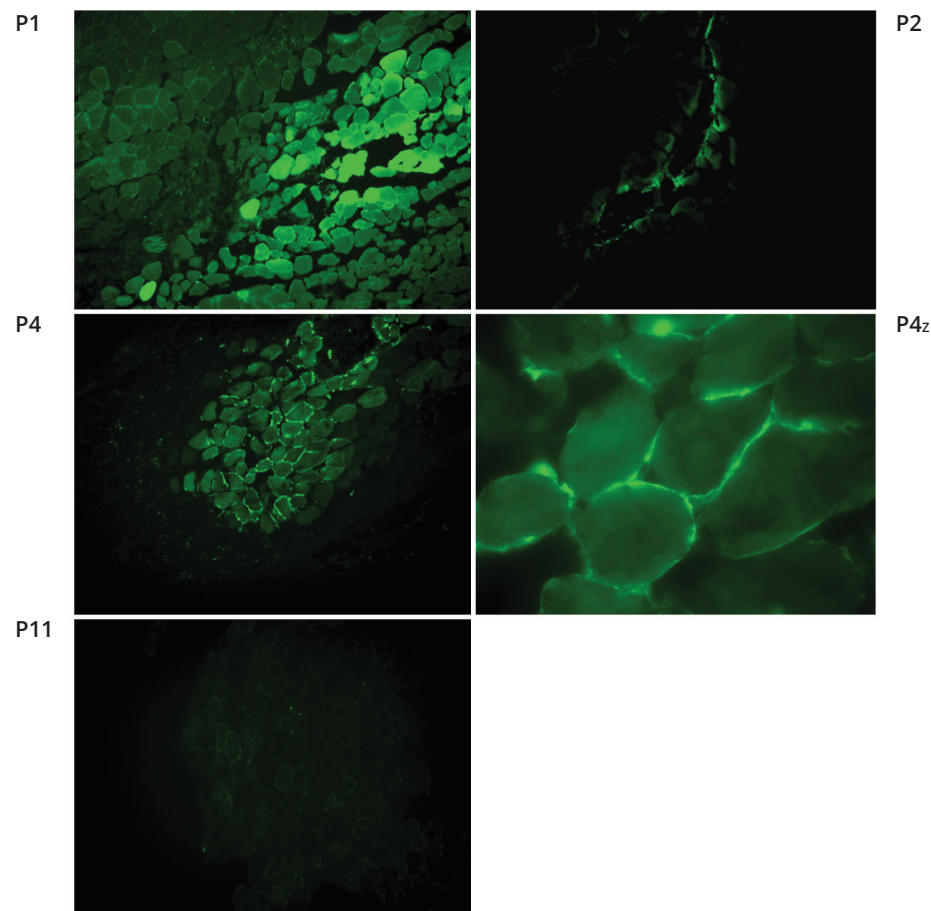


Figure 2. Uptake of FAM-labeled peptides in vivo after intramuscular injection in the mdx mouse model. Four to six weeks old mdx mice were intramuscularly injected with 2.5 nmol FAM-peptide in the gastrocnemius muscle. After 3 days the muscle was isolated and muscle sections were analysed using fluorescence microscopy. Representative pictures are shown. P1, 2, 4 and 11 are candidate peptides. P4z is a 5 times enlargement of P4.

Showing the best results, P4 was conjugated to a 20MePS AON specific for mouse dystrophin exon 23 (23AON), which can induce exon skipping and restore dystrophin in the *mdx* mouse²⁹. 23AON and P4-conjugated 23AON (P4-23AON) were incubated with primary human control myotube cultures without a transfection reagent. To detect the location of the (P4-)23AON, we used a sense DNA oligonucleotide with a Cy5 label and observed more a punctuate fluorescence pattern for P4-23AON compared to 23AON (figure 3).

To confirm that the efficacy of the 23AON is not influenced by the conjugation of the peptide, differentiated C2C12 mouse myogenic cells were incubated with 500 nM of P4-23AON or 23AON with PEI as transfection reagent and without a transfection reagent. RNA was isolated 48 hours after incubation, and exon skipping percentages were determined by RT-PCR (figure 4). No exon skipping was seen when the cells were incubated with P4-23AON or 23AON without the use of a transfection reagent; a possible explanation for this is endosomal entrapment³⁰ of the AONs, as is suggested by the punctuate staining observed in figure 3. PEI is known to facilitate endosomal escape of compounds after transfection and indeed, in cells incubated with PEI as a transfection reagent and AONs, ~50% exon skipping was observed for both 23AON and P4-23AON. This indicates that the conjugation of P4 to the 23AON does not interfere with the exon skipping ability of the 23AON.

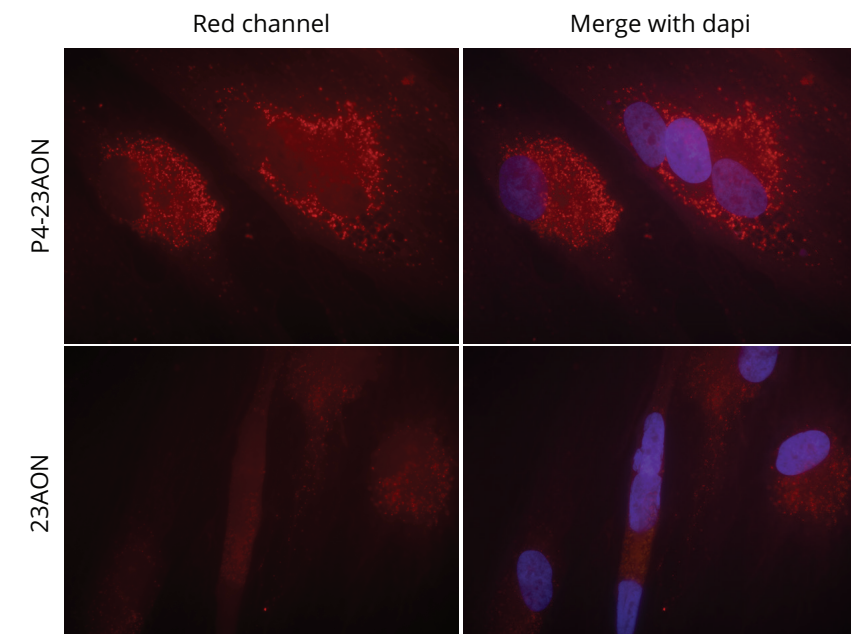


Figure 3. Sense staining of 23AON and P4-23AON transfected primary human control myotube cells. Differentiated primary humane control myotubes were incubated with 2.25 nmol of P4-23AON or 23AON respectively in serum free differentiation medium. After 3 hours 2 ml of differentiation medium with 2% serum was added and 48 hours later the cells were hybridized with a Cy5-labeled sense DNA oligonucleotide and analyzed with fluorescence microscopy. Representative pictures are shown.

Finally, we tested whether this peptide could enhance 23AON uptake by heart and muscle after systemic treatment of an animal model. For 20MePS AONs the optimal dose and route for systemic AON

treatment in *mdx* mice appears to be 200 mg/kg/week by subcutaneous administration^{12,31}, which would correspond to a dose of 16 mg/kg in humans after correcting for differences in body surface area between small and large animals <http://www.fda.gov/downloads/Drugs/GuidanceComplianceRegulatoryInformation/Guidances/ucm078932.pdf>. In this study *mdx* mice (5 per group) were subcutaneously injected with 4 weekly doses of 50 mg/kg of 23AON or the molar equivalent of P4-23AON for 6 weeks. Plasma samples were collected at different time points after the last injection, mice were sacrificed one week later and several tissues were harvested for bioanalysis. AON levels in plasma, organs and tissues were determined. Compared to 23AON, P4-23AON showed higher AON levels in plasma for all time points (figure 5a). This could relate to a higher availability of the conjugate due to lower immediate clearance rate by liver and kidney. In most isolated tissues, P4-23AON levels were slightly higher than 23AON levels, with a significant difference in heart ($p=0.0017$, figure 5b). Since we also observed slightly higher levels in liver and kidney for P4-23AON than 23AON, we calculated the muscle/liver, muscle/kidney, heart/liver, and heart/kidney ratios. This revealed improved relative uptake of the P4-23AON conjugate in muscle and especially heart compared to 23AON for both liver and kidney (figures 5c,d). Accordingly, exon skipping levels were higher in all tissues for P4-23AON with a significant difference for heart and diaphragm ($P=0.02$ and $P=0.001$, respectively, figure 5e)

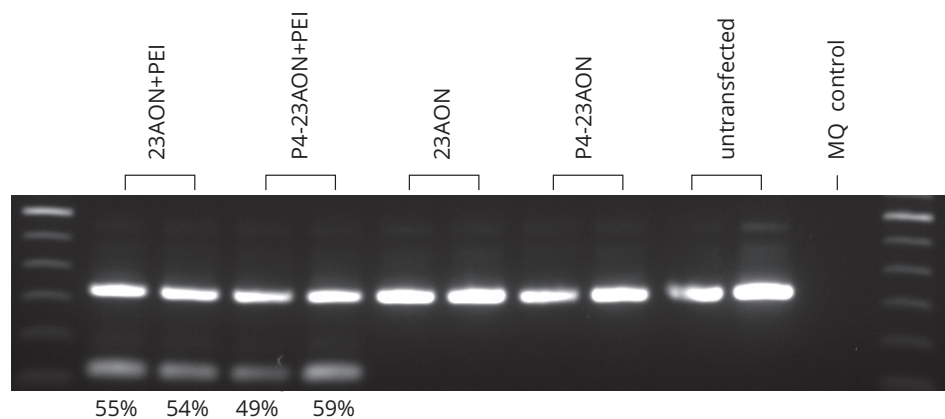


Figure 4. Exon skipping efficacy of 23AON and P4-23AON in differentiated mouse myogenic cells. Mouse myogenic cells were differentiated and transfected in duplo with 500 nM of 23AON or P4-23AON with (1-4) and without (5-8) PEI. The cells were incubated for 48 hours after which RNA was isolated and exon skipping levels analyzed by RT-PCR. Full length and exon skipping fragments were visualized on agarose gel and semi-quantitatively determined by lab-on a chip as the percentages of the total (skip and wild type) product.

To evaluate safety of P4-23AON, body weight was measured over time and plasma parameters for liver and kidney function and damage and muscle integrity were assessed at time of sacrifice (figure 6). Alkaline phosphatase (ALP) a marker for hepatobiliary function, glutamate pyruvic transaminase (GPT) and glutamic oxaloacetic pyruvate transaminase (GOT), which are enzymes that leak in to the bloodstream upon liver and muscle damage, showed no significant differences for P4-23AON and 23AON treated animals and were in the normal ranges for *mdx* mice (figure 6a,b). Also urea (a marker for kidney function) and hemoglobin showed no significant differences between the groups and were within normal levels (figure 6c). We finally measured creatine kinase levels (marker for muscle damage) and observed no difference between P4-23AON and 23AON treated animal (figure 6d). No differences were found when measuring body weight over time (figure 6e).

4. Discussion

For DMD AON-mediated exon skipping has reached phase 3 clinical trials for drisapersen (2OMePS) and eteplirsen (PMO) and seems a promising therapeutic approach. Since over 30% of the human body consists of muscle, systemic treatment is necessary, and seems feasible. However, most of the injected AONs end up in liver and kidney, which decreases the amount that can be taken up by muscle.

Preclinical animal studies suggest that upon systemic AON delivery, body wide dystrophin restoration in skeletal muscles is feasible, while dystrophin restoration in heart may be less effective. There is a possibility that improved muscle function due to dystrophin restoration leads to a higher demand on the heart^{32,33}. Therefore, enhancing uptake of AONs by skeletal but especially cardiac muscle would further improve their therapeutic effect.

Several papers describe arginine rich cell-penetrating peptides to enhance the uptake of PMOs by all tissues¹⁷. The resulting peptide-PMO conjugates (PPMOs) showed increased exon skipping and dystrophin levels in skeletal and cardiac muscle when systemically tested in *mdx* mice. However these peptides are not tissue specific and peptide-related toxicity problems have been observed^{18,19}. In a different approach to improve specific AON uptake by heart and skeletal muscle without using a cell penetrating peptide, we used a phage display peptide library screen to specifically identify muscle and heart homing peptides. Sequencing single colonies after the pre-final and final rounds of selection gave insight in library enrichment. Phage display screenings are known to result in false positive peptides caused by binding to non-target related materials or propagation advantages. Therefore we used Pepbank and Sarotup databases to filter for these false positive peptides^{27,28}.

Samoylova et al describe finding the muscle targeting peptide ASSLNIA²⁴. We did not find this peptide in our biopanning. There are several possible explanations for this. First, we had a different experimental setup (only *in vivo* compared to first *in vitro* than *in vivo*). Second, since one selects peptides from a library containing theoretically 2×10^8 different peptide sequences and analyses only 10-100 clones from the enriched library, it is possible that different peptides are found in different biopanning experiments (including experiments that are performed in parallel). The identification of enriched peptides by DNA sequencing of inserts of 10-100 clones is laborious, while it gives only a small insight in possible candidates and phages that are prone to preferential amplification will constitute a significant subset of sequenced clones. As an alternative approach one can use deep sequencing to analyse millions of insert sequences after a more limiting biopanning³⁴. Third, according to the sarotup target unrelated peptide scanner²⁷, ASSLNIA has a high probability of binding avidin-family proteins, implying that it is possible that this peptide is not entirely target specific.

Ten candidate peptides and 3 control peptides were tested *in vitro*. Of the 3 control peptides, only P8 revealed positive fluorescence *in vitro*, but with lower intensity than some other candidates. Since this peptide was already identified in other biopanning experiments for different targets it is most likely not muscle and/or heart specific²⁷. Control peptide P12 was suggested to target the nuclei of mammary epithelial cells, but was negative for targeting cultured muscle cells; P13 was negative as expected. An interesting finding is the high fluorescence for P4 and the lack of fluorescence for P5, since these peptides only differ in their N-terminal amino acid. This finding highlights the sequence specificity of homing peptides.

Of the four candidate peptides (P1, P2, P4 and P11) selected as promising based on *in vitro* and *in vivo* results, P4 conjugation to 23AON resulted in significantly increased exon skipping in heart and diaphragm. For heart, this is most likely due to the higher levels of P4-23AON compared to 23AON. However, for diaphragm, we did not find significantly improved levels of P4-23AON. Note that it is not possible to distinguish between AONs taken up by cells and AONs sequestered in interstitium with the ELISA used to measure AON levels in tissue homogenates. Therefore there may not always be a clear correlation between the increase in exon skipping and increase of AON levels in the tissues as seen here for the diaphragm. This probably also underlies the fact that exon skipping levels in heart are lower than in skeletal muscles, while AON levels in these tissues are comparable. No significant increase was seen in other skeletal muscle, which is as expected since P4 was selected for uptake by heart (see table 1). The generally higher tissue P4-23AON levels are possibly the result of a lower clearance rate by liver and kidney or faster uptake by muscle. This

is underlined by the higher P4-23AON plasma levels after injection. While we also observed increased P4-23AON levels in liver and kidney at time of sacrifice, the relative levels of P4-23AON in skeletal and cardiac muscle compared to liver and kidney were favourable.

We investigated the safety profile of our P4 conjugate. Based on the fact that all markers for liver and kidney function and damage were unchanged after short term systemic treatment with P4-23AON, we conclude that P4 conjugation does not alter the safety profile of the 23AON in short term treatment of *mdx* mice; however extended studies are required for longer term safety evaluation.

In summary, peptide P4 conjugation slightly enhances skeletal and cardiac muscle uptake of 23AON, resulting in higher exon skipping levels, significant in heart and diaphragm, and is well-tolerated by *mdx* mice after short term treatment. The application of P4 for clinical application will depend on more extensive efficacy and safety studies and mechanism of action, but the approach may be very interesting to further improve the efficacy of both 2OMePS and potentially also PMOs currently in clinical development for DMD.

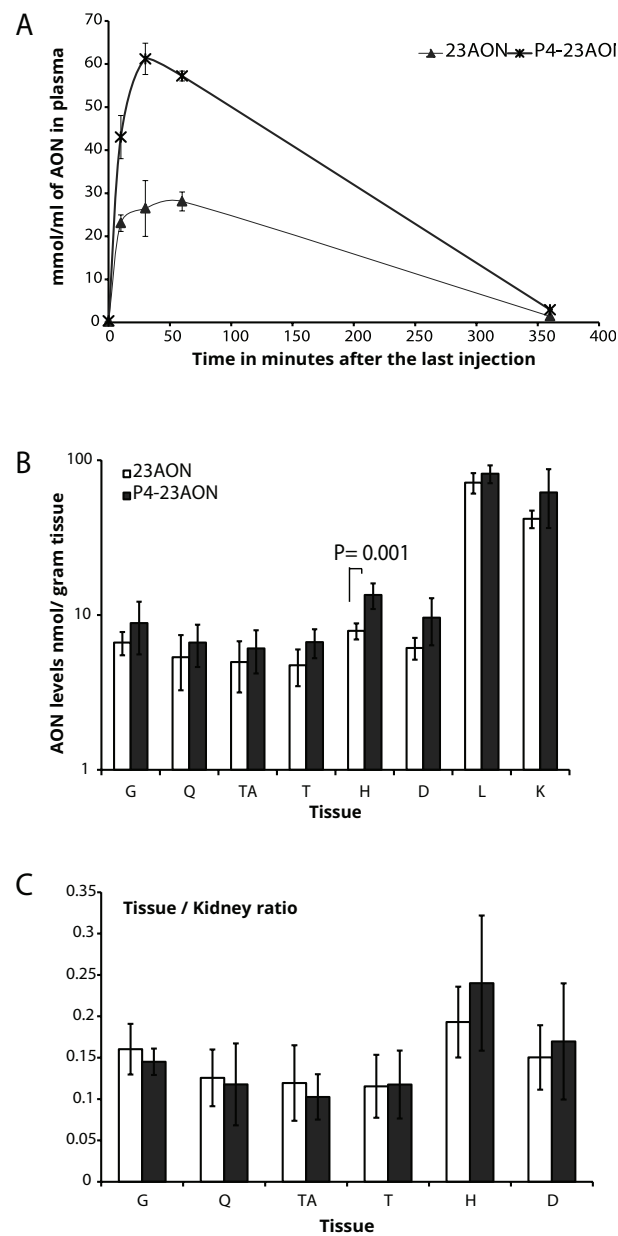
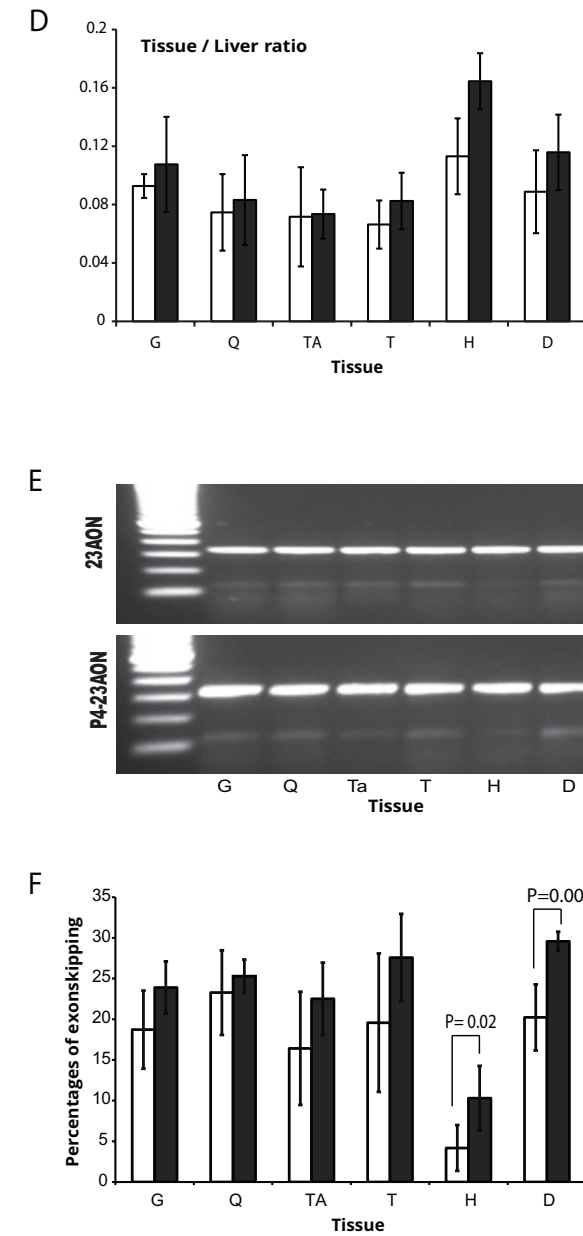


Figure 5. AON levels and exon skipping efficacy after systemic treatment of (P4-)23AON in mdx mice. Mdx mice (5 mice per group) were subcutaneously injected 4 times per week with 50 mg/kg of 23AON or equimolar P4-23AON for 6 weeks. Tissues were harvested for bioanalysis one week after the last injection. A) A hybridization ligation assay was used to measure plasma AON levels before, and 10 minutes, 30 minutes, 1 hour and 6 hours after the last injection. B) The same assay is used to determine tissue AON levels. C) Ratios of AON levels in muscle and heart



compared to kidney. D) Ratios of AON levels in muscle and heart compared to liver. E) Exon skipping assessed by RT-PCR visualized on agarose gel (two representative pictures, one mouse from each group) and semi-quantitatively determined by lab-on-a-chip as the percentages of the total (skip and wild type) product. Bars represent means \pm SD. (T-test for significant $P < 0.05$). G= Gastrocnemius, Q= Quadriceps, TA= Tibialis Anterior, T= Triceps, H= Heart, D= Diaphragm, L= Liver, K=Kidney.

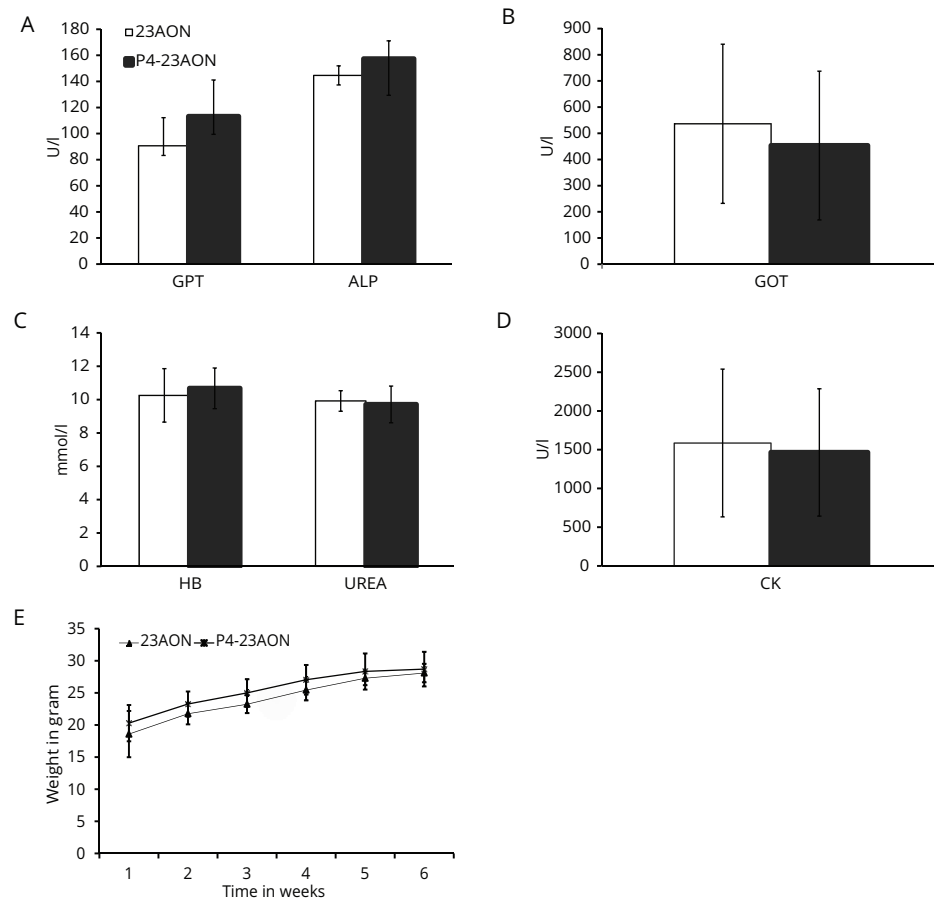


Figure 6. Assessment of safety parameters. *Mdx* mice were subcutaneously injected 4 times per week with 50 mg/kg of 23AON or P4-23AON for 6 weeks. Upon sacrifice (one week after the last injection) blood samples were taken from all mice and plasma was analyzed for levels of A) glutamate pyruvate transaminase (GPT), alkaline phosphates (ALP) B) glutamic oxaloacetic transaminase (GOT) C) hemoglobin (HB), urea and D) creatine kinase (CK). E) Weight over time. Bars represent means \pm SD.

Acknowledgements

This work was funded by a grant from the Dutch Duchenne Parent Project and ZonMw (the Netherlands). All peptides and peptide-AON conjugates were synthesised by Prosensa Therapeutics. All *in vitro* and *in vivo* experiments were performed at the LUMC.

Author disclosure statement

Hans Heemskerk "a", Annemieke Aartsma -Rus "a", and Judith van Deutenkom "b", report being coinventors on patents of the LUMC on exon skipping, licensed by LUMC to Prosensa Therapeutics, and being entitled to a share of royalties. Judith van Deutenkom., Begona Aguilera., Peter de Visser., Anneke Janson., Daan Muilwijk, Kar Him Pang, Rick Vermue and Tatyana G. Karnaoukh report being employed by Prosensa Therapeutics.

Reference

1. Moat, SJ, Bradley, DM, Salmon, R, Clarke, A, Hartley, L (2013) Newborn bloodspot screening for Duchenne muscular dystrophy: 21 years experience in Wales (UK). *Eur J Hum Genet*;
2. Emery, AE (2002) The muscular dystrophies. *Lancet*; 359: 687-695.
3. van Putten M., Aartsma-Rus, A (2011) Opportunities and challenges for the development of antisense treatment in neuromuscular disorders. *Expert Opin Biol Ther*; 11: 1025-1037.
4. Monaco, AP, Bertelson, CJ, Liechti-Gallati, S, Moser, H, Kunkel, LM (1988) An explanation for the phenotypic differences between patients bearing partial deletions of the DMD locus. *Genomics*; 2: 90-95.
5. Muntoni, F, Torelli, S, Ferlini, A (2003) Dystrophin and mutations: one gene, several proteins, multiple phenotypes. *Lancet Neurol*; 2: 731-740.
6. Aartsma-Rus, A, Janson, AA, Kaman, WE, Bremmer-Bout, M, den Dunnen, JT, Baas, F et al. (2003) Therapeutic antisense-induced exon skipping in cultured muscle cells from six different DMD patients. *Hum Mol Genet*; 12: 907-914.
7. Aartsma-Rus, A (2010) Antisense-mediated modulation of splicing: therapeutic implications for Duchenne muscular dystrophy. *RNA Biol*; 7: 453-461.
8. McClorey, G, Moulton, HM, Iversen, PL, Fletcher, S, Wilton, SD (2006) Antisense oligonucleotide-induced exon skipping restores dystrophin expression in vitro in a canine model of DMD. *Gene Ther*; 13: 1373-1381.
9. Yokota, T, Lu, QL, Partridge, T, Kobayashi, M, Nakamura, A, Takeda, S et al. (2009) Efficacy of systemic morpholino exon-skipping in Duchenne dystrophy dogs. *Ann Neurol*; 65: 667-676.
10. Bremmer-Bout, M, Aartsma-Rus, A, de Meijer, EJ, Kaman, WE, Janson, AA, Vossen, RH et al. (2004) Targeted exon skipping in transgenic hDMD mice: A model for direct preclinical screening of human-specific antisense oligonucleotides. *Mol Ther*; 10: 232-240.
11. Fletcher, S, Honeyman, K, Fall, AM, Harding, PL, Johnsen, RD, Wilton, SD (2006) Dystrophin expression in the mdx mouse after localised and systemic administration of a morpholino antisense oligonucleotide. *J Gene Med*; 8: 207-216.
12. Heemskerk, H, de WC, van, KP, Heuvelmans, N, Sabatelli, P, Rimessi, P et al. (2010) Preclinical PK and PD studies on 2'-O-methyl-phosphorothioate RNA antisense oligonucleotides in the mdx mouse model. *Mol Ther*; 18: 1210-1217.
13. Alter, J, Lou, F, Rabinowitz, A, Yin, H, Rosenfeld, J, Wilton, SD et al. (2006) Systemic delivery of morpholino oligonucleotide restores dystrophin expression bodywide and improves dystrophic pathology. *Nat Med*; 12: 175-177.
14. Goemans, NM, Tulinius, M, van den Akker, JT, Burm, BE, Ekhardt, PF, Heuvelmans, N et al. (2011) Systemic administration of PRO051 in Duchenne's muscular dystrophy. *N Engl J Med*; 364: 1513-1522.
15. Cirak, S, Arechavala-Gomez, V, Guglieri, M, Feng, L, Torelli, S, Anthony, K et al. (2011) Exon skipping and dystrophin restoration in patients with Duchenne muscular dystrophy after systemic phosphorodiamidate morpholino oligomer treatment: an open-label, phase 2, dose-escalation study. *Lancet*; 378: 595-605.
16. Heemskerk, HA, de Winter, CL, de Kimpe, SJ, van Kuik-Romeijn, P, Heuvelmans, N, Platenburg, GJ et al. (2009) In vivo comparison of 2'-O-methyl phosphorothioate and morpholino antisense oligonucleotides for Duchenne muscular dystrophy exon skipping. *J Gene Med*; 11: 257-266.
17. Moulton, HM, Wu, B, Jearawiriyapaisarn, N, Sazani, P, Lu, QL, Kole, R (2009) Peptide-morpholino conjugate: a promising therapeutic for Duchenne muscular dystrophy. *Ann N Y Acad Sci*; 1175: 55-60.
18. Moulton, HM, Moulton, JD (2010) Morpholinos and their peptide conjugates: therapeutic promise and challenge for Duchenne muscular dystrophy. *Biochim Biophys Acta*; 1798: 2296-2303.
19. Wu, B, Lu, P, Cloer, C, Shaban, M, Grewal, S, Milazi, S et al. (2012) Long-term rescue of dystrophin expression and improvement in muscle pathology and function in dystrophic mdx mice by peptide-conjugated morpholino. *Am J Pathol*; 181: 392-400.
20. Yin, H, Saleh, AF, Betts, C, Camelliti, P, Seow, Y, Ashraf, S et al. (2011) Pip5 transduction peptides direct high efficiency oligonucleotide-mediated dystrophin exon skipping in heart and phenotypic correction in mdx mice. *Mol Ther*; 19: 1295-1303.
21. Scott, JK, Smith, GP (1990) Searching for peptide ligands with an epitope library. *Science*; 249: 386-390.
22. Kehoe, JW, Kay, BK (2005) Filamentous phage display in the new

- millennium. *Chem Rev*; 105: 4056-4072.
23. Zahid, M, Phillips, BE, Albers, SM, Giannoukakis, N, Watkins, SC, Robbins, PD (2010) Identification of a cardiac specific protein transduction domain by in vivo biopanning using a M13 phage peptide display library in mice. *PLoS One*; 5: e12252.
 24. Samoylova, TI, Smith, BF (1999) Elucidation of muscle-binding peptides by phage display screening. *Muscle Nerve*; 22: 460-466.
 25. Seow, Y, Yin, H, Wood, MJ (2010) Identification of a novel muscle targeting peptide in mdx mice. *Peptides*; 31: 1873-1877.
 26. Yin, H, Moulton, HM, Betts, C, Seow, Y, Boutilier, J, Iverson, PL et al. (2009) A fusion peptide directs enhanced systemic dystrophin exon skipping and functional restoration in dystrophin-deficient mdx mice. *Hum Mol Genet*; 18: 4405-4414.
 27. Huang, J, Ru, B, Li, S, Lin, H, Guo, FB (2010) SAROTUP: scanner and reporter of target-unrelated peptides. *J Biomed Biotechnol*; 2010: 101932.
 28. Shtatland, T, Guettler, D, Kossodo, M, Pivovarov, M, Weissleder, R (2007) PepBank--a database of peptides based on sequence text mining and public peptide data sources. *BMC Bioinformatics*; 8: 280.
 29. Mann, CJ, Honeyman, K, McClorey, G, Fletcher, S, Wilton, SD (2002) Improved antisense oligonucleotide induced exon skipping in the mdx mouse model of muscular dystrophy. *J Gene Med*; 4: 644-654.
 30. Juliano, RL, Ming, X, Nakagawa, O (2012) Cellular uptake and intracellular trafficking of antisense and siRNA oligonucleotides. *Bioconjug Chem*; 23: 147-157.
 31. Verhaart, IE, Tanganyika-de Winter, CL, Karnaoukh, TG, Kolfschoten, IG, de Kimpe, SJ, van Deutekom, JC et al. (2013) Dose-dependent pharmacokinetic profiles of 2'-O-methyl phosphorothioate antisense oligonucleotides in mdx mice. *Nucleic Acid Ther*; 23: 228-237.
 32. Malerba, A, Boldrin, L, Dickson, G (2011) Long-term systemic administration of unconjugated morpholino oligomers for therapeutic expression of dystrophin by exon skipping in skeletal muscle: implications for cardiac muscle integrity. *Nucleic Acid Ther*; 21: 293-298.
 33. Townsend, D, Yasuda, S, Chamberlain, J, Metzger, JM (2009) Cardiac consequences to skeletal muscle-centric therapeutics for Duchenne muscular dystrophy. *Trends Cardiovasc Med*; 19: 50-55.
 34. 't Hoen, PA, Jirka, SM, Ten Broeke, BR, Schultes, EA, Aguilera, B, Pang, KH et al. (2012) Phage display screening without repetitious selection rounds. *Anal Biochem*; 421: 622-631.
 35. Yu, RZ, Baker, B, Chappell, A, Geary, RS, Cheung, E, Levin, AA (2002) Development of an ultrasensitive noncompetitive hybridization-ligation enzyme-linked immunosorbent assay for the determination of phosphorothioate oligodeoxynucleotide in plasma. *Anal Biochem*; 304: 19-25.



Phage display screening without repetitious selection rounds

Peter A.C. 't Hoen, [Silvana M.G. Jirka](#), Bradley R. ten Broeke, Erik A. Schultes, Begoña Aguilera*, Kar Him Pang*, Hans Heemskerk, Annemieke Aartsma-Rus, Gertjan B. van Ommen, Johan T. den Dunnen

From the Center for Human and Clinical Genetics and Leiden Genome Technology Center, Leiden University Medical Center, Leiden, The Netherlands, and *Prosensa Therapeutics B.V., Leiden, The Netherlands

Anal Biochem. 2012 Feb 15;421(2):622-31

Abstract

Phage display screenings are frequently employed to identify high affinity peptides or antibodies. While successful, phage display is a laborious technology and notorious for identification of false positive hits. To accelerate and improve the selection process, we have employed Illumina next generation sequencing to deeply characterize the Ph.D.-7™ M13 peptide phage display library before and after several rounds of biopanning on KS483 osteoblast cells. Sequencing of the naïve library after one round of amplification in bacteria identifies propagation advantage as an important source of false positive hits. Most importantly, our data show that deep sequencing of the phage pool after a first round of biopanning is already sufficient to identify positive phages. While traditional sequencing of a limited number of clones after one or two rounds of selection is uninformative, the required additional rounds of biopanning are associated with the risk of losing promising clones propagating slower than non-binding phages. Confocal and live cell imaging confirm that our screen successfully selected a peptide with very high binding and uptake in osteoblasts. We conclude that next generation sequencing can significantly empower phage display screenings by accelerating the finding of specific binders and restraining the number of false positive hits.

1. Introduction

Phage display is a powerful technique for the identification of peptides, proteins or antibodies with affinity for a specific target [1]. Many different phage libraries have been created and used for different applications, ranging from libraries with short random peptide inserts, to cDNA and classical and VHH antibody libraries [2-4]. In several rounds of affinity selection or “biopanning”, the phage library is gradually enriched for high affinity binders.

Traditionally, peptides enriched after several rounds of selection are identified by DNA sequencing of the inserts of a limited number (tens to hundreds) of clones. Depending on the sequence diversity remaining in the library after selection, the analysis of a such a limited number of clones does not necessarily result in the discovery of the most promising candidates. Moreover, phage display screenings are notorious for their identification of false positive hits. These emerge for two important reasons: binding to non-target related materials used during the selection (such as plastics or albumin) and propagation advantages [5]. A well-known example in the latter category is the greatly accelerated propagation of phages displaying the HAIYPRH peptide in the Ph.D.-7™ library, as a consequence of a mutation in the Shine-Dalgarno box of the phage protein gIIp in this clone [6]. This peptide has been identified in at least 13 independent biopanning experiments [5]. To aid the identification of potential false positives, several

web-based tools have been constructed: PepBank can be used to search for peptides already published in other experiments [7], while SAROTUP searches for peptides binding to unintended materials [8].

With the advance of next generation sequencing (NGS), it is now possible to sequence millions of inserts in parallel [9;10]. Thus, NGS permits a more expedient and higher resolution characterization of the library [11-13]. In this paper, we use NGS to examine the contents and the enrichment process of the Ph.D.-7™ library, the most popular, commercially available phage library for peptide ligand screening. In this library, random 7-mer peptides are displayed at the tip of the pIII minor coat protein of the M13 phage. We employed NGS after each round of selection to carefully characterize the enrichment process and show that positive hits can already be found after one round of selection. By comparison of the content of different libraries and by sequencing of the naïve library, we have found an efficient way to discriminate true binders and false positives such as target-unrelated peptides.

2. Materials and Methods

Cell culture

KS483 cells (murine preosteoblast) were cultured in α -MEM (1x) with glutamax (Gibco BRL, Breda, the Netherlands) supplemented with 10% Fetal Bovine Serum (Gibco BRL, Breda, the Netherlands) and 1% penicillin/streptomycin (Gibco BRL, Breda, the Netherlands) under 5% CO₂. Cells were passaged by 0.05% trypsin-EDTA (Gibco BRL, Breda, the Netherlands) treatment at 3-4 day intervals. The cultured cells were grown to subconfluency. For differentiation, KS483 cells were seeded at a density of 15,000 cells/cm² in a 8.6 cm petridish. Every 3-4 days the medium was changed. From day 4 of culture, full confluence was reached and L(+) ascorbic acid (50 μ g/ml, VWR International, the Netherlands) was added to the culture medium. When compact cell nodules appeared (from day 11 of culture onward), β -glycerolphosphate (5 mmol/L, Fluca) was added to the culture medium. At day 18 of differentiation, the control cells were stained with 3% Alizarin red solution (Sigma-Aldrich, St. Louis, MO) to confirm successful differentiation.

Biopanning

A heptapeptide phage display library (Ph.D.-7™ Phage Display Peptide Library kit, New England Biolabs, Beverly, Massachusetts) was used for the *in vitro* biopanning experiments. KS483 cells, at 4 and 18 days of differentiation, were washed gently with phosphate buffered saline (PBS) and incubated with 5 ml of α -MEM, containing 0.1% (w/v) bovine serum albumin (BSA), for 1 hour at 37°C under 5% CO₂. The cells were gently washed once with 5 ml of PBS before adding the phage library. Phages

(2×10^{11}) were added in 3 ml α -MEM containing 0.1% BSA. Cells were incubated with the phage for 1 hour at 37°C, while shaking at 70 rounds per minute. After the incubation, the cells were gently washed 6 times by incubating with 5 ml of ice cold α -MEM, containing 0.1% BSA, for 5 minutes. Subsequently, the cells were incubated for 10 minutes on ice with 3 ml of 0.1M HCl pH 2.2 to elute cell-surface bound phage. This solution was neutralized by addition of 0.6 ml 0.5M Tris. The cells were then lysed for 1 hour on ice in 3 ml of 30mM Tris.HCl, 1mM EDTA, pH8, to recover the cell-associated phage fraction. Phages from each fraction were titrated and amplified according to the manufacturer's protocol. Each subsequent round of selection employed 2×10^{11} phage derived from the phage library recovered from the previous round.

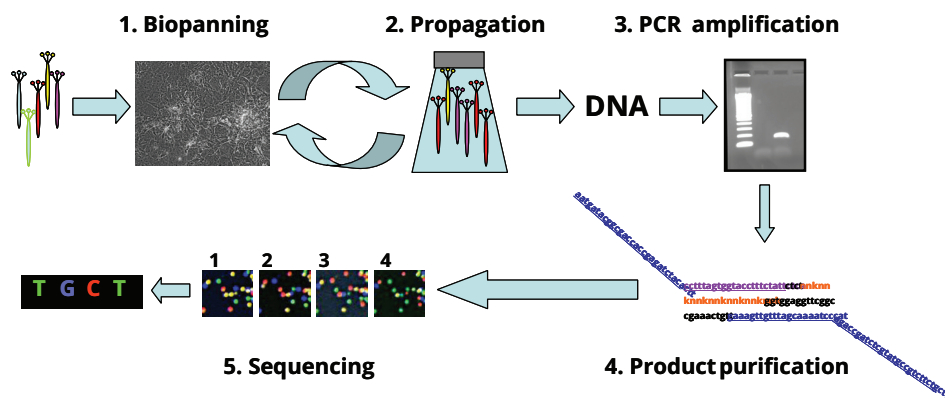


Figure 1: Overview of method. (1) In the biopanning phase, cells are incubated with the phage library. After washing away non-bound phages, binders are isolated and amplified in bacteria. The amplified libraries can be reused in a subsequent round of biopanning. (2) Alternatively, the DNA of the phages can be isolated and (3) amplified with PCR primers complementary to sequences flanking the variable region of the M13 phage DNA. The PCR primers contain tails with the adapter sequences necessary for Illumina sequencing. (4) A 160 bp fragment is purified from gel (lane 1: size marker; lane 2: negative PCR control; lane 3: phage DNA) and sequenced by the Illumina sequencer (5).

DNA preparation and sequencing

Sequencing was performed with the Illumina Whole Genome Analyzer WG2. Phage DNA was isolated from the amplified phage stocks and the naive (unselected) library. For this, 10 μ l of a 1000 times diluted phage stocks were added to 1 ml of a 100 times diluted overnight culture of ER2738 bacteria and grown for 4.5 hours at 37°C while shaking at 200 rpm. Bacteria were centrifuged for 30 sec at 15700g. Then, 500 μ l of the top 80% of the supernatant was precipitated with 200 μ l of PEG/NaCl for 10 minutes at room temperature and the DNA was further isolated according to the manufacturer's protocol. The final pellet was dissolved in 25 μ l of milliQ

water and DNA concentration determined by Nanodrop before freezing at -20°C. Phage DNA was amplified with the following PCR primers:

Forward: AAT GAT ACG GCG ACC ACC GAG ATC TAC ACT TCC TTT AGT GGT ACC TTT CTA TTC TC*A

Reverse: CAA GCA GAA GAC GGC ATA CGA GAT CGG TCT ATG GGA TTT TGC TAA ACA ACT TT*C

where * indicates phosphorothioate bond. PCR primers used to amplify the phage DNA contained a subsequence that recognized the sequence flanking the 21 nucleotides long, unknown insert sequence and the adapters necessary for binding to the Illumina flow cell. The final product of the PCR was 160 base pairs long. The PCR protocol applied was the following: 1 ng of phage DNA was incubated with 2.625 U high fidelity Taq polymerase (Roche Diagnostics, The Netherlands), 20pM of primers in 1x High fidelity PCR buffer containing 15mM $MgCl_2$, and amplified for 20 cycles, each consisting of an incubation for 30 sec at 94°C, 30 sec at 60°C and 30 sec at 72°C. The PCR was stopped in exponential phase to mitigate PCR-induced sequence biases. The final PCR product was purified with the Qiaquick PCR purification kit (Qiagen, Valencia, CA). Concentrations as well as the correct length of the PCR product were established with an Agilent 2100 Bioanalyzer DNA 1000 assay. Each PCR product was applied to a single lane of an Illumina flow cell and subjected to solid phase amplification in the cluster station following the manufacturer's specification (Illumina, San Diego, CA). Single end sequencing for 27-35 cycles (27 cycles are sufficient but runs were sometimes extended to 35 cycles due to requirements for samples in other lanes of the same flow cell) was performed with a custom sequencing primer that started exactly at the first position of the unknown insert sequence (ACA CTT CCT TTA GTG GTA CCT TTC TAT TCT CAC TC*T)

Data analysis

All sequenced lanes were run through the initial Illumina Genome Analyzer Pipeline (Firecrest \Rightarrow Bustard \Rightarrow Gerald) for image analysis, quality control and base calling. Only sequences with the expected 6 nucleotide sequence after the insert (GGTGGA) were used (~95% of the sequences remaining after this filter step). DNA sequences were translated to amino acid sequences with a custom perl script using conventional amino acid codon tables. All reported numbers and sequences refer to the translated peptide sequences. *symbols indicate the presence of a stop codon, while - symbols indicate the presence of an unknown nucleotide in the triplet.

For plotting of phage abundance, a square root transformation was applied on the number of counts in the library, a commonly applied data transformation to stabilize the variance in count data [14].

Simulation of random clone picking

We randomly selected 50 amino acid sequences from the round 1, round 2, round 3, round 4 phage libraries selected for internalization into KS483 cells at day 18 of differentiation. We counted how frequently we selected the most abundant or 10 most abundant peptide sequences, as identified after complete sequencing of the round 4 library. We repeated this 20 times and report the average percentage and standard deviations for the 50 random picks in Figure 3D.

Peptide synthesis

7-mer peptides were synthesized by standard Fmoc solid phase peptide chemistry on a PS3 or Tribute Peptide synthesizer (Protein Technologies), using HCTU (5 eq.) as activating reagent and DIPEA (10 eq.) as base. Resin bound peptides were manually coupled to the fluorescent label by treatment with 5(6)-carboxyfluorescein N-hydroxysuccinimide ester and triethylamine in DMF. After cleavage [TFA/TIS/H₂O 95/2.5/2.5 (v/v) or TFA/thioanisole/TIS/H₂O 90/2.5/2.5/5 (v/v) for peptide sequences containing Met], filtration, precipitation over cold-ether and centrifugation, crude FAM-labeled peptides were obtained. Peptides were purified by RP-HPLC on a Shimadzu Prominence HPLC [Alltima C₁₈ column (5mm, 10 x 250 mm); solvent A (0.1% TFA CH₃CN/H₂O 5/ 95 ; solvent B (0.1% TFA CH₃CN /H₂O 80/20)]. Peptides were analyzed by ESI-MS (positive mode) on a Agilent LC-ion trap mass spectrophotometer. Fluorescent peptide concentrations were determined by spectrophotometric analysis at 490 nm at pH=7.5.

Fluorescent imaging of KS483 cells

KS483 cells were seeded at a density of 15,000 cells/cm² in 6 wells plates with glass cover slides 21x26 mm (Menzel Glaser, Germany) or in Mattek glass bottom dishes with a diameter of 14mm and a glass thickness of 1.5 mm (Mattek corporation) in culture media described above. Cells were gently washed with PBS before adding 2.25 μM of FAM-labeled peptide in medium without serum for 24 or 48 hours. After incubation, cells at 4 days of differentiation were washed three times with PBS, fixed in ice cold methanol for 5 minutes and air dried for 5 minutes. Subsequently, the cells were embedded on microscope slides with Vectashield (Vector laboratories Inc.) and the slides were analyzed with a Leica TCS SP5 DMI6000 confocal microscope (Leica Microsystems, HCX PL APO 63x/1.4 oil-immersion objective, 8 bit resolution, 512x512 pixels, 400Hz speed). Cells at day 18 of differentiation were gently washed with PBS (three times) and supplied with fresh medium before analysis with live cell imaging using a Leica Af6000LX inverted microscope (Leica Microsystems, HCX PL FLUOTAR 63.0x1.25 oil-immersion objective, 12 bit resolution, 1392x1040 pixels).

3. Results

In the current study, we employed NGS technology to characterize the phage display screening process during successive rounds of selection. We used the combination of phage display and NGS to select for peptides that are binding to the surface of and/or internalized by KS483 cells in different stages of differentiation. KS483 are osteoblastic cells that can be efficiently differentiated into mature osteoblasts and form nodules depositing mineralized calcium material within 18 days [15;16]. The identified peptides may ultimately be used for the targeting of pharmaceutical formulations to bone or for enhancing the intracellular uptake of drugs into osteoblasts.

Sequencing of phage display libraries

The preparation of the phage libraries for sequencing is a simple and short procedure, as depicted in Figure 1. After DNA isolation from the entire phage pool, the fragment containing the insert was amplified and equipped with the linkers necessary for NGS in a one-step PCR reaction. The unknown inserts of 21 nucleotides (7 amino acids) were sequenced on the Illumina Whole Genome Analyzer. After quality control and translation of the DNA sequences to amino acid sequences, we obtained around 13 million peptide sequences for each phage display library (Table 1). This provides an ultra-deep profiling of the content of the phage display libraries.

Table 1: Overview of sequencing results phage display experiments

Selection Round	Differentiation	Internalized /surface	#sequences	#unique sequences	most abundant sequence	# counts for most abundant
3	4 days	surface	11,192,802	274,666	GETRAPL	1,279,913
4	4 days	surface	12,858,902	123,972	GETRAPL	3,113,643
3	4 days	internalized	12,357,279	358,844	GETRAPL	397,669
3	18 days	surface	13,146,497	196,615	GETRAPL	3,599,322
1	18 days	internalized	15,595,055	1,913,785	HAIYPRH	41,257
2	18 days	internalized	17,092,798	1,318,281	GETRAPL	547,210
3	18 days	internalized	13,217,869	350,379	RHEPPLA	543,337
4	18 days	internalized	13,880,199	282,266	RHEPPLA	1,413,696
no selection	-	-	6,688,401	3,887,498	HAIYPRH	36

Characterization of the naïve library

Before analyzing the phage display libraries selected against biological targets, we screened for potential sequence biases introduced by the propagation of the phages in bacteria by sequencing the naïve (unselected) library after one round of bacterial amplification. The library of 2×10^{11} phages theoretically contains all of the 2×10^9 heptapeptide sequences. By sequencing millions of peptides only a fraction of the entire library was analyzed. However, we confirmed that the peptide diversity in the

library was high, since more than fifty percent of the peptide sequences in the naïve library were found only once (Table 1). Nevertheless, some peptides were found at higher frequencies than expected by chance. The peptide HAIYPRH was found most frequently (36 times) and is known for its accelerated propagation in phage display experiments due to a mutation in the Shine-Dalgarno box of the phage protein gIIp [6]. Hence, growth advantages unrelated to the target selection emerge even after a single round of bacterial amplification of the naïve phage library. A high number of additional peptides were found more than twice in the naïve library, while the chance on this event based on a Poisson distribution with the current number of sequenced peptides would be only 5.5×10^{-9} . Presumably, these peptides also have growth advantages. We provide a list of these nearly 700,000 peptides and their frequencies in the naïve library in Supplementary Table 1. It seems wise not to choose peptides that are found more than twice in the naïve library for follow-up studies, even when they demonstrate high enrichment after several rounds of selection.

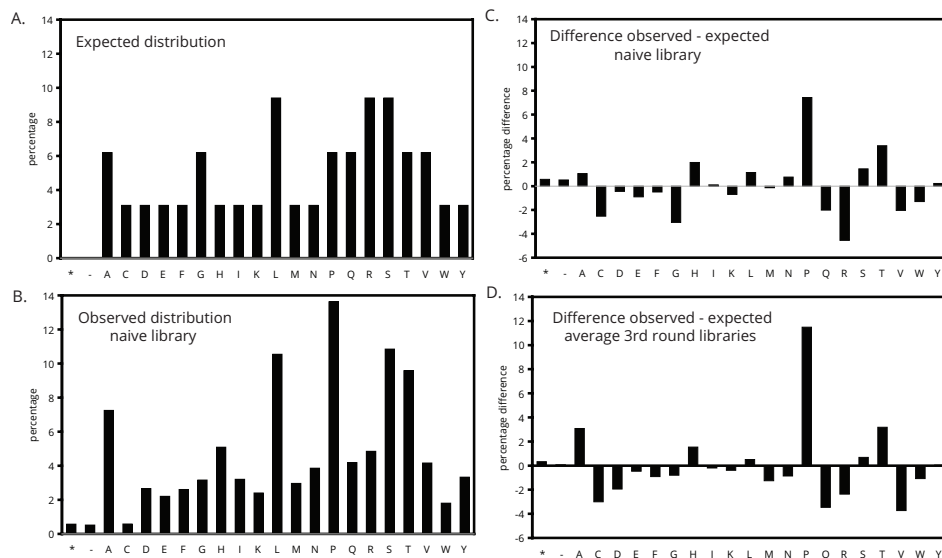


Figure 2: Analysis of amino acid composition of PhD7 library. Overview of the average amino acid composition (in %) of all unique peptides sequenced. A) Theoretical amino acid composition based on the translation of random (NNK)₇ inserts. B) Observed composition in naïve library. C) Difference between the observed composition in the naïve library and the theoretical composition. D) Difference between the average composition in all 3rd round libraries and the theoretical composition. Standard amino acid one letter codes are used; *: one of the nucleotides in the triplet is unknown (N); -: stop codon.

Amino acid composition of peptides from naïve and enriched libraries

The naïve library is generated from a degenerate (NNK)₇ oligonucleotide library where K represents an admixture of 50% T and 50% G. The expected amino acid frequencies resulting from this degenerate code is given in Figure 2A. Already after sequencing 70 random clones, the manufacturer noticed considerable differences between the actual and the expected amino acid composition of the naïve library (see manufacturer's documentation). A much more refined distribution of amino acid frequencies was obtained after sequencing >6 million inserts (Fig. 2B and C). The naïve library suffers from a considerable depletion of cysteine residues (frequency less than 1% of all amino acids). Glycine and arginine residues are also underrepresented but still found at frequencies higher than 2.5%. Proline is the most overrepresented amino acid. After selection, these trends were even stronger (Fig. 2D), suggesting that cysteine residues impede but proline residues enhance the propagation of phages. Some major positional effects were also observed (Supplementary Fig. 1): the most important is the restriction of the overrepresentation of proline residues to positions 2-7, while the first position is actually depleted of proline residues, as noted before [17].

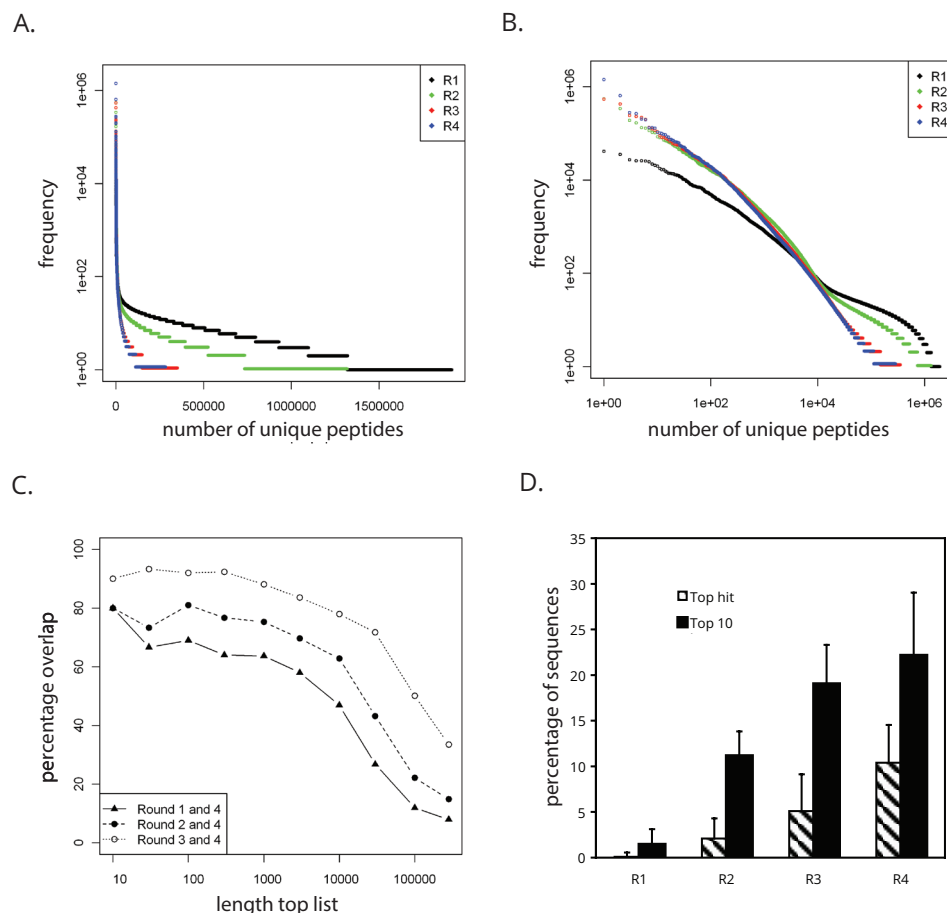


Figure 3: Comparison of round 1, 2, 3, and 4 libraries. AB) Frequency distribution (A: linear scale; B: 10log scale) of all unique peptide sequences (ordered from high to low abundance) after one (black), two (green), three (red), or four (blue) rounds of selection for phages internalizing into differentiated KS483 cells. The horizontal lines at the bottom of the plot represent the peptide sequences that occur once, twice, three times etc, with higher frequencies being more difficult to discriminate. The length of such a line represents the number of peptides with a particular frequency. C) Percentage overlap in the lists of most abundant peptides obtained after different rounds of selection. D) Simulation of traditional picking of 50 clones after round 1, 2, 3, or 4. The percentage of sequences belonging to the most abundant (hashed bars) or 10 most abundant (black bars) phages identified by next generation sequencing of the 4th round library are shown. Standard deviations refer to the variance observed in 20 independent random picks of 50 clones.

Characterization of the enrichment process

To identify phages with high binding affinity for undifferentiated and differentiated osteoblast (KS483) cells, we sequenced phage libraries

extracted from the surface of the cells. Internalizing phages were identified by the sequencing of libraries extracted from cell lysates after removing surface-bound phages. We initially sequenced libraries after 3 or 4 rounds of selection (Table 1), since we observed a significant enrichment, based on titration of output/input ratios, after these rounds (data not shown). To further characterize the enrichment process and the potential for identification of interesting phages from earlier rounds of selection, we also analyzed the phage libraries isolated after one, two, three and four rounds of selection for the internalization of phages on differentiated KS483 cells.

During subsequent rounds of selection the overall diversity decreased, while the frequency of the most enriched peptides steadily increased (Table 1, Fig. 3A and 3B). To illustrate this: the number of unique sequences decreased from 1,913,785 in round 1 to 282,266 in round 4, while the frequency of the highest abundant peptide increased from 0.26% to 10%, and the number of sequences that were found only once decreased from 594,379 to 170,592 (Fig. 3A and 3B). Thus, libraries converge towards certain peptide sequences in later rounds, consistent with expectations behind (traditional) phage display experiments.

There is a high correlation between the counts observed after the different selection rounds (Supplementary Fig. 2). In all comparisons, the correlations are high (Pearson correlation ranging from 0.47 (round 1 vs. 2) to 0.94 (round 3 vs. round 4)). Moreover, the correspondence in the top 1000 most abundant peptides between the different rounds is high, ranging from ~60% between round 1 and 4 to >80% between round 3 and 4 (Fig. 3C). Eight out of the ten most abundant peptides from round 4 are also in the top-10 after the first or second selection round (Fig. 3C). This means that, with the current sequencing depth, (i) further rounds of selection will not lead to the identification of peptides that could not have been found in earlier rounds; (ii) high affinity peptides can already be identified after the first round of selection.

We performed a simulation study to illustrate that this result is in striking contrast with a phage display experiment with traditional clone picking. In Figure 3D, we show that, after the fourth round, around 10% (say 5 out of 50 clones picked) would be derived from the most abundant phage, as identified by sequencing of the complete round 4 library. A further 12% of sequenced clones (say 6 out of 50 clones picked) would be derived from other phages from the top 10 of the complete round 4 library. When sequencing only 50 clones, these top 10 peptides would most likely be sequenced only once, and some of them would not be sequenced at all. The remainder of the 50 randomly picked sequences (78%) are from phages that are not found in the top10 after NGS analysis of the round 4 library. It is clear from Figure 3D that these results are even worse when randomly picking 50 clones from the round 3 library, when only 5% of the sequences

would be derived from the top phage, while sequencing 50 randomly selected phages after round 1 and 2 would be completely uninformative.

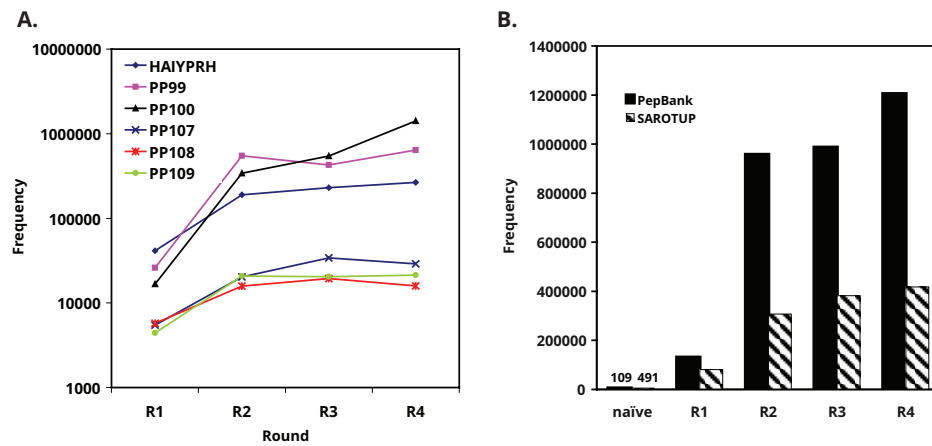


Figure 4: Counts of non-target and target-specific peptide sequences during subsequent rounds of selection. A) Counts for non-target specific peptides HAIYPRH, PP99, and PP100, and target-specific peptides PP107, PP108 and PP109 after four subsequent rounds of selection for phages internalizing into differentiated KS483 cells. B) Percentage of sequences recorded in PepBank (black bars, database of short peptide sequences previously reported in literature) and SAROTUP (hashed bars, database of peptides which bind unintended targets) identified after sequencing of the naïve library and the round 1, 2, 3, and 4 libraries.

Identification of false positives

The selection of one or a few sequences from a library of 10^{11} molecules is an inherently noisy process. There are two principle causes for the high abundance of irrelevant peptide sequences in phage display experiments. On the one hand, phages may have lower than average replication time in bacterial hosts, illustrated by the HAIYPRH example. The impact of these propagation advantages increases with every round of selection and amplification. As an example, HAIYPRH was found 41,257 times after one round of selection and amplification (0.26% of all sequenced peptides) and 237,535 times after three rounds of selection (1.8%) (Fig. 4A). These false positives can be identified by sequencing of the naïve library after one round of amplification in bacteria. On the other hand, peptides may bind to non-target substrates and propagate during subsequent selection rounds without having any affinity to the intended target. These are less easy to identify, since their enrichment pattern may be similar to that of target-specific peptides (Fig. 4A). A notorious example is the GETRAPL peptide, identified in many independent experiments [7]. Most likely, the peptide binds to plastics in general, since it was found at a frequency of 35% in phage display selection for polystyrene binding peptides and demonstrated

considerable affinity for polystyrene [18]. GETRAPL was the most abundant in 6/9 of our libraries selected on KS483 cells and amongst the top ranked peptides in the other libraries. Libraries selected against *in vivo* targets did not have an overabundance of GETRAPL (data not shown), consistent with this peptide's presumed affinity for polystyrene plastics not present in *in vivo* screens. Two databases, PepBank [7] and SAROTUP [8], are very helpful to identify non-target specific peptides. Figure 4B shows that subsequent rounds of biopanning resulted in gradual enrichment for known target-unrelated peptides, amounting to ~10% of all sequences found after round 4. Through comparisons of many deep-sequenced libraries, it is possible to filter for commonly found parasitic peptides.

Table 2: Selected peptide sequences

Group	Peptide sequence	Peptide number (PP)	Counts in naïve library	Counts in Day 4 - surface	Counts in Day 4 - internalized	Counts in Day 18 - surface	Counts in Day 18 - internalized	SAROTUP	Pepbank
0 - Control peptides	LPLTLP	98	16	13,006	29,175	20,988	20,003	Yes	Yes
	GETRAPL	99	15	1,279,913	397,669	3,599,322	427,153	Yes	Yes
	RHEPPLA	100	0	6	0	0	543,337	No	No (*)
1 - Abundant in all selected libraries	AMSSRSL	101	0	15,301	54,629	11,517	134,645	No	No
	YRAPWPP	102	1	34,250	23,765	56,436	55,732	No	No
	ASSSHRS	103	0	73,075	5,033	57,476	24,902	No	No
2 - Surface specific	DLKIPLR	104	0	37,802	0	55,342	59	No	No
	IEFSPLM	105	1	4,765	0	43,697	0	No	No
3 - Day 4 specific (Internalized)	NPWTTRP	106	0	0	50,155	0	0	No	No
4 - Day 18 specific (Internalized)	ALPQIVR	107	0	0	210	0	34,034	No	No
	DERHQHY	108	0	0	0	0	19,404	No	No
	WQSVPTI	109	0	0	0	0	20,390	No	No

Note: The following selection criteria were applied: Control peptides had more than two counts in the naïve library and were included in Pepbank or SAROTUP. Peptides in group 1 had more than 1000 counts in all round three libraries. Peptides in group 2 had more than 1000 counts in all surface but not in internalized libraries. The peptide in group 3 had more than 1000 counts, but only in the internalizing phages at day 4 of differentiation. Peptides in group 4 had more than 1000 counts in internalizing phages at day 18 only. () mentioned as a polystyrene binder in [18]*

Selection of candidate peptide sequences

We were interested to identify peptides that specifically bind to and/or are internalized by KS483 cells. We applied the filter criteria described below to identify candidate peptide sequences from the different libraries, and searched for peptides with different apparent specificities. To exclude any putative false positives, we discarded all peptides with a frequency of 2 or higher in the naïve library and hits in Pepbank and SAROTUP. From the remaining list of peptides, we selected 9 putative target-related peptides (PP101-109) with apparent differences in specificities (Table 2). PP101-103 were most highly enriched in all libraries, while PP104-109 showed at least 100-fold differences in abundance between libraries and were selected for their apparent specificities. PP104-105 were selected as potential binders to the surface of cells at day 4 and day 18 of differentiated cells. We included peptides PP107-109 with apparent specificity towards fully differentiated (day 18) cells. These peptides were gradually enriched during subsequent rounds of selection (Fig. 4A), and were consistently ranked in the top 120. No other phages in the top 120 displayed similar degrees of specificity for internalization in cells at day 18 of differentiation. As negative controls, we selected three non-target related peptides (PP98-100): LPLTPLP (PP98) and GETRAPL (PP99) demonstrated a frequency of 2 or higher in the naïve library and had a hit in Pepbank. RHEPPLA (PP100) had been found to bind to polystyrene in an earlier study [18], but was unexpectedly only found in the libraries selected for internalization at day 18, where it was the most highly enriched peptide (Table 1), and not in any of the other libraries. The presumed non-target related peptides demonstrated similar enrichment profiles as PP107-109 (Fig. 4A). Unfortunately, solubility of PP98 and PP105 was too limited to allow further analysis.

Fluorescent imaging of peptide binding and uptake by KS483 cells

Selected peptides, equipped with a fluorescent FAM-label, were tested for binding to and uptake by KS483 cells at day 4 and day 18 of differentiation. The experiments with cells at day 4 of differentiation were performed three times with duplicated wells in each experiment, using cells with high and low passage numbers and incubation times of 24 and 48 hours, all generating similar results. Day 4 cells were analyzed with confocal microscopy to be able to discriminate between surface binding and internalizing peptides. Confocal microscopy was not possible for day 18 cells since the cells grow on top of each other and deposit thick matrix structures. Therefore, day 18 cells were analyzed by live cell imaging. Representative fluorescent images obtained with the two different technologies are shown in Figure 5 and Supplementary Figure 3. As expected, cells incubated with the PP99 control peptide, which has been found in many other phage display selection experiments according to SAROTUP and Pepbank, do not show any fluorescent signal. Similarly,

PP100, which was found to bind to polystyrene before [18], demonstrated only very weak cellular staining. PP102, which was highly abundant in all selected libraries, indeed displayed strong binding and uptake in day 4 and day 18 cells. Spectrophotometric analysis of the cell lysates confirmed that the majority of the presented peptides were internalized (data not shown). The intracellular distribution of PP102 differed between day 4 and day 18 cells, with more prominent staining of the nucleus on day 4 and more prominent staining of the extracellular matrix on day 18. Surprisingly, PP101 and PP103, also abundant in all selected libraries, displayed very weak or no signal. In line with the selection of PP104 as a surface binding peptide, PP104 demonstrated strong binding to the extracellular matrix. A similar staining pattern was observed for PP106, which was unanticipated since this peptide sequence was discovered in the pool of internalized phages. Peptides PP107 and PP108 were identified in day 18 cells only, and indeed appeared to give stronger staining in day 18 cells than in day 4 cells. Data for PP109 were inconclusive since the peptide was highly aggregation prone.

4. Discussion

In the studies described in the current paper, we have gained significant insight into the phage display selection process. This was achieved by sequencing millions of independent phages after different selection rounds using the latest next generation sequencing technology. We show that the enrichment factor of positive clones gradually increases during subsequent rounds of selection. We have not observed differences in the enrichment kinetics between target-specific and target-unrelated peptides. This is concordant with the observed absence of a correlation between peptide affinity and abundance in other reported phage display experiments [19].

Multiple rounds of selection will be helpful to reduce the background of non-binders and is therefore essential when sequencing a limited number of clones (*cf.* our simulation study in Fig. 3D). In contrast, significant enrichment can already be observed after the first round of selection when sequencing millions of clones. The high correlation between abundances after the first and subsequent rounds suggests that further rounds of enrichment may not have additional value. The large effects of small differences in propagation rates on the final abundances, nicely illustrated in ref. [19], may even result in exclusion or down-weighting of interesting phages from the pool. Instead of performing multiple rounds of selection, it may be preferred to perform the first round of selection in duplicate or triplicate, to account for variability in the stringency of binding conditions.

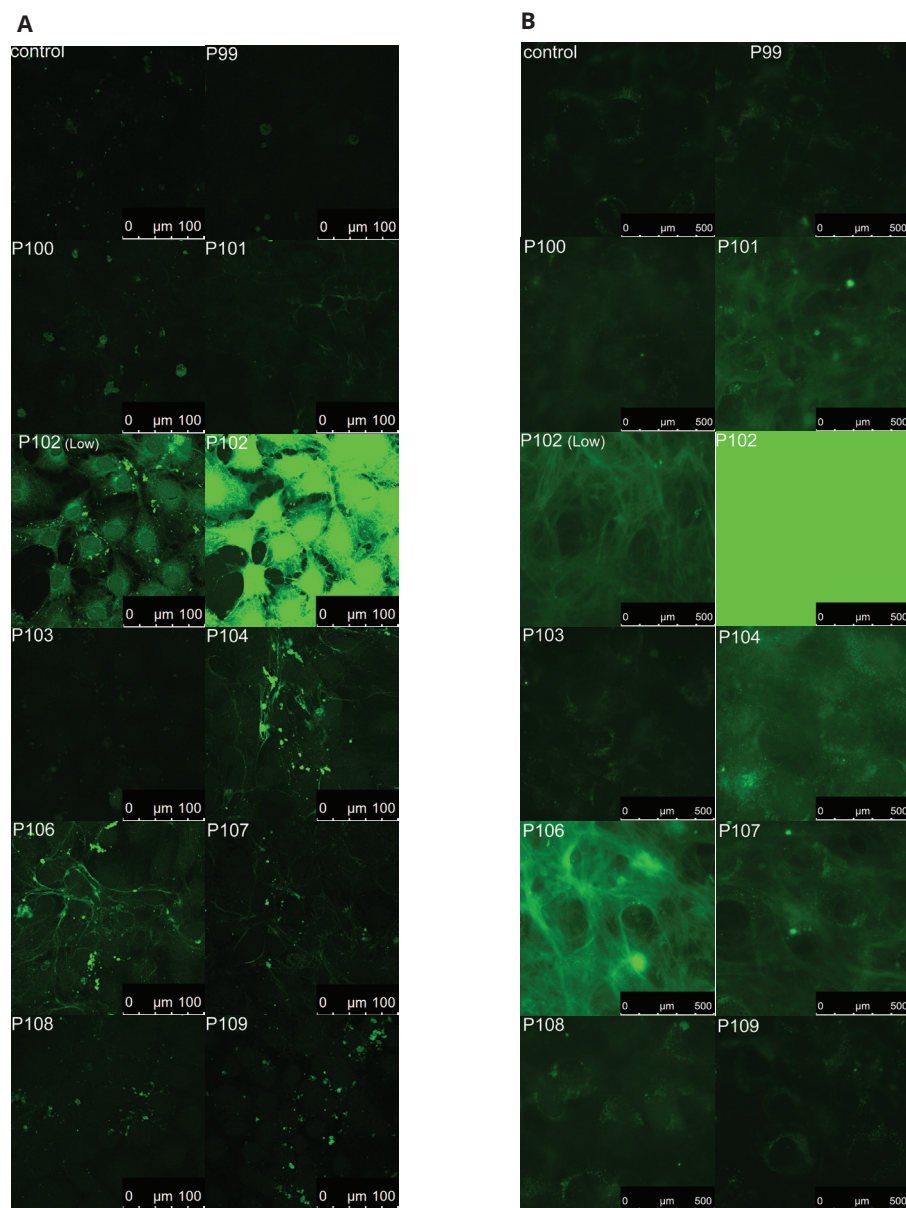


Figure 5: Uptake of fluorescently labeled peptides by KS483 cells. KS483 cells at day 4 (Panel A) or day 18 (Panel B) of differentiation were incubated with 2.25 μM of FAM-labeled peptide in serum free medium and analyzed by confocal microscope (Panel A) or by live cell imaging with an inverted microscope (Panel B). Since the incubation with PP102 resulted in high uptake and very bright fluorescent, images obtained with two different gains (Panel A: 528 (also used for the other peptides) and 424 (labeled with LOW)) or exposure times (Panel B: 220 ms (also used for the other peptides) and 25 ms (labeled with LOW)) are shown.

Thus, our results question the validity of the traditional phage display screening approach: the high number of selection rounds required to arrive at peptides observed multiple times in tens to a few hundred of sequenced clones will come with the risk of an over-reduction in the library complexity and the loss of potentially interesting phages. Moreover, NGS-based characterization of phage display libraries is more cost effective than traditional clone picking because of the lower number of selection rounds required. It is also less laborious than methods previously developed to mitigate amplification biases employing phage amplification in isolated compartments such as monodisperse droplets [20].

Although full characterization of the first round library would require sequencing more than 10 million reads, identification of the most abundant phages requires substantially lower sequencing depth. The required sequencing depth depends on the complexity of the library and the enrichment factor. Generally speaking, sequencing of 1 million reads should be sufficient with relatively low enrichment factors obtained after one round of biopanning, since they would be represented >50 times according to simulated random draws of 1 million sequences from our round one library. This would allow for a high level of multiplexing of different phage display libraries in a single lane of the Illumina sequencer, and thus further reduce sequencing costs.

Previous characterization of phage display libraries were done with Roche 454 sequencing. Dias-Neto *et al.* sequenced around 70,000 phages isolated from human tissues after phage infusion [11]. In their experiment, the number of unique phages recovered was much lower than in our experiment - probably due to the distribution of the phages over different organs and the small biopsies taken - and sequencing of around 40,000 phages was sufficient to fully characterize the library. In an independent study, a cDNA phage display library selected for binding to transglutaminase was characterized by Roche 454 sequencing [21]. After sequencing of 120,000 phages, no decrease in diversity compared to the naïve library was observed. This may have been caused by a lack of high affinity binders in the phage pool and /or an insufficient sequencing depth. Illumina sequencing technology, like SOLiD and Helicos technologies, provides millions of reads. This may be an important reason why we observed a clear decrease in library complexity already after the first round of sequencing.

It is not yet feasible to sequence the complete naïve library, since it is claimed to contain 2 billion different phages. We sequenced a fraction of about 0.3%. Still, the sequencing of the naïve library has proven extremely useful for two reasons. First, it revealed non-random occurrences of the different amino acids at the different positions. We confirm the findings by Krümpe *et al.* obtained by random sequencing of 100-400 phages from

similarly constructed CX7C and X12 M13 phage display libraries [17], and demonstrate that proline residues are overrepresented at all but the first position, and that cysteine residues are significantly underrepresented. Based on the fact that this was already apparent in the naïve library, which went through one round of amplification in bacteria, we tend to explain this by differences in availability of the amino acids, non-random incorporation probabilities during translation and suboptimal codon usage in bacteria. The non-random representation of amino acids reduces the chance to identify the highest affinity binders and therefore some optimization of the identified peptide sequences may still be useful. Second, sequences that were already found at higher frequencies than expected by chance are likely to have a selective or growth advantages. Indeed the GETRAPL peptide (PP99), which was found already 15 times in the naïve library, was not binding to KS483 cells, nor effective as a viral targeting peptide [22]. The lack of signal in our plastic dishes also suggests that GETRAPL is not a polystyrene binding peptide as previously claimed [18]. Its identification in a screening for plastic binding phages may have been caused by the same selection advantage. Moreover, the PCR amplification step applied during sample preparation may introduce biases that would be revealed by sequencing of the naïve library. We therefore strongly recommend to sequence naïve phage display libraries after one round of amplification in bacteria.

Despite our elimination of possible false positives caused by amplification or PCR biases or non-specific binding, other factors appear to contribute to the high false positive rate in peptide phage display screenings and were also observed in our experiment. A likely explanation for this is that the binding of synthetic 7-mer peptides may be largely different from the binding of a phage displaying a 7-mer peptide sequence as part of the phage pIII protein, giving rise to substantial differences in secondary and tertiary structures.

We have identified one peptide (PP102) with exceptionally strong binding and uptake by KS483 cells and two peptides with strong binding to the extracellular matrix. Further research should demonstrate the potential of these peptides to target bioactive agents or drugs to osteoblasts and/or shuttle these across the plasma membrane. PP102 was ranked 14 after the first round of selection and remained in the top-20 during subsequent rounds of selection. Interestingly, there were two independent phage clones coding for the PP102 amino acid sequence: TATAGGGCTCCTTGCCGCCT was the most prominent one followed by TATCGGGCTCCTTGCCGCCT, which was observed at frequencies of approximately 10% of the former. The other selected peptides, which displayed less strong binding to KS483 cells, were not represented by multiple independent phages, since DNA variants were present at frequencies <1%. This suggests that the identification of independent phages displaying the same peptide has positive predictive

value for the affinity of the peptide. Clearly, more research evaluating larger sets of peptides needs to be done to confirm this.

The 1% threshold is our current estimate of the total sequencing error rate for a 21-mer sequence. This estimate is based on the steep increase of the number of DNA variants with a one mismatch difference at frequencies $\leq 1\%$ of the more abundant sequence. Another positive predictive feature would be the identification of related peptides with slightly different amino acid compositions. Single amino acid substitutions at frequencies lower than one percent can be explained by sequencing errors and should not be considered. However, for PP102 we found a second peptide, SRAPWPP, differing by just one amino acid, at DNA sequence-based frequencies ranging between 3 and 20% of the frequency of YRAPWPP (PP102). It proved difficult to perform a systematic search for clusters of related peptide sequences, since existing peptide sequence clustering software is not designed for the clustering of very large sets of very short peptides.

In our experiment, reads of only 21 nucleotides were required to identify unknown 7-mer peptide sequences. Other types of phage display libraries, like cDNA and antibody phage display libraries are also amenable to NGS-based characterization, aided by the much longer read length currently obtained with next generation sequencers. Likewise, NGS was recently applied to characterize the antibody variable regions of bone marrow plasma cells and this proved to be a very efficient method for monoclonal antibody selection [13]. Taken together, NGS can significantly empower phage display screenings and accelerate the finding of specific binders while restraining the number of false positive hits.

Acknowledgements

This research was supported by a grant from the Dutch Ministry of Economic Affairs (IOP-Genomics grant IGE7001), the Centre for Medical Systems Biology within the framework of the Netherlands Genomics Initiative (NGI)/Netherlands Organisation for Scientific Research (NWO), and the Center for Biomedical Genetics.

We would like to thank Annelies Boonzaier-van der Laan (Leiden University Medical Center, department of Molecular and Cellular Biology) for microscopy assistance and dr. Rinse Klooster (Leiden University Medical Center, department of Molecular and Cellular Biology) for comments on the manuscript.

References

1. G.P. Smith, Filamentous fusion phage: novel expression vectors that display cloned antigens on the virion surface. *Science* 228 (1985) 1315-1317.
2. T. Bratkovic, Progress in phage display: evolution of the technique and its application. *Cell Mol.Life Sci.* 67 (2010) 749-767.
3. Y. Georgieva, Z. Konthur, Design and screening of m13 phage display cDNA libraries. *Molecules.* 16 (2011) 1667-1681.
4. C. Hamers-Casterman, T. Atarhouch, S. Muyldermans, G. Robinson, C. Hamers, E.B. Songa, N. Bendahman, R. Hamers, Naturally occurring antibodies devoid of light chains. *Nature* 363 (1993) 446-448.
5. M. Vodnik, U. Zager, B. Strukelj, M. Lunder, Phage display: selecting straws instead of a needle from a haystack. *Molecules.* 16 (2011) 790-817.
6. L.A. Brammer, B. Bolduc, J.L. Kass, K.M. Felice, C.J. Noren, M.F. Hall, A target-unrelated peptide in an M13 phage display library traced to an advantageous mutation in the gene II ribosome-binding site. *Anal. Biochem.* 373 (2008) 88-98.
7. T. Shtatland, D. Guettler, M. Kossodo, M. Pivovarov, R. Weissleder, PepBank--a database of peptides based on sequence text mining and public peptide data sources. *BMC.Bioinformatics.* 8 (2007) 280.
8. J. Huang, B. Ru, S. Li, H. Lin, F.B. Guo, SAROTUP: scanner and reporter of target-unrelated peptides. *J.Biomed.Biotechnol.* 2010 (2010) 101932.
9. D.R. Bentley, Whole-genome re-sequencing. *Curr.Opin.Genet.Dev.* 16 (2006) 545-552.
10. M. Margulies, M. Egholm, W.E. Altman, S. Attiya, J.S. Bader, L.A. Bembien, J. Berka, M.S. Braverman, Y.J. Chen, Z. Chen, S.B. Dewell, L. Du, J.M. Fierro, X.V. Gomes, B.C. Godwin, W. He, S. Helgesen, C.H. Ho, G.P. Irzyk, S.C. Jando, M.L. Alenquer, T.P. Jarvie, K.B. Jirage, J.B. Kim, J.R. Knight, J.R. Lanza, J.H. Leamon, S.M. Lefkowitz, M. Lei, J. Li, K.L. Lohman, H. Lu, V.B. Makhijani, K.E. McDade, M.P. McKenna, E.W. Myers, E. Nickerson, J.R. Nobile, R. Plant, B.P. Puc, M.T. Ronan, G.T. Roth, G.J. Sarkis, J.F. Simons, J.W. Simpson, M. Srinivasan, K.R. Tartaro, A. Tomasz, K.A. Vogt, G.A. Volkmer, S.H. Wang, Y. Wang, M.P. Weiner, P. Yu, R.F. Begley, J.M. Rothberg, Genome sequencing in microfabricated high-density picolitre reactors. *Nature* 437 (2005) 376-380.

11. E. Dias-Neto, D.N. Nunes, R.J. Giordano, J. Sun, G.H. Botz, K. Yang, J.C. Setubal, R. Pasqualini, W. Arap, Next-generation phage display: integrating and comparing available molecular tools to enable cost-effective high-throughput analysis. *PLoS.One.* 4 (2009) e8338.
12. U. Ravn, F. Gueneau, L. Baerlocher, M. Osteras, M. Desmurs, P. Malinge, G. Magistrelli, L. Farinelli, M.H. Kosco-Vilbois, N. Fischer, Bypassing in vitro screening--next generation sequencing technologies applied to antibody display and in silico candidate selection. *Nucleic Acids Res.* 38 (2010) e193.
13. S.T. Reddy, X. Ge, A.E. Miklos, R.A. Hughes, S.H. Kang, K.H. Hoi, C. Chrysostomou, S.P. Hunicke-Smith, B.L. Iverson, P.W. Tucker, A.D. Ellington, G. Georgiou, Monoclonal antibodies isolated without screening by analyzing the variable-gene repertoire of plasma cells. *Nat.Biotechnol.* 28 (2010) 965-969.
14. P.A. 't Hoen, Y. Ariyurek, H.H. Thygesen, E. Vreugdenhil, R.H. Vossen, R.X. de Menezes, J.M. Boer, G.J. van Ommen, J.T. den Dunnen, Deep sequencing-based expression analysis shows major advances in robustness, resolution and inter-lab portability over five microarray platforms. *Nucleic Acids Res.* 36 (2008) e141.
15. T. Yamashita, H. Ishii, K. Shimoda, T.K. Sampath, T. Katagiri, M. Wada, T. Osawa, T. Suda, Subcloning of three osteoblastic cell lines with distinct differentiation phenotypes from the mouse osteoblastic cell line KS-4. *Bone* 19 (1996) 429-436.
16. M.M. Deckers, M. Karperien, C. van der Bent, T. Yamashita, S.E. Papapoulos, C.W. Lowik, Expression of vascular endothelial growth factors and their receptors during osteoblast differentiation. *Endocrinology* 141 (2000) 1667-1674.
17. L.R. Krumpe, A.J. Atkinson, G.W. Smythers, A. Kandel, K.M. Schumacher, J.B. McMahon, L. Makowski, T. Mori, T7 lytic phage-displayed peptide libraries exhibit less sequence bias than M13 filamentous phage-displayed peptide libraries. *Proteomics.* 6 (2006) 4210-4222.
18. T. Serizawa, P. Techawanitchai, H. Matsuno, Isolation of peptides that can recognize syndiotactic polystyrene. *Chembiochem.* 8 (2007) 989-993.
19. R. Derda, S.K. Tang, S.C. Li, S. Ng, W. Matochko, M.R. Jafari, Diversity of phage-displayed libraries of peptides during panning and amplification. *Molecules.* 16 (2011) 1776-1803.
20. R. Derda, S.K. Tang, G.M. Whitesides, Uniform amplification of phage with different growth characteristics in individual compartments consisting of monodisperse droplets. *Angew.Chem.Int.Ed Engl.* 49 (2010) 5301-5304.
21. Di Niro R., A.M. Sulic, F. Mignone, S. D'Angelo, R. Bordoni, M. Iacono, R. Marzari, T. Gaiotto, M. Lavric, A.R. Bradbury, L. Biancone, D. Zevin-Sonkin, B.G. De, C. Santoro, D. Sblattero, Rapid interactome profiling by massive sequencing. *Nucleic Acids Res.* 38 (2010) e110.
22. L.M. Work, S.A. Nicklin, N.J. Brain, K.L. Dishart, D.J. Von Seggern, M. Hallek, H. Buning, A.H. Baker, Development of efficient viral vectors selective for vascular smooth muscle cells. *Mol.Ther.* 9 (2004) 198-208.



Cyclic peptides to improve delivery and exon skipping of antisense oligonucleotides for Duchenne muscular dystrophy

S.M.G. Jirka¹, P.A.C. 't Hoen¹, V. Diaz Parillas², C. Tanganyika-de Winter¹, R.C. Verheul², B. Aquilera²,

P.C. de Visser², A. Aartsma-Rus¹

¹Department of Human Genetics, Leiden University Medical Center, 2300 RC Leiden, The Netherlands

²BioMarin Nederland BV, 2333 CH Leiden, The Netherlands

Submitted

Abstract

Duchenne muscular dystrophy (DMD) is a severe, progressive muscle wasting disorder caused by reading frame disrupting mutations in the *DMD* gene. Exon skipping is a therapeutic approach for DMD. It employs antisense oligonucleotides (AONs) to restore the disrupted open reading frame, allowing the production of shorter, but partly functional dystrophin protein as seen in less severely affected Becker muscular dystrophy patients. To be effective, AONs need to be delivered and effectively taken up by the target cells, which can be accomplished by the conjugation of tissue homing peptides. We performed phage display screens using a cyclic peptide library combined with next generation sequencing analyses to identify candidate muscle-homing peptides. Conjugation of the lead peptide to 2'-*O*-methyl phosphorothioate AONs enabled a significant, two-fold increase in delivery and exon skipping in all analyzed skeletal and cardiac muscle of *mdx* mice and appeared well tolerated. While selected as a muscle homing peptide, uptake was increased in liver and kidney as well. The homing capacity of the peptide may have been overruled by the natural biodistribution of the AON. Nonetheless, our results suggest that the identified peptide has the potential to facilitate delivery of AONs and perhaps other compounds to skeletal and cardiac muscle.

1. Introduction

Duchenne muscular dystrophy (DMD) is a severe, progressive, X-linked muscle wasting disorder affecting 1 in 5,000 newborn boys worldwide (1,2). In general, DMD patients are diagnosed before the age of 5, become wheelchair dependent around the age of 12, need assisted ventilation around 20 years of age and currently have a life expectancy of ~30 years in the Western world (2). DMD is caused by out of frame or nonsense mutations in the *DMD* gene that lead to truncated, non-functional dystrophin proteins. Dystrophin provides stability to the muscle fibers upon contraction (3). Lacking dystrophin, muscle fibers are easily and continuously damaged, and eventually replaced by non-functional fibrotic and adipose tissues. In contrast, Becker muscular dystrophy (BMD) is a muscle wasting disorder caused by mutations in the same gene, but here mutations maintain the open reading frame and allow production of an internally deleted, but partially functional dystrophin protein. The phenotype of patients with BMD is milder and less progressive, and patients have generally near normal life expectancies (2). Restoration of the reading frame in DMD patients would in theory allow the production of a shorter, but partly functional dystrophin protein as seen in patients with BMD (4,5). This restoration can be achieved with antisense oligonucleotides (AONs) that recognize specific exons during pre-mRNA splicing and induce skipping of target exons (6,7). The first exon skipping drug (eteplirsen) was recently approved by the FDA (<http://www.fda.gov/NewsEvents/Newsroom/PressAnnouncements/ucm521263.htm>).

Exon skipping AONs need to be delivered and taken up adequately by the target tissue and enter the target tissue cells to be effective. Furthermore, when taken up by endocytosis, they have to escape from the endosomes and reach the nucleus where splicing takes place. Since the human body consists of 30-40% muscle, body-wide treatment is necessary for DMD. This appeared feasible for AONs, as observed in preclinical animal studies, however in humans it remains challenging to reach a significant clinical benefit for DMD patients (6,8-12). Studies in animal models have revealed that large portions of the AON end up in liver and/or kidney, while uptake and consequently exon skipping levels in skeletal muscle and heart are low and very low, respectively when using AON doses comparable to those used in humans in clinical trials (13-15). Obviously, improved AON delivery to skeletal and cardiac muscle is anticipated to enhance therapeutic effects of AONs.

Non-muscle specific strategies for improving the delivery of AON are the use of nanoparticles, cell penetrating peptide (CPP) conjugation or co-administration of additive compounds to enhance cellular uptake (16-27). Highly cationic CPPs are, however, unsuitable for conjugation to anionic AONs such as 2'-*O*-methyl phosphorothioate AON (2OMePS) due to aggregation issues. For this AON chemistry, we therefore chose to use (non-highly cationic) tissue homing peptides, identified using phage display technology, a well-described technique to identify target specific peptides, antibodies and proteins (Smith, 1985). This approach can be cumbersome and it is well known that many false positive peptides have been identified (28). However, analyzing the outcome of phage display experiments with next generation sequencing (NGS) improves the chance of success greatly (29). NGS allows us to use just a single screening round, preventing parasitic peptide sequences to dominate the outcome and making identification of parasitic peptide sequences easier and more reliable. First encouraging results were reported using a short, linear 7-mer homing peptide selected from *in vivo* phage display biopanning experiments towards skeletal and cardiac muscle using the Ph.D.-7™ phage display library (30). This library expresses a few copies of a linear 7-mer peptide at the N-terminus of the PIII protein of the phage. In addition, a cyclic 7-mer peptide library, Ph.D.-C7C™, is available. This C7C-peptide library shares its features with the linear library but expresses peptides that are cyclized by disulfide bridges between two cysteine residues that are positioned at each end of the random 7-mer peptide. We reasoned that the conformational restriction by cyclization would lead to higher affinity binding, and thus to potentially more efficient targeting peptides.

Here, we explored the identification of muscle homing peptides with new phage display peptide library screens, *in vitro* and *in vivo*, using the Ph.D.-C7C™ peptide library combined with NGS analyses. This allowed the identification of a cyclic peptide (CyPep10) which, upon conjugation to a 2OMePS AON, resulted in a significant, two-fold increase in delivery and exon 23 skipping in all analyzed skeletal muscles and heart of the *mdx* mouse model and appeared well tolerated. Although this peptide was selected for being muscle specific, a more general increased delivery of the conjugate throughout tissues was seen. Nonetheless, results suggests that the identified peptide has the potential to facilitate targeted delivery of AONs and possible other compounds to skeletal and cardiac muscle for DMD.

2. Material and methods

Animal care

All experiments were approved by the animal experimental commission (DEC) of the LUMC and performed according to Dutch regulation for animal experimentation. Mice were housed with a 12 hour light-dark cycles in individually ventilated cages and had access to standard chow and water *ad libitum*. In all studies mice of mixed gender were used.

Cell culture

All cells were cultured in an incubator at 37°C and 5% CO₂.

Human control myoblasts (7304-1 cells (kindly provided by dr. Vincent Mouly (31)), used for phage display biopanning) were grown in NutMix F-10 (HAM) medium supplemented with GlutaMax™-I, 20% fetal bovine serum (FBS) and 1% penicillin/streptomycin (P/S) (all from Gibco-BRL, the Netherlands) in flasks coated with purified bovine dermal collagen (collagen) for cell culture (Nutacon B.V. the Netherlands). Cells were plated on collagen coated petri-dishes and grown to 90% confluence before switching to differentiation medium (Dulbecco's medium (DMEM), without phenol red, with 2% FBS, 1% P/S, 2% GlutaMax™-I and 1% glucose (all from Gibco-BRL, the Netherlands)). Cells were allowed to differentiate for 7-14 days.

Human control myoblasts (Km155.c25 cells, kindly provided by dr. Vincent Mouly) were grown in skeletal muscle cell growth medium (Promocell, C-23160) supplemented with an extra 15% FBS and 50 µg/ml gentamicin (PAA Laboratories, USA) in uncoated flasks until 70-80% confluence was reached. Cells were plated in a six wells plate with 0.5% gelatin coated glass slides (Sigma Aldrich, the Netherlands), at a density of 1x10⁵ cells per well, 48 hours prior to differentiation. Reaching 90% confluence, medium was switched to differentiation medium (DMEM (without phenol red) with 2%

FBS, 50 µg/ml gentamicin, 2% GlutaMax™-I and 1% glucose). Cells were allowed to differentiate for 3-5 days.

Immortalized human cardiomyocytes (Applied Biological Materials, Canada) were grown in Prigrow I medium supplemented with 10% FBS and 1% P/S in collagen coated flasks. Cells were plated in collagen coated glass slides in six wells plates and grown until confluence prior to experiments.

In vitro Biopanning

In vitro biopanning was performed as previously described by 't Hoen *et al* (29). Differentiated human control myoblasts cells (7304-1) were washed three times with phosphate buffered saline (PBS) and incubated with DMEM supplemented with 0.1% bovine serum albumin (BSA) for one hour at 37°C, 5% CO₂. Cells were washed with PBS and incubated with 2x10¹¹ phages from the Ph.D.-C7C™ Phage Display Peptide Library kit (New England Biolabs (NEB), USA) in 3 ml DMEM medium for one hour at 37°C, while shaking at 70 rounds per minute. After incubation, the cells were gently washed six times by incubating with 5 ml of ice cold DMEM containing 0.1% BSA, for five minutes. Subsequently, the cells were incubated for 10 minutes on ice with 3 ml of 0.1M HCl (pH 2.2) to elute cell-surface bound phages, which was neutralized by addition of 0.6 ml 0.5M Tris. To recover the cell-associated phages, cells were lysed for one hour on ice in 3 ml of 30 mM Tris-HCl, 1 mM EDTA, pH 8. Phages from each fraction were titrated and amplified according to the manufacturer's instruction (NEB).

In vivo Biopanning

In total three *mdx* mice (C57Bl/10ScSn-DMD^{*mdx*} /J) were injected intravenously (IV) with 2x10¹¹ phages either from the first round *in vitro* cell-surface bound phages, *in vitro* internalized phages (i.e. second selection round *in vivo*) or the naive Ph.D.-C7C™ library (i.e. first *in vivo* selection round). Phages were circulated for one hour after which mice were under anesthesia perfused with PBS. Quadriceps muscles, heart and liver were isolated from mice injected with phages from the *in vitro* selection. Gastrocnemius and quadriceps muscles, heart, liver and kidney were isolated from the mouse injected with the naive library. Tissues were homogenized in TBS buffer using a MagNalyzer according manufacturer's instruction (Roche Diagnostics, the Netherlands). Phages were titrated and amplified according to manufacturer's instruction (NEB) (from here on referred to as enriched phage library).

DNA isolation and Next Generation Sequencing

Total phage DNA was isolated from all enriched phage libraries, the naive unselected library and the naive library after a single round of bacterial amplification. From each enriched phage library, 2×10^{11} phage particles were added to 500 μ l LB growth media in a 1.5 ml tube. The phages were precipitated with 200 μ l PEG 8000/NaCl (Sigma-Aldrich, the Netherlands) for 3-4 hours at room temperature. Phages were pelleted and DNA was isolated according to the manufacturer's instruction. The final pellet (phage DNA) was dissolved in milliQ water and DNA concentration determined by Nanodrop (ThermoFisher Scientific, the Netherlands) Phage DNA was amplified by PCR using the following primers (* is a phosphorothioate bond):

Forward: AAT GAT ACG GCG ACC ACC GAG ATC TAC ACT TCC TTT AGT GGT ACC TTT CTA TTC TC*A

Reverse: CAA GCA GAA GAC GGC ATA CGA GAT CGG BARCODE TCT ATG GGA TTT TGC TAA ACA ACT TT*C

The PCR primers used to amplify the phage DNA contain a subsequence that recognized the sequence flanking the 27 nucleotides long unknown insert sequence (including the two cysteines), the adapters necessary for binding to the Illumina flow cell and a unique barcode (underlined) for every enriched phage library. The PCR protocol applied was the following: 1 ng of phage DNA was incubated with 2.625 U high fidelity Taq polymerase (Roche Diagnostics, the Netherlands), 20 pM of primers in 1 time high fidelity PCR buffer containing 15 mM MgCl₂ and amplified for 20 cycles, each consisting of an incubation for 30 seconds at 94°C, 30 seconds at 67°C and 30 seconds at 72°C. The PCR was stopped in exponential phase to mitigate PCR-induced sequence biases. The final PCR product was purified with the Qiaquick PCR purification kit (Qiagen, Valencia, CA, USA). Concentrations as well as the correct length of the PCR products were established with an Agilent 2100 Bioanalyzer DNA 1000 assay (Agilent Technologies, USA). All PCR products from the enriched phage libraries were combined in a single lane. Phage fractions from the naive unselected library (with and without amplification) were combined together in another lane of the Illumina flow cell. Both pools were subjected to solid phase amplification in the cluster station following manufacturer's specification (Illumina, USA). Up to 50 cycles of single end sequencing (the minimal amount required for single end sequencing in the department due to presence of unrelated samples in the other lanes) were performed using a custom sequencing primer that started exactly at the first position of the unknown insert sequence (ACA CTT CCT TTA GTG GTA CCT TTC TAT TCT CAC TC*T). Sequencing was performed with the Illumina HiSeq 2000 with a v3 flow cell and reagents (Illumina, USA).

Next generation sequencing analyses

The Illumina CASAVA 1.8.2 software was used to extract fastq files from Illumina BCL files and to split the data based on the individual sample barcodes. For further analyses, sequences were filtered out if they did not fulfill the following criteria: sequences should start with GCT TGT followed by (NNK)₇, and end with TGC GGT GGA GGT, with N being any nucleotide and K being G or T. Subsequently, sequences were translated to amino acid sequences with a custom perl script using conventional amino acid codon tables. When the stop codon TAG was encountered this was changed to a CAG codon according to manufacturer's instruction (NEB). An overview of the coverage is shown in supplementary table 1 and figure 1. All sequenced phage library data was normalized by a square root transformation on the number of counts in the library, a commonly applied data transformation to stabilize the variance in count data (t Hoen et al., 2008a). Subsequently, parasitic sequences were excluded. Parasitic sequences were defined as sequences for which the frequency count in the naive amplified library minus the frequency count in the unamplified naive library was greater than two. Next, two separate analyses were performed. First, sequences with a frequency count higher than two in liver and or kidney were removed from the enriched skeletal and cardiac muscle libraries. Sequences in the skeletal and cardiac muscle libraries were, per individual enriched library, ranked by frequency count and interesting candidates divided in two groups i.e. 'skeletal muscle' and 'cardiac muscle'. Secondly, the threshold for liver and kidney was ignored and skeletal and cardiac muscle libraries ranked based on frequency count. Peptide sequences with higher frequency counts in liver and or kidney compared to skeletal or cardiac muscle were removed. Interesting candidates were selected and combined in the group 'cardiac muscle and skeletal muscle'. A final list of 25 candidate peptides was created (seven peptides for 'skeletal muscle'; seven peptides for 'cardiac muscle' and nine peptides for 'skeletal and cardiac muscle' groups). Finally, sequences with more than two positively charged amino acids (arginines or lysines) were removed from the final candidate list. Of this list, the best 12 candidate peptides were selected for further evaluation (three from 'skeletal muscle', four from 'cardiac muscle', five from 'skeletal and cardiac muscle' group)

Peptides

Fluorescently labeled cyclic and linear (Cys --> Ala substitution) peptides were obtained from Pepscan (Lelystad, the Netherlands). A FITC-label was attached to an Ahx (6-aminohexanoic acid) spacer which was added to the N-terminus of the peptide, the C-terminus was amidated and peptides were made circular by disulfide cyclization.

***In vitro* evaluation of FITC-labeled peptides**

Positive/negative screening. FITC-labeled peptides were dissolved in water and, if necessary, acetic acid was used to help dissolve the peptide (final acetic acid concentration in experiment <0.2% v/v.) Final peptide concentrations were determined by spectrophotometric analysis at 490 nm, pH 7.5 (~20 times diluted in 1M Tris-HCl buffer, pH 7.5)

Human control myotubes and immortalized human cardiomyocytes were washed twice with PBS and incubated with 2.25 μ M of FITC-labeled peptides in serum free media for three hours at 37°C and 5% CO₂. Cells were washed three times with PBS and fixed with cold methanol (-20°C) for five minutes (human control myotubes) or 10 minutes (human cardiomyocytes). Subsequently the glass slides were shortly air dried, and embedded on microscope slides with Vectashield hard set containing DAPI, mounting media (Vector laboratories). After drying 30 minutes, slides were analysed with fluorescence microscopy, 20 times magnification (Leica DM5500 B) using a CCD camera (Leica DFC 360 FX).

Mechanistic uptake experiments. Human control myotubes in six-wells plate on gelatin coated cover glass slips (as previous described), were incubated for 30 minutes at 37°C and 5% CO₂ with 7.7 μ M sodium azide (NaN₃, Riedel-de Haën, Germany), 5 μ g/ml chloroquine diphosphate (Sigma Aldrich, the Netherlands), 75 μ g/ml fucoidan (from *focus vesiculosus*, Sigma Aldrich, the Netherlands), 2 μ g/ml dextran sulfate sodium salt (Sigma Aldrich, the Netherlands), 2.5 μ M chlorpromazine (Sigma Aldrich, the Netherlands), 200 μ M genistein (Sigma Aldrich, the Netherlands) or were kept at 4°C prior to the addition of 2.25 μ M of FITC-labeled peptide and subsequently incubated for another three hours at 37°C and 5% CO₂ or 4°C in the presence of the inhibitors. Cells were washed and slides were analysed as previously described for positive/negative screening of the peptides.

AON and CyPep-AON conjugates

The 5'-carboxylate linker phosphoramidite was purchased from Link Technologies (UK). All solvents and reagents were obtained from Sigma Aldrich (the Netherlands) or Acros (Belgium) and used as received unless indicated otherwise. Cyclic peptides were synthesized by Bachem (Switzerland). Observed molecular weights were corrected for reference standard values.

AON synthesis. 2OMePS AONs modified with a 5'-carboxylate linker were prepared through standard phosphoramidite chemistry protocols, using a 2-chlorotrityl (Clt)-protected amidite for the last coupling (15eq, 20min modified coupling conditions) and final removal of the Clt group. Cleavage/deprotection (0.1M NaOH in MeOH/H₂O 4/1 (v/v), 18h, 55°C), addition of NaCl and desalting by FPLC, and subsequent lyophilization yielded the desired crude AON which was of sufficient purity to use in the next steps.

CyPep10-h45AON synthesis. The 5'-carboxylate modified h45AON (1 μ mol) was added to a solution of HCTU (2.3 eq) and HOBt (2 eq) in DMSO (0.4 mL) for preactivation by shaking for three minutes at RT. CyPep10 (2 μ mol and 2.3 eq DiPEA in 0.1 mL DMF) was added and the reaction mixture was shaken for one hour at RT. RP-HPLC purification was followed by salt exchange using a small excess of NaCl. Excess salt was removed by FPLC and the conjugate was evaporated to dryness three times from MilliQ, yielding CyPep10-h45AON (0.3 μ mol (31%), MW (ESI) calc. 9211.9, found 9211.5).

CyPep6-23AON and CyPep10-23AON synthesis. Both conjugates were obtained through similar procedure as described for CyPep10-h45AON, in larger scale from six separate pooled syntheses: CyPep6-23AON (38 μ mol (37%), MW (ESI) calc. 8005.8, found 8006.5), and CyPep10-23AON (38 μ mol (36%), MW (ESI) calc. 8189.1, found 8188.7)

***In vitro* evaluation of peptide conjugated AON**

Human control myotubes (Km1555.c25, differentiated for 3-5 days) were incubated with 2 or 4 μ M AON or peptide conjugated-AON (CyPep-h45AON) for 96 hours in differentiation medium without a transfection reagent. After incubation cells were washed three times with PBS and RNA was isolated by adding 500 μ L TriPure (Roche diagnostics, the Netherlands) to each well to lyse the cells. This was followed by chloroform extraction in a 1/5 ratio on ice for five minutes. After centrifugation (4°C, 15 minutes, 15,400 rcf) the upper aqueous phase was precipitated for 30 minutes on ice with equal volume of isopropanol. Subsequently, RNA was pelleted down by centrifugation (4°C, 15 minutes, 15,400 rcf) and the pellet washed with 70% ethanol. The final pellet (RNA) was dissolved in Milli-Q water. For complementary DNA (cDNA) synthesis, half of RNA was used in a 20 μ L reaction with a specific primer reverse primer in exon 48 and transcriptase reverse transcriptase (Roche Diagnostics, the Netherlands) for 30 minutes at 55°C and five minutes at 85°C to terminate the reaction. For PCR analysis 3 μ L of cDNA was incubated with 0.625 U AmpliTaq polymerase (Roche Diagnostics, the Netherlands), 10 pM of primers (reverse primer in exon 48, and a forward primer in exon 43), one time supertaq PCR buffer (Enzyme Technologies Ltd, UK) and amplified for 20 cycles each consisting of an incubation for 40 seconds at 94°C, 40 seconds at 60°C and 80 seconds at 72°C. This PCR was followed by a nested PCR in which 1.5 μ L of the first PCR was incubated with 1.25 U AmpliTaq polymerase (Roche Diagnostics, the Netherlands), 20 pM of primers (reverse primer in exon 47 and a forward primer in exon 44) and one time supertaq PCR buffer (Enzyme Technologies Ltd, UK) were amplified for 32 cycles each consisting of an incubation for 40 seconds at 94°C, 40 seconds at 60°C and 60 seconds at 72°C. Exon skipping levels were semi-quantitatively determined as the percentages of the total (wild type and skipped) product with the Agilent 2100 Bioanalyzer.

In vivo evaluation of peptide conjugated AONs

hDMD mice. Four hDMD mice were injected in the gastrocnemius and triceps muscles with cardiotoxin two days prior to injection with 2.9 nmol of h45AON or CyPep10-h45AON contralateral for two consecutive days. One week after the last injection the mice were sacrificed, quadriceps (non-injected control), gastrocnemius, and triceps muscles were isolated to determine exon skip levels as described for the *in vitro* evaluation of peptide conjugated AON.

Mdx mice. Four week old (4-5 mice per group, mixed m/f) *mdx* mice (C57Bl/10ScSn-DMD^{mdx}/J) were subcutaneously (SC) injected with 50 mg/kg AON, molar equivalent of CyPep-AON, or saline four times per week for eight weeks. After the first injection, blood was collected via the tail vein to determine AON levels in plasma at 30 minutes, one hour, three hours and six hours via sparse sampling approach. One week after the last injection blood was collected via the tail vein to determine AON in plasma and assess plasma levels of markers for liver and kidney function and damage. Subsequently, mice were anesthetized, sacrificed by perfusion with PBS and gastrocnemius, quadriceps, tibialis anterior, triceps, diaphragm, heart, kidney and liver were isolated to determine exon skip, AON and dystrophin levels in tissue.

Determination of *in vivo* exon skip levels

Skeletal and cardiac muscles were homogenized in TriPure buffer (Roche Diagnostics, the Netherlands) using the MagNaLyzer and MagNaLyzer green beads (Roche Diagnostics, the Netherlands). Total RNA was isolated as described for the *in vitro* evaluation of peptide conjugated AON.

RT-PCR. cDNA was generated using 400 ng of RNA in a 20 µl reaction with random hexamer primers and transcriptase reverse transcriptase (Roche Diagnostics, the Netherlands) for 45 minutes at 42°C. For PCR analysis 1.5 µl of cDNA was incubated with 1.25 U taq polymerase (Roche Diagnostics, the Netherlands), 20 pM of primers (reverse primer in exon 24, forward primer in exon 22) and one time supertaq PCR buffer (Enzyme Technologies Ltd) and amplified for 30 cycles each consisting of an incubation for 30 seconds at 94°C, 30 seconds at 60°C and 30 seconds at 72°C. Exon skipping levels were semi-quantitatively determined as the percentages of the total (wild type and skipped) product with the Agilent 2100 Bioanalyzer.

ddPCR. cDNA was generated in 20 µl reactions, using 1,000 ng of total RNA with random hexamer primers (Roche Diagnostics, the Netherlands) and transcriptase reverse transcriptase (Roche Diagnostics, the Netherlands) according to the manufacturer's instructions. Digital droplet PCR (ddPCR) was performed in duplicate as previously described (Verheul et al., 2016) on 0.5 µl of cDNA using a Taqman assay spanning the exon 22-23 junction to detect the non-skipped fragment and an assay spanning the exon

22-24 junction to detect the skipped fragment (sequences are listed in supplementary table 2). The concentration (in copies/µl sample mix) of the skipped assay and non-skipped assay was used to calculate the percentage of exon 23 skip [copies/µl skipped/(copies/µl skipped + copies/µl non-skipped)*100].

Determination of AON levels in plasma and tissue

For measuring the concentration of (CyPep)-23AON in plasma and tissue samples a hybridization-ligation assay based on one previously published was used (Yu et al., 2002) following adaptations previously described (Jirka et al, 2015). Tissues were homogenized in 100 mM Tris-HCl pH 8.5, 200 mM NaCl, 0.2% SDS, 5 mM EDTA and 2 mg/mL proteinase K using MagNaLyzer green bead tubes in a MagNaLyzer (Roche Diagnostics, the Netherlands). Samples were diluted 600 and 6,000 times (muscle) or 6,000 and 60,000 (liver and kidney) in pooled control *mdx* tissue in PBS. Calibration curves of the analyzed 23AON prepared in 60 times pooled control mouse *mdx* tissue in PBS were included. All analyses were performed in duplicate. For plasma, the samples were diluted as follow: t = 30 minutes and one hour 10,000 and 100,000 times, t = three hours 1,000 and 10,000 times, t = six hours and sacrifice 100 and 1,000 times, all in pooled control plasma of *mdx* mice in PBS. Calibration curves of the analyzed 23AON prepared in 100 times pooled control plasma of *mdx* mice in PBS were included.

Determination of protein levels by western blot

Quadriceps muscle samples were homogenized in MagNaLyzer green bead tubes with a MagNaLyzer (Roche diagnostics, the Netherlands). Samples were homogenized for 20 seconds at speed 7,000 (2-5 rounds) in 1 ml 125 mM Tris-HCl (pH 6.8) buffer supplemented with 20% (w/v) sodium dodecyl sulfate (SDS). Protein concentrations were determined by the bicinchoninic acid (BCA) protein assay kit (Thermo Fisher Scientific, the Netherlands) using bovine serum albumin as a standard according to manufacturer's instruction. Prior to loading, a sample volume (for muscle tissue and reference samples) representing 25 µg of total protein, was supplemented with loading buffer consisting of 125 mM Tris-HCl (pH 6.8), 20% (v/v) glycerol, 5% (v/v) β-mercaptoethanol and 0.0008% (w/v) bromophenol blue, to reach a final volume of 20 µl. Subsequently this was incubated for five minutes at 95°C. Reference concentration samples were made by diluting total protein from wild type in *mdx* lysates of the same muscle type. Samples were loaded on Criterion XT Tris acetate (polyacrylamide) gels containing 18 slots, with a linear resolving gel gradient of 3-8% (Bio-Rad Laboratories, The Netherlands). Gels were run for one hour at 75 V (~0.07 A), followed by a two hour incubation at 150 V (~0.12 A), on ice, using XT Tricine as running buffer (Bio-Rad Laboratories B.V., the Netherlands). The gel was blotted on a nitrocellulose membrane (Bio-Rad Laboratories B.V., the Netherlands) using the ready to use Trans-Blot Turbo transfer packs

and the Trans-Blot Turbo transfer system from Bio-Rad at 2.5 A (~25 V) for 10 minutes (standard Bio-Rad protocol for high molecular weight proteins). The membrane was blocked for one hour with 5% (w/v) non-fat dried milk powder (ELK Campina Melkunie, the Netherlands) in a Tris-buffered saline buffer (TBS: 10 mM Tris-HCl (pH 8.0) and 0.15 M NaCl). Membranes were washed three times for 10 minutes with TBS-T buffer (TBS buffer with 0.005% (v/v) Tween 20) and incubated with primary antibody for dystrophin (GTX15277, 1:2000, Gene Tex, USA) and primary antibody for loading control, alpha-actinin (AB72592, 1:7500, Abcam, UK) in TBS buffer overnight at room temperature with gentle agitation. Membranes were washed three times for 15 minutes in TBS-T buffer and incubated with secondary antibody IRDye 800 CW for dystrophin (1:5000, IgG, Li-Cor, USA) and IRDye 680TL for alpha actinin (1:10000, Li-Cor, USA) in TBS buffer for one hour. Membranes were washed two times for 15 minutes in TBS-T buffer followed by a final washing step of 15 minutes in TBS buffer. Membranes were analyzed with the Odyssey system and software (Li-Cor, USA)

Safety evaluation

Blood was collected in lithium-heparin coated microvettes CB300 (Sarstedt B.V., the Netherlands). Haemoglobin (HB), urea, alkaline phosphatase (ALP), glutamate pyruvate transaminase (GPT), glutamic oxaloacetic transaminase (GOT), and creatine kinase (CK) levels were determined using Reflotron strips (Roche Diagnostics, the Netherlands) in the Reflotron Plus machine (Roche Diagnostics, the Netherlands) as previously described (30).

Statistical analysis

A one-way ANOVA with a post-hoc test (Bonferroni) was used to determine significant differences in exon skipping levels, AON levels and plasma protein levels. Results were deemed significantly different when $P < 0.05$.

3. Results

Candidate peptide identification

To identify peptides that enhance the delivery of AONs to skeletal and cardiac muscle we used the Ph.D.-C7C™ phage display peptide library. A schematic outline of the screening procedure is given in figure 1. We performed a first round *in vitro* screening using human control myotubes (7304-1) in which internalized and surface bound phages were isolated and amplified. Subsequently, the naive library was also used for a first round *in vivo*, enriched internalized phage fraction and the enriched surface bound phage fraction were used for a second *in vivo* screening round in *mdx* mice, a mouse model for DMD. Gastrocnemius, quadriceps and heart were isolated for positive phage selection. Liver and kidney were isolated for negative phage selection. All enriched libraries from the biopanning selections, and the naive library with and without one round of bacterial amplification, were sequenced using a published NGS sequencing approach (29) with further adaptations and improvements to increase efficiency. First, we barcoded each of the libraries using sample specific barcodes in the reverse primer, allowing all enriched libraries to be pooled in one lane and the two naive libraries to be pooled in a second lane. Results are summarized in supplementary table 1 and supplementary figure 1.

To identify candidate peptides, the enriched phage libraries were first filtered for parasitic sequences with a propagation advantage. Sequences were considered parasitic when the frequency count in the naive amplified library minus the frequency count in the unamplified naive library was greater than two. Secondly, candidate peptides were selected based on the following criteria: A) the candidate peptide sequence has a relatively low frequency count or is absent in liver and kidney, and B) the candidate peptide sequence has either a high frequency count in skeletal muscle and low frequency count in cardiac muscle or vice versa, or C) the candidate peptide sequence has a high frequency count in both skeletal and in cardiac muscle (figure 1). Lastly, we took the charge of the peptides into account: candidate peptide sequences with more than two positively charged residues (arginines or lysines) were removed from the candidate list, because they were expected to likely form aggregates when attempting to couple them to negatively charged AONs.

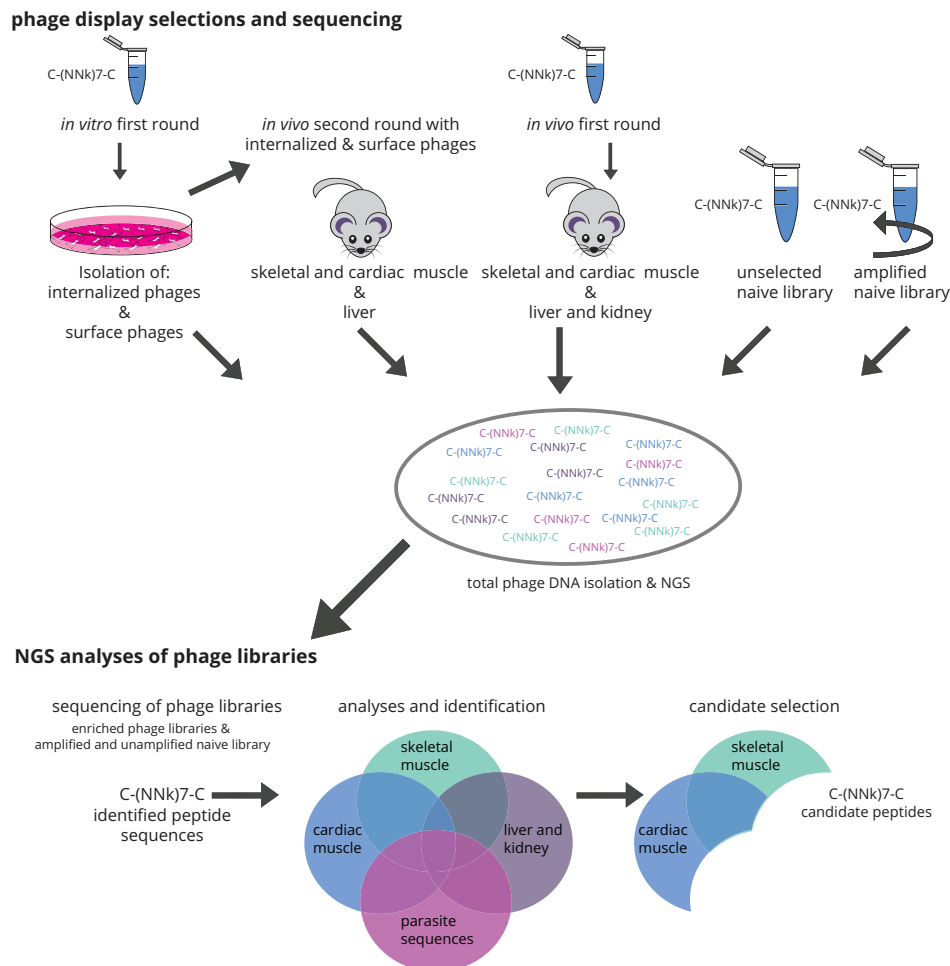


Figure 1. Phage display selections and sequencing. A schematic overview of the phage display selection experiments and candidate peptide identification.

Table 1

Peptide	Sequences	Group
CyPep1	CQVRSNTTC	Muscle
CyPep2	CSLFKNFRC	Muscle/heart
CyPep3	CRADFYTTC	Heart
CyPep4	CRETNHTC	Heart
CyPep5	CWNEDHTWC	Muscle/heart
CyPep6	CLNSLFGSC	Muscle/heart
CyPep7	CLLGHTNNC	Muscle
CyPep8	CFSHTYRVC	Muscle
CyPep9	CTYSPTEVC	Heart
CyPep10	CQLFPLFRC	Muscle/heart
CyPep11	CTLQDQATC	Heart
CyPep12	CMQHSMRVC	Muscle/heart

In vitro evaluation of the peptides

For *in vitro* evaluation of uptake by skeletal and cardiac cells, we synthesized the best 12 candidate peptides equipped with a FITC label (Table 1). Human control myotubes (km155.c25) or human cardiomyocytes cultured on cover glass slips were incubated for three hours with 2.25 μM of candidate peptides. After thorough washing, slides were fixed with methanol and embedded in mounting media containing DAPI to stain the nuclei. Most of the peptides were not taken up based on the absence of fluorescence in the cells. Cells incubated with CyPep2, CyPep8 or CyPep9 were weakly fluorescent, whereas incubation with CyPep6 (CLNSLFGSC) and CyPep10 (CQLFPLFRC) resulted in bright fluorescence throughout the cells with fluorescence also observed in the nuclei (figure 2). When we repeated the experiment using different incubation times, clear fluorescence of CyPep6 and CyPep10 could be seen in human control myotubes after one hour of incubation (figure 3a). In cardiomyocytes, higher fluorescence intensity was observed for CyPep6 compared to CyPep10 after three hours of incubation (figure 3b). Interestingly, incubation with CyPep10 resulted in detectable levels of fluorescence in human control myotubes and human cardiomyocytes cultures, already, after an incubation of 10 minutes (figure 3c), something we did not observe for CyPep6 (data not shown).

To study if the cyclisation of the peptide is crucial for the observed results, FITC-labeled linear forms of CyPep6 and 10 with Cys>Ala substitutions were synthesized. No fluorescence was observed for both peptides suggesting that not only the sequence, but also the cyclisation is responsible for the positive fluorescence observed (figure 3d).

Peptide conjugation does not impair exon skipping *in vitro* and *in vivo*

To investigate if the conjugation of these cyclic peptides to a 2OMePS AON impacts its exon skipping ability, we conjugated CyPep10 to a human AON targeting human dystrophin exon 45 (h45AON). Human control myotubes were incubated with 2 μ M or 4 μ M of h45AON or CyPep10-h45AON for 96 hours without a transfection reagent. Subsequently, the cells were washed, followed by RNA isolation and nested RT-PCR. Exon skipping levels were determined semi-quantitatively by lab-on-a-chip analysis. This revealed no differences in exon skipping levels (figure 4a).

Furthermore, we evaluated CyPep10-h45AON in hDMD mice, a mouse model with the human *DMD* gene integrated in the mouse genome (32). This mouse model has healthy muscle, since human dystrophin compensates for the lack of mouse dystrophin. We pretreated gastrocnemius and triceps muscles intramuscularly (IM) with cardiotoxin injections to induce muscle necrosis and enhance AON uptake (14). Two days later muscles were injected with 2.9 nmol of h45AON or a molar equivalent of CyPep10-h45AON for two consecutive days. One week after the last injection, RNA was isolated, nested RT-PCR performed and exon skipping levels were determined semi-quantitatively by lab-on-a-chip analyses. No differences in exon skipping levels were found, showing that the conjugation of a cyclic peptide to an AON also has no negative influence on its exon skipping ability *in vivo* (figure 4b).

Conjugation of CyPep10 to AONs increases uptake and exon skipping levels after systemic delivery in *mdx* mice

We evaluated CyPep6 and CyPep10 for their ability to enhance delivery and efficacy of AONs in skeletal and cardiac muscle in *mdx* mice upon systemic administration. *Mdx* mice (C57Bl/10ScSn-DMD^{mdx}/J) have a point mutation in exon 23 of the mouse *Dmd* gene, which leads to a premature stop codon, resulting in an absence of the dystrophin protein (Sicinski et al., 1989). Skipping exon 23 in the *mdx* mouse *Dmd* pre-mRNA bypasses the mutation, maintaining the reading frame and results in a shorter but (partly) functional protein. CyPep6 and CyPep10 were conjugated to a 2OMePS AON targeting the exon 23/intron 23 splice site (23AON) (33). We systemically treated four week old *mdx* mice (4-5 per group) subcutaneously (SC) for four times per week with 50 mg/kg 23AON, a molar equivalent of CyPep6-23AON or CyPep10-23AON, or saline for eight weeks. Animals were sacrificed one week after the last injection.

Evaluation of AON levels in plasma, obtained at several time-points (sparse sampling approach) after the first injection, revealed increased levels of CyPep10-23AON in plasma for the first three hours after injection but not for CyPep6-23AON (figure 5a). In tissues, a 2-fold (on average) increase of

CyPep6 and CyPep10-conjugated 23AON was observed in gastrocnemius, quadriceps, tibialis anterior and triceps muscle, and 3 and 2.8-fold increases were observed in diaphragm and heart, respectively. Unexpectedly, 2.5-fold and 3-fold increases were found in liver for CyPep6 and CyPep10 conjugated 23AON. A less prominent and non-significant 1.5 fold increase in kidney was seen for both conjugated 23AONs (figure 5b).

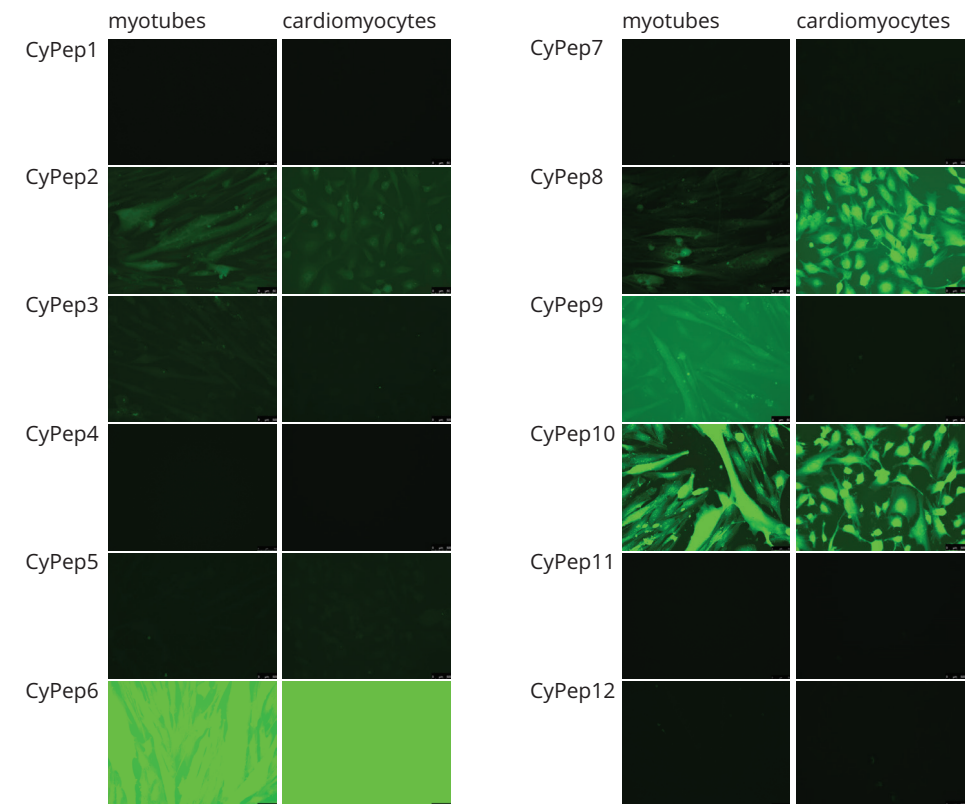


Figure 2. In vitro evaluation of fluorescently labeled cyclic-peptides. Human control myotubes and cardiomyocytes were incubated with 2.25 μ M of FITC-labeled CyPeps for three hours. Slides were embedded in mounting media containing DAPI to stain nuclei. Fluorescence intensities were analyzed with fluorescence microscopy 20 times. magnification, representative pictures are shown. Bright fluorescence in the cells is seen for CyPep6 and CyPep10. CyPep2, CyPep8 and CyPep9 resulted in weak fluorescence. Scale bar = 50 μ m.

Exon skipping levels (single round RT-PCR) in skeletal and cardiac muscle showed a significant, 2-fold increase in exon 23 skipping for CyPep10-23AON compared to the unconjugated 23AON (figure 5c). Surprisingly,

CyPep6-23AON did not show any improvement in exon skipping levels. Dystrophin could be detected in quadriceps of all AON (conjugated and unconjugated) treated mice by western blot analysis. Upon visual inspection, a slight increase seems to be present for mice treated with CyPep10-23AON (figure 5d), but levels were too low for quantification.

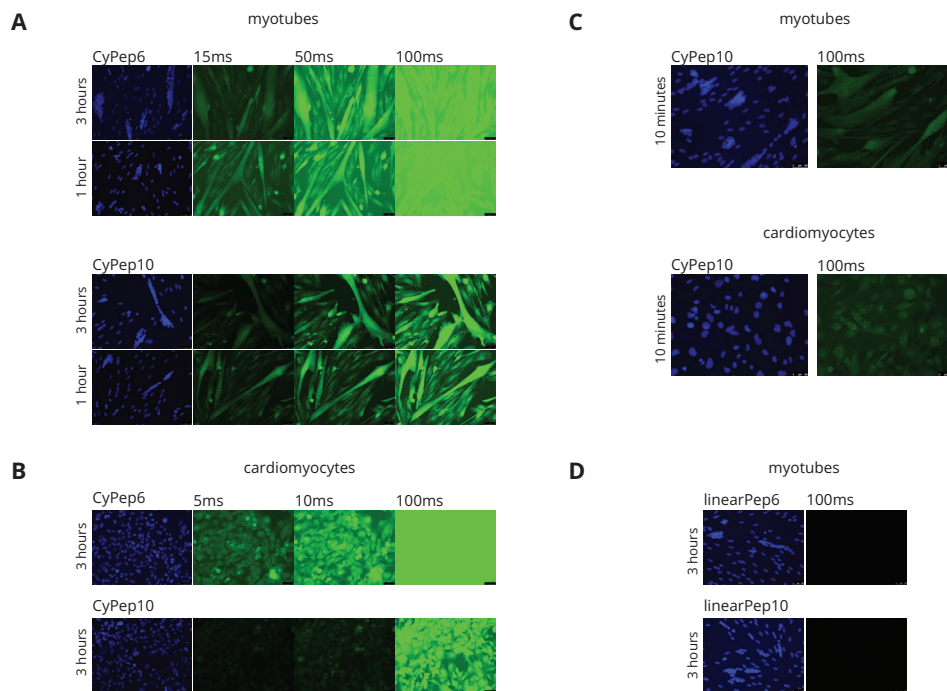


Figure 3. In vitro evaluation of CyPep6 and CyPep10. CyPep6 and CyPep10 were incubated at a dose of 2.25 μ M, slides were embedded in mounting media containing DAPI and analyzed with fluorescence microscopy, 20 times magnification. a) human control myotubes incubated with CyPep6 or CyPep10 for three or one hour. b) human cardiomyocytes incubated with CyPep6 or CyPep10 for three hours. c) human control myotubes or cardiomyocytes incubated with CyPep10 for 10 minutes. d) human control myotubes incubated with linearPep6 or linearPep10 for three hours. Representative pictures are shown. First pictures (left) DAPI staining in blue, exposure time for each picture in milliseconds (ms). Scale bar = 50 μ m.

Results show clear fluorescence throughout the cells and in the nuclei of CyPep6 and CyPep10 at three hours and one hour of incubation for both cell lines. CyPep10 showed already positive fluorescence after 10 minutes for both cell lines. The linear forms of both peptides (with Cys \rightarrow Ala) did not show any fluorescence indicating that not only the sequence but also the cyclisation is of influence.

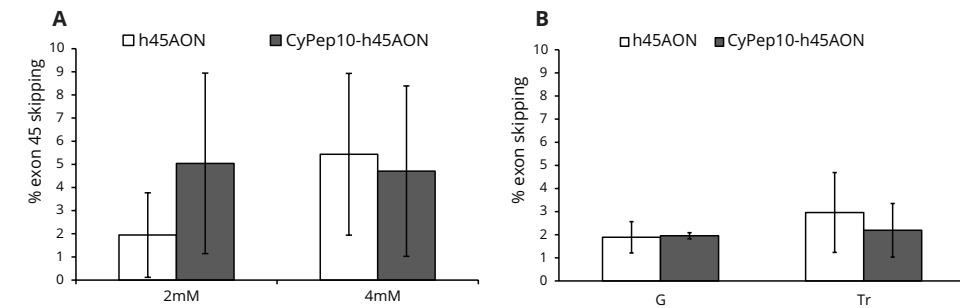


Figure 4. Evaluation of CyPep10 AON-conjugate. CyPep10 was conjugated to an AON targeting human dystrophin exon 45 (h45AON and CyPep10-h45AON) to evaluate if the conjugation of a cyclic peptide has any influence on the exon skipping functionality of the AON. a) human control myotubes incubated with 2 or 4 μ M AON without any transfection reagent for 96 hours. Results show the average exon skipping levels of two independent experiments in duplo. b) IM injection in two hDMD mice (pretreated with cardiotoxin) with 2.9 nmol h45AON of molar equivalent of CyPep10-h45AON for two consecutive days. Results represent an average of two independent experiments in duplo. Results indicate that the conjugation of a cyclic peptide to a 2OMePS AON has no negative influence on the functionality of the AON. G = Gastrocnemius, Tr = Triceps. Bars represent mean \pm SD.

We replicated the RT-PCR results for CyPep10-23AON for gastrocnemius, quadriceps and triceps muscles using a highly quantitative method, i.e. digital droplet PCR (ddPCR) (34). These results showed a 2.4-fold increase on average in exon 23 skipping levels for CyPep10-23AON compared to the unconjugated 23AON. This supports our findings from the RT-PCR (figure 5e).

Lastly, we evaluated blood and plasma parameters for liver and kidney damage and function to determine any possible toxicity of the conjugates used, in samples obtained just prior to sacrifice. Hemoglobin levels, urea (a marker for kidney function) and alkaline phosphatase (ALP, a marker for hepatobiliary function), showed no significant differences between groups and were within the normal range for *mdx* mice. Levels of glutamate pyruvic transaminase (GPT) and glutamic oxaloacetic pyruvate transaminase (GOT), markers for liver and muscle damage and creatine kinase (CK), marker for muscle damage, were evaluated. No significant differences were observed for GPT. GOT levels were slightly lower, but not significantly, for CyPep10-23AON. CK was significantly decreased in CyPep10-23AON treated mice compared to the 23AON, but not compared to saline treated mice due to the high variation observed in this group (supplementary figure 2).

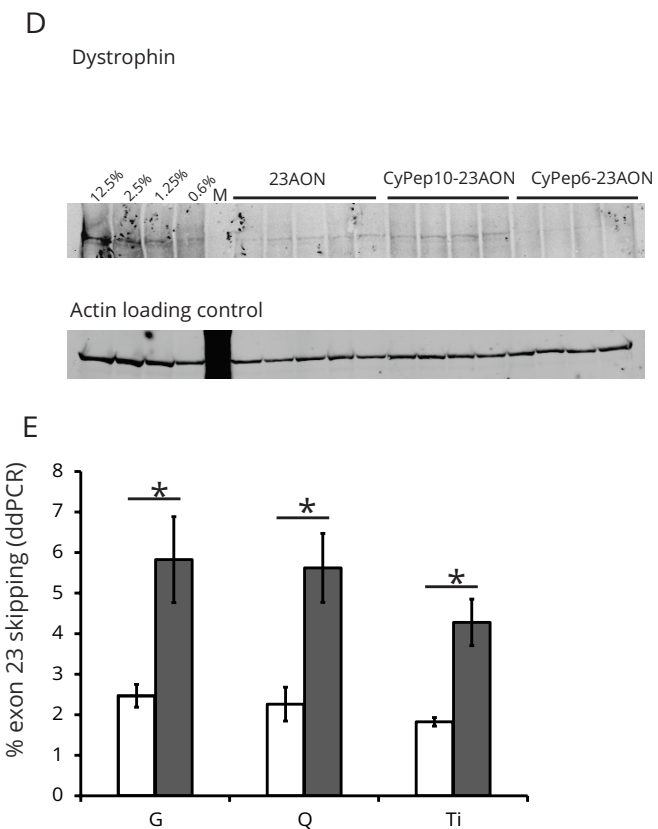
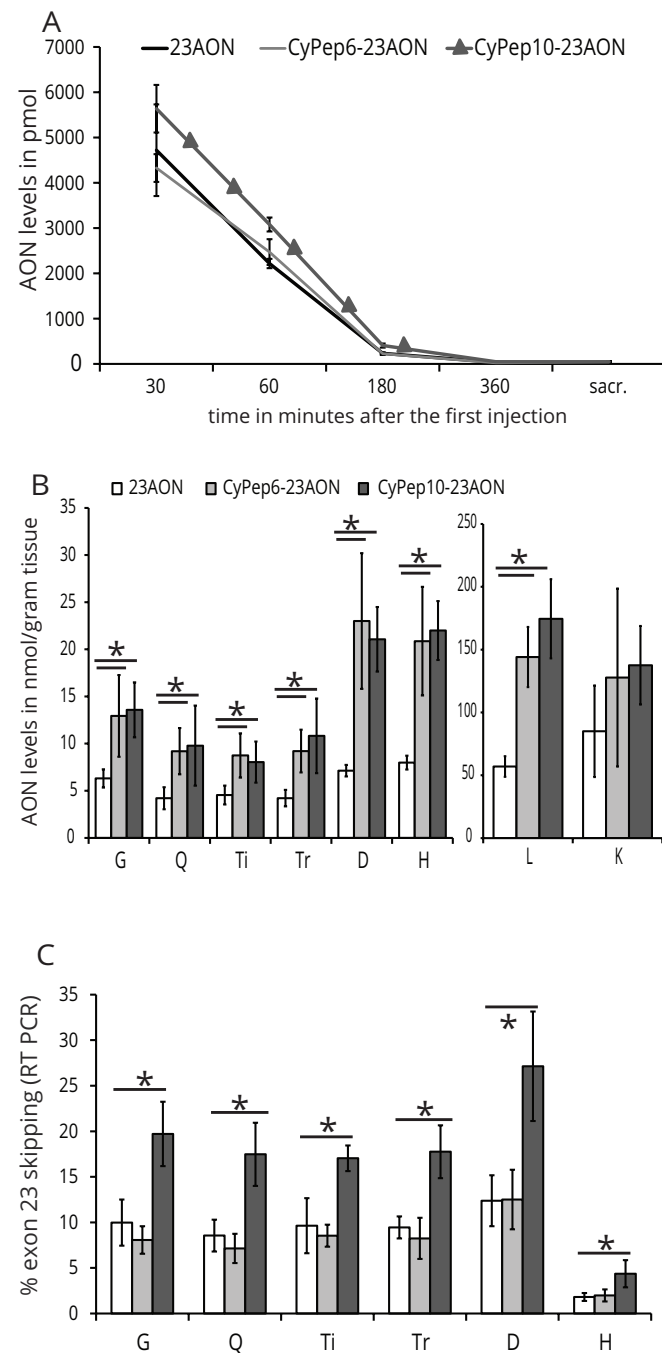


Figure 5. Systemic evaluation of CyPep6 and CyPep10 conjugated AON. Subcutaneous administration of four week old mdx mice (4-5 per group), four times per week, with 50mg/kg of 23AON, a molar equivalent of CyPep6-23AON, CyPep10-23AON or saline for eight weeks. One week after the last injection tissues were isolated. a) After the first injection blood samples were taken at several time points and at sacrifice to determine AON levels in plasma. b) A hybridization-ligation assay was used to determine AON levels in tissue. c) RNA was isolated and exon 23 skipping levels were evaluated by single RT-PCR and semi-quantitatively determined by lab-on-a-chip analysis. d) Dystrophin protein levels of quadriceps muscles were determined by western blot. e) Exon skipping levels in gastrocnemius, quadriceps and triceps muscle were quantified using ddPCR for CyPep10-23AON and 23AON treated mice. Results show a clear increase in AON levels in tissue and plasma for both peptide conjugated AON compared to the unconjugated AON. This resulted in a 2-fold increase in exon skip levels on average for CyPep10-23AON but not for CyPep6-23AON. No clear increase for dystrophin protein levels is observed. Bars represent mean \pm SD. A One-way ANOVA post-hoc test (Bonferroni) used for significance ($P < 0.05^*$). G= Gastrocnemius, Q = Quadriceps, Ti = Tibialis Anterior, Tr = Triceps, D = Diaphragm, H = Heart, L = Liver, K = Kidney.

Investigation of the uptake mechanism points towards receptor mediated uptake

Encouraged by the positive results for CyPep10, we set out to study the possible uptake mechanisms for this peptide. Human control myotubes were incubated with a number of pharmacological inhibitors (Table 2) for 3.5 hours, where 2.25 μM of FITC-CyPep10 was added after 30 minutes. CyPep10 showed a clear energy dependent uptake, as no fluorescence was observed at 4°C and reduced fluorescence was observed after pre-incubation with sodium azide. We speculate that there is no endosomal entrapment of FITC-CyPep10 based on the finding that incubation with 5 $\mu\text{g/ml}$ chloroquine did not result in increased fluorescence. With fucoidan (75 $\mu\text{g/ml}$) and dextran sulfate (2 $\mu\text{g/ml}$) blocking uptake by scavenger receptors, we observed less fluorescence, suggesting that scavenger receptors are involved in the uptake of FITC-labeled CyPep10. Incubation with chlorpromazine (2.5 μM) resulted also in less fluorescence suggesting that clathrin-mediated uptake is involved. In contrast, incubation with genistein (200 μM), an inhibitor of caveolin-mediated uptake, did not show any difference in fluorescence compared to CyPep10 alone. Combined, these results point towards an energy dependent uptake of CyPep10 via scavenger receptors accumulated in clathrin-coated pits of the muscle cell membrane (figure 6).

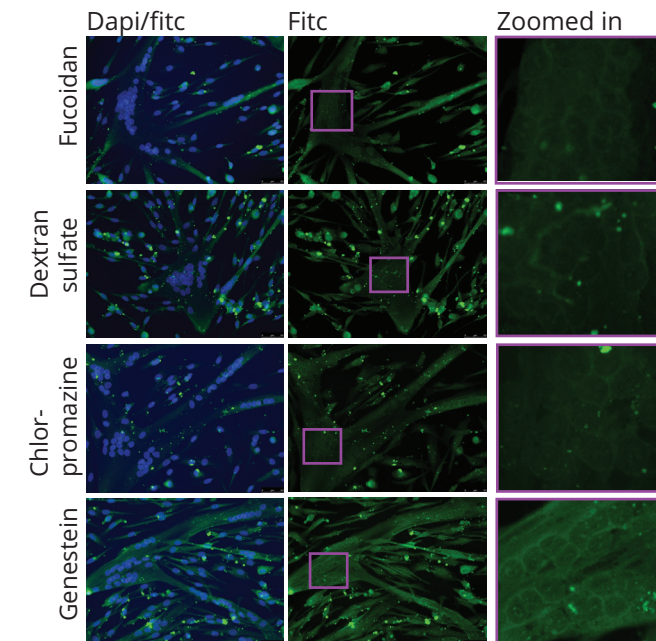
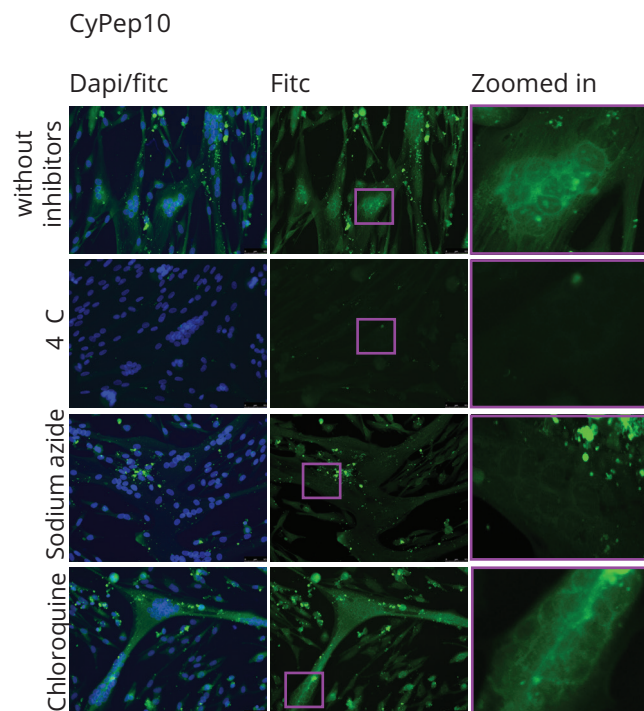


Figure 6. Uptake mechanism of CyPep10. Human control myotubes were incubated with pharmacological inhibitors for 30 minutes prior to a three hour incubation with CyPep10 in the presence of the inhibitors. Results were analyzed with fluorescence microscopy. Representative pictures are shown scale bar = 50 μm .

4. Discussion

Exon skipping is a therapeutic approach for DMD. Improved delivery of AON to the target tissue is anticipated to increase the therapeutic effect. Achieving this in a safe and effective way is challenging, although some progress has been made using PCM polymers, or ZM2 or polymeric nanoparticles (22,23,35). Most progress to increase the delivery and efficacy has been achieved by the conjugation of arginine rich cell penetrating peptides to non-anionic AONs such as peptide nucleic acid (PNA) and phosphorodiamidate morpholino oligomer (PMO). It was found that some of these highly cationic peptides were poorly tolerated in higher animals due to kidney toxicity (25). A different approach is the use of tissue homing peptides, which are not necessarily highly cationic. In 1999, Samoylova *et al.*, described a phage, expressing the 7-mer peptide ASSLNIA, which showed increased fluorescence in murine tissues compared to control phages upon histochemical analyses. Unfortunately, the peptide alone was unable to increase delivery or exon skipping levels in *mdx* mice when conjugated to a PMO (36,37). More recently, Gao *et al.*, reported the M12

peptide RRQPPRSISSHP (38), which, upon conjugation to a PMO, resulted in improved but variable exon skipping levels in *mdx* mice in skeletal muscle but not heart. Previously we described the 7-mer P4 peptide LGAQSNF identified through phage display studies, which, upon conjugation to a 2OMePS AON, resulted in significantly increased exon skipping levels in diaphragm and cardiac muscle tissue of *mdx* mice (30). Taken together, tissue homing peptide conjugation to AONs appears to be a promising strategy.

We believe the approach we have used here (figure 1) facilitates the identification of effective muscle homing peptides from phage display studies further for several reasons. First, as already outlined by other studies (29,39-41), the use of NGS enables to study large numbers of sequences. By sequencing the naive library before and after one round of bacterial amplification one can identify library specific peptide sequences that are overrepresented or have an amplification bias, the so called parasitic sequences (29,41). With our approach we assessed that a little over 1.9 million unique sequences in the naive amplified library are potentially parasitic sequences (around 21% of the total library). In the enriched libraries, ~11% of the unique sequences were represented by these parasitic sequences. However, even with NGS, only a fraction of possible sequences in the enriched libraries are sequenced (for comparison, the naive library contains 1.28×10^9 unique sequences whereas we sequenced approximately $1-2.5 \times 10^6$ sequences of the enriched libraries). Nevertheless, these millions of sequences are a vast improvement over the ~50-100 phage clones generally sequenced with Sanger sequencing (30). Furthermore, many sequences in the enriched library will be present only once or twice with the more abundant sequences primarily being of interest. As such, NGS sequencing will generally provide sufficient depth to identify interesting candidates. Additionally, the databases Pepbank (42) and Sarotup (28) can be used to filter known parasitic sequences or target-unrelated sequences, but are mainly applicable to linear peptides and do not provide sufficient information about cyclic peptides. Secondly, combining a first round *in vitro* screening with a second selection round *in vivo* screening we aimed to increase the potential binding of peptides towards muscle, since peptides with no affinity towards muscle would be deselected in the first round. By isolating phages from liver and kidney we were able to filter peptides which predominately were taken up by these tissues (e.g. target-unrelated sequences).

The 12 selected candidate peptides contained a group of seven that were identified in either skeletal or cardiac muscle (data not shown) and a group of five that were identified in both skeletal and cardiac muscle. *In vitro* evaluation of these candidates in human myotubes and cardiomyocyte cultures left us with two peptides for further study: CyPep6 and CyPep10, both identified in skeletal and cardiac muscle. Interestingly, of the peptides

selected based on presence in skeletal muscle or cardiac muscle, only three out of seven showed some degree of fluorescence. While in the group selected based on presence in skeletal and cardiac muscles, two out of three showed bright fluorescence and one showed some fluorescence. This suggests that for future studies it may be more efficient to focus only on peptides enriched in both skeletal and cardiac muscle tissue.

Systemic administration of CyPep6 and CyPep10-conjugated 23AON in *mdx* mice revealed a 2-fold increase of AON levels in skeletal muscle and around three-fold increase in diaphragm muscle and heart for both peptide conjugates over the unconjugated 23AON. This resulted in a significant 2-fold increase in exon skipping in all tissues analyzed for CyPep10-23AON, but surprisingly not for CyPep6-23AON (figure 5). A potential explanation for the discrepancy between CyPep6-23AON tissue levels and activity may lie in the fact that the peptides were isolated from muscle and heart tissue homogenates, and not selected for their capacity to actually enter the tissue or tissue cells. It is therefore possible that CyPep6-23AON conjugate is trapped somewhere in the endothelium or interstitium. Judged on the fluorescence observed *in vitro*, CyPep6 outperformed CyPep10 for both cell lines at time points one and three hours, except for the 10 minute incubation time point (figure 3). CyPep6 appears to be taken up by cells efficiently however not as fast as CyPep10. This could indicate that different mechanistic uptake pathways are involved and that fast uptake *in vitro* might lead to a better outcome *in vivo*. If CyPep6 alone does enter tissue and tissue cells, conjugation to the larger AON may have negatively affected the tissue- or cellular uptake *in vivo*. The fact that CyPep10-23AON did show increased exon skip levels suggests that this peptide conjugate is taken up by the target cells efficiently. Unfortunately, dystrophin levels were very low and could not be accurately quantified. It is known that dystrophin levels accumulate for 12-24 weeks after treatment initiation (43), so the time of sacrifice (deemed optimal for analysis of AON and exon skipping levels) is probably not optimal for assessing dystrophin levels.

Compared to unconjugated AON, we observed for CyPep10-23AON similar uptake in kidney, but a 2.5-fold increase in AON levels in liver. No clear indication is found in our NGS data that could explain the increased uptake in liver. CyPep10 showed a 4-fold increase in frequency count in the second round *in vivo* in quadriceps and heart compared to the first round *in vitro* (internalized phage fraction). Frequency counts in liver were 2.5 times lower in the second selection round *in vivo* compared to quadriceps and heart. After the first selection round *in vivo*, the counts in liver were 6.5 times lower compared to heart and 1.5 times lower compared to kidney. Thus the kidney and liver levels of CyPep10-AON conjugate may seem surprising given that the peptide was selected based on low uptake in these organs. However, one should not forget that the identified peptide was conjugated, in multiple copies, to a phage, while now it is singly conjugated to a 2OMePS

AON, which is by itself taken up efficiently by liver and kidney. It is not unlikely that this is further facilitated by peptide conjugation and/or that increased levels are due to the increased plasma half-life.

We finally investigated the mechanism by which FITC-labelled CyPep10 is taken up. Results clearly show that uptake of CyPep10 by muscle cells is energy dependent, because incubation at 4°C or with an ATP inhibitor almost completely prevented uptake. The involvement of scavenger receptors accumulated in clathrin-coated pits is also implied, since uptake was inhibited by inhibitors of scavenger receptors and clathrin-mediated uptake. Clathrin-mediated uptake is one of the main and best studied uptake pathways (44). It requires strong receptor/-ligand binding and clustering in clathrin-coated pits in an energy dependent way. The clathrin-coated pits invaginate and pinch off from the membrane into clathrin-coated vesicles, which later on form early and late endosomes. Subsequently, ligand and receptors are sorted and transported to their appropriated cellular destination such as, Golgi Apparatus, liposomes, nucleus or back to the cell membrane. Endosomes appear to play a role after the peptide enters the cell in clathrin-coated vesicles. This is supported by the fact that pre-incubation with chloroquine, an inhibitor of endosomal entrapment, did not result in a clear increase in fluorescence.

In conclusion, we have identified CyPep10 from phage display studies, as a potential candidate for AON delivery. Although this peptide was selected as muscle specific, upon conjugation to the AON, the conjugate showed general improved tissue levels in a mouse model for DMD. Extended studies will be needed to assess if long term treatment leads to beneficial effects on muscle quality and function.

Acknowledgements

We hereby thank the following people for their technical or intellectual input: M. van Putten, J.W. Boertje- van der Meulen, M. Hulsker, L. van Vliet, M. Overzier, A. Harder (student) employed by the LUMC, Leiden the Netherlands. D. Muilwijk, K.H. Pang, R. Vermue, N.A. Datson and J.C.T. van Deutekom employed by BioMarin Nederland BV, Leiden the Netherlands.

Studies were financed by the Dutch Ministry of Economic Affairs to PH (IOP-Genmics grant IGE7001) and a grant from the Prinses Beatrix Spierfonds to AAR (W-OR13-06).

Author disclosure statement

AAR is co-inventor of patents of the LUMC on exon skipping, licensed by LUMC to Prosensa Therapeutics, and being entitled to a share or royalties. SJ, AAR, PH, BA and PCdV are co-inventors on a patent that include the peptides reported in this work. AAR also declares being an ad hoc consultant for Global Guidepoint, GLC consulting, Deerfield Institute, Bioclinica, Grunenthal, Summit PLC, PTC Therapeutics and BioMarin and being a member of the scientific advisory board of ProQR and Philae Pharmaceuticals. Remuneration for these activities go to LUMC. PCdV, RCV BA and VDP are employees of BioMarin Nederland BV.

References

1. Moat, S.J., Bradley, D.M., Salmon, R., Clarke, A. and Hartley, L. (2013) Newborn bloodspot screening for Duchenne muscular dystrophy: 21 years experience in Wales (UK). *Eur.J.Hum.Genet.*
2. Emery, A.E. (2002) The muscular dystrophies. *Lancet*, **359**, 687-695.
3. Blake, D.J., Weir, A., Newey, S.E. and Davies, K.E. (2002) Function and genetics of dystrophin and dystrophin-related proteins in muscle. *Physiol Rev.*, **82**, 291-329.
4. Monaco, A.P., Bertelson, C.J., Liechti-Gallati, S., Moser, H. and Kunkel, L.M. (1988) An explanation for the phenotypic differences between patients bearing partial deletions of the DMD locus. *Genomics*, **2**, 90-95.
5. Muntoni, F., Torelli, S. and Ferlini, A. (2003) Dystrophin and mutations: one gene, several proteins, multiple phenotypes. *The Lancet. Neurology*, **2**, 731-740.
6. Aartsma-Rus, A., Janson, A.A., Kaman, W.E., Bremmer-Bout, M., den Dunnen, J.T., Baas, F., van Ommen, G.J. and van Deutekom, J.C. (2003) Therapeutic antisense-induced exon skipping in cultured muscle cells from six different DMD patients. *Hum.Mol.Genet.*, **12**, 907-914.
7. Aartsma-Rus, A. (2010) Antisense-mediated modulation of splicing: therapeutic implications for Duchenne muscular dystrophy. *RNA.Biol.*, **7**, 453-461.
8. Aartsma-Rus, A. (2014) Dystrophin analysis in clinical trials. *JND*, **1**, 41-53.
9. Flanigan, K.M., Voit, T., Rosales, X.Q., Servais, L., Kraus, J.E., Wardell, C., Morgan, A., Dorricott, S., Nakielny, J., Quarcoo, N. *et al.* (2014) Pharmacokinetics and safety of single doses of drisapersen in non-ambulant subjects with Duchenne muscular dystrophy: results of a double-blind randomized clinical trial. *Neuromuscul.Disord.*, **24**, 16-24.
10. Voit, T., Topaloglu, H., Straub, V., Muntoni, F., Deconinck, N., Campion, G., de Kimpe, S.J., Eagle, M., Guglieri, M., Hood, S. *et al.* (2014) Safety and efficacy of drisapersen for the treatment of Duchenne muscular dystrophy (DEMAND II): an exploratory, randomised, placebo-controlled phase 2 study. *Lancet Neurol.*, **13**, 987-996.
11. Mendell, J.R., Rodino-Klapac, L.R., Sahenk, Z., Roush, K., Bird, L., Lowes, L.P., Alfano, L., Gomez, A.M., Lewis, S., Kota, J. *et al.* (2013) Eteplirsen for the treatment of Duchenne muscular dystrophy. *Ann. Neurol.*, **74**, 637-647.
12. Fall, A.M., Johnsen, R., Honeyman, K., Iversen, P., Fletcher, S. and Wilton, S.D. (2006) Induction of revertant fibres in the mdx mouse using antisense oligonucleotides. *Genetic vaccines and therapy*, **4**, 3.
13. Heemskerk, H.A., de Winter, C.L., de Kimpe, S.J., van Kuik-Romeijn, P., Heuvelmans, N., Platenburg, G.J., van Ommen, G.J., van Deutekom, J.C. and Aartsma-Rus, A. (2009) In vivo comparison of 2'-O-methyl phosphorothioate and morpholino antisense oligonucleotides for Duchenne muscular dystrophy exon skipping. *J.Gene Med.*, **11**, 257-266.
14. Heemskerk, H., de Winter, C., van Kuik, P., Heuvelmans, N., Sabatelli, P., Rimessi, P., Braghetta, P., van Ommen, G.J., de, K.S., Ferlini, A. *et al.* (2010) Preclinical PK and PD studies on 2'-O-methyl-phosphorothioate RNA antisense oligonucleotides in the mdx mouse model. *Mol.Ther.*, **18**, 1210-1217.
15. Wu, B., Xiao, B., Cloer, C., Shaban, M., Sali, A., Lu, P., Li, J., Nagaraju, K., Xiao, X. and Lu, Q.L. (2011) One-year treatment of morpholino antisense oligomer improves skeletal and cardiac muscle functions in dystrophic mdx mice. *Mol.Ther.*, **19**, 576-583.
16. Hu, Y., Wu, B., Zillmer, A., Lu, P., Benrashid, E., Wang, M., Doran, T., Shaban, M., Wu, X. and Lu, Q.L. (2010) Guanine analogues enhance antisense oligonucleotide-induced exon skipping in dystrophin gene in vitro and in vivo. *Mol.Ther.*, **18**, 812-818.
17. Verhaart, I.E. and Aartsma-Rus, A. (2012) The effect of 6-thioguanine on alternative splicing and antisense-mediated exon skipping treatment for duchenne muscular dystrophy. *PLoS.Curr.*, **4**.
18. Kendall, G.C., Mokhonova, E.I., Moran, M., Sejbuk, N.E., Wang, D.W., Silva, O., Wang, R.T., Martinez, L., Lu, Q.L., Damoiseaux, R. *et al.* (2012) Dantrolene enhances antisense-mediated exon skipping in human and mouse models of Duchenne muscular dystrophy. *Sci.Transl.Med.*, **4**, 164ra160.
19. Rimessi, P., Sabatelli, P., Fabris, M., Braghetta, P., Bassi, E., Spitali, P., Vattemi, G., Tomelleri, G., Mari, L., Perrone, D. *et al.* (2009) Cationic PMMA nanoparticles bind and deliver antisense oligoribonucleotides allowing restoration of dystrophin expression in the mdx mouse. *Mol. Ther.*, **17**, 820-827.
20. Mumcuoglu, D., Sardan, M., Tekinay, T., Guler, M.O. and Tekinay, A.B. (2015) Oligonucleotide delivery with cell surface binding and cell

- penetrating Peptide amphiphile nanospheres. *Mol.Pharm.*, **12**, 1584-1591.
21. Ferlini, A., Sabatelli, P., Fabris, M., Bassi, E., Falzarano, S., Vattermi, G., Perrone, D., Gualandi, F., Maraldi, N.M., Merlini, L. *et al.* (2010) Dystrophin restoration in skeletal, heart and skin arrector pili smooth muscle of mdx mice by ZM2 NP-AON complexes. *Gene Ther.*, **17**, 432-438.
 22. Bassi, E., Falzarano, S., Fabris, M., Gualandi, F., Merlini, L., Vattermi, G., Perrone, D., Marchesi, E., Sabatelli, P., Sparnacci, K. *et al.* (2012) Persistent dystrophin protein restoration 90 days after a course of intraperitoneally administered naked 2'OMePS AON and ZM2 NP-AON complexes in mdx mice. *J.Biomed.Biotechnol.*, **2012**, 897076.
 23. Wang, M., Wu, B., Lu, P., Cloer, C., Tucker, J.D. and Lu, Q. (2013) Polyethylenimine-modified pluronics (PCMs) improve morpholino oligomer delivery in cell culture and dystrophic mdx mice. *Mol.Ther.*, **21**, 210-216.
 24. Lehto, T., Castillo, A.A., Gauck, S., Gait, M.J., Coursindel, T., Wood, M.J., Lebleu, B. and Boisguerin, P. (2013) Cellular trafficking determines the exon skipping activity of Pip6a-PMO in mdx skeletal and cardiac muscle cells. *Nucleic Acids Res.*
 25. Moulton, H.M. and Moulton, J.D. (2010) Morpholinos and their peptide conjugates: therapeutic promise and challenge for Duchenne muscular dystrophy. *Biochim.Biophys.Acta*, **1798**, 2296-2303.
 26. Yin, H., Saleh, A.F., Betts, C., Camelliti, P., Seow, Y., Ashraf, S., Arzumanov, A., Hammond, S., Merritt, T., Gait, M.J. *et al.* (2011) Pip5 transduction peptides direct high efficiency oligonucleotide-mediated dystrophin exon skipping in heart and phenotypic correction in mdx mice. *Mol.Ther.*, **19**, 1295-1303.
 27. Betts, C.A., Saleh, A.F., Carr, C.A., Hammond, S.M., Coenen-Stass, A.M., Godfrey, C., McClorey, G., Varela, M.A., Roberts, T.C., Clarke, K. *et al.* (2015) Prevention of exercised induced cardiomyopathy following Pip-PMO treatment in dystrophic mdx mice. *Sci.Rep.*, **5**, 8986.
 28. Huang, J., Ru, B., Li, S., Lin, H. and Guo, F.B. (2010) SAROTUP: scanner and reporter of target-unrelated peptides. *J.Biomed.Biotechnol.*, **2010**, 101932.
 29. 't Hoen, P.A., Jirka, S.M., Ten Broeke, B.R., Schultes, E.A., Aguilera, B., Pang, K.H., Heemskerk, H., Aartsma-Rus, A., van Ommen, G.J. and den Dunnen, J.T. (2012) Phage display screening without repetitious selection rounds. *Anal.Biochem.*, **421**, 622-631.
 30. Jirka, S.M., Heemskerk, H., Tanganyika-de Winter, C.L., Muilwijk, D., Pang, K.H., de Visser, P.C., Janson, A., Karnaoukh, T.G., Vermue, R., 't Hoen, P.A. *et al.* (2013) Peptide Conjugation of 2'-O-methyl Phosphorothioate Antisense Oligonucleotides Enhances Cardiac Uptake and Exon Skipping in mdx Mice. *Nucleic Acid Ther.*
 31. Zhu, C.H., Mouly, V., Cooper, R.N., Mamchaoui, K., Bigot, A., Shay, J.W., Di Santo, J.P., Butler-Browne, G.S. and Wright, W.E. (2007) Cellular senescence in human myoblasts is overcome by human telomerase reverse transcriptase and cyclin-dependent kinase 4: consequences in aging muscle and therapeutic strategies for muscular dystrophies. *Aging Cell*, **6**, 515-523.
 32. 't Hoen, P.A., de Meijer, E.J., Boer, J.M., Vossen, R.H., Turk, R., Maatman, R.G., Davies, K.E., van Ommen, G.J., van Deutekom, J.C. and den Dunnen, J.T. (2008) Generation and characterization of transgenic mice with the full-length human DMD gene. *J.Biol.Chem.*, **283**, 5899-5907.
 33. Mann, C.J., Honeyman, K., McClorey, G., Fletcher, S. and Wilton, S.D. (2002) Improved antisense oligonucleotide induced exon skipping in the mdx mouse model of muscular dystrophy. *J.Gene Med.*, **4**, 644-654.
 34. Verheul, R.C., van Deutekom, J.C. and Datson, N.A. (2016) Digital Droplet PCR for the Absolute Quantification of Exon Skipping Induced by Antisense Oligonucleotides in (Pre-)Clinical Development for Duchenne Muscular Dystrophy. *PLoS one*, **11**, e0162467.
 35. Falzarano, M.S., Bassi, E., Passarelli, C., Braghetta, P. and Ferlini, A. (2014) Biodistribution studies of polymeric nanoparticles for drug delivery in mice. *Hum.Gene Ther.*, **25**, 927-928.
 36. Samoylova, T.I. and Smith, B.F. (1999) Elucidation of muscle-binding peptides by phage display screening. *Muscle Nerve*, **22**, 460-466.
 37. Yin, H., Moulton, H.M., Betts, C., Seow, Y., Boutilier, J., Iverson, P.L. and Wood, M.J. (2009) A fusion peptide directs enhanced systemic dystrophin exon skipping and functional restoration in dystrophin-deficient mdx mice. *Hum.Mol.Genet.*, **18**, 4405-4414.
 38. Gao, X., Zhao, J., Han, G., Zhang, Y., Dong, X., Cao, L., Wang, Q., Moulton, H.M. and Yin, H. (2014) Effective dystrophin restoration by a novel muscle-homing peptide-morpholino conjugate in dystrophin-deficient mdx mice. *Mol.Ther.*, **22**, 1333-1341.

39. Dias-Neto, E., Nunes, D.N., Giordano, R.J., Sun, J., Botz, G.H., Yang, K., Setubal, J.C., Pasqualini, R. and Arap, W. (2009) Next-generation phage display: integrating and comparing available molecular tools to enable cost-effective high-throughput analysis. *PLoS.One.*, **4**, e8338.
40. McLaughlin, M.E. and Sidhu, S.S. (2013) Engineering and analysis of peptide-recognition domain specificities by phage display and deep sequencing. *Methods Enzymol.*, **523**, 327-349.
41. Matochko, W.L., Cory, L.S., Tang, S.K. and Derda, R. (2014) Prospective identification of parasitic sequences in phage display screens. *Nucleic Acids Res.*, **42**, 1784-1798.
42. Shtatland, T., Guettler, D., Kossodo, M., Pivovarov, M. and Weissleder, R. (2007) PepBank--a database of peptides based on sequence text mining and public peptide data sources. *BMC.Bioinformatics.*, **8**, 280.
43. Verhaart, I.E., Dool, v.V.-v.d., Sipkens, J.A., de Kimpe, S.J., Kolfschoten, I.G., van Deutekom, J.C., Liefwaard, L., Ridings, J.E., Hood, S.R. and Aartsma-Rus, A. (2014) The Dynamics of Compound, Transcript, and Protein Effects After Treatment With 2OMePS Antisense Oligonucleotides in mdx Mice. *Mol.Ther.Nucleic Acids*, **3**, e148.
44. McMahon, H.T. and Boucrot, E. (2011) Molecular mechanism and physiological functions of clathrin-mediated endocytosis. *Nat.Rev.Mol. Cell Biol.*, **12**, 517-533.



Evaluation of 2'-deoxy-2'-fluoro antisense oligonucleotides for exon skipping in Duchenne muscular dystrophy

S.M.G. Jirka^a, C.L. Tanganyika-de Winter^a, J.W. Boertje -van der Meulen^a, M. van Putten^a, M. Hiller^a, R. Vermue^b, P.C. de Visser^b and A.M. Aartsma-Rus^a

^a Department of Human Genetics, Leiden University Medical Center, 2300 RC Leiden, The Netherlands

^b Prosensa Therapeutics B.V./ BioMarin, 2333 CH Leiden, The Netherlands

Abstract

Duchenne muscular dystrophy (DMD) is a severe muscle wasting disorder typically caused by frame-shifting mutations in the *DMD* gene. Restoration of the reading frame would allow the production of a shorter but partly functional dystrophin protein as seen in Becker muscular dystrophy patients. This can be achieved with antisense oligonucleotides (AONs) that induce skipping of specific exons during pre-mRNA splicing. Different chemical modifications have been developed to improve AON properties. The 2'-deoxy-2'-fluoro (2F) RNA modification is attractive for exon skipping due to its ability to recruit ILF2/3 proteins to the 2F/pre-mRNA duplex, which resulted in enhanced exon skipping in spinal muscular atrophy models. In this study, we examined the effect of two different 2'-substituted AONs (2'-F phosphorothioate (2FPS) and 2'-O-Me phosphorothioate (2OMePS)) on exon skipping in DMD cell and animal models. In human cell cultures, 2FPS AONs showed higher exon skipping levels than their isosequential 2OMePS counterparts. Interestingly, in the *mdx* mouse model 2FPS was less efficient than 2OMePS and suggested safety issues as evidenced by increased spleen size and weight loss. Our results do not support a clinical application for 2FPS AON.

1. Introduction

Duchenne muscular dystrophy (DMD) is a severe X-linked muscle wasting disorder affecting 1 in 5,000 newborn boys^{1,2}. DMD is caused by out-of-frame or nonsense mutations in the *DMD* gene that lead to a truncated, non-functional dystrophin protein. Dystrophin is an important shock absorbing protein in muscle and without it, muscles are easily damaged. Restoration of the reading frame in DMD patients would in theory allow the production of a shorter, but partly functional dystrophin protein as seen in less severely affected Becker muscular dystrophy (BMD) patients^{3,4}. This can be achieved with antisense oligonucleotides (AONs) that target and induce skipping of specific exons during pre-mRNA splicing^{5,6}. Exon skipping AONs are thought to act by sterically hindering splicing factors in the recognition of the exon and/or splicing sites.

Over the years chemical modifications have been developed to improve AON characteristics, such as improved binding affinity to the target transcript, increased resistance against nuclease degradation and improved cellular uptake⁷. Two different AON chemistries, phosphorodiamidate morpholino oligonucleotides and 2'-O-methyl phosphorothioate (2OMePS), are currently in clinical development for exon skipping in DMD⁸⁻¹².

The 2'-deoxy-2'-fluoro (2F) chemistry may also be an attractive chemistry for exon skipping AONs. Recently it has been shown that the duplex of 2F AON and its target pre-mRNA attracts interleukin enhancer binding factors

2 and 3 (ILF2/3 proteins) resulting in unanticipated exon skipping in a model of spinal muscular atrophy (SMA)¹³. Probably this is based on enhanced steric hindrance by the duplex/protein complex, which impedes binding of splicing factors to splice sites or exonic regions in the pre-mRNA transcript beyond the AON target sequence. As enhanced exon skipping is relevant for DMD therapeutics, we compared the efficiencies of isosequential 2'-F phosphorothioate (2FPS) and 2OMePS AONs targeting exonic regions within different human dystrophin exons, or in the 5' donor splice site of mouse dystrophin exon 23. In *in vitro* transfection experiments, 2FPS AONs outperformed their 2OMePS counterparts, while *in vivo* they appeared less effective.

2. Material and Methods

AONs

Sequences of 2FPS and 2OMePS AONs are provided in Supplementary Table 1. 2FPS AONs contained 2'-deoxy-2'-fluoro RNA with a phosphorothioate backbone (ChemGenes corporation, Wilmington, MA USA). 2OMePS AONs consisted of 2'-O-methyl RNA with a phosphorothioate backbone (Prosensa Therapeutics/BioMarin, Leiden, the Netherlands).

Cell culture

Human myoblasts

Primary human control myoblasts and patient myoblasts with a deletion of exon 45-52 were a kind gift from Vincent Mouly²². Cells were grown in skeletal muscle cell growth medium (Promocell, C-23160) supplemented with an additional 15% fetal bovine serum (FBS) (Gibco-BRL, the Netherlands) and 50 µg/ml gentamicin (PAA Laboratories) in uncoated flasks until 70-80% confluence was reached. Cells were plated in a 6 wells plate coated with 0.5% gelatin (Sigma Aldrich Chemie B.V., the Netherlands), at a density of 10⁵ cells per well, 48 hours prior to differentiation. Reaching 90% confluence, medium was switched to differentiation medium (Dulbecco's medium (without phenol red) with 2% FBS, 50ug/ml gentamicin, 2% glutamax and 1% glucose (all from Gibco-BRL, the Netherlands)). Cells were allowed to differentiate for 4-5 days.

Mouse myoblasts

Mouse myoblasts were grown in Dulbecco's medium (without phenol red) supplemented with 10% FBS, 1% Penicillin/Streptomycin (P/S), 2% Glutamax and 1% glucose (all from Gibco-BRL, the Netherlands) in collagen coated flasks. Cells were seeded in collagen coated 6 wells plates with proliferation medium and grown until confluence. The cells were washed twice with Hank's Balanced Salt Solution (HBSS) and differentiation medium, Dulbecco's medium (without phenol red) supplemented with 2%

horse serum (HS), 1% P/S, 2% glutamax and 1% glucose (all from Gibco-BRL, the Netherlands) was added to induce differentiation. The cells were differentiated for 7-9 days before AON transfection.

Primary myoblasts from mdx mice

Primary myoblasts were isolated from the *extensor digitorum longus* (EDL) muscle of one *mdx* mouse by collagenase treatment followed by single fiber isolation²³. Fibers were grown in SC+ medium (Dulbecco's medium (without phenol red) supplemented with 10% (HS), 30% fetal calf serum, 1% chicken embryonic extract (all from Gibco-BRL, the Netherlands) and 10 μ l/30ml final medium of fibroblast growth factor (Promega) on matrigel (GFR Matrigel BD Biosciences) coated plates. After 3 days myoblasts were separated from fibroblasts by pre-plating in proliferation medium (Dulbecco's medium (without phenol red) supplemented with 10% FBS, 1% P/S, 2% glutamax and 1% glucose (all from Gibco-BRL, the Netherlands)). Finally primary myoblast cells were plated in 12 wells plates at 70-80% confluence, the following day the cells were washed with PBS and differentiation medium (Dulbecco's medium (without phenol red) supplemented with 2% HS, 1% P/S, 2% glutamax and 1% glucose (all from Gibco-BRL, the Netherlands)) was added.

In vitro delivery

AON transfection of myotube cultures

Primary human control, patients myotube and mouse myotube cells were transfected with either 100, 200 or 500 nM of AONs using 6 μ l of Lipofectamin 2000 (according to manufacturer's protocol) per well. After incubation for 3-4 hours at 37 °C and 5% CO₂, cells were washed twice with PBS and 2 ml of fresh differentiation medium was added. Forty-eight hours later, RNA was isolated.

Gymnotic delivery

Primary myoblasts from *mdx* mice were incubated with 2 or 4 μ M of 23M or 23F AON for 96 hours at initiation of differentiation.

In vivo delivery

Intramuscular injection of mdx mice

Two *mdx* mice were IM injected in the *gastrocnemius* and *triceps* muscles with 2.9 nmol of 23M (20 μ g) or 23F AON in contralateral muscles for 2 consecutive days. One week after the last injection the mice were sacrificed, and *quadriceps* (non-injected control), *gastrocnemius* and *triceps* muscles were isolated.

Intramuscular injection of hDMD mice

Two hDMD mice were injected in the *gastrocnemius* and *triceps* muscles with cardiotoxin 2 days prior to injection with 2.9 nmol of 23AON or 2FPS23AON contralateral for 2 consecutive days. One week after the last injection the mice were sacrificed, *quadriceps* (non-injected control), *gastrocnemius* and *triceps* muscles were isolated.

Systemic treatment in mdx mice

Five weeks old *mdx* mice (4-5 mice per group) were subcutaneously injected 4 times per week, with 50 mg/kg of 23M AON in 100 μ l of saline or the molar equivalent (6.8 μ mol) for 23F AON. *Mdx* mice were treated for 8 weeks and sacrificed 1 week after the last injection. All mice were weighed prior to injection and at the day of sacrifice. Blood samples were obtained from the tail vein for plasma pharmacokinetics analysis (PK) at the day of sacrifice. *Gastrocnemius*, *quadriceps*, *tibialis anterior*, *triceps* and *diaphragm* muscles, heart, liver and kidney were isolated to determine exon skipping levels and AON concentrations. The spleen was isolated and weighed.

RNA isolation

RNA isolation and cDNA synthesis of myotube cultures

Human and mouse cells were washed twice with PBS. RNA was isolated by adding 500 μ L TriPure (Roche diagnostics, the Netherlands) to each well to lyse the cells. This was followed by chloroform extraction in a 1:5 ratio on ice for 5 minutes. The remaining cell debris was spin down by centrifugation (4°C, 15 minutes, 15,4000 rcf) and the upper aqueous phase precipitated for 30 minutes on ice with equal volume of isopropanol. The RNA/isopropanol precipitate was centrifuged (4°C, 15 minutes, 15,400 rcf) and the pellet washed with 70% ethanol. The final RNA pellet was dissolved in 15 μ l of RNase/ DNase free water. For complementary DNA (cDNA) synthesis, 11 μ l of RNA was used in a 20 μ l reaction with a specific reverse primer (in human exon 48 for evaluating exon 45 skipping, in human exon 56 for evaluating exon 53 skipping, in mouse exon 26 for evaluating exon 23 skipping) and transcriptase reverse transcriptase (Roche Diagnostics, the Netherlands) for 30 minutes at 55°C and 5 minutes at 85°C to terminate the reaction according to the manufacturer's instructions.

RNA isolation and cDNA synthesis of tissue

Samples were homogenized in TriPure (Roche diagnostics, the Netherlands) solution using a MagNA Lyser (Roche Diagnostics, the Netherlands) and MagNA Lyser green beads (Roche Diagnostics, the Netherlands). Total RNA was isolated and purified according manufacturer's instructions. For the cDNA synthesis, 400 ng of RNA was used in a 20 μ l reaction with random hexamers and transcriptase reverse transcriptase (Roche Diagnostics, the Netherlands) for 45 minutes at 42°C and put on ice.

***In vitro* exon skip evaluation**

Exon skipping was determined by nested RT-PCR. For RT-PCR analysis 3 µl of cDNA was incubated with 0.625 U AmpliTaq polymerase (Roche Diagnostics, the Netherlands), 10 pM of primers (in exon 43 and 48 for exon 45 skipping, for exon 53 skipping in exon 56 and 43 (patient) or exon 50 (control), and mouse exon 21 and 26 for mouse exon 23 skipping) 5pmol of dNTPs and 1 times Supertaq PCR buffer (Sphaero-q, the Netherlands) and amplified for 20 cycles each consisting of 40 seconds at 94 °C, 40 seconds at 60 °C and 80 seconds at 72 °C. This PCR was followed by a nested PCR. For the nested PCR analysis 1.5 µl of the first PCR product was incubated with 1.25 U AmpliTaq polymerase (Roche Diagnostics, the Netherlands), 20 pmol of primers (human exon 44 and 46 for evaluating exon 45 skipping, human exon 55 and 44 (patient) or 51 (control for evaluating exon 53 skipping, and mouse exon 22 and 24 for exon 23 skipping) 10 pmol of dNTPs and 1 times Supertaq PCR buffer and amplified for 32 cycles each consisting of 40 seconds at 94 °C, 40 seconds at 60 °C and 60 seconds at 72 °C. PCR fragments were analyzed using 1.5 % agarose gel electrophoresis. Exon skip levels were semi-quantitatively determined as the percentages of the total (wild type and skipped) product with the Calipur LabChip GX (PerkinElmer, the Netherlands).

***In vivo* exon skip evaluation**

Exon skip evaluation of intramuscular injected mice

Exon skipping was determined by nested RT-PCR and visualized on an agarose gel as described for the myotubes cultures detecting exon 45 skipping (hDMD) or exon 23 skipping (*mdx* mice).

Exon skip evaluation of systemically treated mdx mice

Exon skipping was determined by single RT-PCR. For RT-PCR analysis 1.5 µl of cDNA was incubated with 1.25 U taq polymerase (Roche Diagnostics, the Netherlands), 20 pmol of primers (reverse primer in exon 24, forward primer in exon 22) 10 pmol of dNTPs and 1 times Supertaq PCR buffer (Sphaero-q, the Netherlands) and amplified for 30 cycles each consisting of 30 seconds at 94 °C, 30 seconds at 60 °C and 30 seconds at 72 °C. PCR fragments were analysed by 2% agarose gel electrophoresis.

***In vivo* safety and quantification of AON levels**

Plasma parameters

Blood was collected in lithium-heparin coated microvettes CB300 (Sarstedt B.V. the Netherlands). Glutamate pyruvate transaminase (GPT), alkaline phosphates (ALP) glutamic oxaloacetic transaminase (GOT) hemoglobin (HB), urea and creatine kinase (CK) were determined using Reflotron strips (Roche Diagnostics, the Netherlands) in the Reflotron Plus machine (Roche Diagnostics, the Netherlands).

Quantification of AON levels in tissue of mdx mice

For measuring the concentration of AONs in tissue samples a hybridization-ligation assay based on one previously published was used²⁴. Tissues were homogenized in 100 mM Tris-HCl pH 8.5, 200 mM NaCl, 0.2% SDS, 5 mM EDTA and 2 mg/ml proteinase K using zirconium beads (1.4 mm; OPS Diagnostics, Lebanon, NJ) in a MagNA Lyser (Roche Diagnostics, the Netherlands). Samples were diluted 600 and 6000 times (muscle) or 6000 and 60000 (liver and kidney) in pooled control *mdx* tissue in PBS.

Calibration curves of the analysed exon 23AONs prepared in 60 times pooled control *mdx* tissue in PBS were included. All analyses were performed in duplicate.

Statistical analyses

A Student's T-Test was used to determine significant differences in exon skipping levels, AON levels, plasma protein levels and spleen/bodyweight ratios. Mixed model linear regression analysis was used to determine significant differences in bodyweight over time. Results were deemed significantly different when $P < 0.05$.

3. Results

In vitro evaluation

To test whether 2FPS AONs are capable of inducing dystrophin exon skipping, human control myotube cultures were transfected with 100-500 nM of several 2FPS AONs and their isosequential 2OMePS counterparts¹⁴. These AONs have different activity profiles and target exon 45 or exon 53 (Supplementary table 1, fig. 1). RNA was isolated after 48 hours and exon skipping levels were determined semi-quantitatively by lab-on-a-chip analysis after nested RT-PCR amplification. We observed highest exon 45 skipping levels for each of the 2FPS AONs, with 3 out of 4 of the 2FPS AONs having exon skipping levels over 90% at all concentrations tested (fig. 1A). For exon 53 skipping, although percentages were more variable, all 2FPS AONs induced relatively higher exon skipping levels than their 2OMePS AON counterparts (fig. 1B). This effect was also confirmed in DMD patient-derived $\Delta 45-52$ myotube cultures, in which skipping of exon 53 is frame-restoring and potentially therapeutic (fig. 1C).

We also evaluated the potential of 2FPS AONs targeting mouse dystrophin exon 23¹⁵ in mouse control myotube cultures. Upon the use of a transfection reagent we observed a slight increase in exon 23 skipping with 2FPS AON (23F) compared to the 2OMePS AON (23M) at 500 nM. However, no differences between 23F and 23M were observed at 200nM (fig. 1D). Finally, we also tested the activity of 2FPS AON in primary myoblasts derived from *extensor digitorum longus* (EDL) muscles of an *mdx* mouse, a mouse model for DMD¹⁶. In this case, we did not use a transfection reagent ('gymnotic delivery'). Primary myoblasts were incubated with 2 or 4 μ M of 23M or 23F AON at initiation of differentiation into myotubes. After 96 hours RNA was isolated and analyzed by nested RT-PCR. Exon 23 skipping was confirmed for both AONs at comparable levels (fig. 1E).

In vivo evaluation

Two *mdx* mice were intramuscularly (IM) injected with 2.9 nmol of 23M or 23F AON for 2 consecutive days in *gastrocnemius* and *triceps* muscles. One week after the last injection the mice were sacrificed and the injected muscles harvested for RNA isolation. Exon skipping was determined by nested RT-PCR and visualized on an agarose gel. Surprisingly no clear exon skipping could be detected for the 23F AON, in contrast to the 23M AON (fig. 2A).

In parallel, we evaluated subcutaneous (SC) administration of the 2FPS AON targeting mouse exon 23. Groups of 4-5 *mdx* mice were administered 23M, 23F AON or saline, through 4 weekly injections of 50 mg/kg for 23M AON, or molar equivalent for 23F AON for 8 weeks. One week after the last injection the mice were sacrificed and various muscles and other tissues

were harvested for analysis. Exon skipping was assessed for skeletal- and cardiac muscles by single round RT-PCR and visualized on an agarose gel. Surprisingly, again no exon skipping could be detected in 23F AON treated mice in any of the muscles analyzed, while exon skipping was detectable in the case of 23M AON treated mice for each muscle analyzed (fig. 2B). As anticipated, dystrophin restoration was observed by Western blot for 23M AON treated mice, but not for 23F AON or saline treated mice (Supplementary figure 2).

Assessment of the AON concentrations in different organs revealed lower levels of 23F AON in skeletal and cardiac muscle, liver and kidney compared to 23M AON treated animals (fig. 2C,D). The calculated target tissue muscle/kidney and muscle/liver ratios were higher for 23F AON suggesting that while uptake in muscle is lower for 23F than 23M AON, it is even further reduced in kidney and liver (fig. 2E,F).

Blood and plasma were determined for markers of liver and kidney damage and function as part of the safety profiling of the AONs. Glutamic oxaloacetic pyruvate transaminase (GOT) and glutamate pyruvic transaminase (GPT) are both enzymes that leak into the bloodstream upon liver and muscle damage. No significant differences were observed for GOT, while significantly lower GPT levels were found for mice treated with either AON compared to saline treated mice. Alkaline phosphatase (ALP, a marker for hepatobiliary function), urea (a marker for kidney function), and haemoglobin levels showed no significant differences between the 3 groups and were in the normal range for *mdx* mice. Large variations in individual levels of creatine kinase (CK), an enzyme that leaks into the bloodstream upon muscle damage, prevented comparisons between the groups (fig. 3A-D).

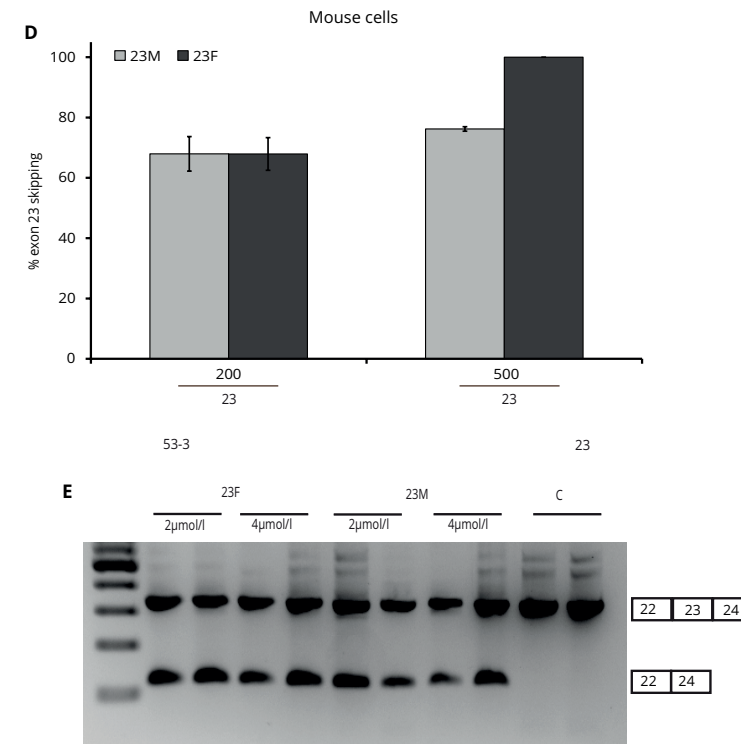
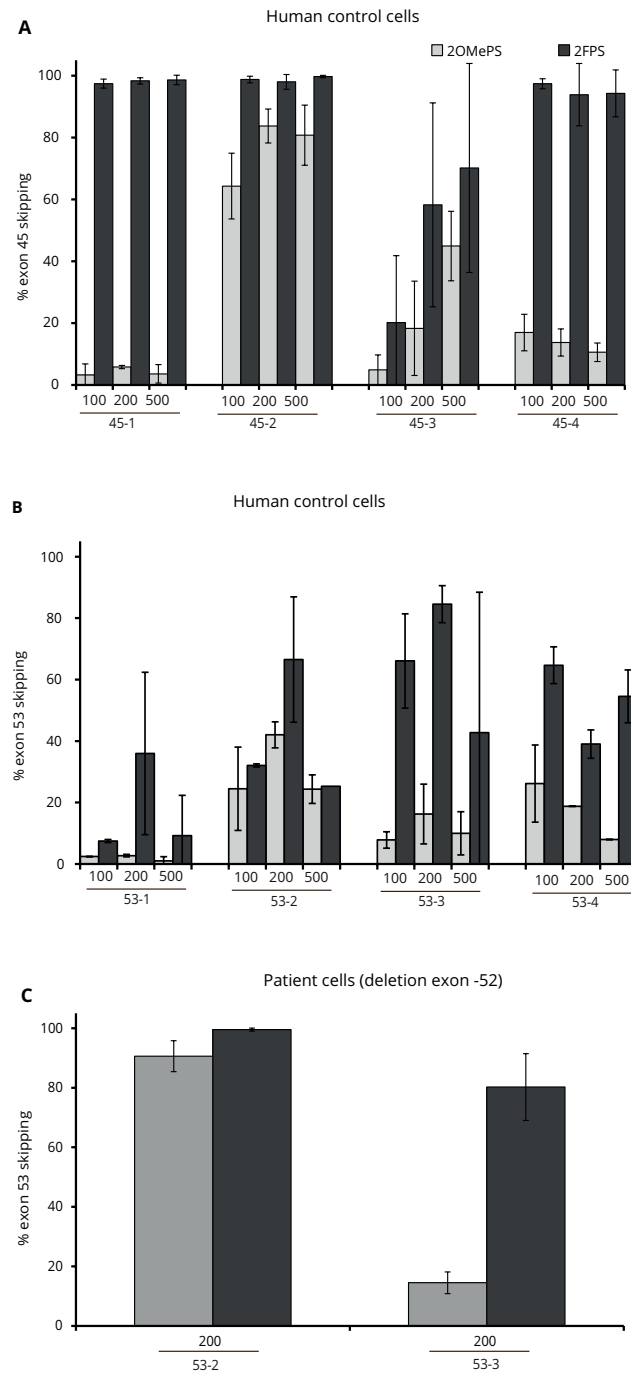


Figure 1. Exon skip evaluation of human and mouse myotube cultures. RT-PCR analysis of human and mouse myotubes transfected with 100-500 nM of 2OMePS or isosequential 2FPS AON (n=4). A) Exon 45 AONs in control myotubes. B) Exon 53 AONs in control myotubes. C) Exon 53 AONs in DMD patient-derived (Δ 45-52) myotubes. D) Mouse exon 23 AONs in mouse myotubes. E) Exon 23 skipping in primary mouse myoblasts without the use of a transfection reagent (gymnotic delivery). Bars represent means \pm SD

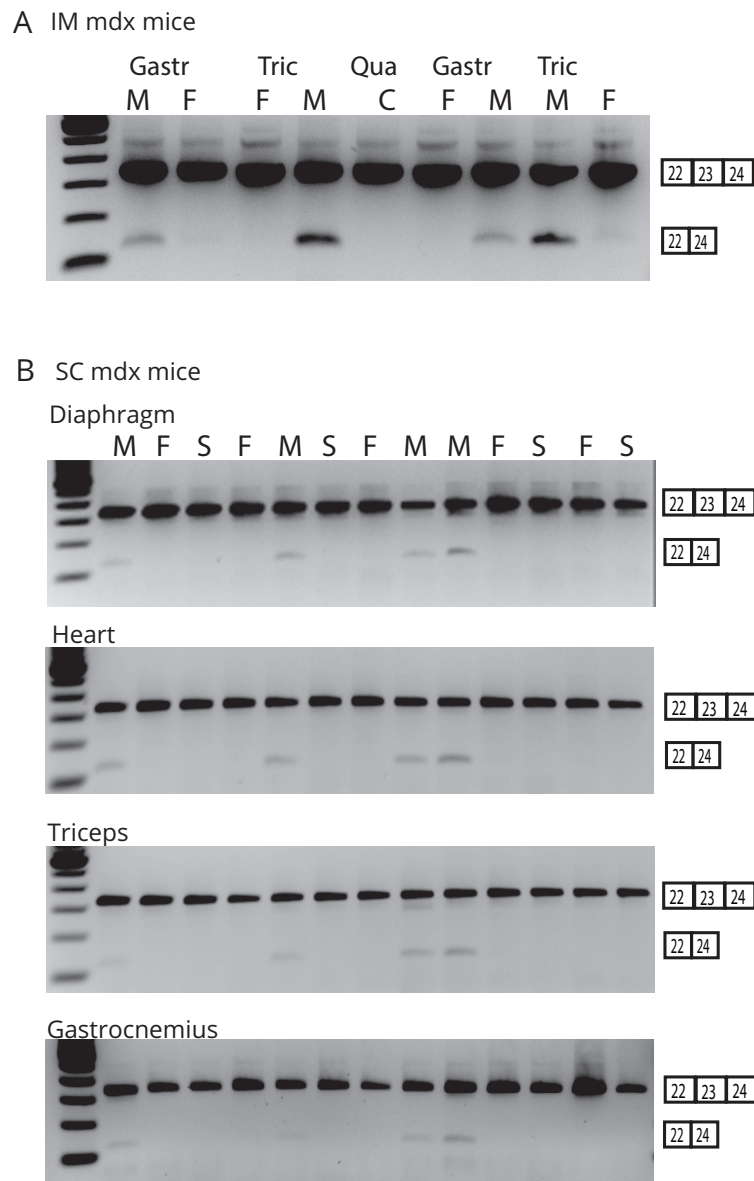
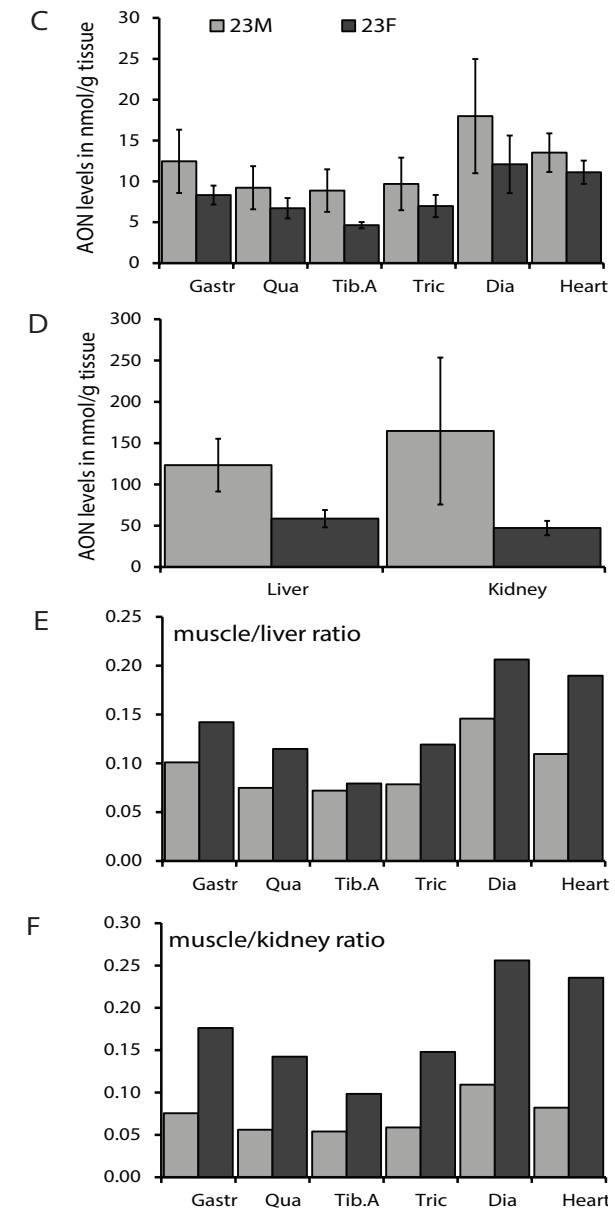


Figure 2. Exon skipping and pharmacokinetic analysis of 23F and 23M-treated mdx mice. A) RT-PCR analysis of muscles from two mdx mice, IM injected with 2.9 nmol of 23M or 23F contralaterally for 2 consecutive days. B) RT-PCR analysis of skeletal and heart muscles isolated from mdx mice (4-5 mice/group) subcutaneously treated 4 times per week with 50 mg/kg of 23M, an equimolar amount of 23F or saline for 8 weeks. C) AON concentrations in skeletal muscles and heart assessed with a



hybridization ligation assay. D) AON concentrations in liver and kidney as assessed with a hybridization ligation assay. E) Ratios of AON levels in muscle compared to kidney. F) Ratios of AON levels in muscle compared to liver. M= 23M, F= 23F, C= untreated control, S= saline, Gastr= gastrocnemius, Qua= quadriceps, Tib.A= tibialis anterior, Tric= triceps, Dia= diaphragm, (*T-test for significant $P < 0.05$). Bars represent means \pm SD

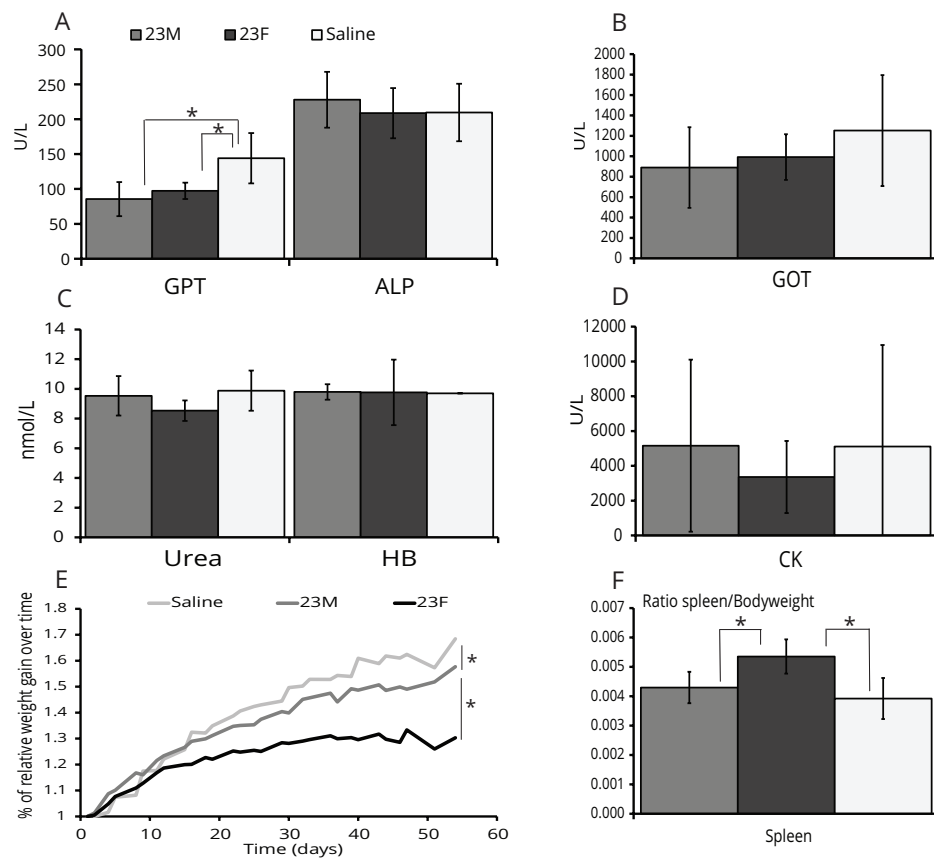


Figure 3. Analysis of plasma protein levels and weight of 23F and 23M-treated mdx mice. A) Glutamate pyruvate transaminase (GPT), alkaline phosphates (ALP), B) glutamic-oxaloacetic transaminase (GOT), C) hemoglobin (Hb), urea, D) creatine kinase (CK), and E) Weight gain over time. Bars represent means \pm SD; F) Ratio spleen/bodyweight.

Notably, 23F AON treated mice had significantly lower increases in body weight over time compared to 23M AON and saline treated mice (fig. 3E). Additionally, we found a significantly higher spleen/bodyweight ratio for mice treated with 23F AON compared to the other groups at sacrifice (fig. 3F).

To assess whether the discrepancy between *in vitro* and *in vivo* results observed for mouse exon 23 AONs also occurred for other exons, we compared a 2FPS and 2OMePS AON targeting human exon 45 *in vivo* in the hDMD mouse model. This mouse model carries the human *DMD* gene integrated in the mouse genome, which compensates for lack of mouse dystrophin resulting in healthy muscle¹⁷. Since AON uptake in *mdx* mice is

facilitated by the dystrophic phenotype we pretreated hDMD *gastrocnemius* and *triceps* muscles with IM cardiotoxin injections to induce muscle necrosis and enhance AON uptake¹⁸. Two days later treated muscles were injected with 2.9 nmol of the most potent 2OMePS AON targeting human exon 45 (45-2M) or isosequential 2FPS AON (45-2F) for 2 consecutive days into *gastrocnemius* and *triceps* muscles. One week after the last injection, RNA was isolated, and exon skip levels were determined by nested RT-PCR and visualized on an agarose gel. Results suggested enhanced exon skipping for 2FPS AON over the 2OMePS AON, which was most pronounced in the *triceps* muscle (fig. 4). These results demonstrate that 2FPS AONs are in fact capable of exon skipping *in vivo* after IM injections and the failure of the 2FPS AON to induce mouse dystrophin exon 23 skipping *in vivo* is not due to an inability of 2FPS AONs to be active *in vivo* per se.

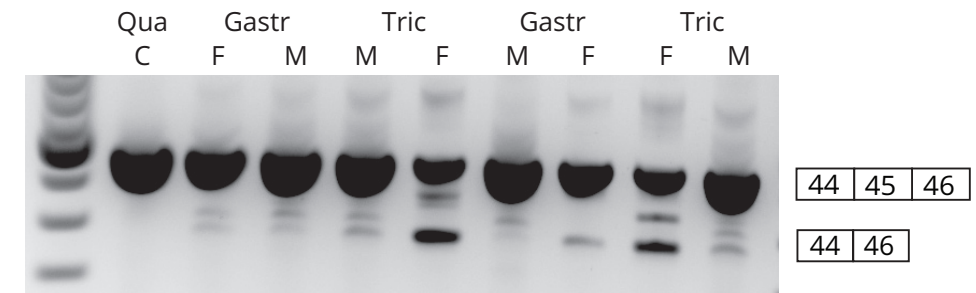


Figure 4. Exon skip evaluation of intramuscular injection of 2FPS AON and 2OMePS counterparts in hDMD mice. Two hDMD mice were intramuscularly injected with cardiotoxin 2 days prior to AON treatment of 2.9 nmol with 2OMePS or 2FPS AON counterpart targeting human exon 45 for 2 consecutive days. RNA was isolated one week after the last injection, subjected to RT-PCR and exon skipping visualized on an agarose gel. M= 23M, F= 23F, C= untreated control, Gastr= gastrocnemius, Qua= quadriceps.

4. Discussion

Exon skipping is a therapeutic approach using AONs to reframe dystrophin transcripts for DMD and is currently evaluated in clinical trials¹¹. 2FPS AONs have shown unanticipated enhanced exon skipping in a model of SMA due to recruitment of ILF2/3 proteins to the 2F/pre-mRNA duplex¹³. For DMD, exon skipping is a desired feature, making 2FPS AONs potentially useful tools for reframing dystrophin transcripts. In this study, we demonstrate *in vitro* that 2FPS AONs have enhanced exon skipping in human and mouse myotube cultures over 2OMePS AON counterparts. The increased efficiency was most pronounced for human exon 45 AONs and least for mouse exon 23 AONs. A possible explanation *in vitro* is the difference in AON target sites and parameters such as AON sequence composition and secondary structure of the target region. For example, the AONs used here to target

human exon 45 or 53, target intraexonic sites whereas the mouse AON targets a donor splice site. It is likely that the added bulkiness of recruited ILF2/3 by fluoro modified AONs is less effective when targeting exon intron boundaries where direct competition takes place with U1 snRNP binding sites than when targeting predicted ESE in intraexonic regions. This is consistent with our previous finding that exonic AONs appear to outperform splice site targeting AONs⁶.

In vivo we demonstrated that 2FPS AONs were not capable of skipping exon 23 in *mdx* mice, in contrast to 2OMePS AONs. A possible explanation for the observed difference between 2OMePS and 2FPS AON *in vivo* is that uptake of 2FPS by skeletal muscles after systemic treatment in *mdx* mice yielded insufficient concentrations to allow exon skipping. However, this does not explain why no exon 23 skipping was detected after IM injections in *mdx* mice. Potentially lower *in vivo* stability of 2FPS AONs could lead to lower tissue levels, but the fact that human exon 45 skipping 2FPS AONs were effective *in vivo* after IM injections argues against this possibility. It should be noted however, that the exon 45 AON was tested in healthy muscle, while it is possible that in the *mdx* mouse the underlying pathology, such as the chronic inflammation and high muscle turnover caused increased 2FPS degradation.

Recently, Shen *et al.*, showed *in vitro* that 2FPS modified AON interfered with splicing proteins and that 2FPS AON treatment of cultured cells resulted in a general disruption of normal splicing¹⁹. We evaluated the accuracy of dystrophin splicing for exons 46 to 53 and the splicing of other genes (Beta-2-Microglobulin, Transforming Growth Factor beta 1, Alpha-1 type I collagen and Activin, chosen because of their involvement in immunogenicity, proliferation, differentiation etc.) in muscle RNA isolated from saline, 2OMePS and 2FPS treated mice, but did not observe any differences between the groups (data not shown). This suggests that the splicing disruptions as observed by Shen *et al.*, might not underlie the lack of exon 23 skipping we observed in the *mdx* mouse. However only a deep analyses of the full dystrophin transcript can rule out the occurrence of splicing abnormalities completely.

Since the first encouraging 2F results were published more than 20 years ago²⁰, only short term *in vivo* experiments (1-3 weeks) have been reported for 2F-modified AONs. Furthermore, only a limited number of tissues was evaluated after intraperitoneal (IP) administration in Spinal Muscular Atrophy (SMA)¹³ or normal mice²¹. To the best of our knowledge, no long term *in vivo* follow up studies have ever been reported for this chemistry.

With respect to safety, in our study of systemic AON treatment targeting mouse exon 23, no clear indications of toxicity were seen in markers for liver, kidney or muscle damage. However, mice treated with 2FPS AON had a significantly higher spleen/bodyweight ratio compared to 2OMePS

AON and saline treated mice. This corroborates the finding²¹ of a dose-dependent increase in spleen weights for mice treated with 2F AONs with flanking and or alternating 2'-O-methoxyethyl nucleotides after three weeks treatment with 6.25- 50 mg/kg twice a week. Lastly, we also noticed that the 2FPS treated *mdx* mice gained significantly less bodyweight than saline and 2OMePS treated mice. On average the 2FPS treated mice weighed 17% less at the end of our experiment. Taken together this suggests that *mdx* mice did not tolerate the treatment with fully modified 2FPS AONs targeting mouse exon 23 very well.

In summary our data shows that 2FPS modified AONs had an improved effect *in vitro* and were effective *in vivo* on *DMD* exon skipping when targeting human exons, but this effect was minimal or absent *in vitro* and *in vivo* targeting mouse *DMD* exon 23. The exact reason for a lack of exon skipping *in vivo* by 2FPS modified AON targeting mouse *DMD* exon 23 is still unclear. In addition, 2FPS AONs revealed possible safety issues for long term *in vivo* application, which needs to be further addressed when one wants to use such AONs in future studies. However, our results do not support a clinical application for 2FPS AON.

Acknowledgements

We would like to thank Vincent Mouly (Institute de Myologie, Paris, France) and colleagues for providing the immortalized primary human control and patients myoblast cells. This work was funded by a grant of the Prinses Beatrix Spierfonds and Spieren voor spieren (the Netherlands).

Author disclosure statement

AAR reports being a coinventor in patents of the LUMC on exon skipping, licensed by LUMC to Prosensa Therapeutics, and being entitled to a share or royalties. AAR also declares being an ad hoc consultant for Global Guidepoint, GLC consulting, Deerfield Institute, PTC Therapeutics and BioMarin and being a member of the scientific advisory board of ProQR. Remuneration for these activities go to LUMC. PCdV and RV report being employed by Prosensa Therapeutics B.V./BioMarin the Netherlands.

References

1. Moat, SJ, Bradley, DM, Salmon, R, Clarke, A, Hartley, L (2013) Newborn bloodspot screening for Duchenne muscular dystrophy: 21 years experience in Wales (UK). *Eur J Hum Genet*;
2. Emery, AE (2002) The muscular dystrophies. *Lancet*; 359: 687-695.
3. Monaco, AP, Bertelson, CJ, Liechti-Gallati, S, Moser, H, Kunkel, LM (1988) An explanation for the phenotypic differences between patients bearing partial deletions of the DMD locus. *Genomics*; 2: 90-95.
4. Muntoni, F, Torelli, S, Ferlini, A (2003) Dystrophin and mutations: one gene, several proteins, multiple phenotypes. *Lancet Neurol*; 2: 731-740.
5. Aartsma-Rus, A, Janson, AA, Kaman, WE, Bremmer-Bout, M, den Dunnen, JT, Baas, F et al. (2003) Therapeutic antisense-induced exon skipping in cultured muscle cells from six different DMD patients. *Hum Mol Genet*; 12: 907-914.
6. Aartsma-Rus, A (2010) Antisense-mediated modulation of splicing: therapeutic implications for Duchenne muscular dystrophy. *RNA Biol*; 7: 453-461.
7. Jarver, P, O'Donovan, L, Gait, MJ (2014) A chemical view of oligonucleotides for exon skipping and related drug applications. *Nucleic Acid Ther*; 24: 37-47.
8. Cirak, S, Arechavala-Gomez, V, Guglieri, M, Feng, L, Torelli, S, Anthony, K et al. (2011) Exon skipping and dystrophin restoration in patients with Duchenne muscular dystrophy after systemic phosphorodiamidate morpholino oligomer treatment: an open-label, phase 2, dose-escalation study. *Lancet*; 378: 595-605.
9. Mendell, JR, Rodino-Klapac, LR, Sahenk, Z, Roush, K, Bird, L, Lowes, LP et al. (2013) Eteplirsen for the treatment of Duchenne muscular dystrophy. *Ann Neurol*; 74: 637-647.
10. Goemans, NM, Tulinius, M, van den Akker, JT, Burm, BE, Ekhardt, PF, Heuvelmans, N et al. (2011) Systemic administration of PRO051 in Duchenne's muscular dystrophy. *N Engl J Med*; 364: 1513-1522.
11. Aartsma-Rus, A (2014) Dystrophin analysis in clinical trials. *JND*; 1: 41-53.
12. Flanigan, KM, Voit, T, Rosales, XQ, Servais, L, Kraus, JE, Wardell, C et al. (2014) Pharmacokinetics and safety of single doses of drisapersen in non-ambulant subjects with Duchenne muscular dystrophy: results of a double-blind randomized clinical trial. *Neuromuscul Disord*; 24: 16-24.
13. Rigo, F, Hua, Y, Chun, SJ, Prakash, TP, Krainer, AR, Bennett, CF (2012) Synthetic oligonucleotides recruit ILF2/3 to RNA transcripts to modulate splicing. *Nat Chem Biol*; 8: 555-561.
14. Aartsma-Rus, A, Kaman, WE, Weij, R, den Dunnen, JT, van Ommen, GJ, van Deutekom, JC (2006) Exploring the frontiers of therapeutic exon skipping for Duchenne muscular dystrophy by double targeting within one or multiple exons. *Mol Ther*; 14: 401-407.
15. Mann, CJ, Honeyman, K, McClorey, G, Fletcher, S, Wilton, SD (2002) Improved antisense oligonucleotide induced exon skipping in the mdx mouse model of muscular dystrophy. *J Gene Med*; 4: 644-654.
16. Sicinski, P, Geng, Y, Ryder-Cook, AS, Barnard, EA, Darlison, MG, Barnard, PJ (1989) The molecular basis of muscular dystrophy in the mdx mouse: a point mutation. *Science*; 244: 1578-1580.
17. 't Hoen, PA, de Meijer, EJ, Boer, JM, Vossen, RH, Turk, R, Maatman, RG et al. (2008) Generation and characterization of transgenic mice with the full-length human DMD gene. *J Biol Chem*; 283: 5899-5907.
18. Heemskerk, H, de, WC, van, KP, Heuvelmans, N, Sabatelli, P, Rimessi, P et al. (2010) Preclinical PK and PD studies on 2'-O-methyl-phosphorothioate RNA antisense oligonucleotides in the mdx mouse model. *Mol Ther*; 18: 1210-1217.
19. Shen, W, Liang, XH, Sun, H, Crooke, ST (2015) 2'-Fluoro-modified phosphorothioate oligonucleotide can cause rapid degradation of P54nrb and PSF. *Nucleic Acids Res*; 43: 4569-4578.
20. Kawasaki, AM, Casper, MD, Freier, SM, Lesnik, EA, Zounes, MC, Cummins, LL et al. (1993) Uniformly modified 2'-deoxy-2'-fluoro phosphorothioate oligonucleotides as nuclease-resistant antisense compounds with high affinity and specificity for RNA targets. *J Med Chem*; 36: 831-841.
21. Davis, S, Propp, S, Freier, SM, Jones, LE, Serra, MJ, Kinberger, G et al. (2009) Potent inhibition of microRNA in vivo without degradation. *Nucleic Acids Res*; 37: 70-77.
22. Zhu, CH, Mouly, V, Cooper, RN, Mamchaoui, K, Bigot, A, Shay, JW et al. (2007) Cellular senescence in human myoblasts is overcome by human telomerase reverse transcriptase and cyclin-dependent

kinase 4: consequences in aging muscle and therapeutic strategies for muscular dystrophies. *Aging Cell*; 6: 515-523.

23. Rosenblatt, JD, Lunt, AI, Parry, DJ, Partridge, TA (1995) Culturing satellite cells from living single muscle fiber explants. *In Vitro Cell Dev Biol Anim*; 31: 773-779.
24. Yu, RZ, Baker, B, Chappell, A, Geary, RS, Cheung, E, Levin, AA (2002) Development of an ultrasensitive noncompetitive hybridization-ligation enzyme-linked immunosorbent assay for the determination of phosphorothioate oligodeoxynucleotide in plasma. *Anal Biochem*; 304: 19-25.



General discussion

General discussion

Efficient drug delivery is a key issue for any potential drug in development. A drug can have a high efficacy *in vitro* but when it fails to reach its target properly *in vivo*, the drug is of no use for humans. Furthermore, a drug needs to be safe and well tolerated. Drugs with severe toxicities or where the side effects are more severe than the disease, are doing more harm than good. A balance between efficient delivery, safety and tolerability will result in a drug with the required efficacy that is suitable to use for humans.

This thesis focusses on delivery of AON to skeletal and cardiac muscle for DMD. Since one cannot treat each muscle individually, systemic treatment is necessary. From pre-clinical studies it is known that this is feasible. Clinical studies have shown that AON (2OMePS and PMO AONs) are safe for humans, however mild to moderate side reactions have been reported. For example subclinical proteinuria is observed in patients treated with 2OMePS AONs but also for patients treated with PMO AONs. Upon subcutaneous administration of 2OMePS AONs injection site reactions and occasionally severe thrombocytopenia have been observed. Upon intravenous administration of PMO AONs vomiting, balance disorders and catheter site pain have been observed (1,2) (www.sarepta.com). Unfortunately, no significant clinical benefit (improvement of 6MWT) has been shown for AON in humans (2OMePS and PMO). While in September 2016 a PMO has been approved by the FDA, this was based on dystrophin restoration (increases of 0.2-0.9% of normal in a subset of patients), and FDA explicitly specified that functional effects still need to be confirmed in future studies. So far results are suggestive of a slower decline in the 6MWT compared to natural history data (chapter 2). Since there is no treatment available besides symptomatic care (chapter 1.3.1), a drug that appears to slow down disease progression is a big achievement where many patients would like to benefit from.

Chemical modifications are an interesting approach to increase the efficacy of AON for DMD. In Chapter 5, fully modified 2FPS AON have been investigated for the first time for DMD (2'-deoxy-2'-fluoro RNA modification (2F)). 2F modified AON resulted in increased exon skipping levels *in vitro* as well as *in vivo* in a model for SMA (3). I observed these findings as well in cultured human myotubes (chapter 6). However, upon systemic administration of *mdx* mice, no exon skipping levels were found in any of the analysed tissues and 2FPS AONs were not well tolerated as suggested by increased spleen weight and decreased body weight compared to 2OMePS AONs. Later, Shen *et al*, found that cells treated with 2F modified oligonucleotides have elevated levels of double stranded breaks (DSB) and more cell death compared to 2'-O- methoxyethyl (2MOE) oligonucleotides (4). They show that the DSB pathway is likely disturbed upon 2F oligonucleotide treatment due to the loss of p54nrb, PSF and PSPC1

proteins, and ultimately leads to a loss of cellular proteins (even limiting the 2F modification to just 4 nucleotides resulted in down regulation of P54nrb). These findings likely explain the lack in weight gain and increased spleen weight observed in *mdx* mice treated with 2FPS AONs. Together these results show that the 2F modification leads to severe toxicity and should not be used in future experiments. Even though there is still room for improvement of AON by chemical modifications, they will not make the AON muscle specific (although they might result in improved muscle uptake due to increased binding affinity).

In my opinion, the lack of significant clinical benefit (meaning at least 30 m differences in 6MWT compared to placebo) is the result of inefficient drug delivery to the target. Since the human body consists of 30-40% of muscle, efficient drug delivery is a major challenge (chapter 1.3.5). Upon systemic administration a large proportion of the administered AONs ends up in liver and or kidney and is lost for targeting muscle. Nevertheless skeletal muscles in DMD patients have leaky membranes, which facilitates the uptake of AONs compared to healthy muscle tissue, yet efficient uptake in cardiac muscle remains challenging as here membranes are intact. Many approaches have been investigated to improve the delivery of AON (chapter 1.3.6) but only a few of them have applied a muscle specific approach (chapter 1.5). I believe this is the preferred option since AON by itself can already distribute throughout the body and be taken up by various tissues (chapter 1.3.5). Improving delivery to and uptake specifically for skeletal and cardiac muscle tissue is key.

To improve the delivery and uptake of AON, muscle specific homing peptides could be ideal candidates to accomplish this. However, the identification of muscle homing peptides from combinatorial phage display peptide libraries is not without challenges e.g. phage display biopanning selections are dominated by parasite sequences (chapter 1.5). In chapter 4 we describe for the first time the implementation of Illumina next generation sequencing (NGS) to analyse the outcome of phage display biopanning selections using the Ph.D.-7™ peptide library (expressing linear 7-mer peptides). We found that sequencing the naïve library after one round of bacterial amplification is a useful tool to identify parasite sequences with a growth advantage. Further, by using NGS a single round of biopanning is enough to identify potential candidate peptides. Databases like Pepbank (5) and Sarotup (6) are versatile tools to check whether your candidate peptide has been found before for a different target (meaning it is not specific for your target), or to inform you whether this is a parasite sequence known from literature (e.g. known to bind albumin, plastic or having a growth advantage). Our NGS results led to a new tool in Sarotup database, PhD7faster. Now other researchers can use this improved tool to filter there data for known 7-mer parasite sequences with a growth advantage (7).

In the last few years Matochko *et al.*, performed more detailed analyses of the peptide libraries, Ph.D.-7TM, Ph.D.-C7CTM and Ph.D.-12TM library (8). They illustrate with statistical analyses how to identify parasite sequences in the naïve library and their behaviour upon bacterial amplification. These results are comparable to ours (Ph.D.-7TM and Ph.D.-C7CTM unpublished). What I found interesting in their analyses compared to ours, are the very high frequency counts found in the naïve library before and after bacterial amplification. Their top 30 peptides have frequency counts between 947 and 5.548 before and between 14.489 and 74.758 after bacterial amplification, whereas in our data set the top frequency count observed in the naïve library was no more than 29 and after bacterial amplification 323. I believe that the library batch used by Matochko *et al.*, is already biased towards parasite sequences through manufacturing/ amplification by the manufacturer/others, or something did not go well in the preparation of the samples for NGS sequencing or a combinations of the above. We did observe a similar issue for our Ph.D.-C7CTM library where the naïve unamplified library (as provided by the manufacturer) showed a frequency distribution in the range of our Ph.D.-7TM library after amplification and observed even further increased frequency counts after bacterial amplification (top 30 peptides Ph.D.-C7CTM library: naïve 103-775, amplified 179-2,106). However these frequency counts are not even close to the counts observed by Matochko *et al.* Nonetheless these findings demand attention from the manufacturer as they can lead to major issues in the phage display field (e.g. limiting the change of identifying true candidate peptides, which by itself is already challenging). Together this does support our finding that it is crucial to sequence your naïve library before and after one round of bacterial amplification to identify parasite sequences with a growth advantage. I believe one has to do this for each library one uses, even for a new batch of the same library.

Matochko *et al.*, also investigated a new method for phage amplification: emulsion amplification (9,10). Here, individual phages are amplified in droplets preventing competition between different phages. This method suppresses fast growing phages and gives other phages more room to amplify, resulting in a more uniform distribution of amplified phages thereby increasing the change of identifying true binders. I find this a valuable approach that should be used in the future by researchers as well as by manufacturers.

Since more researchers are starting to implement NGS sequencing there is a growing need for improved tools which are capable of handling millions of sequences simultaneously. In this area, just recently, improvements became available like PHASTpep (11) and FASTAptamer (12). Further there is an increase in the number of researchers developing and combining high-throughput sequencing with computational analyses (13,14). We have investigated a computational algorithm to predict secondary structure (% of helical content) of all possible 7-mer peptides (1.28 billion) to further improve the analyses of phage display selections (Jirka *et al.*, unpublished). Combining the structure information with the outcome of our NGS data from the naïve unamplified and amplified Ph.D.-7TM library we found a significant increase of peptide sequences with no predicted secondary structure for the parasitic sequence population. This would mean that sequences without a predicted structure have an increased chance of being a parasitic sequence. This finding is not strange since it can be expected that a phage with a peptide sequence without structure would be able to pass the membrane of bacteria much quicker (thereby amplify faster) than a phage with a peptide sequence which does have a structure. This hypothesis still needs to be further investigated using higher resolution algorithms and more thoroughly analyses. Nevertheless the approach has the potential to improve the analysis of phage display selections further and thereby improve the identification of parasite sequences in not only the fraction sequenced by NGS, but for all possible 7-mer peptides. Additionally this approach could be used to characterize parasite sequences further as despite their growth advantage some could still have the potential to bind the target of interest.

In Chapter 3, I describe the identification of muscle homing peptide P4. This peptide is selected from *in vivo* phage display biopanning selections (up to 4 selection rounds) using the Ph.D.-7TM phage display peptide library (without NGS analyses). P4 conjugated 2OMePS AONs resulted, upon systemic administration in *mdx* mice, in increased delivery and exon 23 skipping levels for all muscle tissues analysed and was significant for diaphragm and cardiac muscle tissue. Although increased uptake is seen for liver and kidney as well, the ratio is favoured towards skeletal and cardiac muscle tissue. An outstanding question is whether the modest increase shown would be enough. Looking at the current clinical trial results for 2OMePS AON, low levels of dystrophin protein appear to slow down disease progression. One can hypothesize that a small increase of these low levels can have a serious impact and by this means even small increases have the possibility to further slowdown disease pathology. Pre-clinical studies have shown that improvements in skeletal muscle pathology alone, resulted in increased deterioration of cardiac muscle pathology (15). The significantly increased exon skipping levels seen in diaphragm and cardiac muscle combined with the fact that most DMD patient die of respiratory or cardiac failure, in this manner, illustrates once more the potential of P4.

Although the improvements by P4 are encouraging, ideally we need a better muscle homing peptide. This could be accomplished by chemical modifications of the peptide. Here one could think of amino acid modifications, using non-natural amino acids and alternative conjugation strategies. Continuing to improve the identification methods, new phage display biopanning selections (*in vitro* and *in vivo*) combined with NGS

analyses (using not more than 2 selections rounds) have been performed using a more potent phage display library, Ph.D.-C7C (Chapter 5). This library expresses 7-mer peptides in cyclic conformation from which is thought to have increased binding affinity compared to the linear expressed peptides. This resulted in the identification of muscle homing peptide CyPep10, which upon conjugation to a 2OMePS AON increased the uptake and exon 23 skipping in all skeletal and cardiac muscle tissues analysed, by 2-fold on average and was well tolerated in *mdx* mice. This is a big improvement compared to the P4 peptide and thereby has a lot more potential. Unfortunately, the increase in uptake is also seen for liver and kidney, this might mean that the peptide is not tissue specific. However comparing the frequency counts (number of phages found) of this particular phage (with CyPep10 sequence) in tissues after the biopanning selections, showed higher frequency counts for skeletal and cardiac muscle than liver and kidney. This indicates that CyPep10 should be preferentially taken up by muscle in favour of liver and kidney. Nonetheless, even if the peptide is not muscle specific it remains a potential candidate because the increased uptake seen in liver and kidney did not lead to safety concerns so far. It is possible that the bulkiness of the AON hampers the function of the peptide. Notably, 3-5 copies of the peptide are expressed on the phage coat used in the biopanning experiments and only one is conjugated to the AON. A solution to this problem is to conjugate more than one peptide to the AON, however this requires further research in how to conjugate peptides to 2OMePS AON and the influence of different “linkers” or “spacers” used to accomplish this. Future research is needed to address all these questions and the potential of CyPep10 further.

Muscle homing peptides are not only interesting to enhance delivery of AON for DMD but potentially could help deliver AON for other muscle diseases as well e.g. myotonic dystrophy (DM) or spinal muscular atrophy (SMA) where uptake of AON in muscle is less straightforward due to the absence of leaky muscle fiber membranes as observed in DMD patients. Muscle homing peptides could be interesting for AAV delivery as well (16). The advantage for AAVs is that muscle homing peptides do not need to be conjugated but can be directly integrated in the vectors genome. Another advantage for AAVs is that one does not have to take the charge of the peptide in to account while for 2OMePS AONs only non-cationic homing peptides can be used.

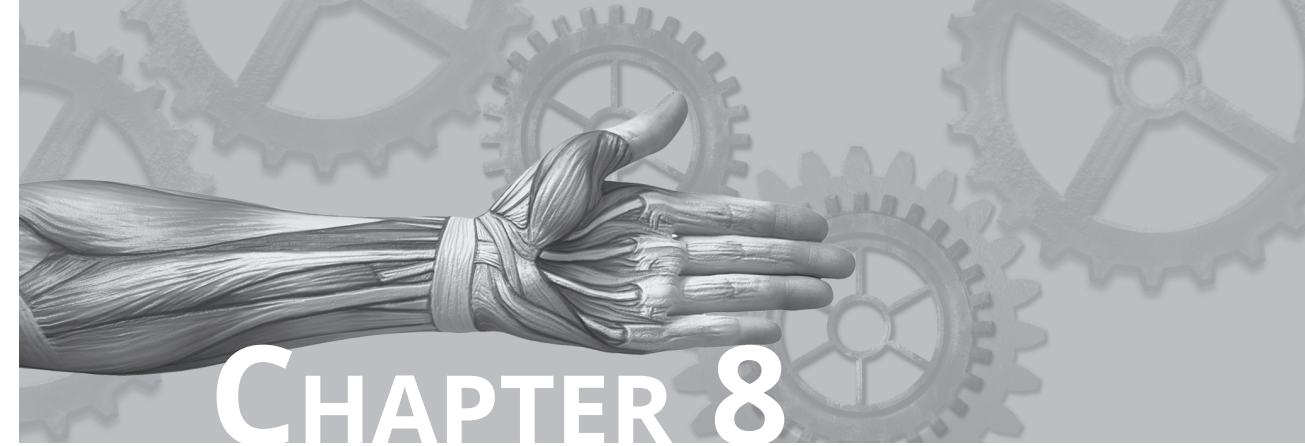
In conclusion, muscle specific homing peptides have the potential to improve the delivery of AON and other compounds towards muscle. By this means they have the potency to improve the balance between delivery, safety and tolerability resulting in an optimized drug with the required efficacy that is necessary for optimal treatment of DMD patients.

References

1. Mendell, J.R., Rodino-Klapac, L.R., Sahenk, Z., Roush, K., Bird, L., Lowes, L.P., Alfano, L., Gomez, A.M., Lewis, S., Kota, J. *et al.* (2013) Eteplirsen for the treatment of Duchenne muscular dystrophy. *Ann. Neurol.*, **74**, 637-647.
2. Voit, T., Topaloglu, H., Straub, V., Muntoni, F., Deconinck, N., Campion, G., de Kimpe, S.J., Eagle, M., Guglieri, M., Hood, S. *et al.* (2014) Safety and efficacy of drisapersen for the treatment of Duchenne muscular dystrophy (DEMAND II): an exploratory, randomised, placebo-controlled phase 2 study. *Lancet Neurol.*, **13**, 987-996.
3. Rigo, F., Hua, Y., Chun, S.J., Prakash, T.P., Krainer, A.R. and Bennett, C.F. (2012) Synthetic oligonucleotides recruit ILF2/3 to RNA transcripts to modulate splicing. *Nat.Chem.Biol.*, **8**, 555-561.
4. Shen, W., Liang, X.H., Sun, H. and Crooke, S.T. (2015) 2'-Fluoro-modified phosphorothioate oligonucleotide can cause rapid degradation of P54nrb and PSF. *Nucleic Acids Res.*, **43**, 4569-4578.
5. Shtatland, T., Guettler, D., Kossodo, M., Pivovarov, M. and Weissleder, R. (2007) PepBank--a database of peptides based on sequence text mining and public peptide data sources. *BMC.Bioinformatics.*, **8**, 280.
6. Huang, J., Ru, B., Li, S., Lin, H. and Guo, F.B. (2010) SAROTUP: scanner and reporter of target-unrelated peptides. *J.Biomed.Biotechnol.*, **2010**, 101932.
7. Ru, B., t Hoen, P.A., Nie, F., Lin, H., Guo, F.B. and Huang, J. (2014) PhD7Faster: predicting clones propagating faster from the Ph.D.-7 phage display peptide library. *Journal of bioinformatics and computational biology*, **12**, 1450005.
8. Matochko, W.L., Cory, L.S., Tang, S.K. and Derda, R. (2014) Prospective identification of parasitic sequences in phage display screens. *Nucleic Acids Res.*, **42**, 1784-1798.
9. Matochko, W.L., Ng, S., Jafari, M.R., Romaniuk, J., Tang, S.K. and Derda, R. (2012) Uniform amplification of phage display libraries in monodisperse emulsions. *Methods*, **58**, 18-27.
10. Derda, R., Tang, S.K. and Whitesides, G.M. (2010) Uniform amplification of phage with different growth characteristics in individual compartments consisting of monodisperse droplets. *Angewandte Chemie (International ed. in English)*, **49**, 5301-5304.
11. Brinton, L.T., Bauknicht, D.K., Dasa, S.S. and Kelly, K.A. (2016)

PHASTpep: Analysis Software for Discovery of Cell-Selective Peptides via Phage Display and Next-Generation Sequencing. *PLoS one*, **11**, e0155244.

12. Alam, K.K., Chang, J.L. and Burke, D.H. (2015) FASTAptamer: A Bioinformatic Toolkit for High-throughput Sequence Analysis of Combinatorial Selections. *Molecular therapy. Nucleic acids*, **4**, e230.
13. Reich, L.L., Dutta, S. and Keating, A.E. (2015) SORTCERY-A High-Throughput Method to Affinity Rank Peptide Ligands. *Journal of molecular biology*, **427**, 2135-2150.
14. Rentero Rebollo, I., Sabisz, M., Baeriswyl, V. and Heinis, C. (2014) Identification of target-binding peptide motifs by high-throughput sequencing of phage-selected peptides. *Nucleic acids research*, **42**, e169.
15. Townsend, D., Yasuda, S., Chamberlain, J. and Metzger, J.M. (2009) Cardiac consequences to skeletal muscle-centric therapeutics for Duchenne muscular dystrophy. *Trends Cardiovasc.Med.*, **19**, 50-55.
16. Korbelin, J., Sieber, T., Michelfelder, S., Lunding, L., Spies, E., Hunger, A., Alawi, M., Rapti, K., Indenbirken, D., Muller, O.J. *et al.* (2016) Pulmonary Targeting of Adeno-associated Viral Vectors by Next-generation Sequencing-guided Screening of Random Capsid Displayed Peptide Libraries. *Molecular therapy : the journal of the American Society of Gene Therapy*, **24**, 1050-1061.



Summary

Efficient drug delivery is a key issue for any potential drug in development. A drug can have a high efficacy in vitro but when it fails to reach its target properly in vivo, the drug is of no use for humans. Furthermore, a drug needs to be safe and well tolerated. Drugs with severe toxicities or where the side effects are more severe than the disease, are doing more harm than good. A balance between efficient delivery, safety and tolerability will result in a drug with the required efficacy that is suitable to use for humans.

Duchenne muscular dystrophy (DMD) is a severe progressive muscle wasting disorder affecting 1 in 5,000 new born boys. DMD is caused by reading frame disrupting mutations in the *DMD* gene resulting in an absence of the dystrophin protein. Dystrophin is an important muscle protein as it provides stability upon muscle fiber contraction. Without this protein muscle fibers are easily damaged and chronic damage leads to muscle fibrosis which in turn results in a loss of muscle function. In general DMD patients are generally diagnosed before the age of five and become wheelchair dependent around the age of 12. Patients need assisted ventilation around the age of 20, an age where in most patients cardiomyopathy is prevalent as well. DMD patients have a life expectancy of around 30 years of age in the western world where respiratory and cardiac failure is the main cause of death. In contrast to DMD, Becker muscular dystrophy (BMD) is a muscle wasting disorder, caused by mutations in the *DMD* gene that not affect the reading frame but result in an internally deleted but partly functional dystrophin protein. The symptoms of BMD are much milder and ranges from mild to moderately severe. The life expectancy of these patients varies from 40-50 years for the more severely affected patients to a nearly normal life expectancy for the milder affected patients.

Currently there is no therapy for the majority of the DMD patients. As part of the standard of care patient receive symptomatic treatment e.g. corticosteroids, respiratory and cardiac support. Various therapeutic approaches are currently under development and in general can be grouped in two main groups. One is focussed on the genetic defect, aiming to restore dystrophin production. The other is focussed on secondary pathology, for example reducing fibrosis and inflammation or improving muscle growth and strength. Most advanced therapeutic approach is aimed at restoring dystrophin production: exon skipping. Here AON are designed to bind a specific exon in the pre-mRNA of the dystrophin transcript. Upon binding the AON hides the exon from the splicing machinery, it is no longer recognized as an exon and thereby spliced out together with the other introns (chapter 1, figure 4c). This results in restoration of the reading frame and the production of a partly functional dystrophin protein as seen in BMD patients (chapter 1, figure 1).

This thesis focusses on delivery of AON to skeletal and cardiac muscle for DMD. Since one cannot treat each muscle individually, systemic treatment

is necessary. From pre-clinical studies it is known that this is feasible. Clinical studies have shown that AON (2OMePS and PMO AONs) are safe for humans, however mild to moderate side effects have been reported. On September 19th 2016 the FDA conditionally approved eteplirsen (a PMO targeting DMD exon 51) for the treatment of DMD patients that benefit from exon 51 skipping. However, upon systemic administration of AON, a large proportion of the administered AONs ends up in liver (2OMePS) and or kidney (2OMePS and PMO) and are lost for targeting muscle.

Strategies taken to improve AON therapy are chemical modification of the AON to enhance nuclease resistance or improve thermodynamic stability, affinity for the target, bio-availability and tissue half-life. In chapter 6 2FPS (substitution of a Fluoro (F) at the 2' position) and isosequential 2OMePS AON counterparts have been compared for DMD. While *in vitro* 2FPS AON resulted in increased exon skipping levels, the modification appeared less effective *in vivo* and was found to be toxic in *mdx* mice (a mouse model for DMD).

Other strategies taken to improve AON therapy are more focussed on the use of a delivery system. Such delivery system should first of all not interfere with the function of the AON, should have a good safety profile and good biostability. Secondly, the delivery system should be small in size to allow efficient uptake by muscle cells and promote endosomal escape. Third, preferably the delivery system is muscle specific thereby limiting or preventing uptake by e.g. liver, kidney and spleen. In this thesis the conjugation of muscle homing peptides, selected from phage display experiments, to 2OMePS AON is described as a delivery system (chapters 3, 4 and 5).

Phage display is a well described, powerful technique to identify peptides, antibodies or other proteins with target specific binding properties from phage libraries. Such a selection is called biopanning and the basic principles are the same for various targets. The phage library is exposed to the target for binding. When all non-binders are removed binding phages are recovered by elution, amplified and prepared for a next biopanning round. After several rounds of biopanning, binding phages are identified by for example sequencing of candidate phage DNA (chapter 1, figure 7). The use of muscle specific homing peptides potentially leads to a delivery system which is safe, small in size, promotes endosomal escape and limits uptake by e.g. liver and kidney.

Focussing on the 7-mer phage display peptide library (Ph.D.-7), the first potential muscle homing peptide for 2OMePS AON, selected from *in vivo* biopanning selections in *mdx* mice, is peptide P4 (7-mer: LGAQSNF). P4 conjugated 2OMePS AONs resulted in small but significantly increased exon skipping levels in diaphragm and cardiac muscle tissue compared to unconjugated AONs, after subcutaneous administration in *mdx* mice

(chapter 3). Despite an increase in AON levels in all tissues was observed, the uptake was favorable for muscle.

In the last couple of years, technology used to analyze phage display outcomes rapidly improved. We integrated for the first time Illumina next generation sequencing (NGS) to analyze phage display biopanning selections (chapter 4). We showed that high throughput sequencing of the naïve library after one round of bacterial amplification is a powerful tool to identify parasite sequences with a growth advantage. We also showed that by using NGS a single biopanning round is enough to identify candidate peptides.

In search for better muscle homing peptides we used NGS sequencing to analyze new *in vitro/in vivo* phage display selection. This, combined with the use of a 7-mer cyclic peptide library (here peptides are more restrained in conformation resulting in higher binding affinity) allowed the identification of new candidates. From these candidates the lead peptide CyPep10 (Cyclic 7-mer: CQLFPLFRC) resulted, upon conjugation to 2OMePS AONs, in 2-3 fold increase in AON levels in all tissues analyzed. Despite increase in AON levels in liver and kidney is seen as well the conjugate has a high potential as it resulted in a significant 2-2.5 fold increase in exon skipping levels in all muscle tissues analyzed (chapter 5).

In conclusion, muscle specific homing peptides have the potential to improve the delivery of AON and other compounds towards muscle. By this means they have the potency to improve the balance between delivery, safety and tolerability resulting in an optimized drug with the required efficacy that is necessary for optimal treatment of DMD patients.



Samenvatting

Een zeer belangrijk onderdeel in de ontwikkeling van nieuwe medicijnen is zorgen dat het medicijn op de plek komt waar het zijn werking moet uitvoeren. Een geneesmiddel kan een goede werkzaamheid hebben, maar wanneer het in het lichaam niet op de plek komt waar het nodig is heeft het geen baat voor mensen. Daarnaast moet een geneesmiddel veilig en verdraagzaam zijn. Geneesmiddelen die leiden tot toxiciteit of waar de bijwerkingen erger zijn dan de te behandelende aandoening, doen uiteindelijk meer kwaad dan goed. Een balans tussen een doeltreffende opname, veiligheid en verdraagzaamheid zal resulteren in een geneesmiddel met het gewenste effect dat geschikt is om mensen mee te behandelen.

Duchenne spierdystrofie (DMD) is een ernstige erfelijke spieraandoening waarbij de spieren worden aangetast en langzaam hun werking verliezen. Het komt voor bij 1:5000 pasgeboren jongens wereldwijd. DMD wordt veroorzaakt door een genetisch defect in het gen dat codeert voor het dystrofine eiwit, het *DMD* gen. Dit heeft het gevolg dat deze patiënten geen dystrofine eiwit kunnen maken.

In de kern van de cellen in ons lichaam is ons DNA opgeslagen. Dit DNA is onze genetische code, ons boek waar in staat beschreven wat en hoe er iets gemaakt moet worden in ons lichaam. De genetische code van ons DNA is opgebouwd uit genen, zoals hoofdstukken in een boek. Genen zijn verder onderverdeeld in intronen en exonen, zoals paragrafen in een boek. In de cel wordt een gen afgelezen en er een exacte kopie van gemaakt genaamd pre-messenger RNA (pre-mRNA). Dit wordt vervolgens gelezen en alle intronen (niet relevante informatie) worden er uitgehaald door middel van een proces wat "splicing" wordt genoemd. Wat overblijft noemen we messenger RNA (mRNA) en bestaat uit exonen (de relevante informatie). Als laatste stap wordt het RNA vertaald in eiwit. Elk gen heeft een begin en eind en net als bij een boek moet het helemaal afgelezen worden om het goed te begrijpen en te vertalen in het juiste eiwit. Als er in een boek een half hoofdstuk ontbreekt mis je een deel van het verhaal en begrijp je niet meer hoe het verhaal verder gaat. Dit is nu juist het geval bij patiënten met DMD, er missen relevante stukken van het gen waardoor de rest van het boek onleesbaar wordt en er uiteindelijk geen dystrofine eiwit kan worden gemaakt.

Het dystrofine eiwit is heel belangrijk voor spieren, het zorgt namelijk voor stevigheid en veerkracht bij beweging. Door het ontbreken van het dystrofine eiwit in de spieren raken deze gemakkelijk beschadigd, verzwakt en verliezen uiteindelijk hun functie. DMD is een aangeboren aandoening, de eerste symptomen zijn al zichtbaar rond het tweede levensjaar en de diagnose wordt meestal gesteld vóór het vijfde levensjaar. De eerste zichtbare symptomen zijn bijvoorbeeld een vertraging in het leren/gaan lopen, het gebruik van de handen om de benen te ondersteunen bij het gaan staan en zichtbaar moeite hebben met rennen en traplopen. Over

het algemeen worden DMD patiënten rolstoel afhankelijk rond het 12^{de} levensjaar, hebben mechanische ondersteuning nodig bij het ademen rond hun 20^{ste} levensjaar, eerst alleen in de nacht later ook overdag. Rond het 10^{de} levensjaar ontwikkelen zich de eerste hartproblemen en vrijwel alle patiënten hebben duidelijk hartfalen vanaf de leeftijd van 20 jaar. De levensverwachting van DMD patiënten in de westerse wereld is zo'n 30 jaar.

Naast DMD is er nog een gerelateerde spieraandoening, Becker spierdystrofie (BMD). BMD patiënten hebben ook een genetisch defect in het *DMD* gen, maar bij deze patiënten wordt er nog wel dystrofine eiwit gemaakt. Echter heeft dit dystrofine eiwit een mindere werking ten opzichte van het gezonde eiwit omdat het kleiner is. Er mist een hoofdstuk van een boek, waardoor je bijvoorbeeld niet weet dat de hoofdpersoon op vakantie is geweest, maar het verhaal is nog steeds duidelijk en leesbaar van begin tot eind. De symptomen voor BMD patiënten variëren van mild tot matig ernstig. BMD patiënten hebben een levensverwachting van 40-50 jaar voor de matig ernstige patiënten tot een normale levensverwachting voor de mildere variant.

Voor de meeste DMD patiënten is er geen geneesmiddel beschikbaar. Behandeling bestaat voornamelijk uit symptoombestrijding zoals het gebruik van corticosteroiden en ondersteuning van de ademhaling en hartfunctie. Hiernaast is een heel team van getraide mensen betrokken (fysiotherapeut, orthopedisch therapeut, longarts, cardioloog, revalidatieartsen e.d.) om het leven zo aangenaam mogelijk te maken. Op dit moment zijn er verschillende potentiële geneesmiddelen voor DMD in ontwikkeling. Over het algemeen kunnen deze in twee hoofdgroepen worden verdeeld. Een groep richt zich op het genetisch defect, het herstellen van de aanmaak van het dystrofine eiwit. De andere groep richt zich op het verbeteren van de bijkomende symptomen zoals het verminderen van de ontsteking of het sterker maken van de spieren. De grootste vooruitgang op het moment is gericht op het herstel van de dystrofine productie: exon skippen. Het geneesmiddel wat hierbij gebruikt wordt heet een antisense oligonucleotide (AON). Deze AON bindt in de celkern van een spiercel aan een speciaal gekozen plek op het pre-mRNA van het *DMD* gen. Daarbij plakt de AON een stuk van een niet functionerend exon op dit pre-mRNA af, het halve hoofdstuk in een boek. Wanneer er vervolgens van pre-mRNA door het proces wat splicing heet mRNA wordt gemaakt, wordt dit afgeplakte stuk pre-mRNA er ook uit gehaald (exon skippen). Nu wordt er een groter stuk weg gehaald, maar wordt het RNA weer leesbaar en kan er een dystrofine eiwit worden gemaakt zoals we zien bij BMD patiënten. Het rare halve hoofdstuk in het boek wordt er uitgehaald (overgeslagen of wel geskipt), en al weet je nu niet dat de hoofdpersoon op vakantie is geweest, het is een mooi leesbaar boek met een duidelijk begin en eind.

Dit proefschrift richt zich op het verbeteren van het gebruik van AON als geneesmiddel voor DMD patiënten. Omdat 30-40% van het menselijk lichaam uit spieren bestaat is het onmogelijk om iedere spier apart te behandelen. Systemische toediening (door het hele lichaam) is nodig. Uit pre-klinisch onderzoek is gebleken dat systemisch toegediende AON in de spieren terecht komen. Het grootste gedeelte komt echter in de lever en nieren terecht en verlaten het lichaam zonder ook maar iets gedaan te hebben. Er zijn verschillende manieren om deze aanpak te verbeteren. Je kan chemisch de AON zelf aanpassen waardoor het stabiel wordt (minder snel afgebroken door het lichaam) of beter aan het mRNA bindt. In hoofdstuk 6 is zo'n chemische aanpassing beschreven. In gekweekte spiercellen in een laboratorium leverde dit een verhoogde activiteit van de AON op. Maar wanneer deze aanpassing in dieren werd getest bleek het helemaal niet te werken en ook nog eens toxisch te zijn.

Een andere mogelijke oplossing is om er voor te zorgen dat meer AON in de spieren terecht komt. Hier zijn verschillende mogelijkheden voor. Binnen dit proefschrift is gekozen voor de ontwikkeling van spier specifieke peptiden (piepkleine eiwitten) die wanneer vast gemaakt aan de AON, deze naar de spieren zou moeten geleiden. Voor de ontwikkeling/identificatie van spier specifieke peptiden is gebruik gemaakt van de techniek faag display. Deze techniek maakt gebruik van een fagenbank (in dit geval peptiden fagen bank) die bestaat uit wel meer dan een miljard fagen (virussen die bacteriën infecteren en zich daar kunnen vermenigvuldigen) die ieder aan hun buitenkant een uniek peptide tot expressie brengen. In een laboratorium is zo'n fagenbank blootgesteld aan spiercellen. Afhankelijk van het peptide dat ze aan de buitenkant hebben zitten, zullen deze fagen wel of niet aan een spiercel binden. De fagen die binden zijn geïdentificeerd en het bijbehorende peptide gekarakteriseerd. Deze peptiden werden vervolgens synthetisch gemaakt. In het laboratorium is onderzocht of ze inderdaad aan spiercellen kunnen binden en bij voorkeur ook de spiercellen in gaan en in de kern van de cel terecht komen (want daar moet uiteindelijk de AON ook heen om zijn werking te kunnen verrichten). Wanneer een peptide gevonden is die aan de juiste voorwaarden voldeed werd deze gekoppeld aan een AON. In diermodellen is er onderzocht of er bijvoorbeeld meer peptiden geconjugeerd AON in de spieren terecht kwam ten opzichte van de AON alleen. Daarnaast is er ook gekeken naar het percentage exon skippen en of er na toediening meer dystrofine eiwit aanwezig is in de spieren. In hoofdstuk 3 is een eerste peptide beschreven (P4) die weliswaar een kleine maar toch significante toename in het percentage exon skippen bewerkstelligt in hart en diafragma (ademhalingsspier). Omdat het wenselijk is om nog betere peptiden te vinden is met behulp van de techniek "next generation sequencing" de analyse van faag display selecties verbeterd, dit staat beschreven in hoofdstuk 4. Nieuwe verbeterde faag display selecties hebben uiteindelijk geresulteerd in de identificatie van peptiden CyPep10, beschreven in hoofdstuk 5. Het CyPep10-AON conjugaat

resulteerde, na systemische toediening, in een significante verdubbeling van de opname van het conjugaat evenals het percentage exon skippen in alle geanalyseerde skeletspieren en hart. Na een eiwitbepaling is er op het oog ook een mogelijk kleine verhoging van het dystrofine eiwit gevonden maar dit is nog niet bewezen.

In conclusie, spier specifieke peptiden hebben de potentie om de opnamen van AON, of andere potentiële geneesmiddelen voor spieren, te verbeteren. Zo gezegd zij hebben de potentie de balans tussen een doeltreffende opname, veiligheid en verdraagzaamheid te verbeteren resulterend in een geneesmiddel met de gewenste werkzaamheid voor de behandeling van DMD patiënten.

Curriculum Vitae

Silvana Jirka was born in Apeldoorn on January 16th 1984. After finishing her Havo degree at the Koninklijke scholen gemeenschap Apeldoorn in 2001 she started to study biology and medical laboratory research at the academic life science and technology, Hogeschool Enschede the Netherlands. She received her Bachelor degree in 2006 and started working as a research technician at the hematology department in the VuMC in Amsterdam the Netherlands under the supervision of Dr. Martine Chamuleau. Here she was involved in studying the TRAIL-R3 expression on leukemic blast cells and the role in apoptosis resistance. In 2008 Silvana started as a research technician at the Department of Human Genetics in the LUMC in Leiden the Netherlands under the supervision of Dr. Peter-Bram 't Hoen. Here she implemented next generation sequencing in the analyses of phage display peptide selections and search for peptides homing to bone. In 2011 she was granted permission to the doctoral and started here PhD in 2012 by Prof. Dr. Gert-Jan van Ommen and Prof. Dr. Annemieke Aartsma-Rus at the Department of Human Genetics in the LUMC in Leiden the Netherlands. The main focus of her PhD research was to improve the delivery of 2'-O-methylphosphorothioate antisense oligonucleotides (AON) to skeletal and cardiac muscle for Duchenne muscular dystrophy (DMD). She used her knowledge on phage display technology and next generation sequencing to identify tissue specific homing peptides to improve the delivery of AON (in collaboration with BioMarin NL). In 2013 she received an award for 'best poster' at the annual meeting of the Oligonucleotide Therapeutic Society (Napels, Italy) and in 2014 she won a travel fellowship to attend the World Muscle Society meeting (Berlin, Germany). In 2015 she again received an award for 'best poster' at the annual meeting of the Oligonucleotide Therapeutic Society (Leiden, Netherlands). She is also co-inventor on patent 16199033.8-1405. All together this resulted in this thesis "developing tissue specific AON-delivery to refine treatment for Duchenne muscular dystrophy. Currently she is continuing her career as a scientist at the Centre for Human Drug Research in Leiden, the Netherlands.

List of Publications

Submitted:

1. **S.M.G. Jirka**, P.A.C. 't Hoen, V. Diaz Parillas, C. Tanganyika-de Winter¹, R.C. Verheul, B. Aguilera, P.C. de Visser, A. Aartsma-Rus
Cyclic peptides to improve delivery and exon skipping of antisense oligonucleotides for Duchenne muscular dystrophy

Published:

1. **S.M.G. Jirka**, C.L. Tanganyika-de Winter, J.W. van der Meulen, M. van Putten, M. Hiller, R. Vermue, P.C. de Visser and A.M. Aartsma-Rus
Evaluation of 2'-deoxy-2'-fluoro antisense oligonucleotides for exon skipping in Duchenne muscular dystrophy
Mol Ther Nucleic Acids. 2015 Dec 1;4:Online
2. **Silvana Jirka** and Annemieke Aartsma-Rus
Update on RNA-targeting therapies for neuromuscular disorders
Curr Opin Neurol. 2015 Oct;28(5):515-21
3. **Silvana M.G. Jirka**, Hans Heemskerk, Christa L. Tanganyika-de Winter, Daan Muilwijk, Kar Him Pang, Peter C. de Visser, Anneke Janson, Tatyana G. Karnaoukh, Rick Vermue, Peter.A.C.'t Hoen, Judith C.T. van Deutekom, Begoña Aguilera and Annemieke Aartsma-Rus.
Peptide conjugation of 2'-O-methyl phosphorothioate antisense oligonucleotides enhances cardiac uptake and exon skipping in mdx mice.
Nucleic Acid Ther. 2014 Feb;24(1):25-36
4. 't Hoen, Peter; **Jirka, Silvana**; ten Broeke, Bradley; Schultes, Erik; Aguilera, Begona; Pang, Kar; Heemskerk, Hans; Aartsma-Rus, Annemieke; van Ommen, G; den Dunnen, Johan. Phage display screening without repetitious selection rounds.
Anal Biochem. 2012 Feb 15;421(2):622-31
5. Chamuleau ME, Ossenkoppele GJ, van Rhenen A, van Dreunen L, **Jirka SMG**, Zevenbergen A, Schuurhuis GJ, van de Loosdrecht AA. High TRAIL-R3 expression on leukemic blasts is associated with poor outcome and induces apoptosis-resistance which can be overcome by targeting TRAIL-R2. Leuk Res. 2011 Jun;35(6):741-9.

Presentations

- Oral:**
- 1)** 25th MGC symposium 2015, Sept 10th, Leiden, the Netherlands
Title: Enhancing the delivery of antisense oligonucleotides for Duchenne muscular dystrophy
 - 2)** COST Action BM1208 meeting 2014, Stockholm, Sweden
Invited speaker, title: Evaluation of exon skipping activity of 2'- deoxy-2'-Fluoro antisense oligonucleotides for Duchenne muscular dystrophy
 - 3)** Genetica Retraite 2013, Kerkrade, the Netherlands
Title: Short peptides to improve delivery of exon skipping compounds in mouse models for Duchenne muscular dystrophy
 - 4)** 4th Next-generation sequencing meeting 2011, Utrecht, the Netherlands
Title : Next-Generation Sequencing of phage display peptide libraries enables fast selection of true and false positive peptide sequences
- Poster:**
- 1)** Nederlandse Vereniging voor Humane Genetica (NVHG), Arnhem, The Netherlands
Title: Enhancing the delivery of antisense oligonucleotides for Duchenne muscular dystrophy
 - 2)** Oligonucleotide Therapeutic Society (OTS),2015, Leiden, The Netherlands
Title: Evaluation of exon skipping activity of 2'- deoxy-2'-fluoro antisense oligonucleotides for Duchenne muscular dystrophy
 - 3)** World muscle society (WMS) 2014, Berlin, Germany
Title: Evaluation of exon skipping activity of 2'- deoxy-2'-fluoro antisense oligonucleotides for Duchenne muscular dystrophy
 - 4)** Oligonucleotide Therapeutic Society (OTS) 2013, Napels, Italy
Title: Peptide conjugation of 2'-O-methyl phosphorothioate antisense oligonucleotides enhances cardiac uptake and exon skipping in mdx mice

Acknowledgements

Kijk hier mijn prachtig proefschrift! Het resultaat van een aantal jaar flink hard werken en veel toewijding. Maar zonder de steun van alle lieve mensen om mij heen had ik dit misschien nooit behaald. Ik zou graag iedereen (vrienden, familie, collega's) willen bedanken die op welke wijze ook heeft bijgedragen aan de totstandkoming van dit proefschrift. Maar een aantal speciale mensen verdienen een extra dankjewel.

Annemieke, mijn dank is groot dat je in mij geloofde en dat ik onder jouw vleugels mocht promoveren, ik had me geen betere promotor kunnen wensen. Peter-Bram, veel dank voor alle wijze woorden, adviezen en ook voor de hulp met al het bioinformatica werk, je bent een waardig co-promotor. Laura, nu oud collega maar nog steeds vriendin, we hebben samen gelachen, gehuild, en hele serieuze discussie gevoerd over goede resultaten of mislukte experimenten. Je hebt het dik verdiend mijn paranimf te zijn! Ivo, mijn redder in nood als het gaat om computer problemen en de voor mij te ingewikkelde bioinformatica analyses. Mijn exon skip collega's (Maaïke, Monika, Pietro, Joke, Svetlana, Margriet, Laura, Christa Nisha, Maurice, Cindy, Marcel, Isabella en Kayleigh) bedankt voor jullie hulp en support. Mijn collaborators bij BioMarin NL, Peter dank voor al je input de afgelopen jaren. Carola & Remco heel veel dank voor alle steun, hulp en heerlijke chocolade door de jaren heen en natuurlijk alle hulp en oppasdagen voor Norah mogen zeker niet vergeten worden! Carola ook jij hebt het dik verdiend mijn paranimf te zijn en Remco veel dank voor het ontwerp en het maken van de layout van dit proefschrift. Hanneke, waar en wanneer ook, we staan voor elkaar klaar, je bent een super meid. Vincent, dank voor al je steun, je bent een geweldige vader. Samen met Norah bewonder ik nog elke dag je teken en illustratie talent. Ik ben er trots op dat je met zo veel toewijding altijd mijn illustraties hebt gemaakt en dat deze nu zijn samengebundeld in dit proefschrift, waar je zelfs mijn persoonlijke draai in hebt weten te verwerken. Marcel & fam en Natasja & fam. Mijn grote broer en zus, al zien we elkaar misschien niet zo veel we zijn er voor elkaar wanneer dat nodig is in voor en tegen spoed en dat waardeer ik enorm. Papa en Mama, van jullie heb ik geleerd om altijd vooruit te kijken naar het doel wat je wil bereiken en vooral om door te zetten. Vol vertrouwen zijn jullie altijd in mij blijven geloven en steunde jullie mij wanneer dat ook maar nodig was. Mijn dank aan jullie is te groot om met geschreven woorden te beschrijven. Norah, dankjewel voor je mooie lach, je stralende ogen en al die lieve knuffels die keer op keer mijn hart verwarmen.

Silvana Jirka